The Role of Mitogen-activated Protein Kinase Phosphatase -2 (MKP-2) In Macrophage Functions

By

Shilan Khayrula Jabbar

Thesis submitted to

University of Strathclyde

Strathclyde Institute of Pharmacy and Biomedical Sciences (SIPBS)

For the degree of

Doctor of Philosophy

September 2018

Glasgow, UK

Publications

Poster presentations

1- **Shilan Jabbar**, Andrew Paul and Robin Plevin.11th November. (2016).The role of MAP Kinase Phosphatase-2 (MKP-2) in Macrophage Functions. SIPBS annual Postgraduate Research Day. University of Strathclyde, Glasgow, UK. (Poster No. 38).
2- **Shilan Jabbar**, Robin Plevin, Kathryn A Mackintosh, Catherin Lawrence, Stuart Woods, Juliane Schroeder and Kirsty Ross.20-22 June. (2016). A Protective role of MAP Kinase Phosphatase-2 in arthritis. Phosphatases and signalling in Health and Disease conference. University of Bath. Bath.UK.

Oral Presentation:

1- **Shilan Jabbar**, Andrew Paul and Robin Plevin.13th November. (2015).The role of MAP Kinase Phosphatase-2 (MKP-2) in Macrophage Functions. Cardiovascular, Cell biology and Neuroscience Postgraduate Research Day. Target validation and drug Discovery group (TVDD).University of Strathclyde, Glasgow, UK.

Papers

- A novel protective role for MAP kinase phosphatase 2 in inflammatory arthritis. 2018. Juliane Schroeder, Kirsty Ross, Kathryn McIntosh, **Shilan Jabber,** Stuart Woods, Jenny Crowe, Janet Paterson Kane, James Alexander, Catherine Lawrence and Robin Plevin. RMD Open. (Submitted and revised).

Declaration

This thesis is the result of the author's original research. It has been composed by the author and had not been previously submitted for examination which has led to the award of a degree.

The copyright of this thesis belongs to the author under the terms of the United Kingdom Copyright Acts as qualified by University of Strathclyde Regulation 3.50. Due acknowledgement must always be made of the use of any material contained in, or derived from, this thesis.

Signed:

Date:

Abstract

Mitogen-activated protein kinase phosphatase-2 (MKP-2) is a type 1 nuclear dual specificity phosphatase which known to play key roles in cellular function through dephosphorylation of the MAPKs (ERK, JNK and p38). MKP-2 has recently been shown to play a significant role in the immune response following parasite and bacterial infections. However, the effect of MKP-2 deletion on a number of other key macrophages functions including phagocytosis, motility and proliferation is yet to be studied. This thesis therefore utilised a novel DUSP4 gene knockout mouse and investigated the effect of cellular MKP-2 removal in bone marrow derived macrophage (BMDMs) using a number of approaches.

Results obtained from macrophage characterisation experiments demonstrated that following LPS stimulation MKP-2 deleted BMDMs showed enhanced JNK activation as opposed to other MAPKs, this effect was found to correlate with enhanced endothelin-1 (EDN1) expression at both gene and protein synthesis level. This is the first study to reveal that EDN1 expression is negatively regulated by MKP-2. MKP-2 deletion also resulted in different kinetic profiles for phagocytosis and migration which was also differed in M1 and M2 stimulated cultures. MKP-2$^{-/-}$ macrophages showed more phagocytic activity but less motility upon LPS activation, this effect was reversed when cells were pre-treated with IL-4 which gave less phagocytic activity but more motility. Also MKP-2 deletion reduced macrophage migration towards C5a suggesting a new role for MKP-2 gene in regulating macrophage motility. Loss of MKP-2 also resulted in decreased macrophage proliferation activity.

Finally, a metabolomics profile was established for both MKP-2$^{+/+}$ and MKP-2$^{-/-}$ macrophages stimulated by different agents. MKP-2 deletion resulted in enhanced production of metabolites associated with glycolysis and the pentose phosphate pathway during the time at which MAPKs were upregulated indicative of a tight correlation between signalling and metabolic changes that underlie macrophage functions. In contrast, the proline and arginine pathway was downregulated in MKP-2 deleted macrophages. This was confirmed by studying nitric oxide production which was downregulated in MKP-2$^{-/-}$ macrophages upon LPS challenge which further correlated with changes in citrulline and ornithine. Collectively, this is the first study to investigate and determine the role of MKP-2 gene in macrophage functions; deletion or inhibition of MKP-2 in macrophages may be a therapeutically desirable approach.

Acknowledgments

I would like to thanks Allah for giving me a good health, facilitating everything in my life and the opportunity to continue my study to this stage. My special thanks goes to my first supervisor Prof. Robin Plevin for his help, support and courage during my PhD and for his endless support in my writing process. The word "Thank you" is very little towards your great efforts and help especially in my hard times you always cheered me up. It is all your support and believe in my abilities that allowed me to grow into an independent researcher without your guidance and believe none of this work would have been possible. Truly you are "a supervisor who plants solid seed to the science to grow many scientists". I am very grateful in working in your lab. My Thanks also goes to my second supervisor Dr. Andrew Paul who always supported me in the daily bases at the lab and solving difficulties that were issued in the lab during long working hours. I am extremely grateful to the one that made our time enjoyable in the lab, the one that gave us endless support whenever needed, the one who spent hours to organise things for us and facilitate the lab running, words can go to infinity here, to whom I ought to all these, to Dr. Kathryn McIntosh and as always I say "you are the heart of Plevin's lab".

To my sister in science Dr. Margaret Cunningham thank you for the courage you gave me along my PhD, having a chat with you means getting great scientific conversation. You always reminded me that the science has to be written to succeed to the next level. I am extremely grateful to Dr. Rothwelle Tate for always encouragement and for his great help in PCR and primer design, the support I got from you helped in shaping my molecular study and thinking. Two people came out from nowhere to train me and help in the confocal imaging, Dr. Musab Bhutta and Graeme Mackenzie,who I am grateful. My special thanks goes to my friend Samyah for her great help in the metabolomics study spending long times in the lab together was our chance to chat about macrophages and having fun while doing such hard experiments. In this context, I would like to thanks Dr. David Watson and his group for facilitating the use of LC-MS machine. A big thank you to the BPU staff Linda Horan, Carole Whitehouse, Lee wheeler and peter for helping in the animal unite in SIPBS. I must not forget the lovely people in SIPBS who always helped in keeping us equipped with autoclaved material, to all autoclave staff I am very grateful. To all secretary and finance staff in SIPBS (Eileen, Grace, Elaistar, Luara, Craige, Philip really you gave me a good view

List of Abbreviations

AMP	Adenine Monophosphate
ANOVA	Analysis of variance
AP-1	Activation protein-1
APC	Antigen presenting cells
APS	Ammonium Persulfate
Arp2/3	Actin-related protein-2/3
ATP	Adenosine Tiphosphate
BMDM	Bone marrow-derived macrophage
BrDU	5-bromo-2'-deoxyuridin
BSA	Bovine Serum Albumin
C5a	Complement component 5a
CAM	Classically activated macrophage
CCR2	CC-chemokine receptor 2
CD	Cluster of differentiation
cDNA	Complementary DNA
CDPs	Common DC precursors
CLPs	Common lymphoid progenitors
CLRs	C-type lectin receptors
CMPs	Common myeloid progenitors
COX-2	Cyclogenase 2
CR3	Complement receptor 3
CSF-1	Colony Stimulating factor 1
CX3CR	CX3C-chemokine receptor 1
CXCR	C-X-C motif chemokine receptor
DAPI	4',6-diamidino-2-phenylindole
DC	Dendritic cells
DMEM	DulBeccos Modified Eagle Medium
DTT	Dithiothreitol
DUSPs	Dual Specificity Phosphatases
E.coli	Escherichia coli
ECACU	European Collection of Authenticated Cell Cultures
ECL	Enhanced chemiluminescene
ECM	Extracellular matrix
EDN1	Endothelin-1
ELISA	Enzyme-Linked Immunosorbent assay
eNOS	endothelial nitric-oxide synthase
ERK	Extracellular signal-regulated kinases
FACs	Fluorescent –activated cell sorting
GM-CSF	Granulocyte/ Monocyte-colony stimulating factor
GMP	Guanine Mono Phosphate
GMPs	Granulocyte/ Macrophage progenitors
GPCR	G-protein coupled receptors

GPCRs	G-protein coupled receptors
HSCs	Haematopoietic stem cells
IAMs	Innate activated macrophages
IFN-γ	Interferon γ
iNOS	Inducible nitric oxide synthase
IRAK	IL-1R-associated kinase
ITAM	Immunoreceptor tyrosine-based activation motif
JNK	c-Jun-N terminal kinase
KO	Knock out
LC-MS	Liquid chromatography–mass spectrometry
LPS	Lipopolysaccharide
LTβ$_4$	Leukotriene beta 4
MAPK	Mitogen activated protein kinases
MCP-1	Monocyte chemoattractant protein 1
M-CSF	Macrophage colony-stimulating factor
MDPs	Macrophage dendritic cells progenitors
MEFs	Mouse embryo fibroblasts
MEPs	Megakaryocyte/Erythrocyte progenitors
MHCII	Major histocompatibility complex class 2
MIF	Macrophage inhibitory factor
MKP-2	Mitogen-activated protein kinase phosphatase
MOI	Multiplicity of infection
MyD88	Myeloid differentiation factor 88
NAD+	Nicotinamide adenine dinucleotide (oxidised form)
NADH	Nicotinamide adenine dinucleotide (reduced form)
NADP+	Nicotinamide adenine dinucleotide phosphate (oxidised form)
NADPH	Nicotinamide adenine dinucleotide phosphate (reduced form)
NEMO	a complex of TRAF6 and NFκB essential modifier)
NF-κB	Nuclear transcription factor κB pathway
NK	Natural killer cells
NK-T	Natural killer T-cells
NO	Nitric oxide
NOD	Nucleotide-binding oligomerization domain-containing protein
NOS2	Nitric oxide synthase 2
OPLAS-DA	(Orthogonal Partial Least Square- discriminant analysis)
OPLSDA	Orthogonal partial least squares - discriminant analysis
P\S	Penicillin/ streptomycin
PAMPs	pathogen-associated molecular patterns
PBS	Phosphate-buffered saline
PC	Phosphorylcholine
PCA	Principal Component Analysis
PCR	Polymerase chain reaction

PFK-1	Phosphofructokinase -1
PI3K	Phosphatidylinositol 3-kinase
PKC	Protein kinase C
PLS-DA	Partial least squares-discriminant analysis
PPP	Pentos phosphate pathway
PRRs	Pattern recognition receptors
PS	Phosphatidylserine
qRT-PCR	Quantitative Real Time Polymerase Chain Reaction amplification
RA	Rheumatoid arthritis
RFU	Relative fluorescent unit
RIG1	Retinoic acid-inducible gen1
RLRs	RIG1-like helicase receptors
ROS	Reactive oxygen species
RPMI	Roswell Park Memorial Institute medium,
SCF	Stem cell factor
SDF-1	Stromal derived factor 1
SEM	Standard errors of the mean
SMICA	Soft-Independent Modelling of Class Analogy
STAT	Signal transducer and activator of transcription
Syk	Spleen tyrosine kinase family
TABs	TAK1-binding proteins
TAK1	Transforming growth factor-β-activated kinase1
TCA	Tricarboxylic acid cycle
TGF	Transforming growth factor
TGFR	Transforming growth factor receptor
TGFβ1	Transforming growth factors -β 1
Th	T helper
TIR	C-terminal Toll /Interleukine-1 receptor
TIR	Toll-IL-1 receptor
TIRAP	TIR-domain–containing adaptor protein
TLRs	Toll- like receptors
TNF-α	Tumour necrosis factor alpha
TRAF6	TNF receptor-associated factor 6
TRIF	TIR-domain–containing adaptor protein-inducing IFNβ
UDP	Uridine Diphosphate
UDP-glucose	Uridine Diphosphate-glucose
UMP	Uridine Monophosphate
UTP	Uridine Triphosphate
WASP	Wiskott-Aldrich Syndrome Patients
WT	Wild type

Contents

Chapter one

Chapter two

Materials and Methods **38**

Chapter three

The role of MKP-2 deletion in MAPK mediated signalling in macrophages and neutrophils 71

Chapter four

Investigating the role of MKP-2 in macrophage phagocytosis, migration, proliferation and the metabolomics profile underlying each process 113

Chapter five

Chapter six

Chapter seven

List of Figures

Chapter one

Chapter two

Chapter three

Chapter four

List of Tables

Chapter One

General Introduction

1.1 Introduction to immune system

The human body encounters a wide variety of invaders such as viruses, bacteria, and other pathogens. Therefore, it establishes many mechanisms or responses to protect itself from these insults. Such responses that protect the body against the invader are called immune responses and are part of normal human physiology. Many organs and tissues are involved in the immune system, for example, bone marrow, spleen, thymus, and lymph nodes (Karp, 2013). These produce the immune cells that are required in immune responses. There are two types of immune responses: innate and adaptive.

1.1.1 Innate and adaptive immune responses

The innate and adaptive responses are activated sequentially but are interlinked at a number of different levels. Innate immune responses are the first line of defence against the invader. They recognise a wide range of pathogens through specific protein or peptide sequences expressed by the microbe known as pathogen-associated molecular patterns (PAMPs). This interaction does not require any other form of previous contact.

When a pathogen enters the body it comes into contact with the innate immune cells that are known as phagocytic cells: macrophages, dendritic cells and neutrophils which recognize the PAMPS on the invader via receptor proteins on their surface called pattern recognition receptors (PRRs). In this context, one of the most important class of pathogen receptor which has been identified are the Toll-like receptors (TLRs) which will be discussed later in this chapter (Akira and Takeda, 2004). Other significant innate responses that involve soluble proteins include the complement pathway which triggers pathogen/cell interactions and the release of pro-inflammatory agents and molecules that aid the destruction of the pathogen (Zhang *et al.*, 2007).

Other cell types participate in the innate immune response. Natural killer cells (NKs) also are a type of innate cell within the immune system that recognise virally infected cells and induces them to undergo apoptosis. In the case of virus infection, the innate response can be mediated indirectly by infected cells themselves via production of substances called interferons, which in turn activates the immune response within the local environment (Le Page *et al.*, 2000). This happens particularly in cases where the innate immune response cannot fully control the microbes (Gonzalez *et al.*, 2011). The same phagocytic and NK cells of the innate immune system are also responsible

in part for initiating the adaptive immune response (Janeway, 2001) by cytokine mediator production or via antigen presentation (APC) to recruit other non-innate immune cells.

The second arm of the immune system is the adaptive immune response. It is more specific when recognising antigens via antigen-specific receptors that are expressed on the surface of T and B- lymphocyte (Karp, 2013). The adaptive immune response is categorized into two types: humoral immunity which comprises antibodies (immunoglobulins) a family of high molecular weight proteins that bind specifically to the pathogen. Secondly, cell mediated immunity in which cells attack the invading pathogen. Both responses are mediated by lymphocytes, two types T and B cells have been identified in humans depending on their differentiation status: B-lymphocytes which differentiate in foetal liver or bone marrow in adult, here early B cells develop into mature B cells. After maturation, B cells leave the bone marrow and migrate either into the circulation to bind specific antigens in lymphoid tissue (as naïve B cells) or migrate to the secondary lymphoid tissue such as spleen and lymph nodes where they will be activated by antigens and form plasma cells which in turn form memory cells (which is dependent on the interaction with T helper cells). (Kurosaki, 2010). In contrast, T-lymphocytes which mediate cell immunity are differentiated in the thymus (Yang *et al.*, 2010).

Unlike the innate response, the adaptive immune response has a "memory" which allows a long lasting attack against pathogens (Karp, 2013). Memory T and B-cells can be reactivated when encountering a specific antigen for a second time due to their production of high affinity and heavy chain antibodies. Studies show that B cell activation may also be dependent on T cells via receptors such as CD40 or can be activated independently of T cells when responding to LPS via direct binding to the PRRs on the cell surface (Chaplin, 2010). Overall, both innate and adaptive immune responses work together to destroy a foreign invader.

1.1.2 Cellular components of the immune responses

The immune system involves many cell subsets that contribute to an immune response over different time frames and with a number of distinct and overlapping functions. These cells are found in the blood stream and called white blood cells (WBC) or leukocytes. Each cell has the ability to detect pathogens and they work together to mediate an immune response (Janeway, 2001). All leukocytes are generated in the bone marrow through a process called haematopoiesis. Haematopoietic stem cells (HSCs) differentiate when responding to internal or external signals for example local ATP release (Barbosa *et al.*, 2011), therefore, they differ in their shape, expression of markers and physiological functions. Haematopoiesis starts from HSCs which differentiate into two cell lineages; common myeloid progenitors (CMPs) and common lymphoid progenitors (CLPs), which in turn differentiate to other types of blood cells (Akashi *et al.*, 2000, Kondo, 2010).

Studies show that lymphoid progenitor cells differentiate further to T-lymphocytes, B-lymphocytes, NKs and NK-T cells (Chaplin, 2010). B-cells are considered the precursors of plasma cells which secrete antibodies. Both B and T-cells are defined by their receptor expression. For example, B cells are recognised by their cell surface receptor (BCR) expression including IgM and IgG (Treanor, 2012, Akashi *et al.*, 2000, Janeway, 2001). NKs are granular lymphocyte-like cells that can recognise cells which are infected with virus or tumour cells themselves via their activating or inhibitory surface receptor functions (Jonsson and Yokoyama, 2009, Orr and Lanier, 2010).

Myloid progenitor's lineages differentiate into other cell types: Megakaryocyte/Erythrocyte progenitors (MEPs) or Granulocyte/ Macrophage progenitors (GMPs) (Akashi *et al.*, 2000, Chaplin, 2010). MEPs in turn differentiate into only two end types, platelets and erythrocytes, whilst GMPs produce many cells: monocytes, mast cells, and granulocytes which include neutrophils, eosinophils and basophils. Mast cells continue their maturation in the tissues and the peripheral circulation, a study has shown that mast cell progenitors express C-X-C motif chemokine receptor 2 (CXCR2) upon differentiation (Hallgren and Gurish, 2011). Another publication indicates that mast cells also require stem cell factor (SCF) for maturation in the tissues, in the absence of SCF, no mast cell maturation was observed (Jamur and Oliver, 2011). Monocytes differentiate further to produce macrophages or dendritic cells (DCs), these antigen presenting cells (APC) are

considered to be the link between innate and adaptive immune responses (Fogg *et al.*, 2006). Furthermore, BM myeloid cells produce reactive oxygen species (ROS) that stimulate myeloid progenitor proliferation (Sugiyama and Nagasawa, 2015).

Another sub lineage that has recently been identified as a new subset of cells which share many characteristics with myeloid progenitors subsets of cells are called macrophage dendritic cell progenitors (MDPs) (Fogg *et al.*, 2006). MPDs give rise to monocytes and common DC precursors (CDPs) (Varol *et al.*, 2007). An illustration of the different lineages is shown in Figure 1.1.
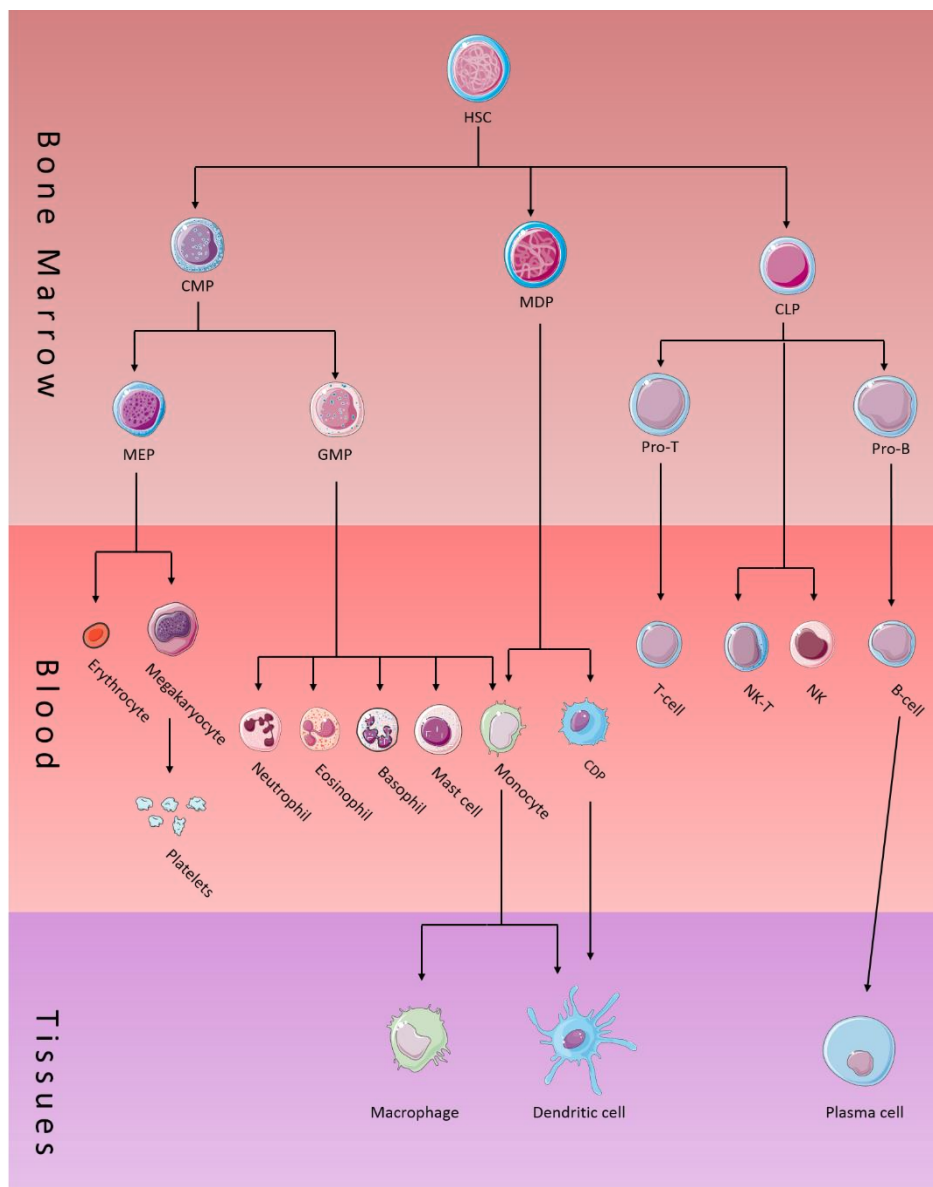
Figure 1. 1 Immune cell lineage

Hematopoietic stem cells (HSCs) differentiation in the bone marrow into common lymphoid progenitors (CLPs) and common myeloid progenitor cells (CMPs). CLPs differentiate to NK, NK-T cells, Pro-B and Pro-T cells which give B-cells and T-cells respectively. CMPs differentiate to Granulocyte/macrophage progenitors (GMPs) and megakaryocyte/erythrocyte progenitors (MEPs). GMPs give rise to monocytes that differentiate peripherally to different subsets of macrophages in different tissues and inflammatory DCs. GMPs also give rise to diverse types of granulocytes including mast cells, eosinophils, neutrophils and basophils. MEPs differentiate to erythrocytes and megakaryocytes which give rise to platelets. Different types of dendritic cells are derived from common DC precursors (CDPs), which are derived from HSCs in bone marrow.

1.1.3 Mononuclear phagocytes (MPs)

After formation of the cells in the bone marrow, three types of cells: monocytes, macrophages and DCs together form a system defined as the mononuclear phagocytic system that was first classified by Van Furth et al.(1979) and reviewed in a paper by Takahashi (2000).These cells responsible for antigen presentation, cytokine production and phagocytosis (Murray and Wynn, 2011). This population is identified by the cell surface expression of CD115, the receptor for macrophage colony stimulating factors CSF- 1R/M-CSFR (Auffray *et al.*, 2009, Van Furth *et al.*, 1972).

Monocytes are MPs that act as important immune effector cells which are derived from bone marrow. They are found in the circulation and localized in tissues as macrophages or DCs. Following infection, monocytes migrate from the blood to the infected tissues following stimulation of cell surface receptors by chemokines, such as chemokine monocyte chemoattractant protein-1 (MCP-1) and CCL2 which activate the monocyte chemokine receptors CCR2 and CXCR1 respectively. Recent studies have shown that deletion of these receptors hinder monocyte ability to migrate towards the atherosclerotic plaque (Geissmann *et al.*, 2010, Lawrence and Natoli, 2011, Gautier *et al.*, 2009). Monocytes are generated from the myeloid progenitor cells which differentiate to monoblasts, the latter in turn differentiate into pro-monocytes which gives rise to monocytes (Gordon and Taylor, 2005, Geissmann *et al.*, 2010).

Numerous studies have demonstrated a number of functions for monocytes and their subsets in human and mice. However, there are still some concerns about the mechanisms and cellular events underpinning these functions. Monocytes were first identified by expression of CD14 which is a part of the lipopolysaccharide (LPS) receptor complex and assumed to be homogeneous population. However, antigenic marker studies showed that monocytes are heterogeneous in peripheral blood (Gordon and Taylor, 2005, Ziegler-Heitbrock, 2015). They are therefore divided into different subsets regulating a diversity of physiological activities. Mice monocytes for example, have been identified by the expression of two markers: CD11b and F4/ 80.

Murine monocytes can be specified into two lineage, inflammatory and residential, depending on their expression of CC-chemokine receptor 2 (CCR2), myeloid marker lymphocyte antigen (LY-6C) and CXC-chemokine receptor,(CX3CR1) (Gordon and Taylor, 2005). Inflammatory monocytes express CCR2, CXCR1^{low} and GR1^{+} while

resident monocytes express CCR2^{-}, CX3CR1[HI]. Both can be found in equal percentages in the blood stream (Passlick *et al.*, 1989) but can vary under different conditions. For example, a study investigating changes in the monocyte receptors during infection with *Leishmania major*, demonstrated that prior to infection monocytes expressing CD11b^{+}, Ly6C[h], and CX3CR1^{+} can be found in large amounts in the blood but are rare in the skin, whilst after infection, monocytes with these markers are highly expressed on the infiltrating monocytes within the dermal site of the infection (Romano *et al.*, 2017). In this context, monocytes can be also classified depending on the differential expression of CD14 and CD16 into classical monocytes (CD14[Hi], CD16^{-}) and non-classical (CD14^{+}, CD16^{+}) which express higher amount of the major histocompatibility complex class 2 (MHC-II) and CD32, these cells have been shown to be similar to mature macrophages but depends on the cytokine regulation of MHC-II (Lee *et al.*, 2017).

Monocytes participate in the clearance of pathogens and cellular debris and toxic molecules by phagocytosis and via production of pro-inflammatory cytokines, nitric oxide (NO), reactive oxygen intermediate (ROI) (Serbina *et al.*, 2008) tumour necrosis factor alpha (TNF-α) and interleukin-1 (IL-1) (Auffray *et al.*, 2009). Meanwhile, these cells can contribute to chronic inflammatory diseases such as atherosclerosis and also have a crucial role in the development of autoimmune diseases (Ingersoll *et al.*, 2011). Overall, monocyte cells have two lineages: one stays resident in the spleen and remains there as a reservoir for macrophage production, whereas the major portion of monocytes circulate within the blood and migrate to different tissues to form either macrophages or DCs as reviewed by Swirski *et al.* (2014). Also, recent evidence found that macrophages can originate from embryonic origin and have a self-renewal ability via proliferation (Guilliams *et al.*, 2014, Swirski *et al.*, 2014).

Macrophages are another class of MPs and considered to be the major phagocytic cells that are distributed within all tissues and have a vital role in the innate immune response to pathogens as well as contributing in the adaptive immune response (Gordon and Taylor, 2005). The next section below describes in detail macrophages, their functions and activation modes.

DCs are a type of MPs that differentiate from monocytes. This cell type was first identified in early 1970s as a novel cell subset in mouse spleen (Steinman and Cohn, 1973). They have an important role in the immune system depending on their maturation status. Immature DCs function as phagocytic cells, once matured they

function to produce cytokines that activate other immune cells (Mellman and Steinman, 2001). Unlike macrophages, tissue DCs transfer to draining lymph nodes through afferent lymphatic vessels, stay for a few days where they mature and present antigens to T- lymphocytes and then finally die (Muller, 2001).

DC activation is initiated via PRRs detection of antigens (Dzopalic *et al.*, 2012). Once DCs are activated, they present antigens to T-cells by increasing their expression of MHC-II and co-stimulatory factors such as CD86, CD80 and CD40 (Boggiatto *et al.*, 2009) and this capability to stimulate naive T cells is a unique function for the DCs as APCs (Howard *et al.*, 2004). This means that although DCs are innate immune cells, they contribute to the adaptive immune response via presenting antigen to T-lymphocytes. In conclusion MPs play a pivotal role in both innate and adaptive immune response. Thus reviewing their function will help to give an insight to the mechanisms and pathways involved in relation to MKP-2 deletion.

1.1.4 Macrophages

Macrophages are major phagocytic cells that differentiate from monocytes in the CMP lineage of haematopoiesis. They are found in blood circulation and migrate to differentiate within the tissues to perform different functions which form a wide variety of macrophages characteristics (Van Furth *et al.*, 1972). These functions vary from maintaining tissue homeostasis to playing a vital role in immune responses upon infection and also during inflammation (Gordon and Taylor, 2005). Recently, another origin has been established for tissue resident macrophages, which is embryonic, which allows these macrophages to proliferate without loss of their differentiation markers (Gentek *et al.*, 2014, Jenkins *et al.*, 2011).

Macrophages can be found in different tissues and often their names differ from one tissue to another. For example, they are known as osteoclasts when found in the bone marrow, microglia in the central nervous system, histiocytes in the connective tissue, Kupffer cells in the liver. They can also found in alveoli, gastrointestinal fluid, spleen and peritoneum (Janeway, 2001, Kumar and Jack, 2006). These different locations allow them to be involved in many important functions across the whole of the body.

Different functions have been identified for macrophages due to their heterogeneity. Mature tissue macrophages for example, perform a significant immune surveillance function. Also, they remove dead and necrotic cells and toxic molecules in order to

maintain tissue health. One example is alveolar macrophages that remove allergens from the lung (Murray and Wynn, 2011). Furthermore, macrophages can engulf foreign molecules or pathogens through the process of phagocytosis which will be described in more detail later in this chapter. This phagocytic activity of macrophages is selective for foreign material (and tumour cells) which means they do not phagocytise normal body cells. Tissue macrophages also supress inflammation mediated by inflammatory monocytes confirming a key role in tissue homeostasis after infection or injury (Epelman *et al.*, 2014). Macrophages also have different PRRs that can recognise signals associated with pathogens during and following phagocytosis. Those receptors include; TLRs, C-type lectin receptor (CLRs), scavenger receptors, retinoic acid-inducible gen1 (RIG1)-like helicase receptors (RLRs), NOD-like receptors (NLRs) and the mannose receptor and macrophage receptors. Of these PRRs the mannose receptor (also known as MR/CD206) is of significance. It is a highly conserved calcium-dependent multi-lectin and a pattern recognition receptor that doesn't require the particle to be opsonised prior to phagocytosis and is also the endocytic receptor for glycan as reviewed in Dangaj *et al.* (2011). Macrophages also express complement and FC receptors that activate the complement cascade (Murray and Wynn, 2011, Dangaj *et al.*, 2011). Signalling via PRRs such as TLRs, NLRs and RLRs activate transcriptional mechanisms that lead to phagocytosis, cellular activation, and also cytokine, chemokine and growth factor production (for further details see section 1.1.6).

Macrophages show a noticeable degree of plasticity depending on stimulation within the micro-environment (Qian and Pollard, 2010). Thus, according to the external stimuli macrophage activation can be classified into four types: innately activated macrophages (IAMs), classically activated macrophages (CAMs), alternatively activated macrophages (AAMs) and regulatory macrophages (Figure 1.2) (Gordon and Taylor, 2005, Martinez and Gordon, 2014). Each type will be described in detail in the next section.

1.1.5 Macrophage activation types

1.1.5.1 Innate activation

When macrophages face microbial stimuli such as LPS, they respond immediately and are activated via TLRs expressed on their surface and form an inflammatory phenotype termed innate activated macrophages (IAMs). Thus, these macrophages produce NO, ROS, inflammatory cytokines and mediators such as TNF-α, IL-6 and

IL-12 (Rodriguez-Prados *et al.*, 2010). Furthermore, IAMs maintain their phagocytic activity after eradicating the pathogen and the dying cells are cleared via the scavenger receptor, this prevents the activation from being prolonged and controlling their activity. However, macrophages cannot fully control the pathogens independently especially in chronic inflammation. Therefore, as mentioned previously this requires the activation of the adaptive immune response including T-helper (Th) lymphocytes which differentiate in response APCs into Th1 and Th2 to promote either classical or alternative macrophage activation (Yan and Hansson, 2007).

1.1.5.2 Classical activation

Classically activated macrophage (CAM) or type 1 macrophage (M1) can be defined as macrophages that are stimulated by interferon γ (IFN-γ) and TNF-α or LPS. IFNγ is released by many other immune cells such as Th1, NK cells and B cells which activate this phenotype of macrophage which is associated with increasing microbicidal activity and antigen-presenting function. In mice, M1 macrophages associated readouts are IL-12, IL-6, IL-1, IL-23, MHC-II and nitric oxide synthase 2 (NOS2), whereas in human M1 has no NOS2 (Mosser and Edwards, 2008). LPS is a component of gram-negative bacteria that triggers different inflammatory mediators in macrophages, DCs and neutrophils (Meng and Lowell, 1997). LPS mediated macrophage activation is characterised by the production of the pro-inflammatory cytokines, TNFα and IL-6, and ROS including NO and super oxide which is important in killing pathogens (Martinez and Gordon, 2014). Macrophages release these cytokines and chemokines to direct other immune cells to the site of infection.

It is well established that the receptor for LPS is TLR4 which couples external pathogenic signal to multiple intracellular signalling pathways that drives macrophages towards the functional outputs above (Palsson-Mcdermott and O'neill, 2004). This is discussed in more detail in section 1.1.6.1 (Roux and Blenis, 2004, Salojin, 2006).

1.1.5.3 Alternative activation

Alternatively activated macrophages, AAMs, are also known as type 2 macrophages, M2. They are associated with parasitic infections and Th2 responses. Their activation is mediated by IL-4 and IL-13 stimulation (Stein *et al.*, 1992). They are identified by their surface markers such as resistin-like-α (also known as FIZZL), arginase-1, chitinase 3-like3 (YMI), IL-10 and the macrophage mannose receptor 1(CD206 or MRC1) which are associated with an inhibition of inflammation and the promotion of wound healing (Murray and Wynn, 2011). Indeed M2 macrophages work as anti-inflammatory and homeostatic agents in wound healing, fibrosis and tissue repair. Furthermore, they produce growth factors that stimulate epithelial cells and fibroblasts including transforming growth factors -β 1(TGFβ1), and they also act as APCs (Lawrence and Natoli, 2011). Another characteristic feature of this phenotype is their unique function to produce arginase-1 which converts ornithine to polyamines and collagen, both are important in wound healing and cell proliferation (Varin and Gordon, 2009).

1.1.5.4 Regulatory macrophages

This phenotype of macrophage was first identified in a study which used a combination of two stimuli such as a TLR ligand plus an immune complex, resulting in macrophages that produce high level of the anti-inflammatory cytokine IL-10 (Sutterwala *et al.*, 1998). This co-stimulation idea has revealed many other inducers for this type of macrophage activation such as adenosine, cAMP, TGF-β, prostaglandin E$_2$, apoptotic cells and IL-10 itself (Gratchev *et al.*, 2008, Peters-Golden, 2009). All these inducers, share the common characteristic of being relatively inefficient at inducing cytokine production from macrophages on their own but in co stimulation with TLR4 they all provide IL-10 to form a regulatory macrophage phenotype. The function of this type of macrophage is to modulate inflammatory immune responses thus limiting tissue damage as a result preventing the immunopathology that is associated with prolonged CAMs and terminating the inflammation (Fleming and Mosser, 2011). Regulatory macrophages have antigen presenting functions and express CD80 and CD86 co-stimulatory molecules (Edwards *et al.*, 2006). Also they are generated as an immune response to some parasites, bacteria and viruses (Mosser and Edwards, 2008).
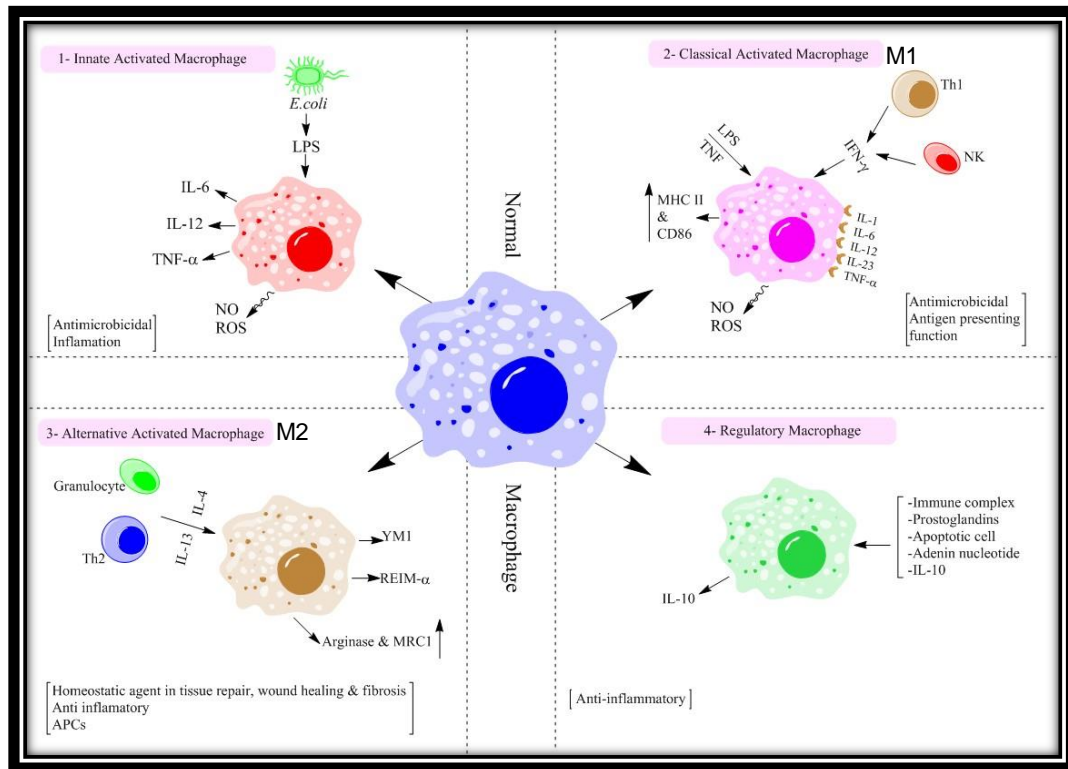
Figure 1. 2 Macrophage activation phenotypes

The microbial product LPS activates macrophages to generate an innate phenotype. This produces TNFα and cytokines which simultaneously works with IFN-γ that is produced by Th1 and NKs and produce classical activation of macrophages. Th2 and granulocytes produce 1L-4 and IL-13 which activate macrophages alternatively. Immune complexes produces regulatory activated macrophage phenotype.

1.1.6 Macrophage functions

1.1.6.1 Pathogen recognition

Macrophages and other immune cells share their ability to recognize a wide variety of pathogens due to their expression of pattern recognition receptors (PRRs) as reviewed in (Takeuchi and Akira, 2010). They are specialised to recognise pathogen associated molecular pattern (PAMPs) which is used by pathogens to survive. These include LPS, beta-glucan, flagellin, peptidoglycan and mannose. According to their functions PRRs are classified into three types: signalling, endocytic and secreted (Janeway, 2001). Both endocytic and signalling receptors are expressed on the surface of macrophages, in the cytoplasm and in the endocytic compartment (Arce *et al.*, 2004, Ivashkiv, 2011), whilst secreted PRRs are used to facilitate the interaction between the pathogen and cell surface receptors.

Endocytic PRRs contribute in recognising and engulfing microbes. Dectin-1, Dectein-2, mannose receptors (MR) and the complement receptor 3, CR3 (also called CD11b/CD18, macrophage receptor-1) all are called C-type lectin receptors (CLRs) and mostly contribute to anti-fungal activity and trigger pro-inflammatory responses such as phagocytosis, oxidative stress and cytokine production (Hardison and Brown, 2012) and reviewed in (Goyal *et al.*, 2018). Dectin-1 and dectin-2 are transmembrane proteins of the CLRs which recognise fungal beta glucan and mannocyl receptors via their single carbohydrate recognition domain (CRD) in their extracellular region (Rizzetto *et al.*, 2013). Dectin-1 couples to intracellular signalling molecules via its immunoreceptor tyrosine based motif (ITAM) located within the cytoplasmic tail whereas Dectin-2 associates with an adaptor, the ITAM containing FC receptor common chain (FcRγ) (Sato *et al.*, 2006). The signalling pathway(s) activated downstream of these receptors leads to the main macrophage functions such as phagocytosis, cytokine production and ROS production, and includes the spleen tyrosine kinase family (Syk) and Src family kinases (Sato *et al.*, 2006). Also it was found recently that FcRγ receptors, via activation of these pathways, play an important role in viral infection via suppression of interferon production from myeloid immune cells, adding another important function of macrophages (Newling *et al.*, 2018).

Other CLRs such as MR also activate macrophages to produce ROS, IL-1, IL-6 and TNF-α (Taylor *et al.*, 2005). Another endocytic receptor is CR3, it consists of integrin subunits β2 (CD18) and CD11b and additionally functions as both an adhesion receptor and a receptor for the secreted PRRs. These endocytic receptors function

via direct recognition by PAMPs such as LPS and β-glucan on the surface of the bacteria or fungi, respectively (Thompson *et al.*, 2011). Receptor recognition of these PAMPs by CR3 has been shown to trigger phagocytosis, nitric oxide (NO) and superoxide production in phagocytes (Matsuno *et al.*, 1998).

Signalling PRRs induce cell activation responses such as gene transcription and cytokine secretion. TLRs represents the prototypical family of signalling PRRs (Janeway, 2001). TLRs are type-I transmembrane receptors with N-terminal leucine-rich repeats and a C-terminal Toll /Interleukin-1 receptor (TIR) domain. So far there are 13 TLRs which have been identified in mice and human and they differ in ligand specification, cellular expression and subcellular localization. They recognise PAMPs and induce signalling by either homo or hetero-dimerization and the association with other receptors or adaptor proteins. This is illustrated in figure 1.3.

The most recognised TLR is TLR4 as the first identified PRR via their interaction with the cytoplasmic drosophila Toll-IL-1 receptor (TIR) domain. This domain and the equivalent domain within the IL-1 receptor, which also signals in the same way, allows the interaction with several proteins which mediate activation of downstream signalling pathways (Doyle and O'neill, 2006). Receptor engagement results in dimerization that initiates multiple downstream signalling pathways (Medzhitov *et al.*, 1997). TLR2 and TLR6 are heterodimers, they can recognise different PAMPs such as diacylated lipopeptids of gram-positive bacteria and yeast derived particles such as zymosan (Ozinsky *et al.*, 2000). Once they recognize their ligands, TLRs mediate the production of inflammatory cytokines, chemokines, MHCs and antimicrobial molecules on the surface of antigen presenting cells (Medzhitov *et al.*, 1997). TLRs coupling to cellular responses is accomplished via two signalling pathways defined as myeloid differentiation factor 88 (MyD88) dependent and MyD88-independent (Akira and Takeda, 2004).

In the MyD88-dependent pathway, MyD88 interacts with the IL-1 receptor (IL-1R) or TLRs to form a protein/protein complex between IL-1R-associated kinase (IRAK) and TNF receptor associated factor 6 (TRAF6), (Deguine and Barton, 2014) which in turn promotes a series of proteins / protein interactions which results in the activation of NEMO (a complex of TRAF6 and NFκB essential modifier) also known as IκB kinase γ (IKKγ). These are polyubiquinated by E3 ubiquitin ligase which forms a complex with E2 ubiquitin-conjugating enzymes. Ubiquinated TRAF6 in turn induces transforming growth factor-β-activated kinase1 (TAK1) and TAK1-binding proteins

(TABs) such as TAB1, TAB2, and TAB3 to form a complex (Adhikari *et al.,* 2007). This complex undergoes further interactions which results in the phosphorylation of IKKs. The IKKs in turn activate NF-κB through IκBα phosphorylation, ubiquitination and degradation by the cellular proteasome (Takeda and Akira, 2004). As a result, NFκB translocates into the nucleus and binds a specific DNA sequences called response element (RE). This process leads to expression of pro-inflammatory cytokine genes and adhesion molecules (Arancibia *et al.,* 2007).

The MyD88-dependent pathway is also responsible for activation of mitogen-activated protein (MAP) kinases. TAK1 activates two members of the MAP kinase kinase family, MKK3 and MKK6 which drives activation of c-Jun-N terminal kinase (JNK) and p38MAPK, respectively. This further leads to ATF2 activation and induction of activation protein-1 (AP-1) (Adhikari *et al.,* 2007). TLR4 more than other TLRs has a unique ability to signal via both the MyD88 dependent pathway to induce pro-inflammatory cytokines through NFκB, and the MYD88-independent pathway through TRIF to induce type 1 IFN via IRF3 (Yamamoto *et al.,* 2003). For further details see Figure 1.3.
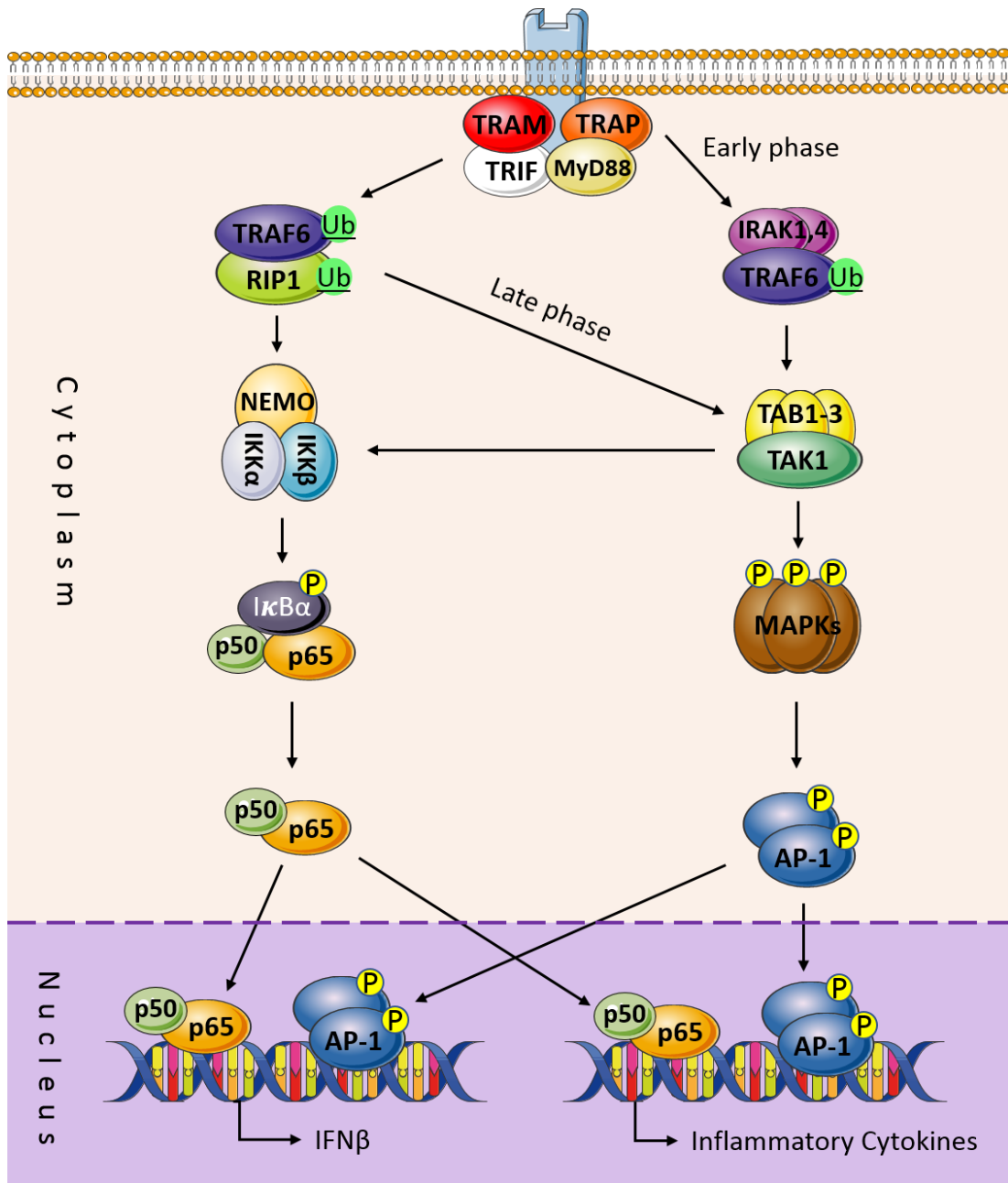
Figure 1. 3 TLRs signalling in MyD88 dependent and independent pathway

TLR4 activates both MyD88 dependent and independent (TRIF-dependent) signalling. MyD88 and TLR4 activate IRAK family, which helps TRAF6 activation. TRAF6 with E3 ligase activate TAK1 which in turn either activates MAPKs or the IKK complex. MAPKs then are activated and phosphorylates AP-1. Activated AP-1 translocates into the nucleus. TAK1, also activates the IKK complex. IKKα, IKKβ and NEMO induce IκB phosphorylation (p), ubiquitination and then degradation leading to NF-κβ which alongside with AP-1 induce inflammatory cytokine production.

1.1.6.2 Macrophage phagocytosis

One of the most important functions of macrophages is their ability to internalize solid particles larger than 0.5µm. These could be apoptotic cells, cell debris or invading pathogens that are recognized by different receptors, thus maintaining homeostasis and clearing the body from harmful agents (Underhill and Goodridge, 2012, Aderem and Underhill, 1999). This process is the key initiator for the adaptive immune response, because macrophage phagocytosed particles or antigens will be presented to the cells of adaptive immune system, thus coordinating a network of immune responses. Due to the varieties of pathogens and particles, macrophages have developed and adapted themselves by expressing relative cell surface receptors that can recognize and phagocytose these agents. These receptors include the complement receptor, mannose receptor and Fcγ receptors (Guzman-Beltran *et al.*, 2012, Zhang *et al.*, 2010).

1.1.6.3 Signalling pathways during phagocytosis

Many pathogens cannot be internalized directly, therefore the immune system response is to enable the coating of these microbes with serum opsonins such as IgG antibodies (Mosser and Zhang, 2011). The cell surface receptor that recognises the IgG-opsonized pathogen is the Fcγ receptor (FcgRs) which binds to the FC region of IgG antibody (Aderem and Underhill, 1999). This binding of pathogen and receptor is followed by a sequence of events that induces actin cytoskeleton rearrangements, phagocytic cup formation and internalization of opsonized particles, illustrated in Figure 1.4 (Niedergang and Chavrier, 2005, Mao and Finnemann, 2015).

Studies of phagocytosis indicate the FC gamma receptor as the main receptor that can couple to signalling pathways that mediate phagocytosis of pathogens. The FcgR is classified into two: firstly, the FcgR1 (CD64) which is high affinity and FcgRIIA which is low affinity, both have immunoreceptor tyrosine-based activation motif (ITAMs) in their intracellular domain. The ITAM recruits tyrosine kinases and activates tyrosine phosphorylation regulated cascades, such as Src kinase (Bezbradica *et al.*, 2014). This type is dependent on expression of accessory γ chain that carries an ITAM; studies demonstrated that deletion of this receptor subunit lead to the functional loss that is activated by Fcγ receptors (Ravetch, 1997).

The second type is FcgRIIB (CD32), an inhibitory receptor that consists of a similar immunoreceptor ITAM based structure. However this coupling, induce phosphatases

such as protein tyrosine phosphatase, SHP-1 and inositol kinase phosphatase SHP-1 both of which inhibit signalling and thus phagocytosis (Fanger *et al.*, 1996, Hart *et al.*, 2004). In a mouse model, deletion of FcgRIIb has been to found to enhance phagocytosis of IgG-opsonised particles compared wild-type counterparts (Clynes *et al.*, 1999) thus confirming the inhibitory effect on phagocytosis.

After IgG coated particles bind to the FcgRs and ITAM phosphorylation takes place intermediates of the focal adhesion kinase family (FAK) or Src are activated which in turn further mediates phosphorylation of Syk. Syk promotes the increase in activity of Rho guanosine exchange factors or VAV and others GTPases such as RAC, molecules well recognised to play key role in cytoskeleton reorganisation. Further RAC mediated kinase activation leads to lamillipodia formation (Swanson and Hoppe, 2004, Tohyama and Yamamura, 2009, Kurokawa *et al.*, 2004). The second pathway initiated from initial ITAM and Src activation involves Cdc42 phosphorylation of WASP (Wiskott-Aldrich Syndrom Patients) which is the key activator of actin polymerization. F-actin formation is important for phagocytic cup formation, as demonstrated by pharmacological studies (Lamprou *et al.*, 2007, Crowley *et al.*, 1997). The final target for activated WASP is the filopodial extensions in the cell periphery (Rougerie *et al.*, 2013).

Actin polymerization is one of the key regulators of FcgRs mediated phagocytosis. The Rho family of GTPases, a member of the RAS superfamily, functions to regulate actin cytoskeleton and thus phagocytosis (Hall, 1998). Three members of the GTPase family, RhoA, RAC1 and Cdc42 control stress fibres and focal adhesion assembly. RAC1 regulates the formation of lamillipodia protrusions and membrane raffles while Cdc42 triggers filopodial extension at the cell periphery. Both RAC1 and Cdc42 activation are required for particle internalization. Also RAC1 mediated formation of lamellipodia and filopodia is essential for cell motility, phagocytosis and the development of substrate adhesion (Parri and Chiarugi, 2010).

Actin filaments were first identified as the key driver of motility at the leading edge, the lamellipodia push upward protrusions to form ruffles (Szent-Gyorgyi, 2004, Small *et al.*, 2002). Lamillipodia is the primary site of actin incorporation and the major filament of the cells that serves in phagocytosis. Filopodia are thin cell extensions consisting of tight bundles of long actin filament covered with cell membrane that work in parallel with lamillipodia in directing cell motility and phagocytosis. Overall this

tightly regulated mechanism ensures that the macrophage can migrate efficiently through tissues to the site of injury or infection. (See Figure 1.4 for further illustration).
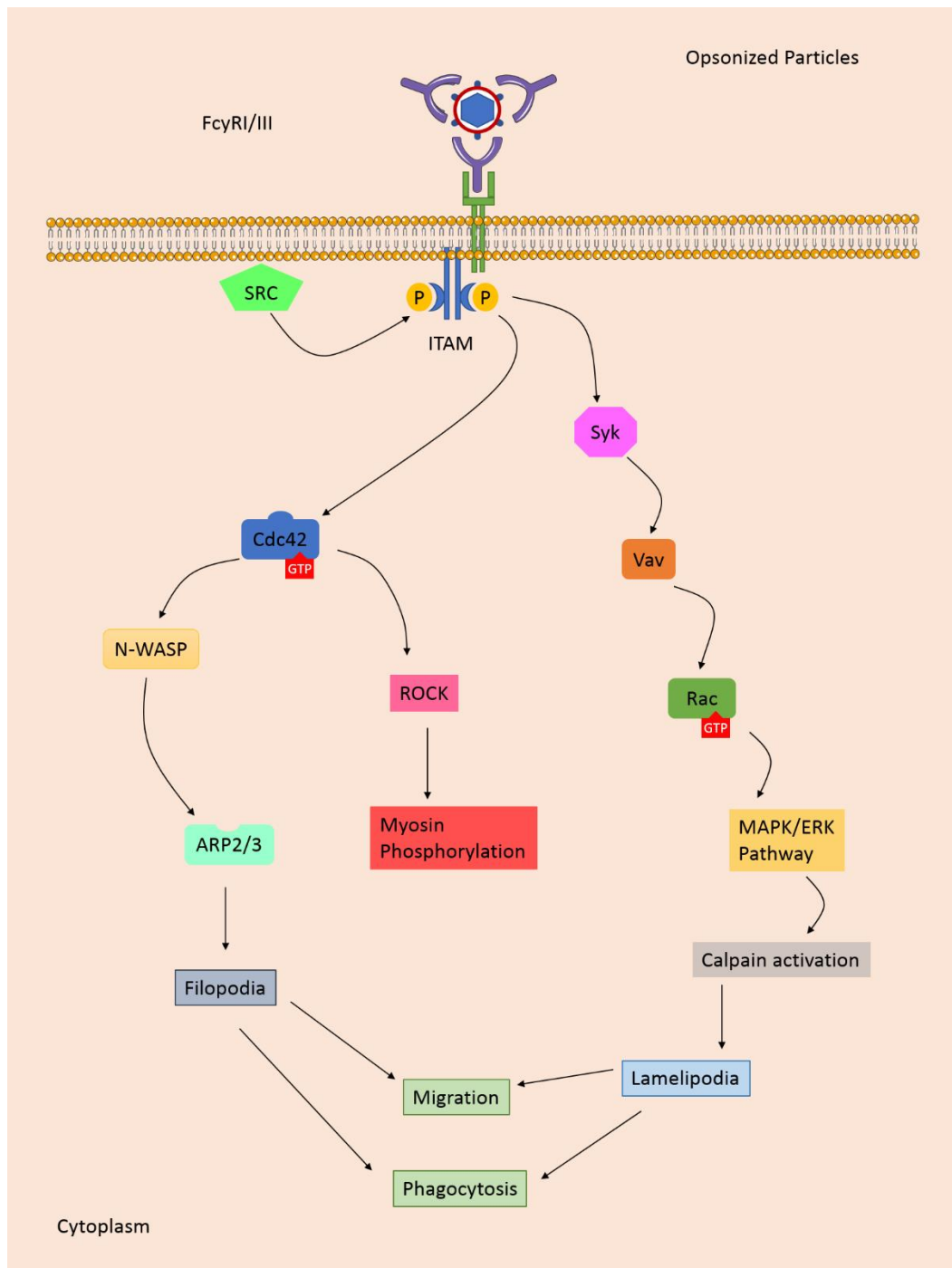
Figure 1. 4 Signalling pathways in phagocytosis and migration

Opsonised pathogen binds to FcgR which crosslinks leading to SRC mediated phosphorylation of ITAM motifs. SYK leads to VAV activation (a GTP/GDP exchange factor). VAV activates RAC/MAPK leading to lamilipodia formation. While, Cdc42 activation further activate WASP and ARP2/3 leading to filopodia formation or it activates ROCK which in turn activate myosin phosphorylation. Both lamilipodia and filopodia play an essential role in cell migration and phagocytosis.

1.1.7 Macrophage migration

In order for macrophages to perform immune functions, they have to migrate first to the site of infection or injury. Once they reach these locations, they engage in phagocytosis and present antigens and cytokines to other immune cells, thus activating the adaptive immune response. Inappropriate macrophage migration has been linked to several autoimmune diseases such as rheumatoid arthritis (Kinne *et al.*, 2000). Also macrophages migrate to and become one of the primary components of atherosclerotic plaques and contribute to cardiovascular disease (Bobryshev *et al.*, 2016). Migration is promoted in response to chemokine and cytokine gradients produced by pathogens or other immune cells in the inflamed tissues (Goerdt and Orfanos, 1999). One such example observed in rheumatoid arthritis (RA), is that synovial fibroblasts over produce CSF-1, this recruits more monocytes from the circulation resulting in more differentiation to macrophages in the joint thus worsen the inflammation (Kinne *et al.*, 2000, Ma and Pope, 2005). Also macrophages produce many pro-inflammatory cytokines which contribute to cartilage and bone destruction. One example is macrophage inhibitory factor (MIF), which has been shown to regulate other cytokines such TNFα, IL-1β and IL-6 in RA. MIF deleted macrophages show lower pro-inflammatory cytokine production in response endotoxins such as LPS resulting in reduced lethality *in vivo* (Bozza *et al.*, 1999, Roger *et al.*, 2001).

Macrophages undergo migration via activation of many signal transduction pathways that govern cell motility. The leading edge of migrating cells is generated by assembly of new actin filament which is regulated by Arp2/3 induced by WASP to promote the nucleation of new actin filament. The upstream kinase pathways involved are illustrated in Figure 1.3 and overlap with those regulating phagocytosis in many instances but can also be distinct depending on the stimulus. The multiple kinase pathways involved are not expanded here but the reader is referred to a number of excellent reviews (Jones, 2000, Pixley, 2012).

1.1.8 Neutrophil/macrophage interactions

Neutrophils are the other key innate immune cells that share with macrophages being the first line of defence against pathogens. Neutrophils have a very short life between 8 to 9 hours. They are the most abundant leukocytes found in the blood. They are generated in bone marrow during haematopoiesis from GMP as shown in Figure 1.1. After their production and storage in the bone marrow they transmigrate through the

sinusoidal endothelium to the circulation (Kruger *et al.*, 2015). The release of neutrophils to the circulation is regulated by chemokines and their receptors such as the stromal derived factor 1 (SDF-1) which is produced in the bone marrow and engages CXCR4 and 7. The interaction of the SDF-1 with CXCR4 leads the release of neutrophils to the circulation while its interaction with CXCR7 keeps neutrophils in the mitotic pool in bone marrow (Burdon *et al.*, 2008, Petit *et al.*, 2007).

Upon infection, neutrophils migrate quicker than macrophages to the site of infection, phagocytose the pathogen and undergo apoptosis by the time macrophages reach the location. Apoptotic neutrophils release an "eat me" signal component such as phosphatidylserine which is a lipid found normally in the inner side of plasma membrane but is exposed to the outer side of the membrane in apoptotic cells. This signals to macrophages to phagocytose apoptotic neutrophils to prevent tissue damage, present antigen to T-helper cells and release anti-inflammatory cytokines thus completing a successful immune response (Koh and Dipietro, 2011, Wang, 2018). Again this whole process is regulated by signalling pathways such as MAPK, well recognised to play key roles in neutrophil function (Huang *et al.*, 2004, Kim and Haynes, 2013, Liu *et al.*, 2012, Lue *et al.*, 2006). These kinases and their role in immune cell function is detailed in the next section.

1.2 Mitogen Activated Protein Kinase family

Mitogen activated protein kinases (MAPKs) is a family of serine/threonine directed enzymes recognized for their regulatory role in different physiological processes such as cell proliferation, differentiation, development, immune and stress responses and cell death (Chang and Karin, 2001, Roux and Blenis, 2004). In mammals, three main MAPKs have been identified and classified depending on structural similarity, differential activation by stimulus and substrate specificity (Enslen *et al.*, 2000). The groups and their variants are the extracellular signal-regulated kinases (ERKs 1 &2) also known as classical MAPKs, and the stress-activated protein kinases including the c-jun n-terminal kinases (JNK1, 2, 3) and the p38 MAP kinases α, β, γ and δ (Pimienta and Pascual, 2007).

All MAPKs contain of a consensus activation sequence TXY in which T refers to threonine, while Y refers to tyrosine. In this context all MAPKS share these two residues. However, they differ from each other in the X residue, being glutamine in ERK, proline in JNK and glycine in p38 (Johnson and Lapadat, 2002). These MAPKs can be activated by a vast assay of external stimuli, such as growth factors,

environmental stresses, phorbol esters, serum, and cytokines (Zhou and Zhang, 2002, Katz *et al.*, 2007). Activation of each kinase subgroup requires dual phosphorylation within the TXY motif by MAPK kinases (MAPKKs) which are activated by MAPK kinase kinases (MAPKKKs) (Marshall, 1994). In mammals 14 different MAPKKKs, seven MAPKKs and 13 MAPKs have been identified. Nevertheless, specificity within the MAPK pathway can be achieved by spatial localization through scaffolding proteins which orientate intermediates of the specific pathway to form a complex, whilst at the same time preventing one protein specific to one pathway from simultaneously engaging in another pathway at the same time (Garrington and Johnson, 1999)

The signalling cascade is coupled to a variety of receptors via a series of upstream intermediates including, kinases, small molecular weight G-proteins and structural connecting proteins (Naor *et al.*, 2000, Fukuyama *et al.*, 2000), some of which have been identified above in the context of macrophage activation (see Figure 1.5). Furthermore, the MAPKs translocate into the nucleus to regulate a number of transcription factors to regulate the expression of a given target genes such as ELK1, c-Jun, ATF2, and CREB (Turjanski *et al.*, 2007) or in several instances are retained within the cytosol where they phosphorylate a number of cytosolic targets such as MAPKAP Kinase-2/3 (Stokoe *et al.*, 1992).
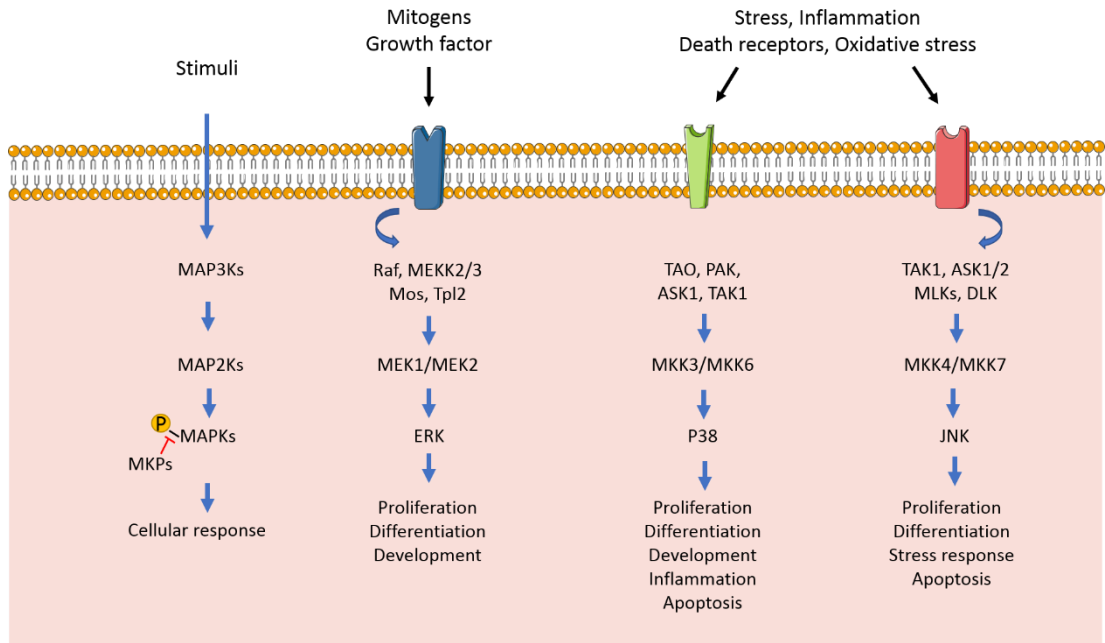
Figure 1. 5 MAPK pathways (Adapted from Morrison, 2012)

Mitogen and growth factors activates Raf mediated MEK1/2 activation which leads to ERK activation leading to cell proliferation or differentiation. Whilst, stress and death receptors mediates TAK1 (transforming factor β-activated kinase 1) which either activate p38 phosphorylation through MKK3/MKK6 or JNK phosphorylation via MKK4/MKK7 activation leading to cellular responses such as proliferation, inflammation and apoptosis.

1.2.1 Extracellular signal-regulated kinase (ERK) family

The ERK family is considered to be the most intensely studied kinase family to date, originally identified by Ray and Sturgill in 1984 investigating the cellular actions of insulin (Sturgill and Ray, 1986). ERK is expressed as many isoforms including ERKs1-5 and ERKs 7/8 depending on their molecular weight and substrate specificity (Roux and Blenis, 2004). Originally characterised as a 43 kDa mitogen-activated protein kinase (MAPK) it is now known as ERK-1 due to the wide variety of extracellular signals that can activate it. The ERK-2 isoform, usually activated simultaneously to ERK-1 is slightly smaller being a 41 kDa protein and has 83% amino acid identity with ERK-1 (Avruch, 2007). As indicated above, in mammals ERKs 1&2 are recognised components of the classical mitogen-activated cascade that consists of Ras/Raf/MEK/ERK. Thus, many studies have demonstrated the involvement of ERK in the control of cell proliferation (Chambard *et al.*, 2007) and inhibitors of the ERK pathway have potential as anticancer agents.

Many receptors couple to ERK1&2 activation including; G-protein coupled receptors (GPCRs), receptor tyrosine kinase receptors (RTKs) and integrins. As indicated above activation is through dual phosphorylation on threonine 183 and tyrosine 185 residues with the TGY motif. The MAPKKs for the classic ERK1/2 module are MEK1 and MEK2, while the MAPKKKs involve members of the Raf family (Mos and Tpl2) (Morrison, 2012). Once ERK1 and ERK2 are activated they in turn phosphorylate a wide range of nuclear substrates including NF-AT, Elk-1, c-fos and STAT 3. ERK also phosphorylates plasma membrane proteins such as CD120, calnexin and Syk and several cytoskeletal proteins for example neurofilaments and paxillin (Aouadi *et al.*, 2006). These interactions result in the regulation of a number of important cellular outcomes such as proliferation, migration and phagocytosis. For example, blockage of PI3K-dependant ERK activation promotes cytotoxicity in NKs (Jiang *et al.*, 2002), whilst ERK regulates paxillin signalling, switching the interaction between FAK-Paxillin which is required for cells to migrate (Huang *et al.*, 2004).

A number of molecular approaches including expression of dominant negative mutants, antisense and siRNA have been used to identify the role of ERK in cellular function. This has been further aided by the development of compounds such as UO126 and PD98059, both MEK1 inhibitors, which have been used widely to demonstrate a role for ERKs in cellular events such as differentiation and proliferation (Dudley *et al.*, 1995, Favata *et al.*, 1998). However, these chemicals act on both

ERK1&2 and cannot differentiate between these two isoforms. Other approaches including the use of isoform specific knockout mice have enabled the role of ERK to be identified both *in vitro* and *in vivo*. For instance, ERK1/2[-/-] mice have reduced thymocyte maturation compared to wild type controls (Pages *et al.*, 1999) whilst another study has shown that ERK1 deficiency decreases adiposity and adipose differentiation (Aouadi *et al.*, 2006). These and other studies suggest a significant role for ERK in different functions in different cells.

1.2.2 C-Jun amino- terminal Kinases (JNK)

This family of MAPKs is also known as stress-activated protein kinases having been initially identified in mice treated with actinomycin (Avruch, 2007). Three members of this family are JNK1, 2 and JNK3 also known as SAPKγ, SAPKα and SAPKβ respectively, which differs from each other in their localisation and tissue distribution, with a total of 10 or more spliced forms. Molecular weights vary between 46 kDa and 55 kDa. These kinases, as their name suggests are strongly activated in cells in response to cellular stresses including; UV irradiation, increased osmolality, cytokines, growth factor deprivation and agents which interfere with DNA and protein synthesis. Furthermore, JNK is activated to some extent by serum, ligands for some GPCRs and growth factors. This activation of SAPKs is through phosphorylation of both Thr and Tyr residues in the TPY motif (Morrison, 2012). Activated JNKs translocate to the nucleus and activate associated transcription factors such as c-Jun, Jun A, ATF2, Elk1, STAT-3 and p53 (Gupta *et al.*, 1996).

JNKs are involved in many physiological activities in cells such as cytokine production, adhesion molecule expression and apoptosis (see below). Similar approaches to studies of the ERK pathway, including the use of isoform selective knockout mice, have revealed roles for JNK 1 and 2 in a number of outcomes. In the central nervous system for example, studies found that JNK1 acts to maintain basic physiological activity while JNK2 functions in long term potentiation (Sahara *et al.*, 2008, Okazawa and Estus, 2002, Yang *et al.*, 1997). In contrast, the expression of JNK3 is restricted primarily to brain where it has an active role in neuronal apoptosis resulting in compromised hippocampal function (Yang *et al.*, 1997). Many other groups have revealed roles for JNKs in many human conditions such as chronic inflammation, birth defects, cancer and ischemia/reperfusion injury (Johnson and Nakamura, 2007, Biteau *et al.*, 2008).

1.2.3 p38 MAP Kinase

This MAPK was first identified as 38 kDa protein and has four isoforms (α, β, γ and δ) (Enslen *et al.*, 2000). The α and β isoforms are found in many cells, whilst γ and δ isoforms are far less widespread. Like ERK and JNK, p38 family members are activated through phosphorylation of both threonine and tyrosine residues however this is via the The-Gly-Tyr motif within the activation loop. All p38 isoforms are activated as part of the classical three tiered cascade involving the MAPKKs, MAPKK3 and MAPKK6 and MEKKs (Keesler *et al.*, 1998). As with JNK, the activation of p38 is very marked in response to UV irradiation, osmotic pressure and temperature stress, cytokines such as TNF-α and growth factors such as CSF-1. However, a number of G-protein coupled receptors have also been shown to strongly activate this cascade (Yamauchi *et al.*, 1997, Grimsey *et al.*, 2015). Unsurprisingly, p38 is involved in apoptosis, the cell cycle, and the expression of inflammatory genes and cytokines (Zarubin and Han, 2005). Establishing a role for p38 in adult physiology has proved difficult, deletion of the p38 gene in mice leads to death during embryogenesis and is required for the formation of organs in the placental stages (Wakeman *et al.*, 2012). However, as with ERK, defining the roles of p38 MAPK in cellular function has been aided by the development of a series of inhibitors such as SB203580, SB202190, BIRB796, and LY3007113.

1.2.4 The role of MAP kinases in the immune response

As mentioned earlier in this chapter, immune cell receptors recognise PAMPs and initiate a sequence of signalling pathway that regulates the overall cellular response. In this context, MAPKs are one of the most extensively studied for their activation in different diseases. This insight is relevant when considering diseases where immune dysfunction underpins the disease such as rheumatoid arthritis or where inflammation has been recently implicated for example, the neurodegenerative disorders of Alzheimer's disease, Parkinson's and amyotrophic lateral sclerosis (Kim and Choi, 2015).

Many studies have shown the MAPKs as playing a critical role in regulating immune function (Arthur and Ley, 2013, Crowell *et al.*, 2014). A range of relevant responses in immune cells would include proliferation, differentiation, survival and inflammatory gene expression (Dong *et al.*, 2001). For example ERK1 and ERK2 activation correlates with cell proliferation and differentiation in vascular fibroblasts, monocyte and T cells (Comalada *et al.*, 2012, Jin *et al.*, 2018). ERK is the main kinase that

contributes to the migration of different cell types for example, in mouse embryo fibroblasts (MEFs), pre-treatment with PD98059 and UO125 reduces cell motility (Huang *et al.*, 2004). ERK also regulates migration via downstream kinases such as Mucin like chain kinase (MLCK)/myosin/membrane protrusion loop, or via FAK/paxillin interaction.

A number of other studies have characterised the role of JNKs in the immune response. Yang et al revealed in their study that there are low basal levels of JNK 1 & 2 in naïve CD4+ and CD8+ T-cells but demonstrated a significant effect of JNK1 on IL-2 production (Yang *et al.*, 1998). A number of studies also suggest that JNK1&2 have different functions within the immune system. In JNK1 deficient mice for example, there is enhanced Th2 differentiation, CD8+ T-cells lacking JNK1 are hypo-proliferative and show lower production of Th2 while in contrast, JNK2 deficiency causes hyper-proliferation and enhanced production of IL-2 (Arbour *et al.*, 2002). Thus, JNK1 is likely to be involved in the development of Th1 response whereas JNK2 organizes CD8+ T-cells (Arthur and Ley, 2013).

The p38 MAPK pathway has key functions in different immune cells. Particularly of note is its role in the differentiation of naïve CD4+ T-cells into effector cells and enhancement of IFNγ production and Th1 differentiation. One study demonstrates that p38 isoforms play an important role in regulating the expression of pattern recognition receptors such as TLRs in macrophages (Bode *et al.*, 2012). More recently, a novel role has been discovered for p38 MAPK in macrophage activation through a downstream signalling product, named ARL11 which drives the production of pro-inflammatory cytokines such as TNFα and IL-6 (Platko *et al.*, 2018).

The studies outlined above are a small part of a large body of evidence which identifies key roles for the MAPKs in immune function. Therefore understanding the mechanisms which regulate the magnitude and duration of the activity of each kinase is important in defining the cellular response. To achieve this understanding the role of phosphatases which switch off these kinases through dephosphorylation is required. These dual specific phosphatases (DUSPs) will be discussed in detail in the next section.

1.3 Dual specificity MAP kinase phosphatases (MKPs)

Studies have shown the participation of a number of phosphatases involved in the inactivation of the MAP kinase pathway. A number operate upstream in the pathway for example PP2A is recognised to dephosphorylate ERK whilst tyrosine phosphatases are able to switch off early events mediated by tyrosine kinase receptors (Letourneux *et al.*, 2006, Mills *et al.*, 1998). However, the best recognised family of enzymes which switches off the MAP kinase pathway involves a group of enzymes known as the Dual Specific Phosphatases or DUSPs, alternatively delineated as the MAP kinase phosphatases or MKPs (Farooq and Zhou, 2004). Negative regulation of MAP kinase activity is via dephosphorylation on both threonine and tyrosine residues within the TXY motif.

The DUSP family can be classified into two groups; typical and atypical DUSPs. These types can be recognized by their amino acid alignments whereby the typical phosphatases contain a MAP kinase binding (MKB), while those lacking this domain and a related kinase interacting motif are classified as atypical DUSPs (Huang and Tan, 2012). The atypical DUSP which dephosphorylate a number of substrates other than the MAPKs themselves and are the topic of a number of excellent reviews to which the reader is refered to (Patterson *et al.*, 2009, Lee *et al.*, 2015).

Typical MKPs, originally identified by Keyse and co-workers (Keyse, 2000), can be further classified to three subgroups depending principally on their location within the cell, nuclear, cytoplasmic or dually- located, but also their substrate specificity and also the potential to be induced by extracellular stimuli or to be constitutively expressed (Kondoh and Nishida, 2007, Caunt and Keyse, 2013). The nuclear MKPs all contain at least one nuclear location sequence (NLS) except in the case of MKP-2 (Sloss *et al.*, 2005) and includes the prototypic MKP-1(DUSP1), MKP-2(DUSP4), PAC-1(DUSP2) and DUSP5. Cytoplasmic DUSPs are DUSP6 (MKP3), DUSP7 (MKP-X) and DUSP9 (MKP-4) and do not express an NLS but an NES which prevents nuclear access. Studies show that blocking or mutating this sequence results in nuclear retention for some of these MPKs (Stanciu and Defranco, 2002).

Other MKPs DUSP16 (MKP-7), DUSP8 (M3\6) and DUSP10 (MKP-5) can be dually located (Huang and Tan, 2012) due to the presence of both NLS and NES. (See figure 1.6)
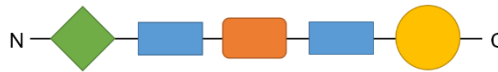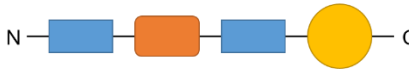
Figure 1. 6 A diagram of DUSP proteins sequences

DUSP family is classified into typical and atypical. The typical DUSPs are located in nucleus such as DUSP1, 2, 4 or in the cytoplasm such as DUSPs 6, 7, 9 or it can be dually located in both nucleus and cytoplasm such as DUSPs 8, 10, 16.NLS (nuclear localization sequence), NES (nuclear export sequence), KIM (kinase-interaction motif), PEST (Pro-Glu-Ser-Thr) sequences adapted from (Lawan *et al.*, 2012).

All DUSPs share common mechanisms of activation through phosphorylation or acetylation (Chi and Flavell, 2008). Significantly, the MKPs also have restricted or overlapping substrate specificities, this helps to regulate a single or a number of MAPKs within a given cellular location. MKP-3 for example, is largely specific for ERK1 and ERK2 over JNK and p38 MAP kinase whilst PAC-1 is selective for ERK and p38 MAP kinase. Only MKP-1 and MKP-2 have the capacity to dephosphorylate all MAPKs at least *in vitro* (Chu *et al.*, 1996), however KO mice models have revealed some restriction in specificity (Al-Mutairi *et al.*, 2010, Cornell *et al.*, 2012).

Whilst studies assessing the role of MKPs are much fewer than those examining MAPK function, these enzymes are now regarded as crucial in the regulation of the cascade. In this context some of the DUSP family have been studied for their active role in immune responses in particular using KO mouse models, as unlike their MAP kinase counterparts, gene deletion does not usually result in embryonic lethality. These are; MKP-1, MKP-2, PAC-1, MKP-5 and MKP-7. The particular role of each MKP in immune response will be detailed further in the next section.

1.3.1 The role of MKPs in immune responses and inflammation

MKP-1 was the first DUSP identified as being able to dephosphorylate both tyrosine and threonine residues in the MAPKs (Charles *et al.*, 1993). It is now one of the most intensely studied MKPs and its role is frequently examined in the innate immune response. It is well recognized as a negative regulator of cytokine production via inactivation of both JNK and p38 MAPKs (Chi, 2006, Cornell *et al.*, 2012). Studies of MKP-1 knock out macrophages show elevated levels of several pro-inflammatory cytokines such as IL-6, IL-12 and TNF-α compared to wild type mice following LPS treatment (Zhao, 2005). In addition, NO production is also upregulated and this exacerbates tissue damage following LPS treatment (Keyse, 2000). MKP-1 function has been established in other conditions linked to immune cell function such as obesity (Wu *et al.*, 2006). Another MKP-1 deletion study revealed that glucocorticoid-mediated induction of DUSP1 results in the suppression of JNK and p38 activation which contributes to the anti-inflammatory induction of glucocorticoid (Abraham *et al.*, 2006). In this context, MKP-1 has been found to play a key role in the immune response by controlling the ability of macrophages to switch between proliferation and activation. A recent paper showed that macrophage proliferation, following stimulation with M-CSF, requires a short period of ERK phosphorylation but for "activation" with LPS needs a longer period; inhibition of MKP-1 increased the kinetics of ERK

activation and blocked macrophage proliferation but enhanced macrophage activation (Comalada *et al.*, 2012).

In addition to MKP-1, another DUSP studied due to the development of a suitable KO mouse model is PAC-1 (DUSP2). It is also a nuclear MKP cloned as an immediate early gene from human T-cells (Rohan *et al.*, 1993). It is expressed in many human cells such as mast cells, neutrophils, eosinophils, B and T-lymphocytes, macrophages and mast cells (Jeffrey, 2006). A key mouse study shows PAC-1 as a negative regulator of ERK and p38 MAPKs which results in significant changes in T- cell function (Jeffrey, 2006). However in the same study macrophages lacking PAC-1 also show a significant increase in JNK activity suggesting cell type specific regulation of different kinases by the same DUSP. The function of PAC-1 seems to be selective to certain cells, for example DUSP2 deletion results in no effect upon obesity-associated inflammation or insulin resistance in mice despite the relevant MAPKs playing a role in both outcomes (Lancaster *et al.*, 2014). Several additional studies are required to better fully understand the role of this DUSP in immune function.

MKP-5 is another more recently described member of the MKP family. Identified in 1999, this newer member has an extended N-terminal MAPK binding domain (150 amino acids), is dual located and selective for p38 and JNK MAPKs (Theodosiou *et al.*, 1999). MKP-5 is also able to regulate innate immunity negatively, and according to mice studies, through specific dephosphorylation of JNK isoforms. Thus, MKP-5 deficient macrophages show increased JNK activity following LPS stimulation and also enhanced cytokine production (Dickinson, 2002, Zhang *et al.*, 2004). The regulation of MAPK activity by MKP-5 has been shown recently by its induction in fibrotic tissue and deleting this gene improves muscular repair in an animal model of muscular dystrophy (Tzouvelekis *et al.*, 2016).

MKP-7 (DUSP16) is another member of the DUSP family that is dually located in cytoplasm or nucleus initially identified as a shuttle protein and selective for JNK (Masuda *et al.*, 2001). The role of this MKP in the immune response is in the regulation of macrophage activation and cytokine release upon infection by Mycobacterium tuberculosis which results in activation of the phosphatase by an acetylation at Lys 55 of MKP-7. This, in turn, regulates JNK dependent autophagy, phagocyte maturation and ROS production in macrophages (Kim *et al.*, 2012). Recently, two different isoforms of MKP-7, A1 and B1, were found to be induced in macrophages and dendritic cells following TLR stimulation. MKP-7 deleted macrophages showed

overexpression of the cytokine IL-12p40 due to an upregulation of JNK which was not observed in WT counterparts (Niedzielska *et al.*, 2014).

MKP-2 is a type 1 nuclear DUSP which has not been studied to the same extent as MKP-1. It consists of 394 amino acids (M.W. 43k Da). Both MKP-1 and MKP-2 share 60% sequence homology especially in their structure and splicing pattern (Guan and Butch, 1995). However, they differ in their tissue localization which may explain differences in their physiological function, although many studies consider MKP-2 to be a functional surrogate to MKP-1. Like other MKPs, MKP-2 can be induced by a range of agents such as growth factors, gonadotropin-releasing hormone(GnRH), serum, retinoic acid, UV-light, oxidative stress and the tumour suppressor p53 suggesting a multitude of signalling pathways and transcription factors which may regulate promoter activity (Misra-Press *et al.*, 1995, Zhang *et al.*, 2001). Other studies report that MKP-2 selectivity between JNK and ERK may vary depending on the cell type (Lawan *et al.*, 2012). Furthermore, several articles show that MKP-2 can regulate either ERK (Misra-Press *et al.*, 1995) or JNK (Zhu *et al.*, 2001).

A recent study also shows that both MKP-1 and MKP-2 are expressed in macrophages (Chen, 2002, Crowell *et al.*, 2014) and their levels can be increased via TLR ligands. Another study demonstrates that MKP-2 stability is decreased when the ERK pathway is inhibited suggesting post-translational modification is important in defining the cellular levels of MKP-2(Crowell *et al.*, 2014).

More recently, studies using a number of different DUSP-4 knockout mice models including those from the Plevin laboratory have revealed an important role for MKP-2 in different biological processes, such as macrophage development, gene expression and apoptosis (Al-Mutairi *et al.*, 2010). Two studies reported a role for MKP-2 in increasing the immune response to infection by parasites such as *Trepanosoma gondii* and *Lieshmania* (Woods *et al.*, 2013, Schroeder *et al.*, 2013). This is partly through increased arginase-1 expression and down regulation of iNOS, both of which interact to control parasite replication (Shweash, 2010, Al-Mutairi *et al.*, 2010). In this context, and opposite to MKP-1, MKP-2 has host protective role. Interestingly, a very recent study found that glycyrrhizic acid, which is an immunomodulatory agent known to suppress leishmania infection, upregulates MKP-2 expression during the infection (Parveen *et al.*, 2018). Also, a novel role has been described for MKP-2 in autoimmune encephalitis via regulation by the transcription factor STAT5 and control of T cell proliferation (Hsiao *et al.*, 2015). These studies indicate that DUSP4 as much

as any other DUSP is likely to play a key role in immune protection from infection and gives rise to the notion that therapeutic strategies in parasite infection may include targeting MKP-2. However, clearly further studies in macrophages, neutrophils and other cells types are required. Also other types of analysis could be useful in defining the function of MKP-2 in the immune response. One strategy recently developed is in the understanding of the metabolic changes that follow macrophage activation.

1.4 Metabolic pathways, immune responses and MKPs

The link between metabolic changes and immune response is relatively old. In the 1950s neutrophils were found to use aerobic glycolysis for ATP production despite having few mitochondria. Even early than this, Otto Warburg described the metabolic profile of tumours in normoxic conditions whereby the end product of the glycolysis pathway pyruvate does not enter the tricarboxylic acid cycle (TCA) but instead generates lactate which produces highly proliferative activity in tumour cells (Warburg *et al.*, 1927, Borregaard and Herlin, 1982). Since then, studies have demonstrated a strong link between cell activities and metabolic pathways which is governed by intracellular signalling cascades in a way more orchestrated than previously realised. For example, the metabolic state and phenotype of a macrophage population are linked and this relationship is found to be bidirectional depending on the micro-environment. So the M1 macrophage phenotype is reliant on an increase in glycolysis whilst the M2 phenotype is dependent on an increase fatty acids (Tannahill *et al.*, 2013). Understanding this correlation can help to identify the role of macrophage metabolism in different stages of atherosclerosis (Tabas and Bornfeldt, 2016).

It is now accepted that metabolic changes in immune cells are regulated by cell signalling events, for example MAPKs are involved in driving the metabolic changes and the energy demands that is needed for macrophage activation and inflammatory responses. A study conducted by (Traves *et al.*, 2012) showed that ERK inhibition leads to decreased glucose consumption and lactate production and the ratio between oxidative and non-oxidative metabolites of the pentose phosphate pathway was also altered. Another study correlated the increase in ERK activation to the induction of glutamine uptake, linking the function of ERK with the TCA cycle (Carr *et al.*, 2010). JNK signalling has also been implicated in metabolic disease, JNK phosphorylation was found to be elevated in obesity and JNK inhibition increased insulin receptor signalling to offset the condition (Hirosumi, 2002). This effect was later

found to be via phosphofructokinase-1 (PFK-1) activation, and thus an effect upon the glycolysis pathway (Deng *et al.*, 2008).

Whilst recent studies have established a link between MAPK signalling and cellular metabolism there are very few studies which do the same for the DUSP family. From all the DUSPs identified to date, the only member that has been studied for its contribution to metabolism is unsurprisingly, MKP-1. Monocytes and macrophages from MKP-1 deletion mice showed dysfunctional cellular migration linked to metabolic changes when both ERK and p38 MAPK were upregulated (Kim and Asmis, 2017). This indicates a potential new area of study for MKPs.

From the literature demonstrated above, using the MKP-2 knock out mouse model, developed in the Plevin laboratory has the potential to further uncover many biological questions surrounding cell differentiation, proliferation and immune response to inflammation. This includes examination of phagocytosis and migration two key events in macrophage function. Furthermore, using a metabolic approach may link metabolic changes to these and other functions and reveal a novel function for MKP-2.

1.5 Aims of the study

Recent studies from our laboratory and others revealed a role for MKP-2 in immune responses via the regulation of the MAPK pathway in macrophages. Using an MKP-2 KO mouse model has helped in the investigation of this gene in response to pathogens and especially parasite infection such as *Toxoplasma* and *Lieshmania*. However, the cellular events which comprise such immune responses such as phagocytosis, motility and proliferation and the role of MKP-2 in the regulation of these events have not been investigated to date.

This PhD study aimed to;

- Characterise macrophage phenotypes in both MKP-2 wild type macrophages and MKP-2 deleted macrophages
- Identify the effect of MKP-2 deletion in MAPK signalling in macrophages and in neutrophils.
- Link changes in MAPK function in MKP-2 deletion macrophages to effects on the expression of the EDN1 gene
- Correlate MKP-2 deletion with macrophage phagocytosis, migration and proliferation.
- Investigate the metabolomics profile to determine metabolic changes underlying each function and correlate this with MKP-2 gene deletion.

Chapter Two

Materials and Methods

2.1 Materials

All materials were of highest commercial grade available and obtained from chemical company Sigma-Aldrich Co. Ltd. (Poole, Dorset, UK) unless otherwise stated.

2.1.1 Cell culture reagents and equipment

Materials	Suppliers	Catalogue #
Dulbecco's Modified Eagle Medium (DMEM)	Gibco (distributer: Life technologies, Paisly, UK)	21969-035
RPMI Media 1640	Gibco (as above)	31870-025
L-glutamine	Gibco (as above)	25030-024
Penicillin/Streptomycin	Gibco (as above)	15140-122
TrypIE™ Express	Gibco (as above)	12604-013
Fetal Bovine Serum (FBS)	Gibco (as above)	10270-106
Cell scraper 25cm /1.8cm non pyrogenic	Corning, Mexico	3010
Cell strainer 70µm	Greiner bio-one, UK	542070
6-well tissue culture plate	Thermo Fisher Scientific	140658
12-well tissue culture plate	Thermo Fisher Scientific	150628
24-well tissue culture plate	Thermo Fisher Scientific	142485
Bacteriological Petri dishes	Thermo Fisher Scientific	121V
T75 Tissue culture flasks	Corning Inc. (USA)	430641U
96-well tissue culture plates	TPP,Techno,Plastic Products AG, Switzerland)	92096
BD falcon cell culture Triple layer Multi-flask	Corning	353143
Trypan blue solution 0.4%	Sigma	T8154

2.1.2 Western blotting chemicals/reagents and equipment

Materials	Suppliers	Catalogue #
Sampling buffer, Bromophenol Blue sodium salt	Sigma, USA	B8026-5G
Glycine	Sigma	G7126-5KG
Trizma base minimum	Sigma	T1503-5KG
Sodium chloride	Sigma	S3014-5KG
P-Coumaric acid	Sigma	C9008-5G
Luminol	Sigma, USA	A8511-5G
Ammonium Persulfate (APS)	Sigma, Germany	215589-100 G

Amersham™ Protram™ , Nitrocellulose Blotting Membrane 0.45µMnc	GE Healthcare Ltd, UK (via Sigma)	GE10600003
Whatman filter paper	GE Healthcare Ltd, UK (via Sigma	3017-915
Acrylamide	Carl Roth GmbH+ Co. , Germany	3029.1
TEMED: N,N,N,N-tetramethyle-ethylene diamine	Sigma	T9281
DTT: DL-Dithiothreitol	Sigma	D91163-5G
Hydrogen peroxidase solution, 30 %(w/w)	Sigma, Germany	H1009-100ml
Pre-stained SDS-Page molecular weight markers	Bio-Rad Laboratories (Hertfordshire, UK)	1610304
Tween-20	Sigma-Aldrich, France	P1379
Glycerol	Sigma	G5516
Sodium dodecyl sulphate (SDS)	Sigma	L3771
2-Mercaptoethanol	Sigma / Germany	M6250
Bovine serum albumin (BSA)	Fisher Sientific International, Inc. (Leicestershire,UK)	161-0374
Sodium phosphate dibasic	Sigma	S7907
Potassium phosphate monobasic	Sigma	P5655
Autoradiography film	Santa cruze Biotechnology, UK	Sc-201696

2.1.3 Western blotting antibodies and optimised conditions

Antibody	Suppliers	Cat #	Dilution conditions
P. ERK p.p44/42 MAPK rabbit	Cell signalling technology, Inc. distributer: New England Biolabs, UK.	4377	1µl: 1500µl, in 3% BSA in TBST, at 4℃
p.SAPK/JNK rabbit	Cell signalling technology, Inc. distributer: New England Biolabs, UK	9251	1µl: 1500µl, in 3% BSA in TBST, at 4℃
p-p38 MAPK rabbit	Cell signalling technology, Inc. distributer: New England Biolabs, UK	9211	1µl: 1500µl, in 3% BSA in TBST, at 4℃
MKP-2(s-18) rabbit	Santa cruz biotechnology,Inc.(distributor: Insight Biotechnology Ltd, UK	Sc-1200	1µl: 1000 µl, in 5% milk in TBST, at 4℃

Anti-p38 rabbit	Cell signalling technology, Inc. distributer: New England Biolabs, UK	9212	1 µl : 7500 µl, in 3% BSA in TBST, at RT
Anti-JNK rabbit	Santa cruz biotechnology,Inc.(distributor: Insight Biotechnology Ltd, UK	Sc-571	1 µl : 7500 µl, in 3% BSA in TBST, at RT
Anti-ERK (C-9) rabbit	Santa cruz biotechnology,Inc.(distributor: Insight Biotechnology Ltd, UK	Sc-514302	1 µl : 7500 µl, in 3% BSA in TBST, at RT
Peroxidase-conjugated affinipure Goat Anti-Rabbit IgG	Jackson Immuno Research Laboratories Inc.	111-035-144	1 µl : 7500 µl, in 1% Milk in TBST at RT

2.1.4 Flow cytometry material/ antibodies

Materials	Suppliers	Cat #
5ml Falcon Polystyrene tubes	Fisher Scientific International	10088710
Ethylenediaminetetra acetic acid (EDTA)	Sigma	E6758
Anti-Mouse CD16/CD32	eBioscience™ (via ThermoFisher Scientific)	16-0161-85
Anti-Mouse F4/80,FITC, Clone BM8	eBioscience™ (via ThermoFisher Scientific)	11-4801-81
Anti-Mouse CD11b, APC Clone M1/70	eBioscience™ (via ThermoFisher Scientific	17-0112-81

2.1.5 Phagocytosis study

Materials	Suppliers	Cat #
Zymosan A bioparticles, Alexa Fluor 594 conjugate	Molecular Probes , by Life technologies, USA	Z-23374
Zymosan opsonizing reagent	Molecular Probes , by Life technologies, USA	Z-2850
Paraformaldehyde 4% in PBS	Santa cruze Biotechnology	CAS 30525-89-4)
Triton 100 x	Sigma	T9284
FITC Labelled Phalloidin	Sigma	PS282

DAPI	Molecular Probes , by Life technologies, USA	D1306
Coverslips-Round,13mm	VWR	631-1578
Mowiol 4-88	Millipore, UK	475904
Microscope slides		7101
Lieca TCS SP5 confocal microscope	Leica Microsystems CMS GmbH,Germany	
Cytoselect ™ 96-well phagocytosis kit	Cell biolabs, Inc. USA	CBA-224

2.1.6 Migration study

Materials	Suppliers	Cat #
ThinCert for 24 well plate, translucent, 0.8µm	Greiner Bio One, UK	662638
Calcein AM	eBioscience	65-0853-78
TrypLE™ Express Enzyme (1X), no phenol	Gibco by Thermofisher Scientific	12604-013
Black/Clear flat bottom TC-treated 96 well plate	ThermoFisher Scientific	10530753
Corning™ 96-Well Clear Bottom Black Polystyrene 96 well Microplates	Fisher Scientific International	10530753
PolarStar Omega fluorescence plate reader	BMG, Labtech, Germany	

2.1.7 Proliferation Study

Material	Suppliers	Cat #
BrdU Cell Proliferation Assay Kit	Cell signalling (distributor: New England Biolabs, UK	6813

2.1.8 Genotyping and PCR study

Materials/ Reagents	Suppliers	Cat #
Thermo Scientific Phire animal tissue direct PCR master mix	ThermoFisher Scientific	F- 170s

0.5 ml PCR tube flat cap	Star Lab Ltd. , UK	11405-8100
Agarose for molecular biology	Sigma / USA	A9539
Ethidium bromide solution	Sigma	E1510
Isolate II RNA Mini Kit	Bioline Reagents Ltd, UK	BIO-52072
Tetro cDNA synthesis kit	Bioline Reagent Ltd, UK	BIO-65042
Micro Amp ^{R} Fast 96-well reaction plate(0.1ml)	Applied Biosystems by life technologies	4346907
MicroAmp™ optical Adhesive film kit	Applied Biosystems by ThermoFisher Scientific	4313663
Power Up™ SYBR Green Master Mix	Applied Biosystems by life technologies	A25741
DNAase, RNase-None detected Water for qPCR	Sigma, USA	W4502

2.1.9 Untargeted metabolomics Study (gifted from Dr David Watson's lab, SIPBS)

Material	Suppliers	Lot #
Methanol	VWR	Lot #15A190510
Acetonitrile	VWR	Lot #14D028945
Ammonium carbonate	Sigma-Aldrich	Lot #BCBQ6156V
HPLC grade water	Thermo Fisher sceintific	Lot #1708940
A ZICpHILIC column (150 x 4.6 mm x 5 µm)	Merck,Germany	Lot #P130326
Conical glass insert 200uL	ThermoFisher sceintific	Lot # 00219799
Auto sampler vials	Thermo Fisher sceintific	Lot# 44383092515DM
Cell shaker	Thermomixer comfort, eppendorf,MTB	
LC-MS	Orbitrap mass spectrometer ,Thermo Fisher Scientific , Germany	
mzmatch	http://mzmatch.sourceforge.net/	
MZmine-2.10 ans 2.17	http://mzmine.github.io/download.html	
SIMCA	Version 14, Umetrics, Umeå, Sweden	
Metaboanalyst 4.0	http://www.metaboanalyst.ca/	

Thermo Xcalibur 2.2 SP1.48-August 12, 2011	Thermo Fisher sceintific inc.	
Thermo ToxID 2.1.2 SP2.17-September 9,2011	Thermo Fisher sceintific inc	

2.1.10 Enzyme-Linked Immunosorbent Assay (ELISA)

Materials/ reagents	Suppliers	Cat #
Mouse EDN1/ Endothelin 1 ELISA kit (Sandwich ELISA)	LifeSpan BioSciences, Inc., USA (distributor: Cambridge Bioscience, UK)	LS-F2783
Mouse IL-1β Duo Set ELISA	R &D system , UK	DY401
IL-1β capture Ab	R &D system , UK	840134
IL-1β detection	R &D system , UK	840135
IL-1β standards	R &D system , UK	840136
IL-1β streptavidin-horseradish peroxidase conjugate	R &D system , UK	893975
Mouse IL-10	BD Biosciences, USA	555252
IL-10 capture Ab	BD Biosciences, USA	51-26571E
IL-10 detection	BD Biosciences, USA	51-26572E
IL-10 streptavidin-horseradish peroxidase conjugate	BD Biosciences, USA	51-9002208
IL-10 Standards	BD Biosciences, USA	51-26576E
SureBlue™ TMB 1-Component Microwell Peroxidase Substrate	KPL immunoassay research(distributor: VWR,UK)	52-00-03
Stop solution	Invitrogen by ThermoFisher Scientific	SS04

2.1.11 Nitric oxide assay

Material/chemicals	Suppliers	Cat #
Sodium nitrite, $NaNO_2$	BDH, England	10256
Sulfanilamide, P- Aminobenzene Sulphonamide, $C_6H_8N_2O_2S$	Sigma, Germany	s-9251
N-(1-Naphthyl)ethylenediamine dihydrochloride, $C_{12}H_{14}N_2.2HCL$	Sigma, Germany	222488

2.1.12 MAPK inhibitors

Material/chemicals	Suppliers	Cat #
UO126,MEK1/2 inhibitor	Millipore by sigma	19-147
SP600125, JNK inhibitor	sigma	S5567
SB203580, p38 inhibitor	sigma	S8307
Dimethyl sulfoxide	Sigma / France	D5879

2.1.13 Stimulants

Chemicals	Suppliers	Cat #
LPS from Escherichia coli 055:B5	Sigma	L2880
rIL-4 (recombinant mouse IL-4	R &D system, UK	404-ML
Recombinant mouse M-CSF	R &D system, UK	416-ML
Recombinant mouse C5a	R &D system, UK	2150-C5
Leukotriene β_4	Tocris biosciences, UK	71160-24-2

2.2 Methods

2.2.1 Animals

MKP-2 (DUSP-4) deleted mice were generated as previously described (Al-Mutairi *et al.*, 2010). MKP-2$^{-/-}$ and MKP-2$^{+/+}$ littermate controls bred on a C57BL/6 background (7th and 8th generation backcross) were used in this project. These mice were bred and maintained within the Biological Procedure animal Unit within the Strathclyde Institute of Pharmacy and Biomedical Sciences. Animals were used at 6 - 8 weeks of age and were age matched within each experiment.

2.2.2. DNA preparation for mouse genotyping

2.2.2.1 DNA extraction

Thermo-scientific phire animal tissue direct PCR master mix (F- 170s) kit was used for mouse genotyping. A small section of ear or tail tips were collected from the mice and placed in sterile 1.5 micro centrifuge tubes. A mixture of 20 µl dilution buffer and 0.5 µl DNA release buffer was vortexed and added to each tissue sample. Then samples spun down at 13,000 xg for 30 seconds and incubated at room temperature for 3 minutes. After that, reaction tubes were placed in the PCR machine set for 98 ºC for 2 minutes. This was followed by sample vortexing to digest the remaining DNA in the ear tissues. The remaining tissue was centrifuged at 13,000 xg for 30 seconds. Sample supernatants (genomic DNA) were transferred to new PCR tubes and stored at -20ºC. 1 µl of this genomic DNA was used per PCR reaction for genotyping.

2.2.2.2 Polymerase chain reaction (PCR) amplification

The extracted genomic DNA was used directly for PCR using MKP-2 primers for wild type (MKP-2$^{+/+}$) and knock out (MKP-2$^{-/-}$) mice. Two reaction tubes were prepared for each sample; one for wild type primers (group A) and one for knock out primers (group B). MKP-2 primers:

WT forward primer 5'-CTTCAGACTGTCCCAATCAC-3'

WT reverse primer 5'-GACTCTGGATTTGGGGTCC-3'

KO forward primer 5'-TGACTAGGGGAGGAGTAGAAGGTGGC- 3'

KO reverse primer 5'- ATAGTGACGCAATGGCATCTCCAGG- 3'

PCR master mix was prepared as below:

PCR reaction	Group A tubes	Group B tubes
H$_2$O	7µl	7µl
2x phire tissue direct PCR master mix	10µl	10µl
Forward primer	1µl	1µl
Reverse primer	1µl	1µl

The PCR master mix was scaled up according to the number of samples, mixed well and 19 µl added to each tube. Finally, 1 µl of genomic DNA was added to each tube so the total volume of the PCR reaction was 20 µl. Negative controls contained everything as above, with the exception of the DNA. Whilst, positive controls composed of 8.6 µl H$_2$O, 10 µl of 2x phire tissue direct PCR master mix and 0.4 µl control primer (provided within the kit) and DNA sample that was chosen randomly.

PCR conditions for MKP-2 genotyping: Initial denaturation 95ºC for 2 minutes. This was followed by 35 cycles of denaturation at 95 ºC for 30 seconds, annealing at 58ºC for 30 seconds and extension at 72ºC for 3 minutes. After this a final extension step at 72ºC for 5minutes. The reaction was stopped by a final hold on 4ºC. The PCR products were separated by agarose gel electrophoresis.

2.2.2.3 DNA detection

Agarose gel (1% w/v) electrophoresis was used to analyse and detect resulting amplified PCR product. One gram of agarose (molecular biology grade) was added to 100 ml of 1x TAE (consisting of 40 mM Tris, 20 mM acetic acid, and 1 mM EDTA) mixed well and heated for 3-4 min in a standard microwave until the agarose was dissolved. 2 µl of Ethidium bromide was directly added to the agarose gel solution in the fume cupboard. The resulting solution was transferred into the gel cast to allow for solidification, this was then transferred to the electrophoresis chamber containing 1X TAE buffer. Gels were run at 90-120 volts for 45-90 min. For sample loading, 10 µl of the PCR genotyping reactions were loaded into the wells of the gel, along with 5µl of a 1KB ladder. DNA bands were visualized under UV-light (302 nm) in a gel documentation system (InGenius from Syngene). Routinely mice were genotyped by PCR of tail or ear tip DNA and backcrosses of 8th generation were used.

2.2.3 Preparation of L- conditional medium

Growing and culturing bone- marrow derived macrophages (BMDMs) requires large quantities of macrophage colony stimulating factor (M-CSF). This factor was derived using L929 cells (ECACU). An aliquot of L929 cells was thawed in the water bath at 37°C and centrifuged at 1400 xg for 5 minutes. The pellet was re-suspended in 10 ml of complete DMEM containing sodium pyruvate, pyridoxine hydrochloride, high glucose, 10 % FCS,1 % L\Glutamine 2 mM, 1 % P\S (100 U/ml Penicillin: 1 µg/ml streptomycin). Cells were cultured in a T.75 cm^2 tissue culture flask for 5-7 days in a 5% CO_2 incubator at 37°C until confluent 100%. After that the media was aspirated from the flask and replaced with 5ml cold PBS and left in the fridge for 10 minutes. Cells were then scraped gently using a 30 cm cell scraper, the cell suspension was collected in a 50 ml tube and centrifuged at 1400 xg for 5 minutes. The supernatant was removed, and the pellet was re-suspended in 10 ml complete DMEM. To each 10 x T-75 flasks 9 ml of complete DMEM media was added, followed by1 ml of cell suspension and incubated until 80%-90% confluent. After this, media was aspirated from the flasks and 2 ml of Triple E was added to each flask and incubated for 2 to 3 minutes to allow cells to detach. Then 10 ml of complete DMEM was added to each flask, to ensure all cells de-attached from the walls of the flasks; media was flushed and pipetted onto the walls. All cell suspension was collected in one flask and mixed well to avoid cell clumps. Triple layer flasks were prepared as below:

In a 3- layer tissue culture –treated 525 cm2 (353/43) flask, 6 ml cell suspension was added to each layer of the flasks. Then complete DMEM was added up to 150 ml and mixed well in which each layer had the same amount of media. Triple layer flasks were then incubated for 7 days in 5% CO2 incubation at 37°C or until confluent. After 7 days incubation, supernatant media was collected from the flasks and transferred to 50ml tubes, spun at 3000 xg for 5 minutes and filtered using a Millipore filter unit (which was attached to a vacuum). The filtered media was then collected into 50 ml tubes, adding 45ml to each and stored at -20 °C as supplementary media (a source of M-CSF for macrophages).

2.2.4 Bone marrow isolation (the generation of macrophages)

BMDMs were obtained from 6-8 weeks old male C57BL/6, MKP-2$^{+/+}$ and MKP-2$^{-/-}$ mice. Mice were sacrificed by cervical dislocation. Using 70 % ethanol the legs were sprayed and sterilized first. Then bones of the femurs and tibias were dissected free of adherent tissue and sprayed with 70 % ethanol. Bones were transported in sterile

media to the cell culture lab. In the cell culture hood, the ends of the bones were cut off and the marrow tissue eluted by irrigation in a syringe with 5 ml of media per each one using a 21G needle and collected in a 50 ml tube.

The media for BMDMs was freshly prepared on the day of isolation and consists of: Dulbecco's Modified Eagle Medium (DMEM) supplemented with 10% FCS, 1% L/G, 1% P/S, and 30 % L-cell conditional medium as a source of M-CSF (the growth factor for macrophages). Cells were then suspended by flushing using a 25 - gauge needle for dis aggregation and then by vigorous pipetting to produce a single cell suspension. The cell suspension was then filtered using a 70 μm cell strainer, centrifuged at 1400 rpm for 5 minutes and the resulting pellet was re-suspended in 10 ml fresh media and counted. After counting $2x10^6$ cells/ml were transferred into 10 cm^2 petri-dishes containing 6 ml complete DMEM supplemented with 3 ml L-conditional media. Dishes were then incubated at 37 °C in a 5 % CO_2 incubator for 7 days (the day of dissection was considered day 0). After 3 days (day 4 from dissection) of incubation macrophage dishes were supplemented with an additional 10 ml L-conditional media to be a total of 20 ml. On day 7 macrophages were confluent and ready to harvest.

2.2.5 Cell harvesting on day 7

To harvest the macrophages the media was removed and replaced by 5 ml cold sterile complete RPMI-1640 media to de-attach the cells. Cells were harvested from the petri dishes using a cell scraper and collected in 50 ml tubes. The same step was repeated with 3 ml RPMI-1640 to ensure harvesting all the cells. Cell suspension was flushed by using 21-gauge syringes to mix the cells and to avoid cell clumps. The collected suspension was then spun at 1400 rpm for 5 minutes. That was followed by washing the pellet twice (once with cold RPMI-1640 nothing added and once with warm complete RPMI-1640 (supplemented with 10 % FCS, 1 % L/G, 1 % P/S), finally, the resulting pellet was re-suspended in 5 ml-10 ml (depending on the pellet) of complete RPMI-1640. Cells were then counted from a diluted cell suspension in a haemocytometer and diluted according to the desired cell number. For MAPKs $1x10^6$ cells were seeded into each well of 12- well plates and $2x10^6$ cells were seeded in each well of a 6-well plate for MKP-2 western blotting.

2.2.6 Neutrophil Isolation protocol

MKP-2$^{+/+}$ and MKP-2$^{-/-}$ mice were sacrificed and bones of femur and tibia were isolated as described in 2.2.4. All steps of bone marrow cell isolation were as described for macrophages except using cold RPMI-1640 complete media for neutrophils instead of DMEM. Primary bone marrow derived neutrophils were isolated using Anti-Ly-6G Microbeads kit specific for mouse (Miltney biotech cat # 130-092-332). Ly-6G is highly expressed on neutrophils, thus was used to positively isolate just neutrophils. After getting single cell suspension from bone marrow, cells were magnetically labelled. First, cell suspension was centrifuged at 1400 xg for 10 minutes. Then supernatant was aspirated and the pellet was re-suspended in 10-40 ml (depending on the pellet) complete RPMI-1640 media. Cell number was determined and a protocol was followed as set by the kit instructions in which all amounts was set to 1x10^8 cells (for bigger cell numbers the amount of materials was scaled up accordingly). Before magnetic labelling cell suspension were passed through a 30 μm nylon mesh (Pre- separation filter 30 μm, Miltney biotech, cat# 130-041- 407) to remove cell clumps which may clog the column. The filter was moistened with MACS buffer (pH=7.2, 0.5 % BSA (Bovine Serum Albumin), 2mM EDTA) before use. Cells were then spun at 1400 xg for 10 minutes and the resulting supernatant was removed completely. The cell pellet was re-suspended in 200 μl of cold MACs buffer per 1x10^8 total cells. This was followed by addition of 50 μl of Anti-Ly- 6G Biotin antibody per 1x10^8 total cells , mixed well and incubated for 10 minutes at 4°C, rotating in order to allow magnetic labelling. After this, 150 μl of MACs buffer and 100 μl of Anti-Biotin Microbeads was added per 10^8 total cells, mixed well and incubated for 15 minutes at 4°C on the roller. During this time, a magnetic separation that is suitable for LS separation column was placed inside the tissue culture hood to be ready to use after 15 minutes. Cells were then washed with 5 ml MACs buffer and centrifuged at 1400 xg for 10 minutes. Supernatant was aspirated completely and the cell pellet was re-suspended in 500 μl of MACs buffer. As mentioned above a magnetic separation column was prepared and attached to a suitable magnetic plate. Two universal tubes were prepared and one was labelled as negative (to collect waste) and the other was labelled as positive (to collect neutrophils). A 70 μm cell strainer was applied to the LS separation column that was rinsed with 3 ml MACs buffer before adding 500 μl MACs buffer to the cell strainer. After this, cell suspension was added to the filter that was adjusted in the top of the column and the flow-through was collected in the negative tube. Finally, the LS column was removed from the magnetic separator and

placed on the positive tube, and then 5 ml of MACs buffer was added to the column and the flow-through collected in the positive tube this contained the isolated neutrophils. The neutrophil suspension was then centrifuged at 1400 xg for 10 minutes and re-suspended in complete RPMI-1640. Isolated neutrophils were then counted and each 1×10^6 cells/ml was placed in 1.5 ml Eppendorf tubes because they are suspension cells and left to rest in the incubator at $37\,^{\circ}\text{C}$ and 5% CO_2 for one hour before utilising for experiments.

2.3 Fluorescent –activated cell sorting (FACS)

In to each FACS tube, 1×10^6 BMDMs was added, washed with FACS buffer (PBS +0.05 % BSA+2mM EDTA) and centrifuged at 1400 xg for 5 minutes. Cells were then incubated for 5 minutes with CD16/CD32-Fc receptor blocker (1:50 in FACS buffer) to reduce nonspecific antibody binding. Additional 50µl of FACS buffer was added to each sample and stained with macrophage cell surface markers antibodies specific to mature macrophage population. One sample was left unstained as control, and two tubes were labelled for single stain of either F4/80 (FITC) or CD11b (APC) antibodies. Whilst for the last tube, both stains were added. After this cell were incubated with antibodies for 25 minutes in dark at 4 ºC. this was followed by one more wash with FACS buffer and spun at 1400 xg for 5 minutes. Cell were then re-suspended in 300 µl of FACs buffer and vortexed to produce single cell suspension. Fluorescent minus one (FMO) was used to measure cell surface markers. Cells that were positive for both F4/80 and CD11b characterised as mature macrophage population. Flowjo software was used for further analysis of cell phenotype.

2.4. Western blotting

2.4.1 Preparation of whole cell extracts

Cells were grown to 1×10^6 cells/ml in 12-well plates for MAPKs or up to 2×10^6 cells/ml in 6-well plates for MKP-2 and then stimulated with different concentrations of LPS from *E.coli* (LPS; 30 ng/ml, 100 ng/ml and 1 µg/ml) for the desired period of time for the macrophages. Whilst neutrophils were stimulated with either 100 ng/ml LPS, 20 nM C5a or 300nM of LTβ4. The plates were then placed on ice to stop the reaction. Cells were immediately washed twice with ice-cold PBS before addition of 150-200 µl of pre-heated Laemmli sample buffer (63 mM Tris-HCl (pH6.8), 2 mM $Na_4P_2O_7$, 5 mM EDTA, 10% (v/v) glycerol, 2% (w/v) SDS, 50 mM DTT, 0.007% (w/v) bromophenol blue) was added. The cells were then scraped from the wells and the protein was

sheared by repeatedly flushing through a 21 gauge needle. The samples were then transferred to labelled micro- centrifuge tubes and boiled for 3 -5 min for protein denaturation, before storing at -20 °C until required.

2.4.2 SDS-Polyacrylamide Gel Electrophoresis (SDS-PAGE)

Gel kit apparatus was first cleaned in 70% ethanol before assembly, then glass plates were checked for leaks prior to use. Resolving gels were prepared containing (10% (w/v) acrylamide: (N, N'-methylenebis-acrylamide (30:0.8), 0.375 M Tris (pH8.8), 0.1% (w/v) SDS and 10% (w/v) ammonium persulphate (APS)). Gels were polymerized by the addition of 0.05% (v/v) N, N, N', N'- tetramethylethylenediamine (TEMED) and poured between two glass plates assembled in a vertical slab configuration according to the manufacturer's instruction (Bio-Rad). A thin layer of 200 µl 0.1% (w/v) SDS was then added to disperse bubbles from the top of the resolving gel. Following gel polymerisation the layer of 0.1% SDS (w/v) was removed and a stacking gel containing (10% (v/v) acrylamide: N, -methylenebis-acrylamide (30:0.8) in 125 mM Tris (pH6.8), 0.1% (w/v) SDS, 0.05% (w/v) ammonium persulfate and 0.05% (v/v) TEMED) was poured on top of the resolving gel and a comb placed to create the wells. After the loading gel polymerized the comb was removed and the gel was ready for electrophoresis.

Polyacrylamide gels were assembled in a Bio-Rad Mini-PROTEAN-3 electrophoresis tank and filled with electrophoresis buffer (25 mM Tris, 129 mM glycine, 0.1% (w/v) SDS). Aliquots of the denatured protein samples were added equally to the wells with a glass syringe. A pre-stained SDS-PAGE molecular weight ladder of known molecular weights was run concurrently in order to help identify the protein of interest. Samples were electrophoresed at a constant voltage of 130 V, until the bromophenol dye had reached and left the bottom of the gel.

2.4.3 Electrophoretic Transfer of Proteins to Nitrocellulose Membrane

In this step, the separated proteins by SDS-PAGE were transferred to nitrocellulose membranes by electrophoretic blotting following a standard protocol (Towbin *et al.*, 1979). The gel was pressed firmly against a nitrocellulose sheet and assembled in a transfer cassette sandwiched between two pieces of Whatman 3MM paper and two sponge pads. The cassette was immersed in transfer buffer (25 M Tris, 19 mM glycine, 20% (v/v) methanol) in a Bio-Rad Mini Trans-Blot™ tank and a constant current of 300 mA was applied for 105 minutes, whilst the tank was cooled by inclusion

of an ice reservoir. The resolving gel contains SDS which confers a negative charge on the protein. Therefore, the cassette was oriented with the nitrocellulose towards the anode.

2.4.4 Immunological Detection of Proteins

Following transfer of the proteins to the nitrocellulose membrane, the membrane was removed and any remaining protein blocked by incubation in a solution of 1% (w/v) milk in TBS 1X which consists of 20 mM Tris-HCL and 150 mM NaCl, pH 7.6 for 1 hr with gentle agitation on a platform shaker. The blocking buffer was then removed and membranes washed 3 times with TBS 1X(10 minutes each) incubated overnight with a primary antibody specific to the target protein diluted in TBST (TBS 1x + 0.1% (v/v) tween 20) buffer containing 3% (w/v) BSA as described in 2.1.3. On the following day membranes were washed in TBST every 10 min for 30 min with gentle agitation. The membranes were then incubated for a further 2 hr at room temperature with secondary horseradish peroxidase-conjugated IgG directed against the primary antibody diluted to approximately 1:7500 in 1% milk in TBST. After three additional washes in TBST as described before, immunoreactivity protein bands were detected by incubation in enhanced chemiluminescent (ECL) reagent. Equal amounts of each ECL 1 [0.1 M Tris-HCl (pH 8.5), 25 M luminol and 25 M Coumaric acid] and ECL 2 [0.1 M Tris-HCl (pH 8.5) and 6.27 mM H_2O_2] was added for 3 min with agitation. The membranes were blotted onto a paper towel to remove any excess liquid. The blots were then mounted onto an exposure cassette and covered with cling film, then exposed to X-ray film (Kodak Ls XOMAT) for the required time under darkroom conditions and developed using X-OMAT machine (KODAK M35-M X-OMAT processor). Resulting films were scanned and protein expression was quantified by densitometry (background pixel intensity subtracted from corresponding band pixel intensity) using Scion Image software (Scion Corp, Maryland, USA).

2.4.5 Nitrocellulose membrane stripping and re-probing

Exposed nitrocellulose membranes were stored in sealed dishes and then stripped and re-probed for the detection of other cellulose bound proteins. In this step, antibodies were stripped from nitrocellulose membranes by incubating in 15 ml stripping buffer (0.05 M Tis-HCl, 2% SDS, and 0.1 M of β-mercaptoethanol) for 60 minutes at 70°C in an incubator/shaker (Stuart Science Equipment). After incubation, the stripping buffer was discarded in a fume hood and the membrane washed three times with TBST buffer (pH 7.4) at 15 min intervals to remove residual stripping buffer.

After washing, membranes were incubated overnight with primary antibody prepared in 3% BSA (w/v) in TBST buffer. On the following day, membranes were washed with TBST buffer three times over 30 min. Finally, the blots were ready for the immunological detection protocol mentioned previously in section 2.4.4.

2.5 Phagocytosis assay

Macrophages were harvested on day seven of the culture and 0.5×10^6 cells were seeded on coverslips in each well of a 12-well plate in complete RPMI media (10% FBS, 1% P/S, 1% L/G) and incubated overnight at 37ºC, 5% CO_2 incubator to allow the cells to attach. Cells were pre-treated with 100 ng/ml of LPS or IL-4 for 2 hours. Next steps were performed in the dark following a protocol from (Weischenfeldt and Porse, 2008). Next day 5 µl of fluorescently labelled zymosan A bio particles, Alexa Fluor 594 conjugate (cat# Z-23374, Molecular probes, Abs= 590, Em= 617) and 5 µl opsonizing reagent (cat# Z-2850) were added to 1.5 reaction tube containing 500 µl PBS and vortexed before incubation for one hour. After that opsonized bio particles were washed twice with 1 ml PBS and centrifuged at 1250 xg for 15 minutes. The pellet was re-suspended in 100 µl PBS, vortexed and the bio particles were counted under a fluorescent microscope to obtain the multiplicity of infection (MOI) of 10. Then the 100 µl opsonized bio particles was added to 30 ml of PBS (depending on the numbers of the coverslips) and mixed well. 1 ml of this mix was added to each well of the 12-well plate. Then the plate was centrifuged at 500 xg for two minutes, (this step is to enhance the zymosan bio particles movement towards the macrophages) followed by one hour incubation in humidified 37ºC, 5% CO_2 incubator (negative control was included here). The phagocytosis was stopped by adding ice-cold PBS. BMDMs were then washed four times with cold PBS before fixing in freshly prepared 4% paraformaldehyde by adding 500µl to each well for 20 minutes. The cover slips were washed twice in PBS and cells permeabilized with PBS containing 1% FBS and 0.5% Triton x-100 for 15 minutes. Then cells were washed three times with PBS 1% FBS (no triton). After this cells were stained with 1 µg/ml FITC-labelled phalloidin in PBS containing 10% FBS for 30 minutes. Finally cells were stained with 0.1 µg/ml DAPI in PBS containing 1% FBS for 10 minutes at room temperature. Then coverslips were washed twice in PBS containing 1% FBS and air dried before mounting with 10 µl of mowiol on the slides. Phagocytosis was quantified using the total number of internalized zymosan particles per 100 cells using Leica TCS SP5 confocal microscope. Phagocytosis index and the morphological changes where checked by

giving anonymous slides to other lab members to further manual count which was near the authors results.

2.5.1 Quantification of phagocytosis

In order to confirm macrophage phagocytosis of zymosan, Cytoselect ™ 96- well phagocytosis assay was used. A description of the process and the assay principles is presented in figure 2.1 according to the manufacturer's instructions. Macrophages from both MKP-2$^{+/+}$ and MKP-2$^{-/-}$ mice were cultured for seven days in macrophage growing media. Cells were then harvested and 2x10^5 cells/100 µl were seeded in each well of a 96-well plate and incubated overnight at 37 ⁰C, 5% CO_2. Macrophages were then pre-treated with either 100 ng/ml LPS, 20 nM C5a or 100 ng/ml IL-4 or 2 µM Cytochalasin D (was used as a positive control of phagocytosis inhibition) for 1 hour prior to the addition of zymosan. Then, 10 µl of opsonized zymosan suspension (5x10^8 particles/ml) was added to each well and incubated for one hour in the cell culture incubator. Each sample including a negative control without zymosan was assayed in duplicate. After this, cell culture media was removed by inverting the plate and blotting on a paper towel and tapping gently several times. Wells were replenished with 200 µl of cold, serum free RPMI media and washed three times.

External particles were removed and blocked by adding 100 µl fixing solution to each well and incubated for 5 minutes at room temperature. Fixing solution was then aspirated and wells washed twice with 1x PBS buffer. 100 µl of pre-diluted 1x blocking reagent was added to each well and the plate incubated for 60 minutes at room temperature on an orbital shaker. After this, the blocking reagent was aspirated and the plate washed three times with 1xPBS.

Next step was detection of internalized zymosan particles. After the last wash the PBS was removed and 100 µl of pre-diluted 1x permeabilisation solution added to each well and incubated for 5 minutes at room temperature. The permeabilisation solution was removed and wells washed once with 1X PBS before adding 100 µl of the 1x detection reagent to each well for 60 minutes at room temperature on an orbital shaker. After removal of the detection reagent, wells were washed 3 times with 1X PBS. This was followed by adding 50 µl of detection buffer to each well and incubating for 10 minutes at room temperature on the orbital shaker. The reaction was initiated by adding 100 µl of substrate and incubated for 15 minutes at 37⁰C. Finally, the reaction was stopped by adding 50 µl of the stop solution and the plate was placed

on the orbital shaker for 30 seconds. The absorbance of each well was read at 405 nm using a polar star omega plate reader (BMG Labtech).
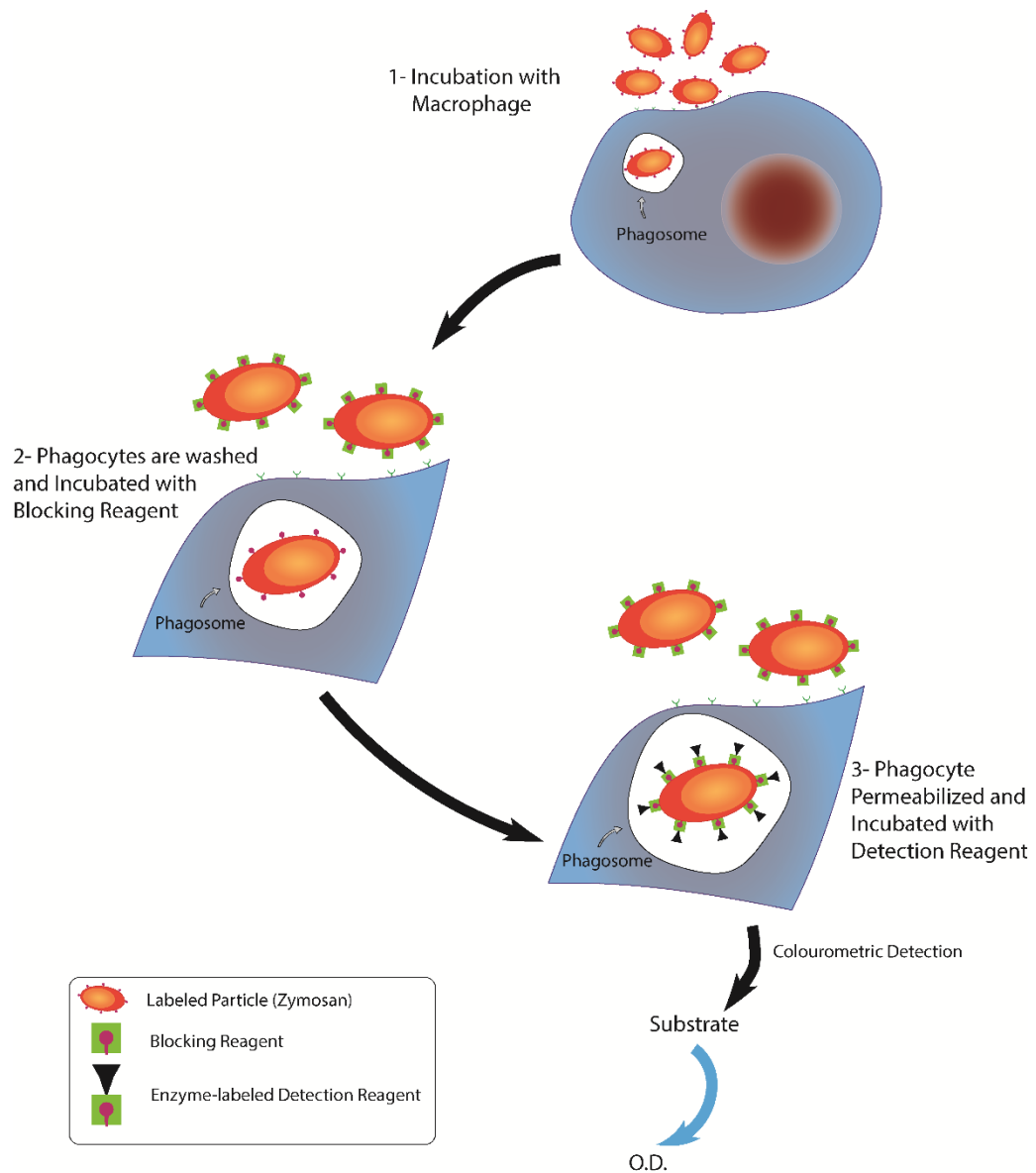
Figure 2. 1 Phagocytosis quantification experiment

Opsonised zymosan particles are incubated with macrophages to allow phagocytosis. Then un-internalized particles were blocked by incubating with blocking reagent. The reaction started by incubating with detection reagent which was then visualised by adding substrate and the colorimetric reaction was measured by reading the optical density (OD) at 405 nm. Adapted and modified from Cell Biolabs, Inc.

2.6 Cell migration assay

To asses macrophage migration, Boyden chambers were prepared by immersing a thin-cert filter with an 8.0 µm pore size into a 24-well, flat-bottom microtiter plate (Thin Cert cat # 662638, Greiner Bio One, UK). The plate contained 600 µl of either serum free DMEM, complete DMEM (containing 10% FCS, 1% L/G, 1% P/S), 100 ng/ml LPS, 20 nM C5a, 100 ng IL-4 or zymosan particles MOI of 10. MKP-2$^{+/+}$ and MKP-2$^{-/-}$ BMDMs were harvested on day seven of the culture and $2x10^5$ cells were seeded in 200 µl of serum free DMEM and added to the upper chamber of the insert. The plate was incubated at 37 ℃ and 5% CO_2 for 24 hours. Next day media was removed from the lower chamber and replaced with 450 µl serum free media containing 3.6 µl of Calcein-AM (8 µM, MW= 994.87) per well. Calcein-AM is a non-fluorescent permeable derivative of Calcein which becomes fluorescent on hydrolysis by cells. The plate was covered with foil after Calcein-AM addition and incubated for 45 minutes at 37 ℃ and 5% CO_2 incubator. After this, media was removed carefully from the upper chamber of the insert. The insert was transferred into a new well of a 24- well plate that contained 500 µl of pre-warmed Triple E and the plate was incubated for 10 minutes. The Plate was agitated 2-3 times during the 10 minutes to ensure all macrophages that attached in the inner part of the filter are detached and mixed into the triple E. The insert was discarded and 150 µl of this mix was then added to each well of 96 well plates (black-96-well plates with clear bottom). The amount of the fluorescence, which represented the number of migratory cells, was measured using the fluorescent plate reader POLARstar Omega – BMG Labtech GmbH (Rotenberg, Germany) on the excitation of 485 nm and emission of 520 nm. The relative fluorescence units (RFU) were correlated linearly with the number of cells. A schematic diagram illustrates the migration experiment and is shown in Figure 2.2.

1. Cell culture for 24 hours

Tissue culture plate
ThinCert ™
Upper chamber
PET membrane
Lower chamber

Without Serum

With Serum

2. Labelling of cells

Calcein-AM

3. Detachment of Cells

Trypl E ™

4. Fluorescence reading

485 nm – 520 nm
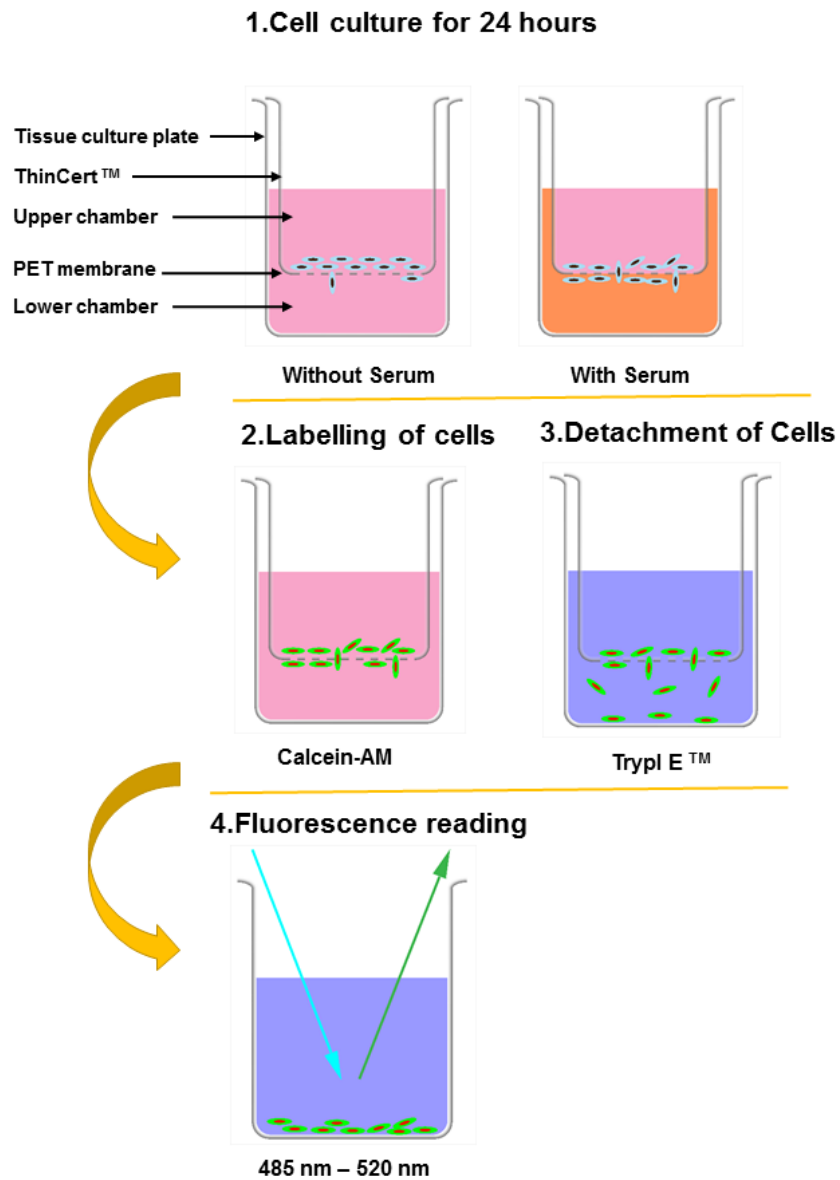
Figure 2. 2 Schematic illustration of cell migration assay

A ThinCert ™ cell culture insert is placed in the well of a 24-well plate. The migration chamber consists of an upper and lower compartment with a porous PET membrane in between. Active cells migrate from the upper to the lower compartment. Migration steps are schematically illustrated. The method was adapted and modified from Greiner Bio-one.

2.7 Cell Proliferation assay

Macrophages were isolated from both MKP-2$^{+/+}$ and MKP-2$^{-/-}$ mice and harvested on the third day of the culture. Cells were then seeded at a density of 4×10^4 per well of 96-well plate and allowed to attach overnight in complete DMEM media (10% FCS, 1% P/S and 1% L/G) without L-media. Next day, macrophages were pre-treated for 2 hours with either 100 ng/ml of LPS or with 100 ng/ml of rIL-4. This was followed by further stimulation with 10 ng/ml of M-CSF for 24, 48, 72 hours or left untreated as controls. Macrophage proliferation from both groups was assessed by using an anti-BrDU antibody detection assay kit which detects 5-bromo-2'-deoxyuridin (BrDU) incorporated into cellular DNA during cell proliferation. On each of the above time points, 10 µM BrDU was added to the plate and cells incubated for 6 hours at 37° C and 5% CO_2 incubator (the BrDU was added at the last 6 hours of each time point). Following the manufacturer's protocol, after the incubation with BrDU, media was removed from wells and 100 µl of the fixing and denaturation solution was added to each well and incubated at room temperature for 30 minutes. After this, the solution was removed and replaced by 100 µl BrDU detection antibody solution and the plate was incubated at room temperature for 1 hour. Following this step, the solution was aspirated from the wells and the plate was washed 3 times with 200 µl of 1x wash buffer (provided with kit). After last wash, 100 µl of freshly prepared 1x HRP-conjugated secondary antibody solution was added to each well and incubated at room temperature for 30 minutes. The solution was then aspirated and wells were washed for another 3 times with the 1x wash buffer. After the last wash, 100 µl of TMB substrate was added for 15-30 minutes at room temperature. The reaction was stopped by adding 100 µl stop solution and the BrDU was immediately measured using the polar star omega plate reader at absorbance 450 nm.

2.8 Polymerase chain reaction (PCR) amplification

In order to measure the endothelin-1 gene expression, quantitative real-time PCR technique was used as a quantified method that ensures high-quality, reproducible and biologically relevant results.

2.8.1 Sample preparation for gene expression study

Macrophages were cultured for seven days, then harvested and seeded in 6 –well plates in a density of $2x10^6$ cell / well in complete RPMI-1460 media. Two wells were used for each condition (meaning 4 million cells for each sample). Cells were left to rest overnight and next day, media was replaced by fresh media in all wells. Control cells were left without any treatment, other wells were treated with LPS (100 ng/ ml) for a time course from 0h, 2h, 4h, 6h, 8h, and 24 hours. Cells were processed to extract RNA.

2.8.2 RNA extraction using BioLine Isolate II RNA Mini Kit

Media was aspirated and 454.5 µl of prepared lysis buffer (450 µl RLY buffer+ 4.5 µl of 2 Mercaptoethanol) was added to the first well of each conditions and gently the plate were swirled and the 1ml syringe rubber was used to gently rub the cells down the well. Then this was transferred to the second well of the same condition and the same process was repeated to collect the cell lysate. Lysates were then loaded onto an isolate II filter (placed on 2 ml collection tube) and centrifuged for 1 minute at 11,000 xg. The flow though were passed 4-5 times through a nuclease –free 23 gauge needle. RNA binding condition was adjusted by adding equal amount of 70 % ethanol to the homogenised lysate and mixed by pipetting five times. This mixture was loaded onto an isolate II RNA mini column placed on a 2 ml collection tube. The column was further spun for 30 second at 11,000 xg. The membrane was desalted by adding 350 µl of desalting buffer (MEM). The membrane was dried by spinning for 1 minute at 11,000 xg. Next, DNA digestion buffer (15 µl of DNase + 135 µl reaction buffer for DNase, RDN) was added to the membrane in the column and incubated for 30 minutes at room temperature (this step is to remove any genomic DNA contamination). The membrane was washed once with RW1 buffer followed by two washes with RW2 before drying the membrane by centrifuge at 11,000 xg for 2 minutes (this step helps to remove genomic DNA and protein contaminants). RNA samples were eluted with 40 µl RNase-free water and spun for one minute at 11,000

xg. Total RNA was directly proceeded to RNA concentration step or stored at – 80˚C until use.

2.8.2.1 RNA concentration

Measuring RNA concentration is an important step when investigating gene expression changes. Thus normalising the RNA concentrations to use equal amounts of RNA from all conditions. NanoDrop (ND – 2000C, Thermoscientific), 220-750 nm spectrophotometer was used to measure the total RNA concentration. First, 2 µl of RNAs free-water was used as a blank. After this, the sampling platform cleaned each time prior to adding 2 µl from each sample to measure RNA concentration. The software displays the sample absorption curve as well as the calculated RNA concentration. Ratio of A 260 nm / 230 nm; A280 nm is also displayed. A ratio of A260 nm / A 230 nm of around 2.0 indicates low salt contamination or carryover. The ratio of A260 nm/ A280 nm should also be around 2.0 for pure RNA. All extracted RNA samples in this study had acceptable purity ratios 260/280 and 260/230.

2.8.3 cDNA synthesis using reverse transcriptase (RT)

To quantify the mRNA transcripts of genes under investigation, RNA was reverse transcribed to complementary DNA (cDNA) using Tetro cDNA synthesis kit (Bioline, USA) following the manufacturers manual. RNA concentrations were normalised between samples to 1µg. The volume was adjusted to 12 µl by adding RNase free-water. A master mix containing 1 µl of oligo (dt) as first –strand synthesis primer, 1 µl of 10mM dNTP mixture, 4 µl of 5 x RT buffer, 1 µl of Ribosafe RNase Inhibitor and 1 µl of Tetro Reverse Transcriptase (200 µg/µl) was added to each sample(containing the 12 µl RNA mixture). These samples were labelled "RT+". In order to check for the persisting contaminating genomic DNA, an additional reaction tube, labelled "RT-"was set up in parallel for each RNA samples. This reaction contained everything as described for the RT+ samples with the exception of the Tetro Reversed Transcriptase. After addition of all components, the reaction was mixed gently by pipetting, and incubated at 45˚C for 30 minutes. The reaction was terminated by incubating in at 85˚C for 5 minutes. cDNA samples were then stored at -20˚C until used as templates for the quantitative real-time PCR for gene expression analysis.

2.8.4 Primer design for SYBER select Master Mix assay

This section's aim is to design primers that only bind to selected target. This is to avoid primer dimers and non-specific products in SYBR®. Gene Runner software was

used to design primers which was then checked for being unique and specific using BLAST function of the National Centre for Biotechnology Information (NCBI) genome browser https://www.ncbi.nlm.nih.gov/tools/primer-blast/. Primer nucleotide sequence are shown in table 2.1.

Table 2. 1 Nucleotide sequences of the primers used for the analysis of gene expression by q RT-PCR

Primer name	Forward Primer (5' – 3')	Reverse Primer (5' – 3')
QARS	5'- GGA CTC CAG CTG AGC GCT GCT C 3'	5'-GGT GGA CTC CAC AGC TTC AAT-3'
Edn-1	5'- ACA CTC CCG AGC GCG TCG TA -3'	5'- TCT TGT CTT TTT GGT GAG CGC ACT G -3'

2.8.5 Quantitative Real-Time Polymerase Chain Reaction amplification (RT-qPCR)

The RT- qPCR assay was carried out using 2x Fast SYBR Green master mix (Life technologies). Into each well of Micro Amp ® Fast 96-well reaction plate (Applied Biosystems), 19 µl of a master mix was added plus 1 µl cDNA to be a final volume of 20 µl. The master mix consisted of 10 µl Power up SYBR green, 1 µl from each forward and reverse primers, and 7 µl nuclease free-water. RT- cDNA samples were included here and also a negative sample with no template (water instead) and a positive control of known primer was included as well. Plates were sealed with an optical adhesive cover (Applied Biosystems). The PCR reaction was performed in the Applied Biosystems Step One Plus real-time PCR system. The thermal cycle started by an initial Uracil-DNA glycosylase activation at 50 ˚C for 2 minutes and a second holding stage of Dual-Lock DNA polymerase at 95 ˚C for 2 minutes. This was followed by 40 cycle denaturation of 95 ˚C for 3 seconds and annealing of 60 ℃ for 30 seconds. The negative controls such as RT- and water blank gave undetermined Ct values as expected. Primers were obtained from Integrated DNA technologies.

2.8.6 Quantification method

Relative quantitative ΔΔCt also known as the comparative threshold method, was used to quantify real-time RT-qPCR results (Livak and Schmittgen, 2001). Levels of EDN1 expression were normalised to the levels of an endogenous housekeeping gene (QARS). The comparative threshold method was used to quantify relative gene expression compared to control using formula: Fold change = $2^{-\Delta\Delta Ct}$

Were ΔCt control = (Ct target gene – Ct reference gene); ΔCt stimulated = (Ct target gene – Ct reference gene); and $\Delta\Delta$Ct = ΔCt stimulated - ΔCt control.

2.9 Enzyme-Linked Immunosorbent assay (ELISA)

2.9.1 Measurements of Endothelin-1 (EDN1)

BMDMs were plated in 6-well plates and treated with LPS time course or inhibitors (cells were used for the RNA extraction and PCR). 1 ml of supernatant from each well was collected and used immediately for ELISA. In order to measure the protein levels of EDN1, mouse EDN1 ELISA kit (sandwich ELISA) was used from Lifespan biosciences, USA. The microtiter 96-well plate was pre-coated with a target specific capture antibody. Following manufacturer's instructions, 100 µl of standards (3.908 – 250 pg/ml), blanks or samples was added per well, covered with a plate sealer and incubated for 90 minutes at 37℃. After this, liquid was aspirated and 100 µl of 1x detection antibody was added to each well, covered as before, gently agitated and incubated for 1 hour at 37℃. Wells were than washed with wash buffer containing 0.1M PBS for three times allowing to sit 1-2 minutes before completely aspirating. The plate was dried then on clean absorbent paper. 100 µl of an Avidin Biotin- Peroxidase Complex (ABS) was added to each well, covered as before and incubated for 30 minutes at 37℃. Unbound ABS was washed 5 times as before. Then 90 µl of TMB substrate was added to each well, covered with a new plate sealer and incubated in dark for 15-30 minutes at 37℃ until optimal colour development was achieved. Finally, 100 µl of stop solution was added to each well and immediately was read at 450 nm by polar star omega plate reader (BMG Labtech).

2.9.2 Measurement of IL-1β

Supernatants from the metabolomics study were collected and stored at -20℃ until use. Mouse IL-1β ELISA kit (R&D system, Abingdon, UK) was used to measure production of IL-1β. Following manufacturer's instructions, 96 well ELISA plates, high binding (Greiner Bio One, UK) were prepared by adding 50 µl capture antibody (4µg/ml) diluted in coating buffer (PBS, PH 7.2). Plates were then washed three times in wash buffer containing (PBS, 0.5 % Tween 20) and dried by blotting. 200 µl assay diluent (PBS, 2 % BSA) was used for blocking and incubated at room temperature for 1 hour. After this, plates were washed as above and 50 µl of samples, blanks and standards (15.6-1000 pg/ml) were added to each well and incubated at 4 ˚C overnight. Next day, plates were washed five times in the wash buffer and dried. 50 µl of diluted

detection antibody (500 ng/ml) was added to each well and plates were incubated for 2 hours. This was followed by 5 times washes before adding the enzyme-streptavidin conjugate (diluted in assay diluent) and incubated for 20 minutes. Plates were washed for 7 times and dried before addition of 50 µl of TMB substrate solution until colour development. The reaction was stopped by adding 25 µl of $2NH_2SO_4$ and read at 450nm as before.

2.9.3 Measurement of IL-10

ELISA procedure for IL-10 was performed as mentioned above using the following;

- Capture antibody: Anti-mouse IL-10
- Detection Ab: Biotinylated Anti-mouse IL-10
- Streptavidin-horseradish peroxisome conjugate
- Standards: recombinant mouse IL-10 in serial dilutions of 31.3-2000 pg/ml.

2.10 Measurements of nitric oxide (NO) production in BMDMs

Macrophages were plated and stimulated with LPS (100 ng/ml) for a time course up to 48 hours. Supernatants were collected, centrifuged at 1000 rpm for 3 minutes and stored at -20°C until use. Samples were then thawed and 50 µl was added into each well of 96-well plates (triplicate wells included for each condition) also 50 µl of nitrite standards (doubling dilutions from 100 µM in RPMI media) was added as duplicate into the wells. Greiss reagent were mixed in a ratio of 1:1 [2% (w/v) sulphanilamide in 5% (v/v) H3PO4: 0.2% (w/v) naphylethylenediamine HCl in water]. 50 µl from this mixture was added to each well. The plate was incubated for 10 minutes at room temperature in the dark. The absorbance was read on a plate reader at 540 nm. The nitrite concentration (µM) for the samples were determined from the standard curve plotted using the standards ran on the same plate (Grisham *et al.*, 1996).

2.11 Macrophage treatment conditions for untargeted metabolomics study

BMDMs from both MKP-2^{+/+} and MKP-2^{-/-} mice were harvested on day 7 of culturing and mature macrophage populations were identified by flow cytometry. Macrophages were then plated at a density of $2x10^6$ cells / well of a 6- well plate containing 2 ml of complete RPMI-1640 (Gibco). Three replicates were used for each condition. Seeded macrophages were then left incubated in humidified incubator at 37°C and 5% CO_2 overnight to rest and attach:

1- To study the effect of LPS on MKP-2$^{+/+}$ and MKP-2$^{-/-}$ macrophage metabolome. LPS from *E.coli* was used at a concentration of 100 ng/ml for different time points (control, 5 minutes, 15 minutes (when MAPK is peaked), 2 hours (when MKP-2 is peaked) and 24 hours. After LPS stimulation, MKP-2$^{+/+}$ and MKP-2$^{-/-}$ treated macrophages were subsequently prepared for metabolite extraction to study the role of MKP-2 in metabolic changes induced by LPS in comparison to unstimulated macrophages.

2- Metabolic changes that occur during macrophage phagocytosis of zymosan particles in both MKP-2$^{+/+}$ and MKP-2$^{-/-}$ was studied. Same parameters that used in LPS was used simultaneously for zymosan. Zymosan particles were added at the same concentration that was used for the phagocytosis assay which was MOI of 10 for the same time points also. Treated extracts were used to compare and analyse the metabolic profile underlying MKP-2$^{+/+}$ and MKP-2$^{-/-}$ macrophage phagocytosis of zymosan.

3- To understand the differences in the migratory activity obtained between MKP-2$^{+/+}$ and MKP-2$^{-/-}$ towards a C5a gradient. C5a was added at a concentration of 20 nM which was exactly the same amount used for migration experiments. As in the LPS and zymosan, C5a was added for up to 24 hours. C5a treated cell extracts were used to identify and compare MKP-2$^{+/+}$ metabolome profile and MKP-2$^{-/-}$ metabolome profile.

All extracts (which were prepared in section 2.11.1) from 1, 2 and 3 were run on an Accela HPLC pump coupled to an Exactive (orbitrap) mass spectrometer, detailed in section 2.11.2, for untargeted metabolomics profiling.

2.11.1 Macrophage metabolites extraction protocol

After stimulation, supernatant media was aspirated and cell extracts were prepared by washing with warm PBS once. Then 1 ml of chilled extraction solution mix containing (Me OH / Me CN / H_2O, 50: 30:20 v/v) was added to each well that had 2×10^6 macrophages. A cell scraper was used to harvest cells. Cell lysates were then collected and shaken for 20 minutes at 1200 xg on a shaker at 4 ℃ before spinning at 0 ℃ at 13,000 xg for 15 minutes. Cell supernatants were then collected and transferred into auto sampler vials specific for loading into the LC-MS auto sampler.

2.11.2 Liquid chromatography / mass spectroscopy (LC-MS)

The conditions for the chromatography were set as fellow: AZICpHILIC column (150 x 4.6 mm x 5 μm) was eluted with a linear gradient over 30 minutes between 20 mM $(NH_4)2$ CO_3 (PH 9.2) / Me CN (20: 80) at 0 minute and 20 mM (NH4)2 CO_3 (PH 9.2) / Me CN (20: 80) at 30 minutes with a flow rate of 0.3 ml / minute. This was followed by washing with 20 mM $(NH_4)2$ CO_3 Me CN (95: 5) for 5 minutes which was followed by re – equilibration with the starting conditions for 10 minutes. LC/MS was carried out by using an Accela HPLC pump coupled to an Exactive (Orbitrap) mass spectrometer from Thermo Fisher Scientific (Bremen, Germany).

The spray voltage was 4.5 kV and 4.0 kV for the positive and the negative mode respectively. The ion transfer temperature was 275°C and sheath and auxiliary gas were 50 and 17 arbitrary units, respectively. A 75 to 12000 m/z was used as a full scan range for both positive and negative modes. The Xcalibur 2.1.0 software package (Thermo Fisher Scientific) was used to record the data. The signals of 83.0604 m/z (2x CAN + H) and 91.0037 m/z (2x formate – H) were selected as lock masses for positive and negative modes, respectively, during each analytical run. The orbital raw data was then processed using the software discussed in 2.11.3. A summary of metabolomics work flow is showed in Figure 2.3 below.
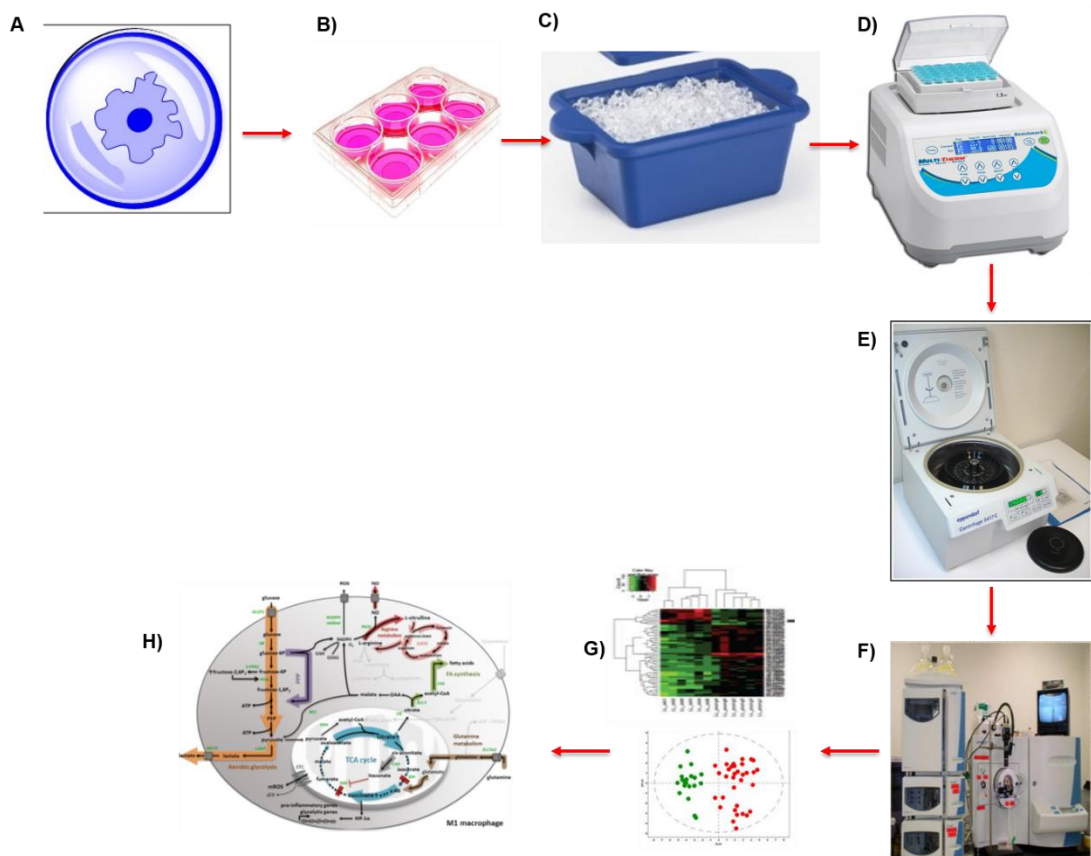
Figure 2. 3 Metabolomics work flow diagram

Macrophage metabolomics consisted of eight sequential steps: A- macrophage culturing and harvesting. B- Cell culture stimulation. C- Stopping metabolic reaction followed by metabolite extraction. D- Shaking cell extracts for further extraction. E- Centrifugation and collection of metabolite extracts. F- Data acquisition using MS-based spectroscopy techniques to generate chromatograms and MS spectra. G- Metabolic analysis and chemo metric analysis including univariate and multivariate analysis. H- Biological interpretation linking metabolomics to macrophage functions using metabolic network. Some of the illustration are adapted from (Geeraerts *et al.*, 2017)

2.11.3 Metabolomics data analysis

Raw data obtained from the untargeted metabolomics study was processed using Mzmine (Pluskal *et al.*, 2010). In order to further identify metabolites properly, data were processed in which metabolites that had low intensities and those that did not show any significant fold changes were excluded due to the difficulties in accurate detection and quantification.

Next, putatively identified metabolites were then further analysed and validated with SMICA version 14 (Umetrics, Umea, Sweden). Analysis involves univariate and multivariate analysis; cluster model creation using PCA (Principal Component Analysis) which provides a crude dataset overview and is used for initial exploration analysis and OPLAS-DA (Orthogonal Partial Least Square- discriminant analysis), for class discrimination, which integrates orthogonal signal correction. Partitioning of predictor variables improves both model transparency and interpretability (Bylesjo *et al.*, 2006, Trygg *et al.*, 2007).

The use of SIMCA software also will provide validity testing; outliers check; permutation, AUROC, regression analysis and cross validation (sensitivity and specificity of the created OPLS-AD model). Metabolite concentrations in some of the treatments designed above, were log- transformed to account for non – normal distribution of metabolite data, mean – cantered to improve interpretability of the models generated and scaled to unit variance in order to insure that all metabolites, both high range and low range, were treated equally when analysed. However, all fold changes were calculated from original intensities and not from transformed intensities. Xcalibure software / ToxID software were used for checking metabolites of interests to confirm existence of true peaks in comparison to standards.

In summary, samples were run on LC-MS to determine changes in the metabolite concentration in MKP-2$^{+/+}$ and MKP-2$^{-/-}$ macrophages. The programme, MZ mine 2.14, was used to search against the data base and matching standards, thousands of metabolites were identified to their exact mass and retention time in both groups. Univariate analysis of raw data followed by paired t-test and fold changes (ratio) was used to compare all time points in both group (see figures 1-9 in the appendixes). The selection of these relevant variables that have been significantly changed as a response to these impacts was based on calculation of the significance value of the variables ($P<0.05$). Metabolites were then analysed using MetaboAnalyst online server to match their pathways and categorised depending on this. Also each

metabolite was checked in the human metabolome database (HMDB) for their being registered and identified metabolites.

2.12 Data analysis

All data shown in this thesis were expressed as Mean ± SEM and were representative of at least three separate experiments. Statistical analysis was performed using Graph Pad Prism version 5.0 (Graph Pad Software, California). The statistical significance of differences between mean values from all groups were determined by one – way analysis of variance (ANOVA) with Bonferroni's multiple comparison test unless otherwise stated.

Chapter Three

The role of MKP-2 deletion in MAPK mediated signalling in macrophages and neutrophils

3.1 Introduction

As outlined in the introduction, the immune system has two arms of defence against pathogens; one is the innate immune response which is the first line to defend our body, the other the adaptive immune response that can be initiated by the innate response. Many immune cells contribute to these immune responses and interact with each other in a network to eliminate a pathogen. Amongst these cells, macrophages and neutrophils are intensely studied due to their critical functions and linked biological processes that are associated with inflammation and immune dysfunction. Both macrophages and neutrophils can behave differently depending on the stimuli and the microenvironment they are exposed to. Macrophages for example, have many cell surface receptors that interact with different stimuli to generate an innate immune response. These receptors include TLRs, scavenger receptors, complement receptors and Fc receptors (Taylor *et al.*, 2005).

Following receptor stimulation, a number of intracellular transduction pathways are activated which results in increased expression of a number of inflammatory genes. Understanding the contribution of each signalling cassette in these events and their dysregulation is an important step in understanding disease and possible routes to new therapies. Herein, the mitogen-activated protein kinase (MAPK) pathway is recognised as a major signalling cascade involved in modulating macrophage functions. As outlined previously, the major MAP kinases are extracellular signal regulated kinase (ERK), c-Jun NH_2-terminal kinase (JNK), and p38 MAP kinase which regulate many cell functions via their phosphorylation and activation of downstream substrates linked to macrophage responses (Huang and Tan, 2012, Bode *et al.*, 2012)

MKP-2 is one of a phosphatase family, known as the DUSPs, that inactivates MAPKs through de-phosphorylation at both phospho-threonine and phospho-tyrosine residues (Canagarajah *et al.*, 1997) Recent studies reveal that similar to the MAPKs, the MKPs have also crucial role in regulating cellular responses which in turn influence innate and adaptive immunity (Liu *et al.*, 2007, Crowell *et al.*, 2014). For example, MKP-2 can regulate the inflammatory responses via modulating MAPK pathways in macrophages (Cornell *et al.*, 2012, Barbour *et al.*, 2016). The deletion of MKP-2 was found to be associated with an increase in macrophage activity and cytokine production thought to be induced by JNK and p38 (Al-Mutairi *et al.*, 2010). Deletion of MKP-2 also affects macrophage growth and differentiation. This suggests a potential link between these kinases and MKP-2 in regulating macrophage functions.

Therefore, the aims of this chapter were first to establish the characteristics of macrophages in the context of LPS exposure. For this, activation of ERK, JNK, and p38 MAPK was assessed. These parameters where also examined in the context of MKP-2 expression. The importance of MKP-2 in the regulation of these kinases after LPS stimulation was then investigated in bone marrow derived macrophages (BMDMs) from both MKP-2 deleted mice (MKP-2$^{-/-}$) and MKP-2 wild type (MKP-2$^{+/+}$). The effect of MKP-2 deletion on the expression of the endothelin-1 gene (EDN1) was also assessed to determine if changes in MAP kinase signalling could be correlated with gene expression.

3.2 Results

3.2.1 The effect of innate activation on MAPK phosphorylation and signalling in BMDMs

Firstly, experiments were carried out in C57BL/6 mice as a background to the MKP-2 deleted mouse (MKP-2$^{-/-}$), MKP-2$^{-/-}$ mice were then used alongside their wild type counterparts (MKP-2$^{+/+}$) to study MKP-2 expression upon LPS stimulation in BMDMs.

Different concentration of LPS were used over a time course to produce innately and classically activated macrophages, then the deletion of MKP-2 correlated with changes in MAPK signalling. For this, different concentrations of LPS were prepared (1µg/ml, 100ng/ml as mentioned in 2.2.3-1). Normally, LPS is able to stimulate the MAPK signalling cascade in macrophages via the interaction with TLR-4 (Shweash, 2010). A time course of up to two hours stimulation with the two different concentrations of LPS was examined.

Results show increased phosphorylation of ERK (p-ERK) (figure 3.1) after 15 minutes stimulation with 100ng/ml LPS and from as early as 5 minutes when stimulated with 1µg/ml. Levels of p-ERK were highest after 15 minutes exposure to LPS at both 100ng/ml and 1µg/ml producing a fold increase of 67.79 fold ± 1.41 and 62.00 fold ± 2.12 respectively. The phosphorylation of ERK decreased gradually after 30 minutes stimulation and by 120 minutes returned towards basal for both concentrations (100ng/ml = 23.64 fold ± 2.01, 1µg/ml = 13.64 fold ± 2.16). This data confirms that phosphorylation of ERK is time dependent upon LPS stimulation and that both concentrations of LPS caused stimulation.

Results in figure 3.2 show a gradual increase in the phosphorylation of JNK (p-JNK) from 5 minutes exposure to LPS at both 100ng/ml and 1µg/ml. This increase in expression peaked at 30 minutes at 65.81 fold ± 4.55 (100ng/ml) and 53.43 fold ± 3.81 (1µg/ml) and then subsided over time such that at 120 minutes stimulations were 6.19 fold ± 3.86 and 14.04 fold ± 5.72 respectively. These results demonstrate that JNK phosphorylation is time dependant when activated with both concentrations of LPS with similar levels of stimulation.

Using same approach, levels of p38 phosphorylation were next examined (figure 3.3). A rapid increase in p38 phosphorylation (p-p38) was observed after 5 minutes stimulation with 100ng/ml and 1µg/ml LPS, producing an increase of 63.44 fold ± 1.99 and 65.50 fold ± 2.52 respectively. This increase was maintained at 15 minutes at

68.49 fold ± 3.50 (100ng/ml) and 68.98 fold ± 1.88 (1µg/ml). Levels of p-p38 then decreased by 60 and 120 minutes, however started to increase again when stimulated with 1µg/ml to 47.91 fold ± 5.06. These results indicate that overall the activation of p38 by LPS is also time dependent.
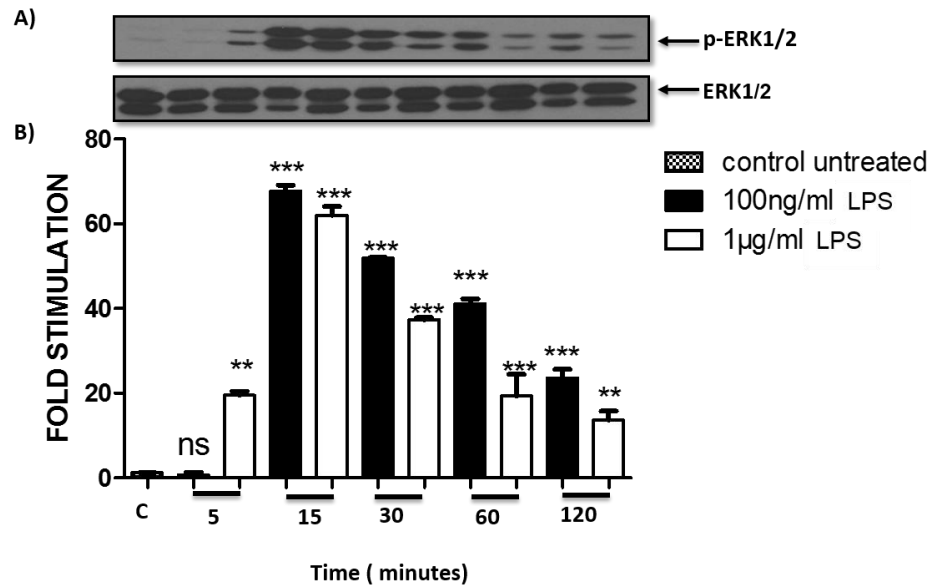
Figure 3. 1 LPS - mediated ERK phosphorylation in BMDMs

BMDMs were incubated in media or stimulated with 100ng/ml or 1µg/ml LPS for the indicated period of time. Whole cell extracts were prepared and protein levels were analysed by Western blotting and semi - quantified using densitometry. Results show (A) Western blot of p- ERK (42/44) kDa. Expression of total ERK was measured as a loading control. (B) Graph of p-ERK. Error bars represent the mean ± SEM of n=3. Data was analysed using one–way ANOVA test, * $P < 0.05$, ** $P < 0.01$, *** $P < 0.001$ compared to control.
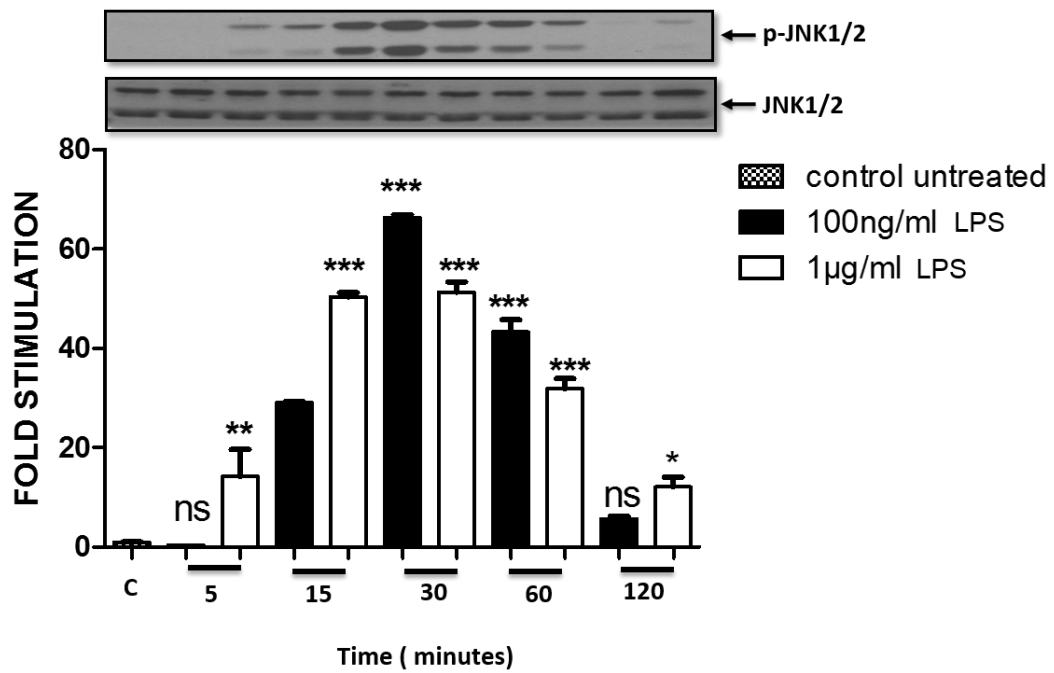
Figure 3. 2 LPS - mediated JNK phosphorylation in BMDMs

BMDMs were incubated in media or stimulated with 100ng/ml or 1µg/ml LPS for the indicated period of time. Whole cell extracts were prepared and protein levels were analysed by Western blotting and semi - quantified using densitometry. Results show (A) Western blot of p- JNK (46/54) kDa. Expression of total JNK was measured as a loading control. (B) Graph of p-JNK. Error bars represent the mean ± SEM of n=3. Data was analysed using one–way ANOVA test, * P < 0.05, ** P < 0.01, *** P < 0.001 compared to control.
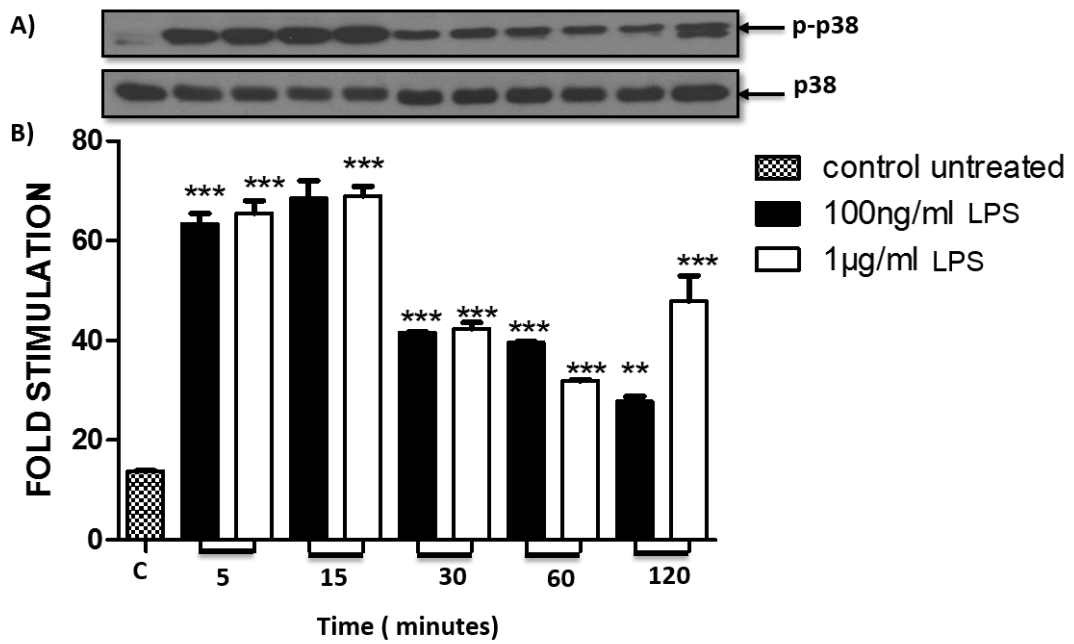
Figure 3. 3 LPS - mediated p38 phosphorylation in BMDMs

BMDMs were incubated in media or stimulated with 100ng/ml or 1µg/ml LPS for the indicated period of time. Whole cell extracts were prepared and protein levels were analysed by Western blotting and semi-quantified using densitometry. Results show (A) western blot of p-p38 (38 kDa). Expression of total p38 was measured as a loading control. (B) Graph of p-p38. Error bars represent the mean ± SEM of n=3. Data was analysed using one–way ANOVA test, ** $P < 0.01$, *** $P < 0.001$ compared to control.

3.2.2 Characterisation of the DUSP-4$^{-/-}$ mouse colony

Having established that macrophages could be properly isolated, cultured and stimulated appropriately, the next step involved assessing the respective DUSP4 colonies which had been back-crossed over 8 generations. In order to confirm MKP-2 deletion, mouse genotyping was repeated on a regular bases to ensure the purity of both MKP-2$^{+/+}$ and MKP-2$^{-/-}$ mice for macrophage generation. For this, tail or ear tips were collected from 6-week old, MKP-2 $^{+/+}$ and MKP-2$^{-/-}$ mice by the BPU staff and labled anonymously. Then, tissues were digested and genomic DNA extracted and analysed by PCR as mentioned in section 2.2.2. Genotyping identifed the MKP-2$^{+/+}$ allelle as a 1.2 kb band while the MKP-2$^{-/-}$ allelle was detected at 2.4 kb (figure 3.4). This result was consistent with previous findings (Al-Mutairi *et al.*, 2010). Deletion of MKP-2 protein was further confirmed later in this chapter by Western blotting.

3.2.3 Effect of MKP-2 deletion on the macrophage population

Before designing further experiments, macrophage populations from both MKP-2$^{+/+}$ and MKP-2$^{-/-}$ mice where characterised. To confirm that both mice give a mature macrophage population following culture, two unique macrophage surface markers F4/80 and CD11b were utilised. A cell population with dual staining for F4/80 and CD11b is considered as mature macrophages and thus can be used for further experiments. Results in figure 3.5 show that dual staining was observed in 93.9%, and 91.7% of MKP-2$^{+/+}$ and MKP-2$^{-/-}$ macrophages respectively. This indicates that deletion of the MKP-2 gene does not significantly alter macrophage characteristics, allowing furhter experiments to be conducted. Macrophage phenotype analysis continued alongside other experiments throughout the project to ensure that macrophages from both groups remained comparable. A dual positively stained population was routinely between 92 and 98% of the total cell population.
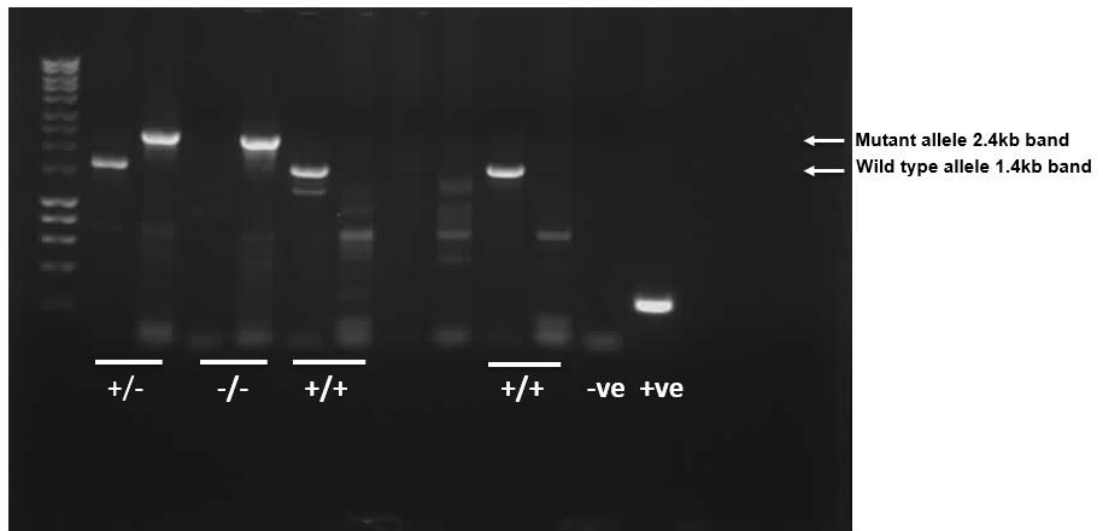
Figure 3. 4 Confirmation of MKP-2 deletion by genotyping

DNA was extracted from MKP-2$^{+/+}$ and MKP-2$^{-/-}$ ear tips and PCR performed using Thermoscentific Direct PCR master mix (as mentioned in the method section 2.2.2). Results show a 1.4 kb amplicon for the MKP-2$^{+/+}$ genotype and a 2.4 kb amplicon for the MKP-2$^{-/-}$ genotype. The PCR amplicon was resolved on a 1% (w/v) agarose gel. A 1 kb DNA ladder was used as a loading control. This data is representative of at least 4 other individual experiments.
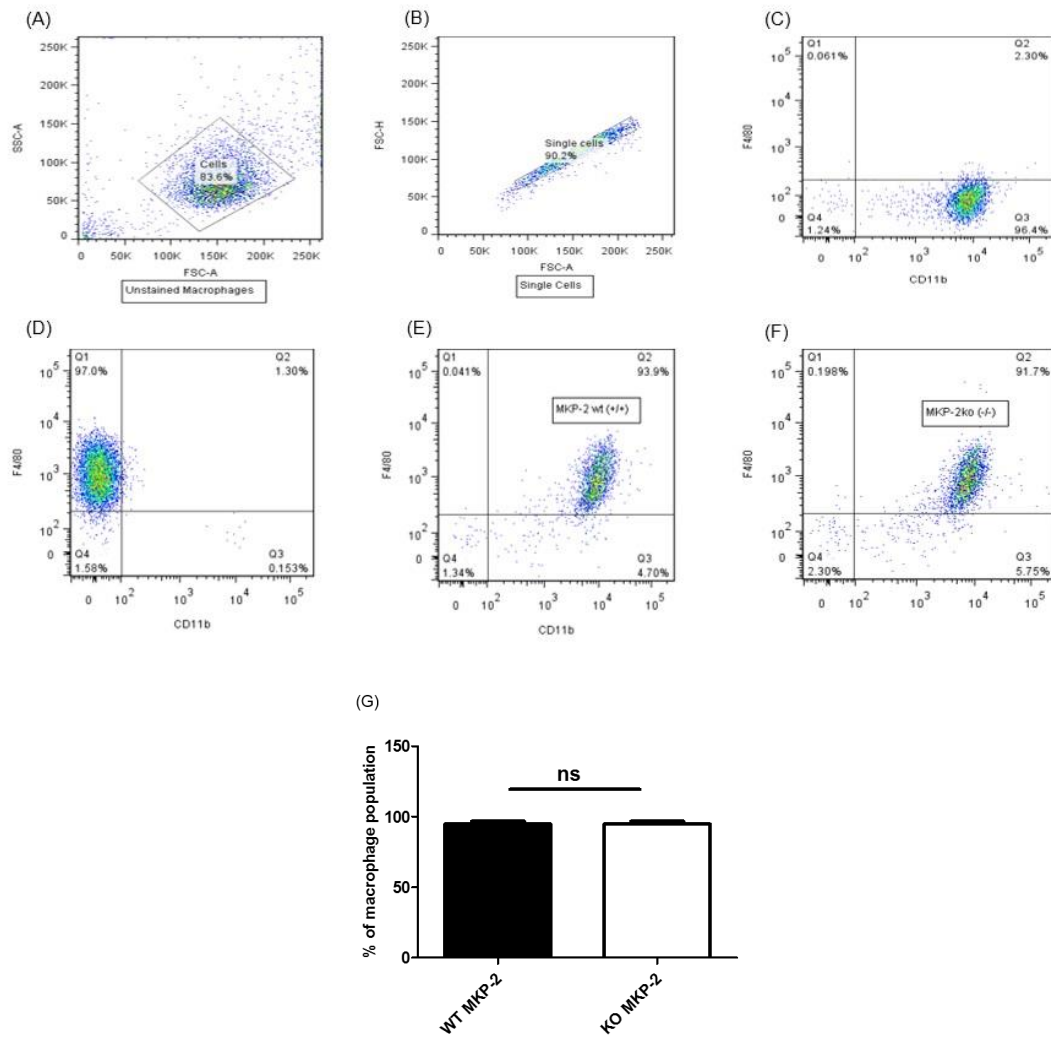
Figure 3. 5 MKP-2 gene deletion does not alter the macrophage population

BMDMs from MKP-2$^{+/+}$ and MKP-2$^{-/-}$ were cultured for 7 days and analysed by FACs analysis for F4/80 and CD11b as described in section 2.3. Gating represents A- unstained macrophages, B- single cells, C- CD11b positive cells, D- F4/80 positive cells, E & F- F4/80 and CD11b positive population of MKP-2$^{+/+}$ and MKP-2$^{-/-}$ respectively, G- macrophage population percentages. Gating performed according to FMO controls. FACS data represents the mean ± SEM of three seprate experiments. Data analysed using two- tailed unpaired t-test, P<0.05 in WT MKP-2 versus KO MKP-2.

3.2.4 The effect of MKP-2 deletion on LPS- mediated MAPK phosphorylation

The effect of LPS stimulation on BMDMs from wild type MKP-2 (MKP-2$^{+/+}$) and knock out (MKP-2$^{-/-}$) mice was studied in this section. As described earlier in this chapter macrophages from C57BL/6 mice were used initially to examine LPS concentrations that could activate MAPK signalling. Of these 100ng/ml of LPS successfully activated all three MAPK pathways and therefore this concentration was used to study this M1 phenotype in MKP-2$^{-/-}$ mice.

Figure 3.6 shows a significant increase in p-ERK levels after 5 minutes stimulation with LPS in both MKP-2$^{+/+}$ and MKP $^{-/-}$ macrophages. Fold stimimulations were 45.16 ± 1.41 and 41.55 fold ± 1.33 respectively when compared to controls. In general MKP-2$^{+/+}$ tended to have higher levels of ERK phosphorylation than MKP-2$^{-/-}$ macrophages but this trend did not reach significance. Stimulation in both populations was transient, levels decreased after 30 minutes and by 120 minutes were back to near basal levels in both wild type and MKP-2 deleted macrophages. This data demonstrates that LPS activates p-ERK in time-dependent manner, with the highest level of phosphorylation produced after 15 minutes of exposure. No significant differences were observed in p-ERK levels between MKP-2$^{+/+}$ and MKP-2$^{-/-}$ macrophages.

Similar to the findings produced in section 3.2.1, levels of p-JNK increased after 5 minutes exposure to LPS in both MKP-2 $^{-/-}$ and MKP-2$^{+/+}$ macrophages (Figure 3.7).

Intrestingly, over a number of experiments MKP-2$^{-/-}$ macrophages produced a higher increase in p-JNK at 5 minutes when compared to MKP-2$^{+/+}$ cells (54.61 fold ± 4.63 versus 44.42 fold ± 14.47). This difference was also recorded at both 15 (76.06 fold ± 0.45 versus 67.16 fold ± 9.72) and 30 minutes (57.88 fold ± 4.52 and 52.23 fold ± 14.95) for MKP-2 $^{-/-}$ versus MKP-2 $^{+/+}$ macrophage populations. Levels of p-JNK then decreased to almost basal levels at 60 and 120 minutes in both groups. These results demonstrate a possible role for MKP-2 in the regulation of JNK during M1 phenotype activation. The p38 results also showed a slightly increased p-p38 signal in MKP-2$^{-/-}$ macophages over MKP-2 $^{+/+}$ counteparts when exposed to LPS (figure 3.8). However again these results were not significant. Overall, these results indicate that deleting MKP-2 gene upregulates MAPK to some extent. This was observed clearly in the JNK levels more than p38 and ERK expression compared to the MKP-2 wild type counterparts.
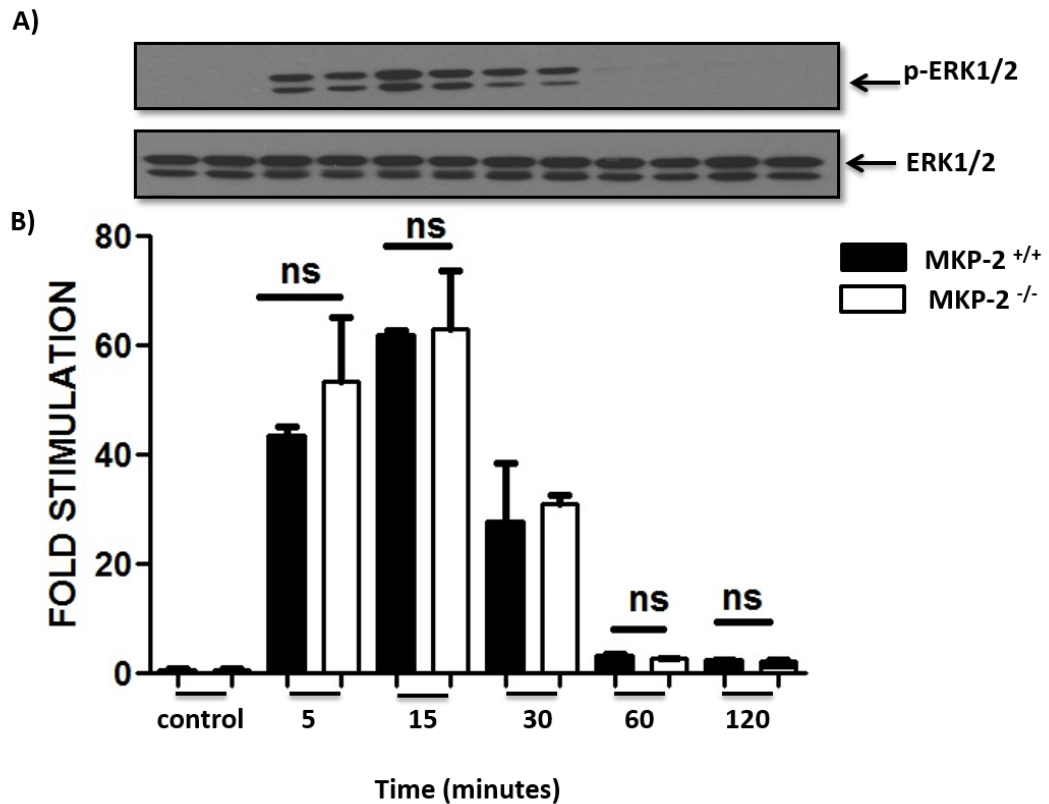
Figure 3. 6 The effect of MKP-2 deletion on LPS - mediated ERK phosphorylation in BMDMs

BMDMs from MKP-2$^{+/+}$ and MKP-2 $^{-/-}$ were incubated in media or stimulated with 100ng/ml LPS for the times indicated. Whole cell extracts were prepared and protein levels analysed by Western blotting and semi - quantified using densitometry. Results show (A) Western blot of p-ERK, 42/44 kDa. Total ERK was measured as a loading control. (B) Graph of p-ERK expression levels. Error bars represents the mean ± SEM of three individual experiments. Data was analysed using one-way ANOVA test, ns= not significant between MKP-2$^{+/+}$ versus MKP-2$^{-/-}$ mice.
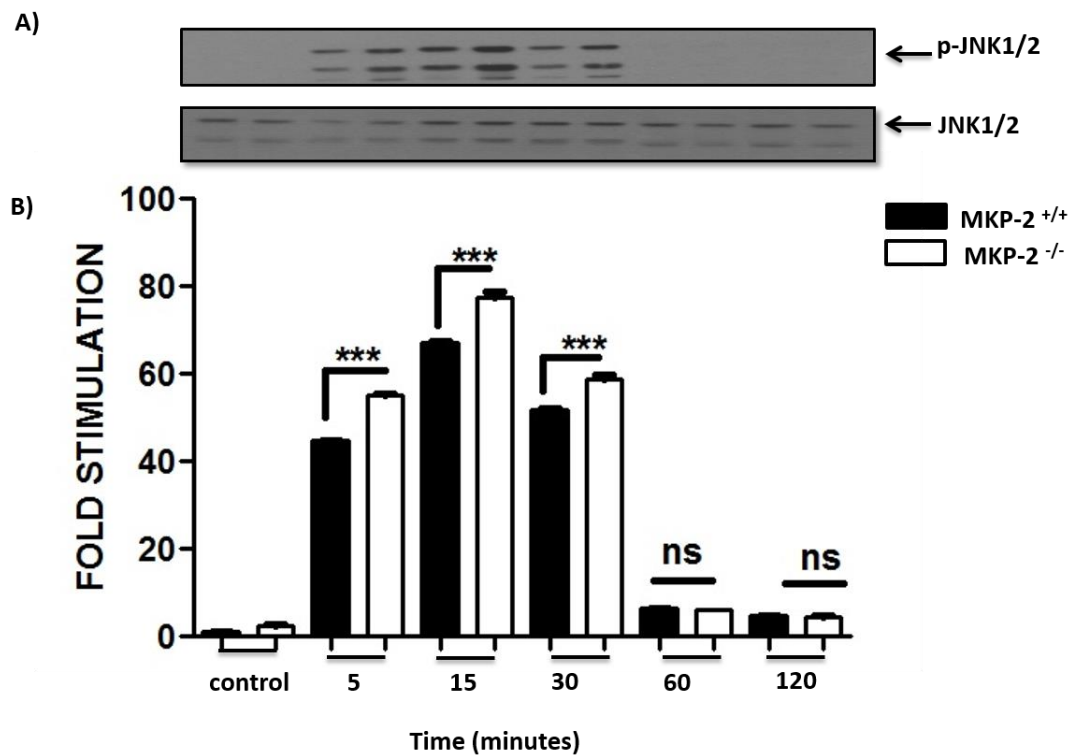
Figure 3. 7 The effect of MKP-2 deletion on LPS - mediated JNK phosphorylation in BMDMs

BMDMs from MKP-2^{+/+} and MKP-2 [-/-] were incubated in media or stimulated with 100ng/ml LPS for the indicated period of time. Whole cell extracts were prepared and protein levels analysed by Western blotting and semi-quantified using densitometry. Results show (A) Western blot of p-JNK (46/54) kDa. Expression of total JNK was measured as a loading control. (B) graph of p-JNK expression levels. Error bars represents the mean ± SEM of three individual experiments. Data was analysed using one-way ANOVA test were ns= no significance, *** $P < 0.001$ for MKP-2 [-/-] versus MKP-2^{+/+}.
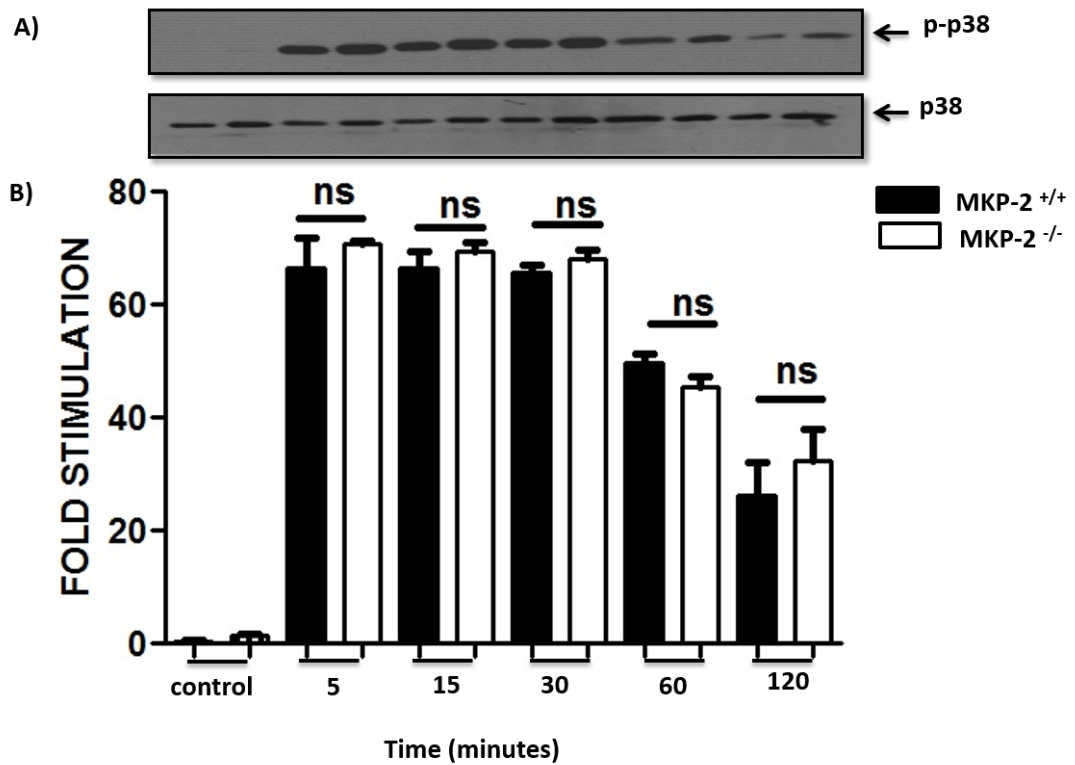
Figure 3. 8 The effect of MKP-2 deletion on LPS - mediated p38 phosphorylation in BMDMs

BMDMs from MKP-2$^{+/+}$ and MKP-2$^{-/-}$ mice were incubated in media or stimulated with 100ng/ml LPS for the times indicated. Whole cell extracts were prepared and protein levels analysed by Western blotting and semi-quantified using densitometry. Results show (A) Western blot of p-p38 (38 kDa). Expression of total p38 was measured as a loading control. (B) graph of p-p38 MAPK expression levels. Error bars represents the mean ± SEM of three individual experiments. Data was analysed using one-way ANOVA test were ns= no significance MKP-2 $^{-/-}$ versus MKP-2$^{+/+}$.

3.2.5 The effect of LPS on MKP-2 protein expression

In order to investigate the role of M1 activation of macrophages in MKP-2$^{+/+}$ mice, MKP-2$^{+/+}$ macrophages were stimulated with 100ng/ml LPS over a time course up to 9 hours. MKP-2 protein expression (figure 3.9) was significantly increased after 30 minutes to 55.29 fold ± 4.45 compared to the untreated control cells. MKP-2 expression continued to increase until two hours after which MKP-2 levels declined at 4 hours but then remained at approximately 30 fold basal values until 6 hours. The level of MKP-2 then dropped back to near the basal level after 9 hours of LPS stimulation the longest time point examined. These results suggests that M1 stimulation upregulates MKP-2 expression in a time dependent manner.
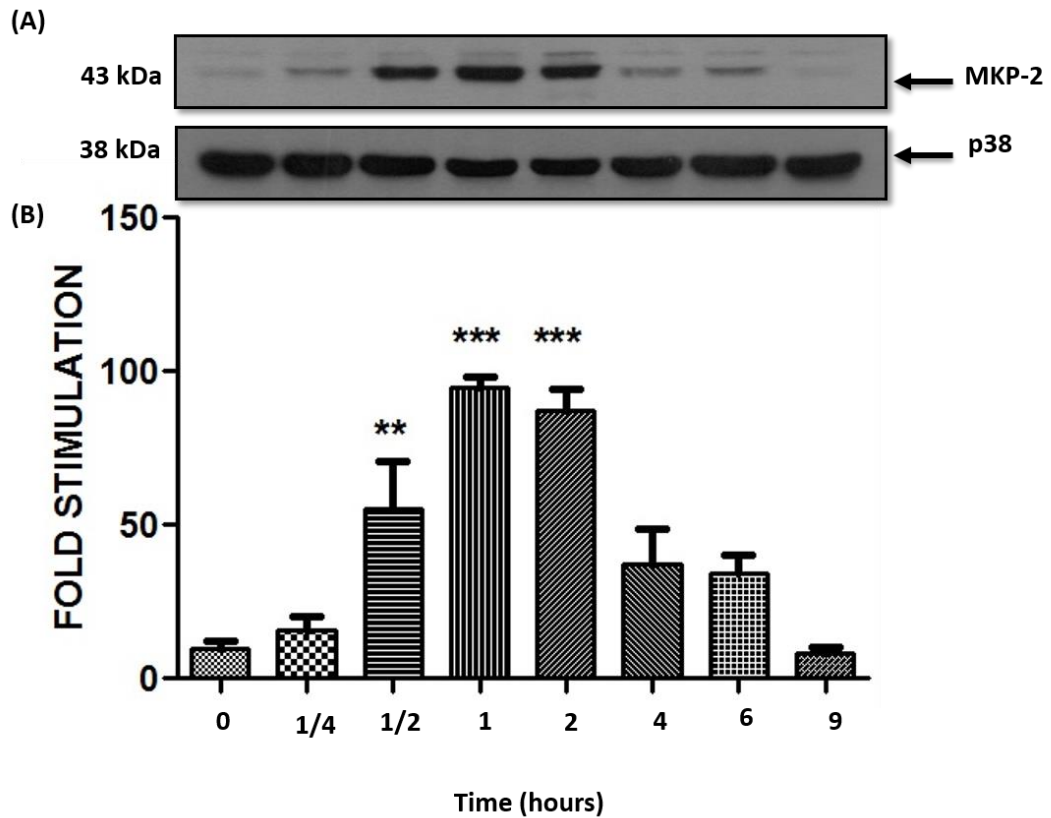
Figure 3. 9 MKP-2 upregulation in M1 activated macrophage phenotype

BMDMs from MKP-2 [+/+] mice were incubated in media or stimulated with 100ng/ml LPS for the indicated period of time. Whole cell extracts were prepared and protein levels were analysed by Western blotting and semi - quantified using densitometry. Result show (A) Western blot for MKP-2 (43 kDa). Expression of total p38 was measured as a loading control. (B) graph of MKP-2 expression levels. Error bars represents the mean ± SEM of three individual experiments. Data was analysed using one-way ANOVA test were ** $P < 0.01$, *** $P < 0.001$ verus control (0 h), n=3.

3.2.6 The Effect of MAPK inhibitors on MKP-2 protein expression

Since LPS stimulated activation of all three major MAP kinases and strongly induced MKP-2 protein expression it was decided to investigate the role of each MAP kinase in this process. This was achieved by utilising known selective inhibitors of each MAP kinase pathway. Macrophages were treated for 60 minutes with each compound to ensure adequate cellular penetration and cells stimulated with LPS for 2 hours, the time at which maximum MKP-2 expression was previously recorded.

Results in figure 3-10 show that LPS, as expected, stimulated an increase in MKP-2 expression to 44.44 fold ± 3.73 when compared to controls. However, the effect of LPS was decreased by approximately 50% to 23.23 fold ± 5.31 when macrophages were pre-treated with the MEK inhibitor, UO126, although there was also a small non-significant inhibitor effect of the DMSO vehicle. When MKP-2$^{+/+}$ macrophages were pre-treated with the p38 inhibitor SB203580 or the JNK inhibitor 6100025, there was no significant inhibitory effect. These results indicate that ERK is the main target that signals to MKP-2 expression and that ERK inhibition in turn reduces MKP-2 expression. In contrast, results also demonstrate that inhibition of JNK and p38 MAPK does not markedly alter MKP-2 expression.
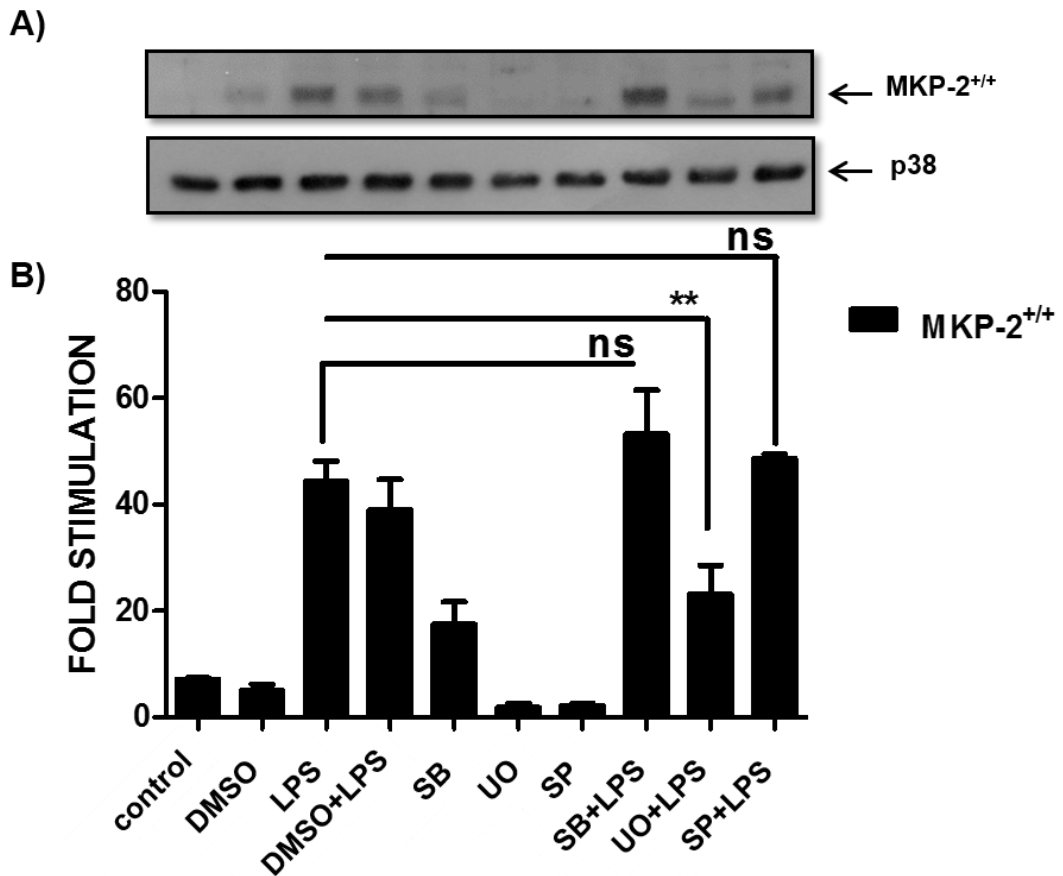
Figure 3. 10 ERK dependent MKP-2 expression

BMDMs from MKP-2 [+/+] mice were pre-treated with either DMSO or 10μM of SB203580 (SB), UO126 (UO) or SP600125 (SP) for one hour prior to stimulation with 100ng/ml LPS for two hours. Whole cell extracts were prepared and protein levels were analysed by Western blotting and semi - quantified using densitometry. Result show (A) Western blot of MKP-2 (43 kDa). Expression of total p38 was measured as a loading control. (B) graph of MKP-2 expression levels. Data represents the mean ± SEM of three individual experiments. Data was analysed using one-way ANOVA test, **$P < 0.01$ in WT LPS versus WT LPS + MAPK inhibitors.

3.2.7 The effect of MKP-2 deletion on neutrophil MAPK signalling

Having established the effects of MKP-2 deletion on MAP kinase signalling in macrophages it was decided to test if a similar effect was observed in neutrophils as a comparison. As mentioned earlier in this chapter, neutrophil responses differ depending on the stimulus and the surrounding environment. Amongst a number of inflammatory stimuli, LPS is reported to activate neutrophils via phosphorylation of MAPKs (Kim and Haynes, 2013). One major signalling pathway that drives neutrophil activation is p38 MAPK (Nick *et al.*, 1999). ERK is also involved in neutrophil functions (Simard *et al.*, 2015).

MKP-2$^{+/+}$ and MKP-2$^{-/-}$ neutrophils were isolated as described in section 2.2.6 and left to rest for 60 minutes before stimulation with 100ng/ml LPS. Surprisingly, results in figure 3.11 showed weak ERK activation in both wild type and MKP-2 deficient neutrophils after LPS stimulation. Basal values were variable and in MKP-2$^{+/+}$ higher than in MKP-2$^{-/-}$, whilst stimulation with LPS resulted in a decrease in the levels of ERK phosphorylation. There was no significant differences in ERK activation between MKP-2$^{+/+}$ and MKP-2$^{-/-}$ neutrophils. Similarly for p38 MAP kinase there was no consistent increase in p38 phosphorylation over the time course studied although there was a general lower level of phosphorylation in MKP-2$^{-/-}$ neutrophils (figure 3.12). Although samples were run for JNK, no signal was seen in any neutrophil samples.
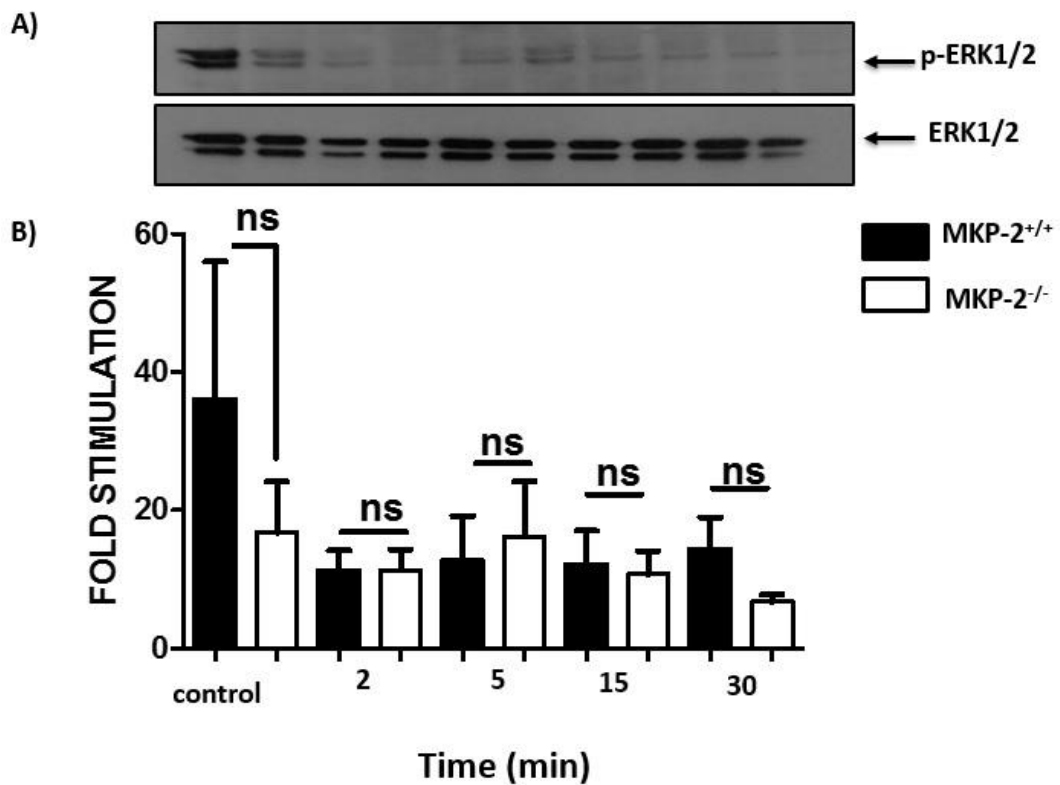
Figure 3. 11 The effect of MKP-2 deletion on LPS induced ERK signalling in neutrophils

Neutrophils were isolated from both MKP-2^{+/+} and MKP-2^{-/-} mice using Anti-LY-6G microbeads (specific for mouse) as described in section 2.2.6. After isolation, neutrophils were left one hour before stimulation with 100ng/ml LPS for the indicated time points. Whole cell extracts were prepared, and protein levels were analysed by Western blotting and semi - quantified using densitometry. Results show (A) Western blot of p-ERK (42/44) kDa in the MKP-2^{+/+} and MKP-2^{-/-} neutrophils respectively. Expression of total ERK was measured as a loading control. (B) Graph of p-ERK expression levels. Data represents the mean ± SEM of three individual experiments. Data was analysed using one-way ANOVA test, ns means no significance in MKP-2^{+/+} versus MKP-2^{-/-} neutrophils   .
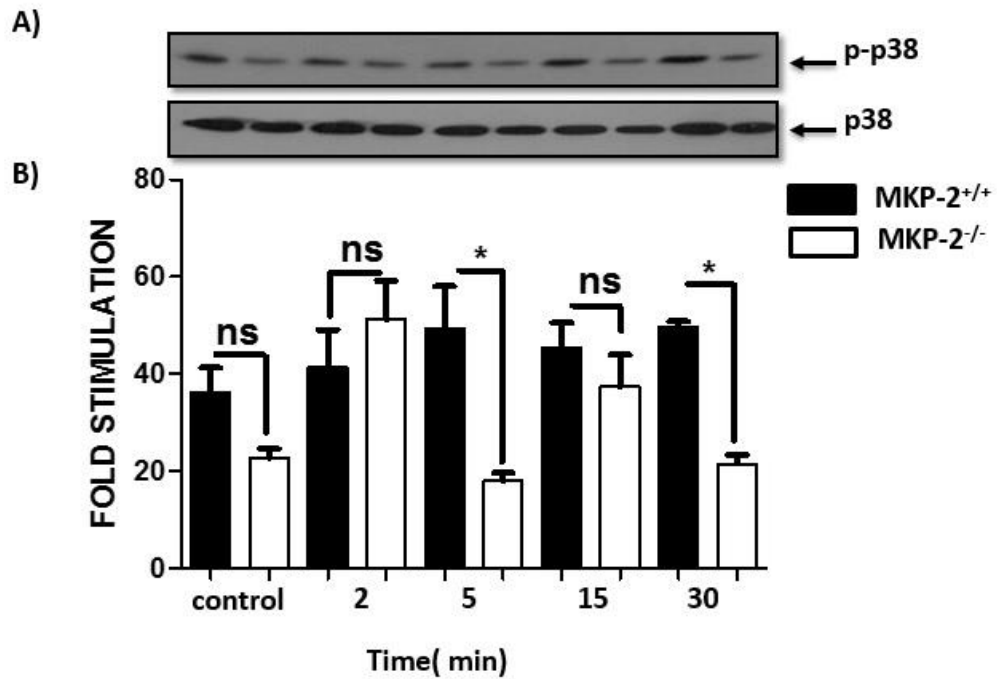
Figure 3. 12 The effect of MKP-2 deletion on LPS - mediated p38 signalling in neutrophils

Neutrophils were isolated from both MKP-2^{+/+} and MKP-2^{-/-} mice using Anti-LY-6G microbeads (specific for mouse) as described in section 2.2.6. After isolation, neutrophils were left one hour before stimulation with 100 ng/ml LPS for the indicated time points. Whole cell extracts were prepared, and protein levels were analysed by Western blotting and semi - quantified using densitometry. Results show (A) Western blot of p-p38 (38kDa) in the MKP-2^{+/+} and MKP-2^{-/-} neutrophils respectively. Expression of total p38 was measured as a loading control. (B) Graph of p-p38 expression levels. Error bars represents the mean ± SEM of three individual experiments. Data was analysed using one-way ANOVA test, * $P < 0.05$ in MKP-2^{+/+} and MKP-2^{-/-} neutrophils and compared to their controls.

Given the poor results with LPS it was decided to track MAPK signalling in neutrophils via the stimulation of the complement C5a or the leukotriene β_4 (LTβ_4) receptors. Both are G-protein coupled receptors and linked to neutrophil responses and functions. Results in figure 3.13 showed a rapid increase of ERK phosphorylation in MKP-2$^{+/+}$ neutrophils, reaching about 2-fold (2.13 ± 0.34) after 2 minutes following C5a treatment. This increased after 5 minutes to approximately to 6 fold (6.17 ± 1.65). In contrast there was very little stimulation in MKP-2$^{-/-}$ counterparts, the maximum stimulation observed was less than 1.5 fold (1.35 ± 0.18). C5a activation of ERK phosphorylation was reduced after 15 minutes and returned to basal values after 30 minutes in wild type neutrophils. These results demonstrate that MKP-2 deletion reduces C5a induced ERK activation in neutrophils.

Next, p38 MAP kinase activation was investigated in MKP-2$^{+/+}$and MKP-2$^{-/-}$ neutrophils following C5a stimulation. Results in figure 3.14 showed increased p38 phosphorylation after 2 minutes to about 2-fold of basal values (2.08 ± 0.43) in MKP-2$^{+/+}$ and to 1.5 fold (1.47 ± 0.12) in MKP-2$^{-/-}$ neutrophils although over a number of experiments this difference did not reach significance. Phosphorylation levels returned to near basal values by 30 minutes.
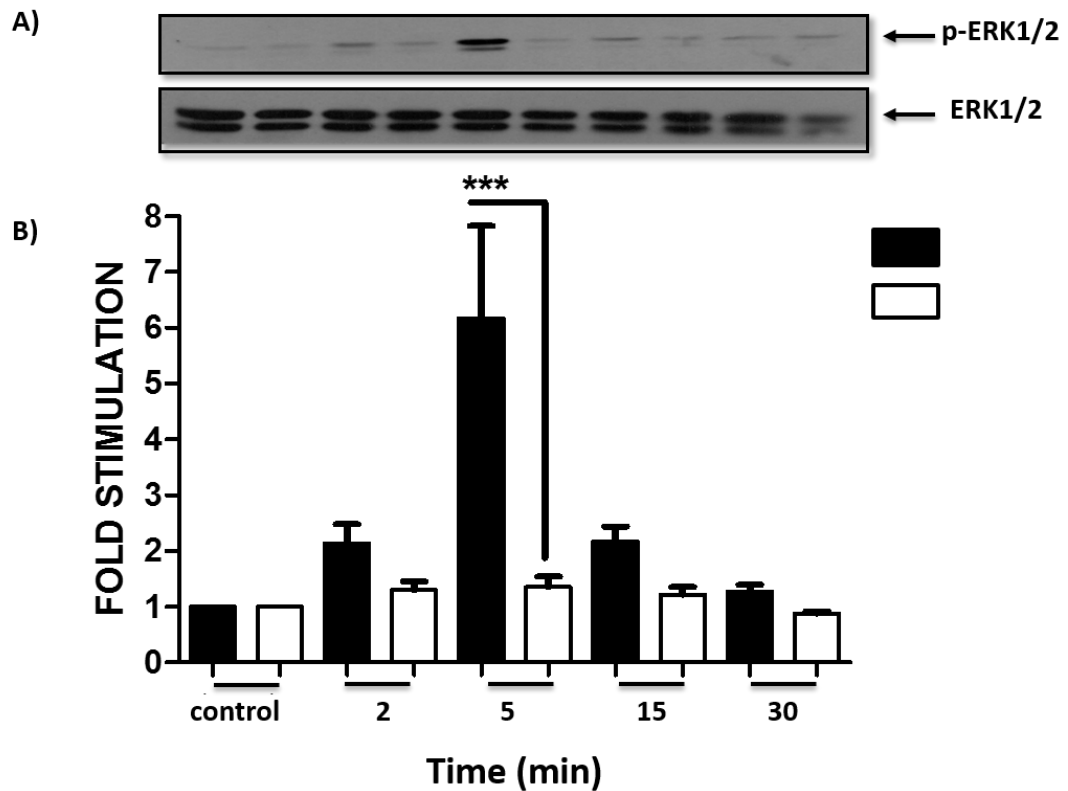
Figure 3. 13 MKP-2 deletion reduces C5a induced ERK activation in neutrophils

Neutrophils were isolated from both MKP-2$^{+/+}$ and MKP-2$^{-/-}$ mice using Anti-LY-6G microbeads (specific for mouse) as described in section 2.2.6. After isolation, neutrophils were left one hour before stimulation with 20 nM C5a for the indicated time points. Whole cell extracts were prepared, and protein levels were analysed by Western blotting and semi-quantified using densitometry. Results show (A) Western blot of p-ERK (42/44) kDa in the MKP-2$^{+/+}$ and MKP-2$^{-/-}$ neutrophils respectively. Expression of total ERK was measured as a loading control. (B) Graph of p-ERK expression levels. Error bars represents the mean ± SEM of three individual experiments. Data was analysed using one-way ANOVA test, *** P < 0.001 for MKP-2$^{+/+}$ versus MKP-2$^{-/-}$.
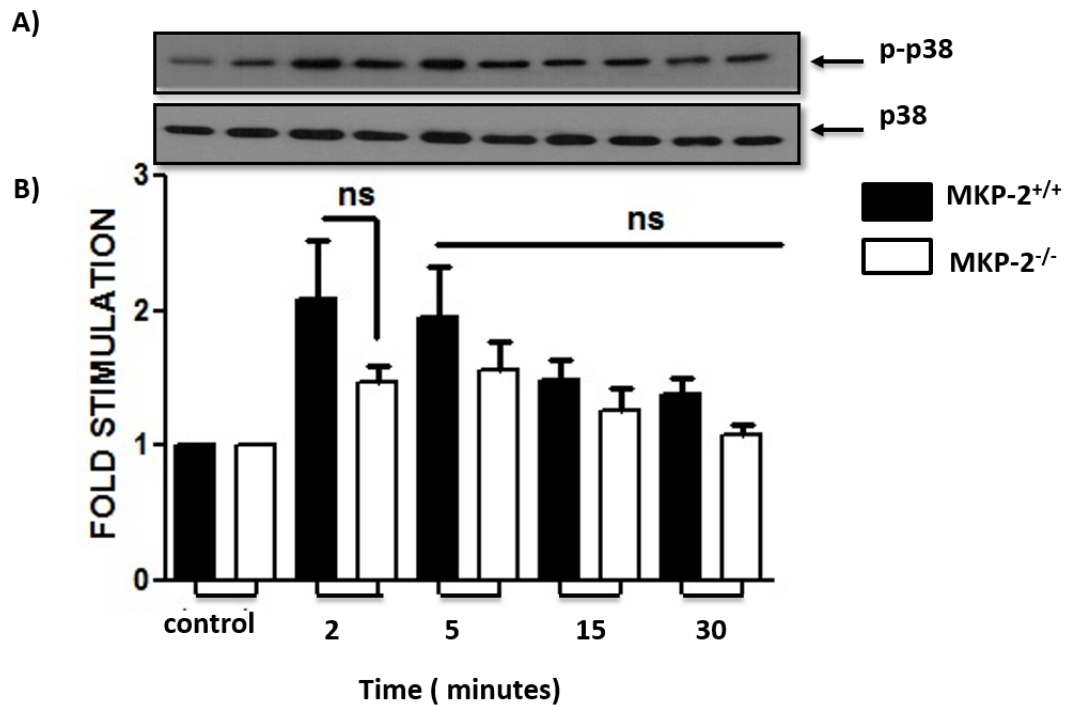
Figure 3. 14 MKP-2 deletion does not alter C5a induced p38 activation in neutrophils

Neutrophils were isolated from both MKP-2^{+/+} and MKP-2^{-/-} mice using Anti-LY-6G microbeads (specific for mouse) as described in section 2.2.6. After isolation, neutrophils were left one hour to rest before stimulation with 20 nM C5a for the indicated time points. Whole cell extracts were prepared, and protein levels were analysed by Western blotting and semi - quantified using densitometry. Results show (A) Western blot of p-p38 (38 kDa) in the MKP-2^{+/+} and MKP-2^{-/-} neutrophils respectively. Expression of total p38 was measured as a loading control. (B) Graph of p-p38 expression levels. Error bars represents the mean ± SEM of three individual experiments. Data was analysed using one-way ANOVA test, n.s means no significance in MKP-2^{+/+} versus MKP-2^{-/-}.

In additional experiments LTβ_4 was used to investigate the effect of MKP-2 deletion on neutrophil MAPK signalling as shown in figure 3.15. The results were similar to those observed with C5a. LTβ_4 stimulated a significant, 13 fold increase (13.44 ± 2.95) in phospho ERK in MKP-2$^{+/+}$ neutrophils at the 5 minute time point. In contrast, the response was much lower in MKP-2$^{-/-}$ neutrophils (8.67 ± 1.89). This was not due to reduced levels of total ERK in MKP-2$^{-/-}$ which were similar to MKP-2$^{+/+}$ neutrophils throughout.

Results in figure 3.16 show that LTβ_4 did not activate p38 pathway to the same extent shown for ERK pathway in neutrophils. MKP-2 deletion had no significant effect on this parameter.
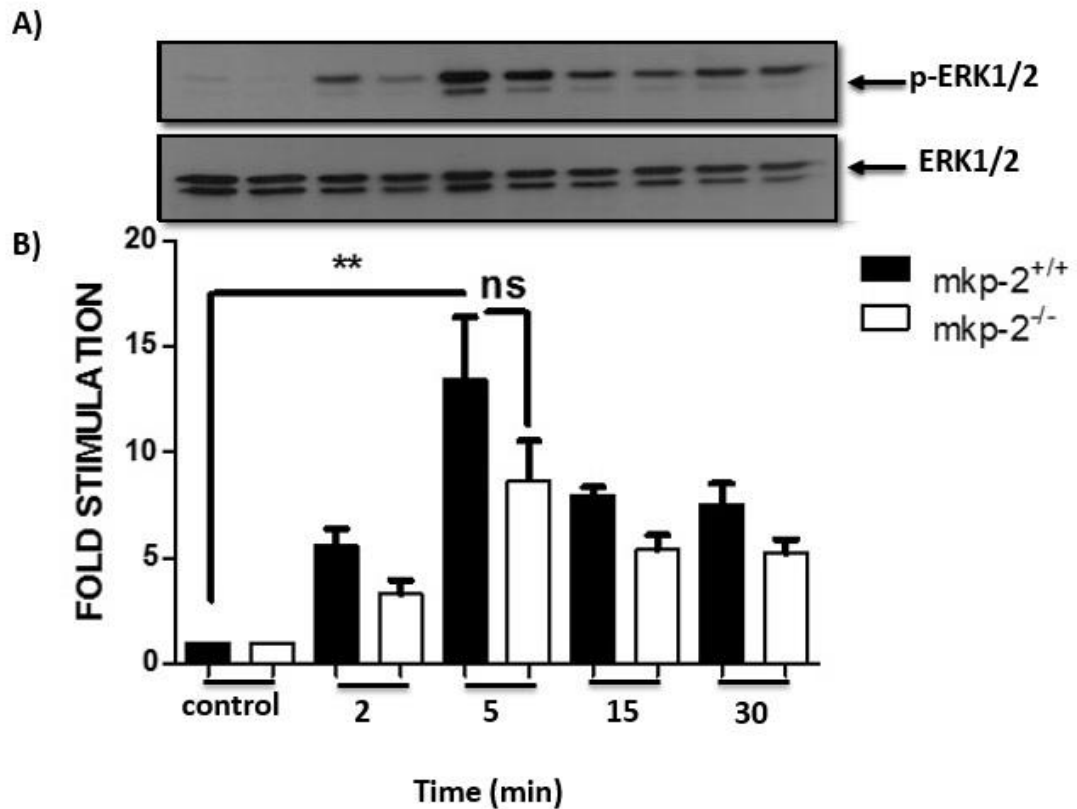
Figure 3. 15 The effect of MKP-2 deletion on LTβ₄ induced ERK phosphorylation in neutrophils

Neutrophils were isolated from both MKP-2$^{+/+}$ and MKP-2$^{-/-}$ mice using Anti-LY-6G microbeads (specific for mouse) as described in section 2.2.6. After isolation, neutrophils were left one hour before stimulation with 300 nM LTβ₄ for the indicated time points. Whole cell extracts were prepared, and protein levels were analysed by Western blotting and semi - quantified using densitometry. Results show (A) Western blot of p-ERK (42/44) kDa in MKP-2$^{+/+}$ and MKP-2$^{-/-}$ neutrophils respectively. Expression of total ERK was measured as a loading control. (B) Graph of p-ERK expression levels. Error bars represents the mean ± SEM of three individual experiments. Data was analysed using one-way ANOVA test, ** $P < 0.01$ in MKP-2$^{+/+}$ and MKP-2$^{-/-}$ versus controls.
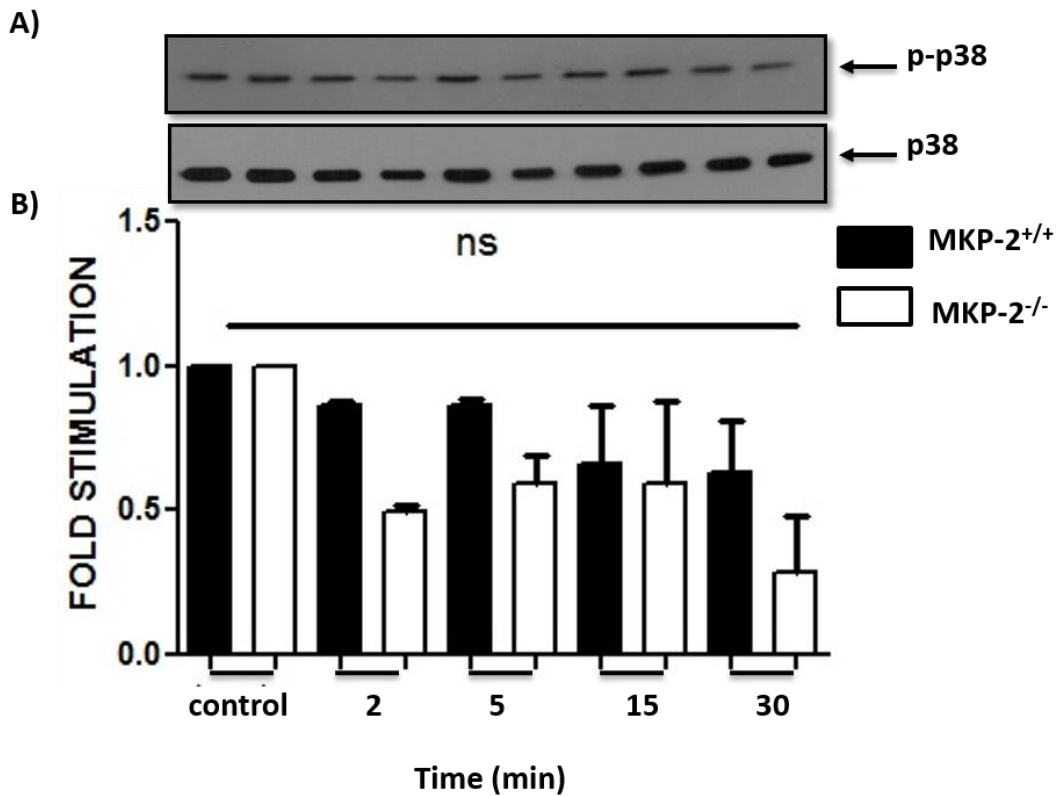
Figure 3. 16 The effect of MKP-2 deletion on LTβ₄ induced p38 activation

Neutrophils were isolated from both MKP-2$^{+/+}$ and MKP-2$^{-/-}$ mice using Anti-LY-6G microbeads (specific for mouse) as described in section 2.2.6. After isolation, neutrophils were left one hour to rest before stimulation with 300 nM LTβ₄ for the indicated time points. Whole cell extracts were prepared, and protein levels were analysed by Western blotting and semi - quantified using densitometry. Results show (A) Western blot of p-p38 (38kDa) in MKP-2$^{+/+}$ and MKP-2$^{-/-}$ neutrophils respectively. Expression of total p38 was measured as a loading control. (B) Graph of p-p38 expression levels. Error bars represents the mean ± SEM of three individual experiments. Data was analysed using one-way ANOVA test, ns = not significant in MKP-2$^{+/+}$ and MKP-2$^{-/-}$ versus controls.

3.2.8 The effect of MKP-2 deletion on endothelin-1 expression

Having established that LPS is associated with a small but significant up regulation of JNK, experiments were conducted to establish if a change in JNK signalling could be related to increased expression of JNK-dependent genes. Previous results from the laboratory have found that MKP-2 deletion is linked with enhanced IL-6, COX-2 and TNF-α expression (Al-Mutairi *et al.*, 2010). These genes are regulated at least in part by JNK signalling and many studies showed that expression of these genes are attenuated after JNK inhibition (Nieminen *et al.*, 2006, Ogata *et al.*, 2007, Kitanaka *et al.*, 2017). Whole genome array previously conducted in the Plevin's laboratory identified a number of macrophage genes up regulated following DUSP-4 deletion (Neamatallah, 2014). One of these genes encoded Endothelin-1 (EDN-1). Endothelin-1 is a vasoconstrictor protein originally found to be released by endothelial cells (Yanagisawa *et al.*, 1988), but also more recently in macrophages (Wahl *et al.*, 2005, Sikkeland *et al.*, 2012).

3.2.8.1 The effect of MKP-2 deletion on LPS mediated endothelin -1 (EDN1) gene expression in BMDMs

As mentioned above, data obtained from the gene array analysis that was carried out previously in Plevin's laboratory suggested that MKP-2 gene deletion affected the expression of other genes. From these genes, EDN1 was one of the genes that was elevated in MKP-2$^{-/-}$ macrophages compared to MKP-2$^{+/+}$ counterparts after 4 hours LPS stimulation, see table 3.1 data obtained from Neamatallah, 2014.

From this information, experiments were conducted to confirm the kinetics of EDN1 produced by macrophages following LPS challenge. As shown in Figure 3.17. LPS, in both set of macrophages, stimulated a significant increase in the EDN1 gene which peaked after 4 hours stimulation before returning to basal values over 24 hours. However, following MKP-2 deletion there was a significant potentiation of EDN1 expression to more than double that observed in wild type macrophages. Furthermore, whilst EDN1 expression decreased for both groups after 6 and 8 hours, levels remained significantly higher in MKP-2$^{-/-}$ macrophages at each time point. EDN1 gene expression levels then returned to the baseline after 24 h stimulation in both groups.

Table 3. 1 Endothelin 1 gene upregulation obtained from the gene array data from (Neamatallah, 2014) and selected to further investigation in the current thesis

Probe name	FC-MKP-2$^{+/+}$	FC-MKP-2$^{-/-}$	Gene symbol	Gene name
A_55_P2128144	4717.09	3292.84	Il19	interleukin 19
A_51_P363187	2975.03	1604.87	Cxcl1	chemokine (C-X-C motif) ligand 1
A_51_P254855	1850.59	1746.34	Ptgs2	prostaglandin-endoperoxide synthase 2
A_52_P100926	1758.98	1369.49	Il1α	interleukin 1 alpha
A_55_P1977008	1574.15	663.96	Gfi1	growth factor independent 1
A-51-P115005	1094.3	5176.78	Edn1	Endothelin 1
A_55_P1997756	769.02	742.88	Il6	interleukin 6
A_51_P217463	710.97	446.13	Cxcl2	chemokine (C-X-C motif) ligand 2
A_52_P399934	434.82	425.43	Dusp2	dual specificity phosphatase 2
A_51_P212782	423.49	494.97	Il1β	interleukin 1 beta
A_66_P109708	304.13	69.88	Il1f6	interleukin 1 family, member 6
A_55_P1971889	272.36	32.41	F3	coagulation factor III
A_51_P140710	46.82	110.86	Ccl3	chemokine (C-C motif) ligand 3

Macrophages from both MKP-2$^{+/+}$ and MKP-2$^{-/-}$ were stimulated for 4 hours with 100ng/ml LPS and data analysed for gene array analysis according to the above reference. Fold changes represents LPS treated cells and compared to that of untreated cells using one way ANOVA, $P<0.05$.
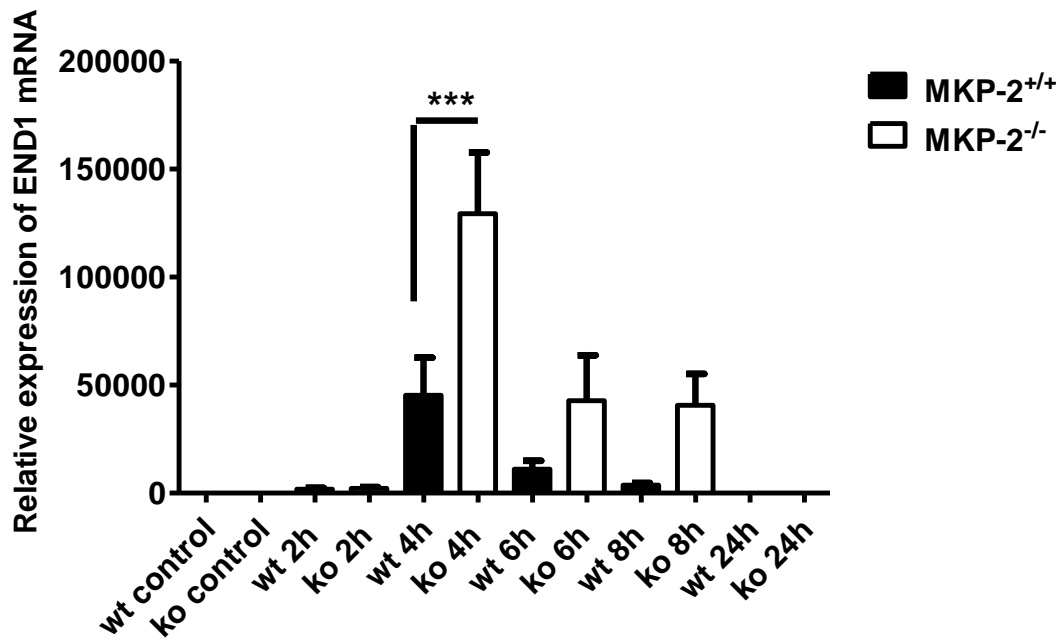
Figure 3. 17 MKP-2 deletion enhances LPS mediated EDN1 gene expression in BMDMs

BMDMs were harvested, seeded into 6 -well plates (2×10^6) then stimulated with LPS (100ng/ml) for the indicated times. Control cells were left untreated. Total RNA was prepared from cells and analysed by quantitative RT-PCR designed to detect EDN1 as described in section 2.8. Relative expression levels of EDN1 mRNA transcripts were normalized to the reference gene QARS using $2^{-\Delta\Delta CT}$ method (Livak and Schmittgen, 2001). Error bars represents the mean ± SEM from 5 individual experiments. ***P<0.001, Bonferroni's Multiple Comparison Test comparing MKP-2$^{+/+}$ vs MKP-2$^{-/-}$.

3.2.8.2 The effect of MAPKs inhibition on LPS-mediated EDN1 gene expression in MKP-2 deficient BMDMs

The previous section established that EDN1 was significantly elevated in MKP-2 deleted macrophages following LPS stimulation. This suggests a potential contribution by MAPKs shown to be increased following MKP-2 deletion. Cells were pre-treated with 10μM of MAPK inhibitors as follows: SB203580 (specific for p38), UO126 (specific for MEK1/2) or SP600125 (for JNK1/2) for one hour prior to LPS stimulation for 4 hours, the time at which the EDN1 expression was maximal. Cells were prepared as previously described for q RT-PCR analysis.

Results in Figure 3.18 show that LPS induced EDN1 gene expression in both groups as identified previously with again higher expression of EDN-1 in MKP-2$^{-/-}$ versus MKP-2$^{+/+}$ macrophages (*P<0.05). Treatment of cells with the inhibitors revealed different sensitivities in the expression of EDN1. Results showed that macrophage pre-treatment with the p38 inhibitor (SB203580), substantially reduced LPS-mediated EDN1 expression significantly in both groups by over 90% (26450 ± 378.80 to 2094 ± 222.25, LPS vs inhibitors in MKP-2$^{+/+}$; 43925.53 ± 7464.42 to 5647.53 ± 1300.41 in MKP-2$^{-/-}$). An almost equally pronounced level of inhibition was observed with the MEK1/2 inhibitor (UO126), reducing the LPS response by over 80%. For both inhibitors it was shown that the MKP-2$^{-/-}$ cells were a little bit more resistant to the inhibitors. However, for the JNK1/2 inhibitor (SP600125), at the concentration employed, there was a much smaller level of inhibition of the EDN1 gene, values were not significantly different to LPS stimulated levels. These results suggests that EDN1 gene expression might be correlated with p38 or ERK1/2 signalling rather than JNK.
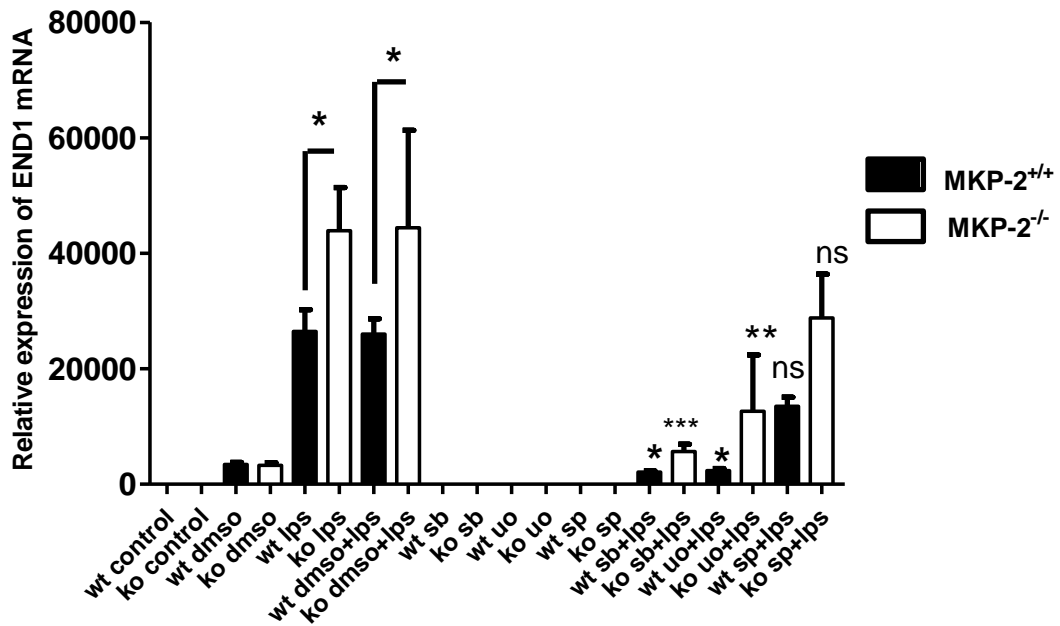
Figure 3. 18 The effect of MAPK inhibitors on LPS induced EDN1 gene expression in BMDMs

Macrophages were harvested, seeded into 6-well plates ($2x10^6$) and pre-stimulated with 10μM of either p38 inhibitor (SB203580), ERK1/2 (UO126) or JNK1/2inhibitors for one hour prior stimulation with LPS (100ng/ml) for 4 hours. Control cells were left untreated. Total RNA was prepared from cells and analysed by quantitative RT-qPCR designed to detect EDN1 as described in section 2.8. Relative expression levels of EDN1 mRNA transcripts were normalized to the reference gene QARS using $2^{-\Delta\Delta CT}$ method (Livak and Schmittgen, 2001). Error bars represents the mean ± SEM from 5 individual experiments.*P<0.05, **P<0.01, ***P<0.001, Bonferroni's Multiple Comparison Test comparing MKP-2$^{+/+}$ vs MKP-2$^{-/-}$.

3.2.8.3 Detection of EDN1 protein expression by ELISA

Having established that EDN1 mRNA levels were markedly increased in MKP-2$^{-/-}$ compared to MKP-2$^{+/+}$ macrophages, an ELISA assay was performed to confirm that this effect was reflected in protein synthesis. Macrophages were stimulated with 100ng/ml of LPS over a time course up to 24 hours and supernatants collected to determine the presence and levels of EDN1 protein. As shown in Figure 3.19, EDN1 protein levels increased significantly in both wild type and MKP-2 deleted macrophages stimulated in response to LPS. The expression of END1 increased more rapidly in MKP-2$^{-/-}$ macrophages and after 4 hours had reached approximately 9 fold compared to a negligible release in MKP-2$^{+/+}$ macrophages (KO= 9.49 ± 0.57 vs WT=0.16 ± 0.04 pg/ml, n=3). After 6 hours EDN1 protein peaked for both groups but again was markedly higher in MKP-2$^{-/-}$ compared to MKP-2$^{+/+}$ macrophages (WT=34.55 ± 4.07 vs KO, 55.52 ± 1.53 pg/ml, n=3). This trend remained consistent after 8 hours stimulation with LPS before returning basal levels after 24 hours. Collectively, these results confirms that EDN1 expression is upregulated following MKP-2 deletion at both the mRNA and protein levels.
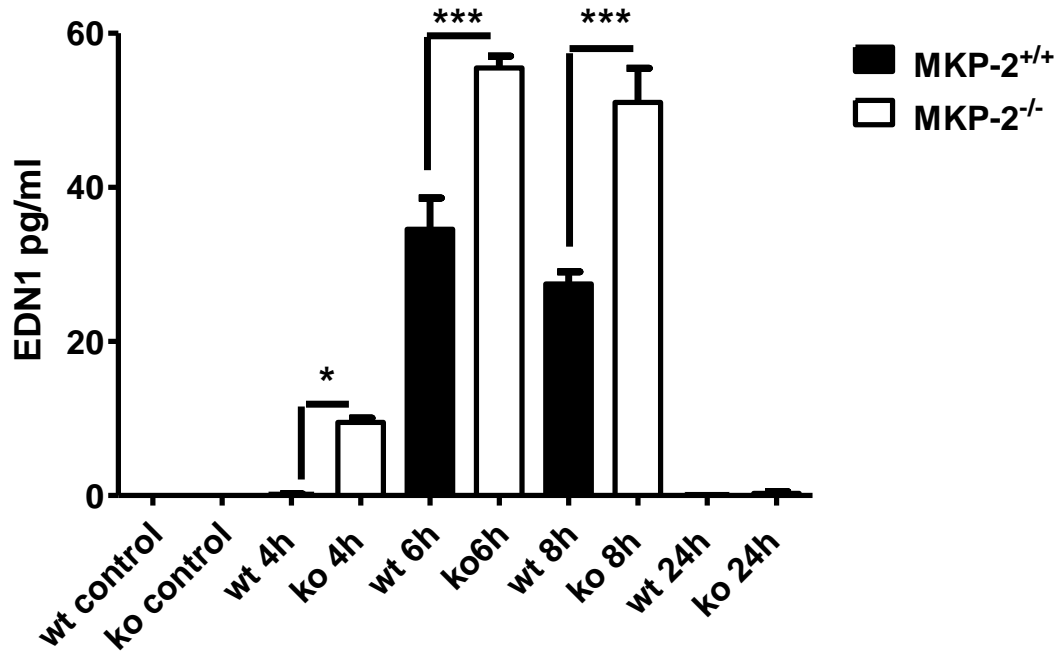
Figure 3. 19 Enhanced EDN1 protein expression in MKP-2$^{-/-}$ BMDMs

Macrophages were harvested, seeded into 6-well plate at a density of $2x10^6$ and incubated overnight. Cells were then stimulated with LPS (100ng/ml) for the indicated periods of time. Controls were left untreated. Supernatant were collected and used immediately to assess EDN1 protein levels by ELISA as described in section 2.9.1. The graph shows representative data from three individual experiments. Error bars represents the Mean ± SEM. *P<0.05, ***P<0.001, Bonferroni's Multiple Comparison Test comparing MKP-2$^{+/+}$ vs MKP-2$^{-/-}$.

3.2.8.4 The effect of MAPK inhibition on LPS-mediated EDN1 protein levels in MKP-2 deficient BMDMs

After confirming the expression of EDN1 protein by ELISA, the next challenge was to investigate the effect of MAPK inhibitors on LPS induced EDN1 protein release. Macrophages were pre-treated with 10µM of either UO126, SP600125 or SB203580 for one hour prior to LPS stimulation for a further 6 hours. Results shown in Figure 3.20 were contradictory to those obtained when examining mRNA levels. Experiments revealed that none of the MAPK inhibitors had a significant inhibitory effect on LPS induced EDN1 production in either macrophage population. In MKP-2$^{-/-}$ macrophages there was a slight decrease in EDN1 level when macrophages were pre-treated with ERK1/2 and JNK1/2 inhibitors but this effect was not statistically significant.

Surprisingly, the p38 inhibitor increased LPS induced EDN1 in both groups by almost as much as 100%. In short, results demonstrated that enhanced EDN1 production and release in MKP-2 deleted macrophage was not MAPK dependent and another cellular event might drive this effect.
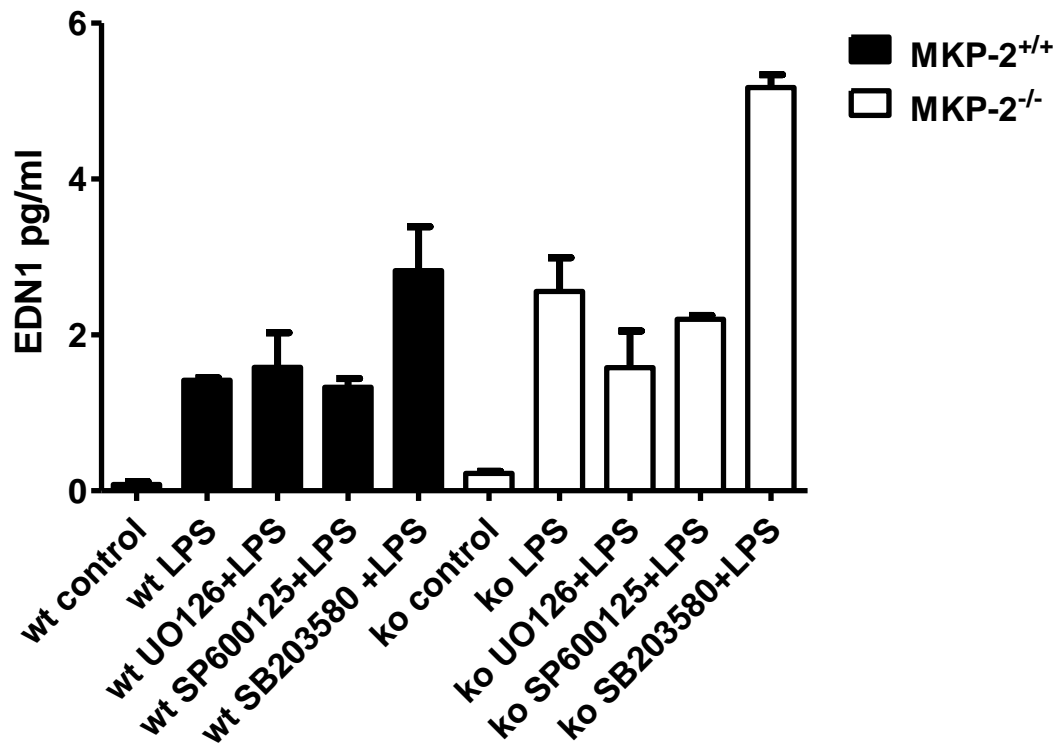
Figure 3. 20 The effect of MAPK inhibitors on the expression of EDN1 protein

Macrophages were harvested, seeded into 6 - well plates ($2x10^6$) and pre-stimulated with 10μl of either p38 inhibitor (SB203580), ERK1/2 (UO126) or JNK1/2 inhibitor (6000125) for one hour prior stimulation with LPS (100ng/ml) for 6 hours. Control cells were left untreated. Supernatant media were collected and used immediately to assess EDN1 protein expression by ELISA as described in section 2.9.1. Data represents mean ± SEM from two individual experiments.

3.3 Discussion

MKP-2 is a type 1 member of the dual specificity phosphatase (DUSP) family that has been shown to regulate the inflammatory response to pathogens such as *Leishmania*, *toxoplasma* and viral infection (Al-Mutairi *et al.*, 2010, Woods *et al.*, 2013, Jiao and Zhang, 2014). This regulation is different depending on the stimuli and the cell type. However, the role of MKP-2 in other immune responses has not been extensively investigated in different classes of innate immune cells.

Generating a DUSP-4 knock out mice has helped to further dissect the role of MKP-2 in the immune response in a way similar to MKP-1 (DUSP-1) and MKP-3 (DUSP-6) (Al-Mutairi *et al.*, 2010). Our lab successfully generated such a model and initially used it to study macrophage function in relation to parasite infection (Woods *et al.*, 2013, Schroeder *et al.*, 2013). However, mice from early backcrosses where utilised can lead to misleading results due to genetic variation of the background C57BL/6 strain. In this study, cells from the 8th generation were utilised and found to be functionally similar in both WT and KO mice as defined by known macrophage markers F4/80 and CD11b.

LPS stimulation was initially used to drive macrophages into the "M1 phenotype" a pro-inflammatory phenotype. Present results showed that LPS mediated ERK, JNK and p38 phosphorylation was time and concentration dependent. All three kinases increased and peaked between 15 - 30 minutes after stimulation. These results were consistent with other studies findings which showed increased ERK, JNK and p38 after LPS stimulation in murine macrophages (Zhou *et al.*, 2014, Guo *et al.*, 2015, Hashimoto *et al.*, 2017). Other studies have demonstrated that this is mediated via TLR-4, macrophages from TLR4 KO mice showed substantial reduction in activation of all three MAPKs (Shweash *et al.*, 2011).

Next, the effect of MKP-2 deletion on LPS - mediated MAPK phosphorylation was studied. MKP-2$^{-/-}$ macrophages showed slightly increased ERK levels (figure 3.7) after 5 minutes exposure to LPS compared to MKP-2$^{+/+}$ macrophages . This is similar to a previous study from our laboratory using early generation macrophages (Al-Mutairi *et al.*, 2010). Another study using a different DUSP-4 deletion model (Cornell *et al.*, 2012) demonstrated an increase in ERK signalling in the absence of MKP-2. Interestingly, levels of JNK were elevated significantly in MKP-2 deleted macrophages (figure 3.8) compared to MKP-2$^{+/+}$ macrophages. This confirms the negative regulatory effect of MKP-2 on JNK that was found previously in our laboratory (Al-

Mutairi *et al.*, 2010). Interestingly ERK rather than JNK is the preferred substrate for MKP-2 at least *in vitro* (Misra-Press *et al.*, 1995). However, it has been previously shown that adenoviral mediated infection with MKP-2 inhibits JNK activity (Al-Mutairi *et al.*, 2010, Lawan *et al.*, 2012). Furthermore, it was found in this study that MKP-2 deletion did not result in any effect on p38 MAPK phosphorylation. Other groups using their own DUSP-4 KO model (Cornell *et al.*, 2010) found decreased JNK and p38 MAPK after MKP-2 knockdown in alveolar macrophages. Also another group demonstrated that MKP-1 is a stronger regulator of p38 inhibition in LPS treated macrophages (Hu *et al.*, 2007). These data indicate that this p38 is not the preferred substrate for MKP-2 activation.

As mentioned earlier LPS drives macrophages to a pro-inflammatory phenotype. Therefore, It was decided to investigate the role of "M1 activation" on MKP-2 protein expression in MKP-2$^{+/+}$ macrophages and correlate this with the MAPK signalling pathway. Results show (figure 3.9) that LPS stimulated induced the upregulation of MKP-2 expression in a time dependent manner. MKP-2 protein levels peaked at 1-2 hours after LPS activation. These results were largely consistent with the kinetics of MAP kinase activation particularly JNK. The results are also similar to those obtained by other reports that studied induction of MKP-2 activity after TLR4 stimulation of BMDMs (Al-Mutairi *et al.*, 2010) and alveolar macrophages (Cornell *et al.*, 2012).

Furthermore, the study also implicated a role for ERK signalling in the expression of MKP-2 itself as shown by the strong inhibition of expression by the MEK1, 2 inhibitor USO126. This is consistent with a number of studies showing reduced expression of MKP-1 and MKP-2 following ERK inhibition, indicative of a regulatory effect for ERK in RAW264.7 macrophages (Crowell *et al.*, 2014). Other pathways have also been implicated and these include p53 (a tumour suppressor protein) (Zhang *et al.*, 2015). For human MKP-2, few studies have been able to identify the mechanisms regulating expression (Balko *et al.*, 2013).

The second part of the chapter examined whether the effect of MKP-2 deletion in macrophages was consistent with neutrophils, another immune cell implicated in the response to pathogens (Nick *et al.*, 1999). The interaction between neutrophils and macrophages triggers an inflammatory response that involves both cells working together in eliminating a pathogen and resolution of inflammation (Gomes *et al.*, 2010).

Initial results however, showed weak ERK activation in both MKP-2 $^{+/+}$ and MKP-2 $^{-/-}$ neutrophil populations in response to LPS. Similarly, other reports found that LPS alone did not activate ERK and JNK phosphorylation in neutrophils (Riedemann *et al.*, 2004, Crowell *et al.*, 2014). Other research has also demonstrated no or low CD14 and TLR4 expression in LPS stimulated neutrophils (Gomes *et al.*, 2010). So as an alternative, two other known neutrophil activators were tested namely C5a and LTβ_4 (Riedemann *et al.*, 2004). The cognate receptors for both agonists have been shown to be linked to ERK and p38 MAP kinase pathways but with less of an effect on JNK (Jiang *et al.*, 2015). For both stimulants it was found that ERK activation was reduced following MKP-2 deletion. These results are not as expected; MKP-2 deletion might be expected to enhance ERK signalling and again suggests that DUSP-4 deletion has an effect on cells which is independent of effects upon MAPK signalling. The results in this chapter represents the first attempt to characterise the role of MKP-2 gene deletion in neutrophil MAPK activation by C5a. However, a similar phenomenon has been observed previously using macrophage progenitors stimulated with GM-CSF, a pronounced reduction in ERK signalling with no effect on p38 (Neamatallah, 2014) suggesting a bonafide phenomenon. It is unclear if this effect is linked to the mechanism of action of ERK by all GPCRs or is restricted to certain classes or even different cell types.

Irrespective of the mechanisms underpinning the deletion for the C5a and also LTβ_4 the results do have implications for neutrophil function. ERK is known to act as a negative regulator of neutrophil migration (Liu *et al.*, 2012) whilst p38 and JNK are known as positive regulators (Moriwaki and Asahi, 2017, Rosa *et al.*, 2016). Therefore, the selective loss of ERK stimulation will result in enhanced migration to a number of target tissues and organs. In addition, ERK regulates the production of cytokines including IL-6 (Riedemann *et al.*, 2004, Seow *et al.*, 2013) which is known to prevent migratory function from being excessive and terminating the immune response via STAT3 (Fielding *et al.*, 2008). There are a number of disease conditions where neutrophil migration is enhanced therefore MKP-2 may have a role in limiting this function.

A final element of the chapter was to correlate the increase in JNK activity with JNK dependent gene expression. Previously, in the laboratory it has been shown that deletion of MKP-2 can enhance COX-2 expression. COX-2 expression is known to be regulated by number of signalling pathways including JNK (Nieminen *et al.*, 2006,

Kitanaka *et al.*, 2017, Park *et al.*, 2007). Therefore rather than examine COX-2 as a JNK dependent gene another gene was chosen, EDN1. This target identified by a macrophage gene array study.

An initial finding in this chapter was that LPS strongly induced the EDN1 gene and this result was consistent with findings from other groups. For example, another study demonstrated that 6 hours stimulation with LPS increased EDN1 gene expression levels in hepatic macrophages and also in BMDMs (Mckenna *et al.*, 2015). The latter study and others suggested that this increase in expression was NF-κB dependent in macrophages but not in endothelial cells (Sen and Smale, 2010, Quehenberger *et al.*, 2000). Another group demonstrated that c-Src dependent activation of ERK and JNK is required to induce EDN1 in vascular smooth muscle cells (Simo-Cheyou *et al.*, 2016). These data point to cellular differences in the predominant pathway regulating EDN1 expression.

In order to further dissect the exact signalling pathway that is involved and to determine if the enhanced expression of EDN1 is a reflection of the enhanced activation of JNK signalling, MAPKs inhibitors were used. The results showed that the expression of EDN1 gene may be regulated by ERK activation or by p38 and to a far lesser less extent by JNK. The correlation was even less marked when EDN1 protein release was analysed by ELISA, there was no apparent inhibitory effect of any of the compounds and indeed there was substantial enhancement of END1 released following p38 inhibition. It is possible that a substantial inhibition of mRNA still allows sufficient synthesis and release of the protein or that substantial END1 protein is already stored and only requires intracellular trafficking and post translational modification. However, this remains unlikely. The results do however point to a substantial effect of MKP-2 deletion on EDN1 synthesis but the effect is again unlikely to involve a mechanism linked to MAPK activation.

Nevertheless the observations regarding EDN1 are intriguing. A number of studies have correlated increased levels of EDN1 with LPS induced endothelial cell injury which promotes smooth muscle cell contraction to increase vasomotor tone (Freeman *et al.*, 2014, Horinouchi *et al.*, 2013). Furthermore, macrophage release of EDN-1 from hepatic macrophages is far greater than from endothelial cells suggesting a new source of EDN1 which could be used therapeutically in sepsis (Mckenna *et al.*, 2015).

A number of studies also suggest strong cross talk between EDN1 expression and NO production (Rapoport, 2014, Labonte *et al.*, 2008, Bourque *et al.*, 2011). Both are

produced in opposition to each other and the ratio between them is the key regulator in maintaining cardiovascular homeostasis and preventing endothelial dysfunction (Labonte *et al*., 2008). In this regard it is interesting that previous results from the Plevin laboratory show reduced iNOS progression and a diminution of NO production in MKP-2$^{-/-}$ macrophages (Al-Mutairi *et al*., 2010). Given these contradictory outcomes it would have been of interest to examine the overall effects in smooth muscle cells since macrophage infiltration into the vessel can result in profound remodelling effects (Friedl and Weigelin, 2008). In a preliminary experiment carried out using Trans well assay system, results showed an increase in VSMC proliferation in the presence of MKP-2 deleted macrophages stimulated with LPS, suggesting the expression and release of END1 is potentially significant.

In summary, in this chapter it has been shown that there are some changes in kinase activation following MKP-2 deletion in the two white blood cell types. In macrophages this is JNK and in neutrophils, ERK. However, ascribing these effects to expression of genes such as EDN1 in macrophages has not been convincing. It seems likely that in addition to effects upon MAPK signalling there is an additional mechanism which underpins the profound changes MKP-2 deletion has on macrophage function.

Chapter Four

Investigating the role of MKP-2 in macrophage phagocytosis, migration, proliferation and the metabolomics profile underlying each process

4.1 Introduction

Macrophages display a wide range of functions that regulate both innate and adaptive immune responses due to their plasticity. They express many cell surface receptors that recognise pathogens and engulf them by phagocytosis (Rougerie *et al.*, 2013). Macrophages also migrate to the site of infection and contribute to the inflammatory response by releasing pro- inflammatory or anti- inflammatory cytokines depending on the surrounding environment (Italiani, 2017). Proliferation is another function that has been found to play a critical role in the development of metabolic syndrome where macrophage proliferation acts reduce blood glucose (Nawaz *et al.*, 2017, Amano *et al.*, 2014). Through these functions macrophages are now thought to be a critical therapeutic target in many human diseases such as, atherosclerosis, cancer, diabetes, fibrosis and other immune diseases (Na *et al.*, 2018).

The processes outlined above are regulated by a number of cell signalling pathways including the MAPK cascade, for example in one study ERK has been shown to play a vital role in macrophage proliferation and migration but inhibition of p38 and JNK promotes macrophage proliferation and suppresses motility and apoptosis (Guo *et al.*, 2018, Rao *et al.*, 2002) In addition, p38 has been implicated in the inflammatory response of macrophages via the upregulation of TNF-α, IL-10 and COX2 expression (Meng *et al.*, 2014, Yang *et al.*, 2014). Another study by Guo *et al.*,2015 showed that inhibiting MAPK, ERK, p38, or JNK could supress macrophage activation in adipocytes via peroxiredoxin (PRX)-like-2 activated in macrophages (PAM), thus enhancing anti-inflammatory function (Guo *et al.*, 2015).

However in contrast, little work has been done on regulation of MAP kinase signalling by MKPs in the context of these events. Amongst the DUSP family only MKP-1 has been studied for balancing macrophage migration and phagocytosis via MAPK dephosphorylation (Lloberas *et al.*, 2016), although one recent paper has revealed an inhibitory role of MKP-2 in this process (Jiao *et al.*, 2015). The hypothesis presented here is given that MKP-2 is implicated in regulating immune responses in response to infection by *Leismania* and *Toxoplasma* (Al-Mutairi *et al.*, 2010, Woods *et al.*, 2013, Parveen *et al.*, 2018) this response may involve changes in macrophage phagocytosis and motility.

In order for macrophages to perform functions listed above, they require metabolic changes to match the energy demands (Traves *et al.*, 2012, Nathan, 2002) and recent studies have linked macrophage functions to their metabolic status. It is well

established that activating macrophages to a pro-inflammatory phenotype upregulates nitric oxide synthase (iNOS) which results in the catabolism of arginine to citrulline and nitric oxide, which in turn, plays a vital role in the intracellular killing of pathogens (Galvan-Pena and O'neill, 2014). In contrast, the same group and others demonstrated that activating macrophages to an anti-inflammatory phenotype produces Arginase-1 which in turn produces urea, polyamine and ornithine, all key factors in the wound healing action of this phenotype (Shearer *et al.*, 1997, Witte and Barbul, 2003, Lulai *et al.*, 2015).

Recently there has been an explosion in metabolomics; the systematic assessment of all metabolites produced by a given organism. This has opened up new insights into the metabolic pathways which support physiological functions. A number of studies have shown that the metabolomic profiles linked to the inflammatory phenotype is important in bacterial killing and resolution, such as itaconate which directly inhibits microbial isocitrate or limits inflammation by controlling succinate accumulation (Michelucci *et al.*, 2013, Tannahill *et al.*, 2013). By contrast, the anti-inflammatory phenotype macrophage has shown to be more related to mitochondrial oxidation thus, controlling the triglyceride uptake that is necessary in fatty acid oxidation (Huang *et al.*, 2014). Another metabolomics analysis demonstrated that cellular metabolism controls macrophage function and that by controlling glycolysis in arthritis and reducing succinate uptake inflammation was reduced (Littlewood-Evans *et al.*, 2016). It is now well established that signal transduction can also regulate metabolism and signalling pathways activated by growth factors or different stimuli. It is now established that signalling pathways can also regulate metabolomics profiles which in turn regulates processes such as proliferation, migration and phagocytosis. As mentioned above, amongst MAPKs, ERK has been well established to link signal transduction, to metabolism and thus to macrophage activities (Traves *et al.*, 2012).

The previous chapter demonstrated the potential for MKP-2 to regulate MAP kinase activity. Therefore, this chapter will investigate the role of MKP-2 in macrophage activity. Firstly to determine whether MKP-2 deletion affects phagocytosis. Secondly, to assess the role of MKP-2 in macrophage migration towards different chemoattractants. This will be followed by mapping the proliferative activity in both MKP-2$^{+/+}$ and MKP-2$^{-/-}$ macrophages to get an overall picture of MKP-2 function in these three key elements. Finally, the metabolomics profile underlying these activities and the role of MKP-2 will be examined.

4.2 Results

4.2.1 MKP-2 deletion alters macrophage phagocytosis

Macrophages are the major phagocytes that take up and degrade infectious pathogens, apoptotic and necrotic cells and as part of the innate response. Through this process they also orchestrate a series of processes which activate the adaptive immune system by presenting antigens to other immune cells (Jutras and Desjardins, 2005). Phagocytosis therefore plays a critical role in pathogen clearance, tissue remodelling and inflammation.

Here, it was investigated as to whether deleting the MKP-2 gene would affect the phagocytic activity and function of macrophages in both M1 and M2 phenotypes. For this zymosan bio particles (*Saccharomyces cerevisiae*) were used to assess phagocytosis in both MKP-2$^{+/+}$and MKP-2$^{-/-}$ macrophages. The assay was optimized and in the first set of experiments it was established that the assay is working when utilising MKP-2$^{+/+}$ macrophages alone (Figure 4.1). The results showed that after 60 minutes approximately 37.5% of total macrophages in the field engulfed red zymosan particles. Staining F-actin with phalloidin (green) showed the actin polymerization and cell membrane elongation and filopodia. DAPI was used to stain the nucleus with blue to recognise the cell morphology in this process.

Closer examination of the macrophages indicated that all the well-recognised stages of phagocytosis could be observed (figure 4.2). Firstly when zymosan particles (red) were attracted to the surface of the macrophage step 1, then actin polymerization of the membrane and elongation in step 2, to engulf the particles and phagosome formation in step 3, followed by particles killing and digestion inside the macrophages, step 4. Therefore, these initial results enabled additional phagocytosis experiments to be carried out, under these optimised conditions.
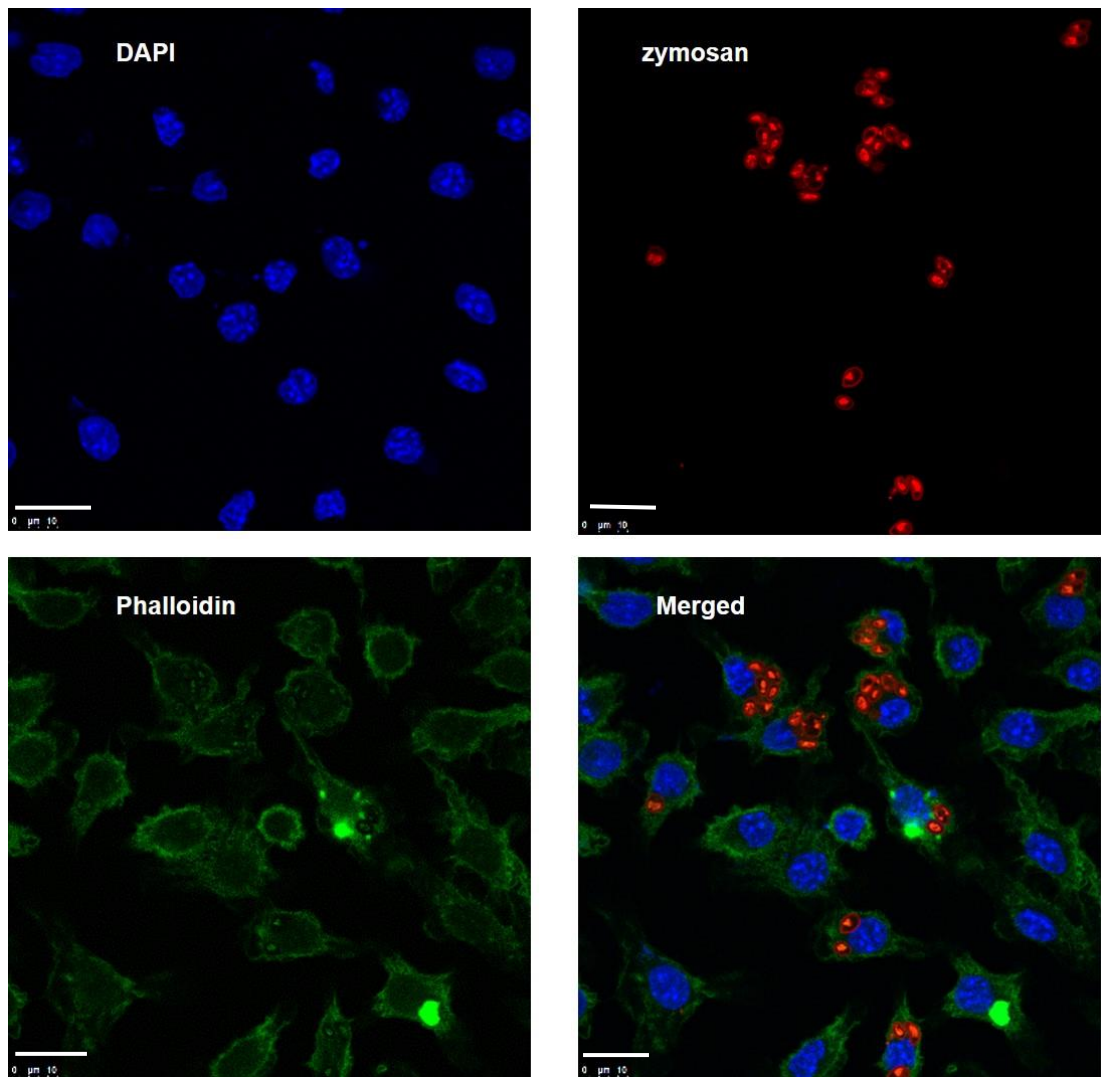
Figure 4. 1 Macrophage phagocytosis of zymosan bio-particles in MKP-2^{+/+} BMDMs

BMDMs were harvested on day 7 of culture and 0.5×10^6 cells were seeded on each coverslip in a 12-well plate and left to attach overnight. Zymosan particles (red), Alexa Fluor 594 conjugate (MOI=10) were added to the wells for 1 hour to allow phagocytosis and the assay carried out as outlined in section 2.5. Cells were then fixed with 4% paraformaldehyde, stained with DAPI (blue), whilst the actin cytoskeleton was stained by FITC phalloidin (green). Cells were visualized by confocal microscope using a 40x oil lense. Scale bars are 10µm. This figure is representative of three other experiments analysing 3-5 coverslips for each.

Phagocytosis stages

1- Chemotaxis   2- engulfment   3- autophagosom

4- Killing and digestion
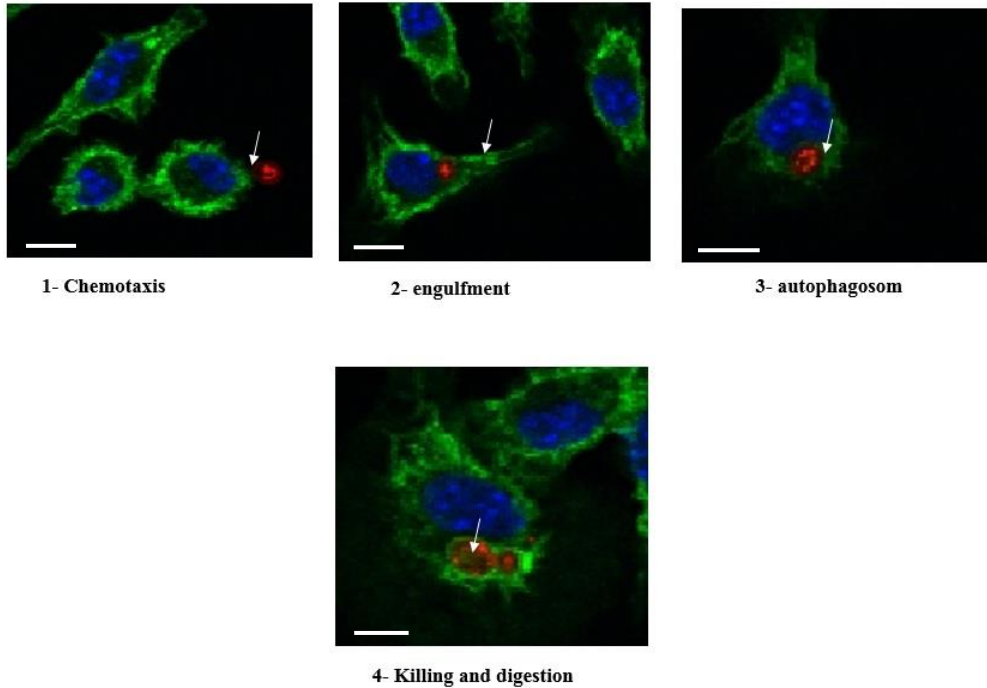
Figure 4. 2 Macrophage phagocytosis steps in MKP-2$^{+/+}$ BMDMs

Macrophages were harvested on day 7 of culture and 0.5x10^6 cells seeded on each coverslip in 12-well plate and left to attach overnight. Then opsonized zymosan particles (red) (MOI=10) was added to the wells for 1 hour to allow phagocytosis and the assay carried out as mentioned in section 2.5. Cells were then fixed with 4% paraformaldehyde, stained with DAPI (blue) for the nucleus, FITC phalloidin (green) for actin cytoskeleton. Cells were visualized by confocal microscope using 40x oil lenses. Scale bars are 10µm.

In further experiments, phagocytosis was examined in both WT and MKP-2 KO macrophages for both M1 and M2 activation phenotypes, stimulated by ether LPS or IL-4, and shown in figure 4.3 (as representative images). Figure 4.3 panel A and 4.4 shows consistent staining with infection at 10 zymosan for each macrophage. In the control cells that were cultured with media alone and untreated, the morphology of cells is shown as oval cell bodies with dense cytoplasm in an area surrounding the inner side of the cell membrane, the nucleus was mostly localised in the centre of the cells in the WT MKP-2. The MKP-2$^{-/-}$ control cells showed similar morphology with some differences in the shape which was more oval and the nucleus which was localised to one end of the cell other than being in the centre, also the cell membrane tended to be thinner than those of the wild type. In both group, cells had few pseudopods (cell membrane feature of phagocytes).

Macrophages that were pre-treated with LPS showed a similar cell shape as their wild type counterparts, but had more pseudopods that were thick and long as shown in figure 4.3, panel B and figure 4.5. MKP-2$^{-/-}$ macrophages differed from their wild type in the shape appearance which was a more elongated oval shape and the nucleus was indistinguishable from the cytoplasm. They also had longer pseudopods that were terminated in a thin ramification with extensive branches that ended in thin filaments. In contrast, the morphology of IL-4 pre-treated macrophages tended to be more flattened stellar shape in both groups. Here, a consistent observations was observed in the MKP-2 deleted macrophages which showed more lamellipodial cell membrane extensions and pseudopods with more branches (see Figure 4.3 panel C and figure 4.6.).
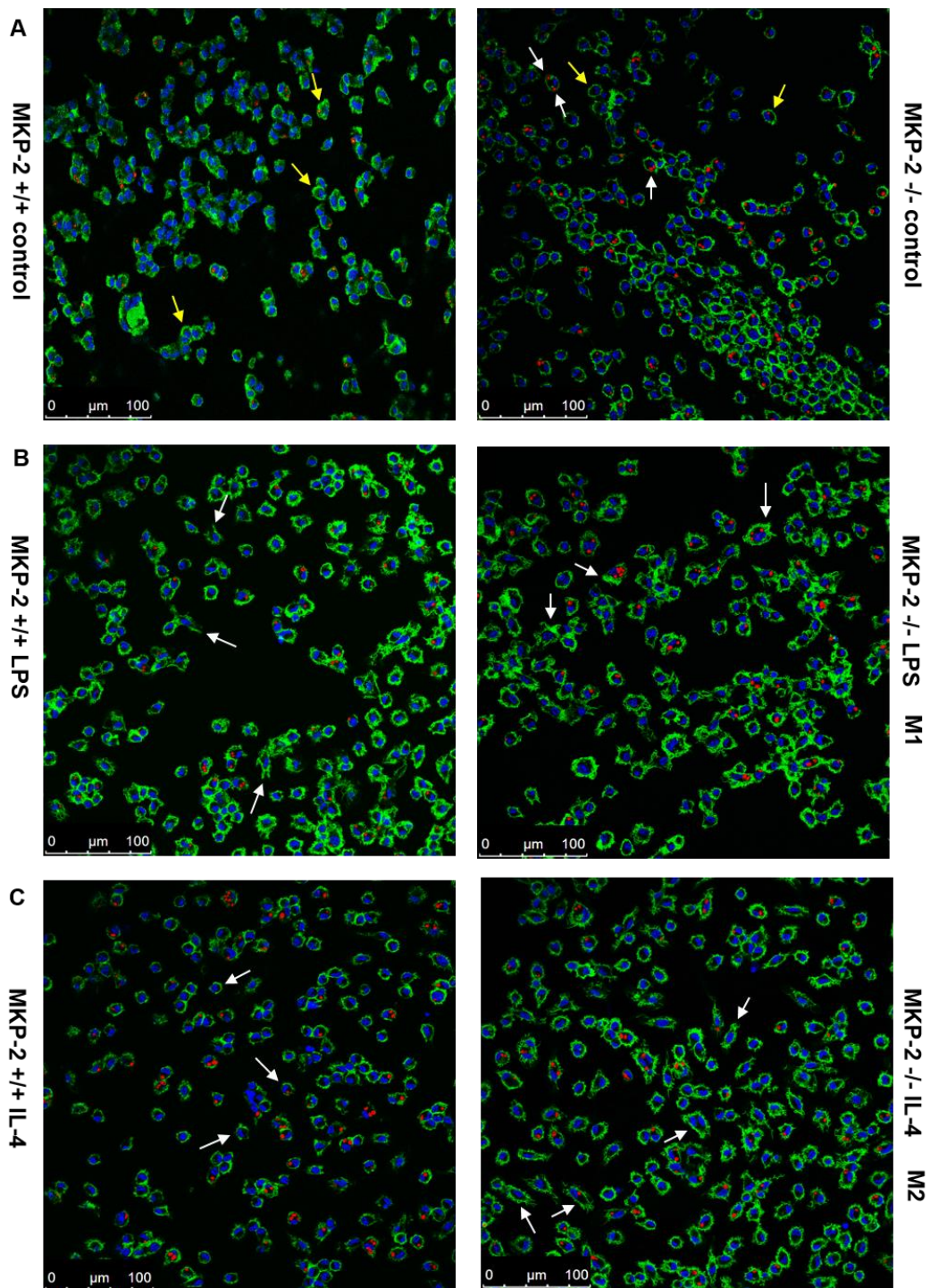
Figure 4. 3 The effect of LPS and IL-4 on macrophage phagocytosis

BMDMs assessed for phagocytosis as described in 2.5. White arrows show nucleus located near one end in MKP-2$^{-/-}$ in panel A while yellow arrows refer to thinner cell membrane than MKP-2$^{+/+}$. Panel B shows that LPS treated MKP-2$^{-/-}$ had more pseudopods as pointed in arrows. Panel C shows IL-4 treated cells were elongated more in MKP-2$^{-/-}$ BMDMs.
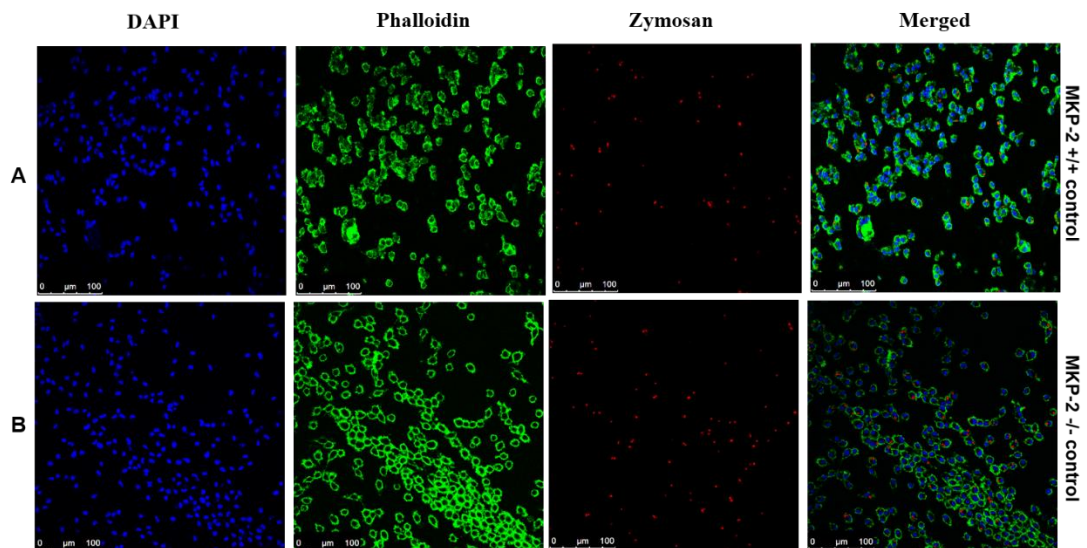
Figure 4. 4 The effect of MKP-2 deletion on phagocytosis morphology

BMDMs were harvested on day 7 of culture and 0.5 x10^6 cells seeded on coverslips in 12-well plates and left to attach overnight. Cells were left untreated as controls or opsonized zymosan particles (MOI: 10) added for one hour and phagocytosis assayed as outlined in section 2.5. Panel (A) represents MKP-2 $^{+/+}$ and panel (B) represents MKP-2 $^{-/-}$. Each condition was performed in triplicate and 5 fields assessed for each coverslip (3-5 coverslips per each conditions). Scale bars are 100μm. n=3. Each figure is representative of at least 3 experiments and represented as bar chart in Figure 4.7.
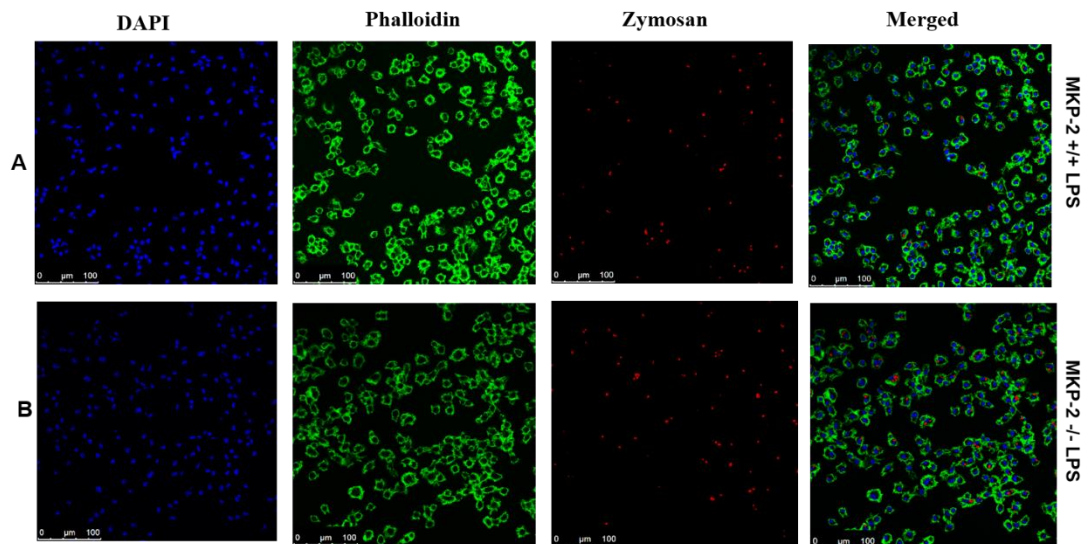
Figure 4. 5 The effect of MKP-2 deletion on LPS-stimulated macrophage phagocytosis

BMDMs were harvested on day 7 of culture and 0.5 x10^6 cells seeded on coverslips in 12-well plates and left to attach overnight. Next day cells were stimulated with 100ng/ml LPS or left untreated as controls one hour before adding opsonized zymosan particles for further one hour and phagocytosis assayed as described in section 2.5. Panel (A) represents MKP-2 $^{+/+}$ and panel (B) represents MKP-2 $^{-/-}$. Each condition was performed in triplicate and 5 fields assessed for each coverslip (3-5 coverslips per each conditions). Scale bars are 100µm. n=3. Each figure is representative of at least 3 experiments and represented as bar chart in Figure 4.7.
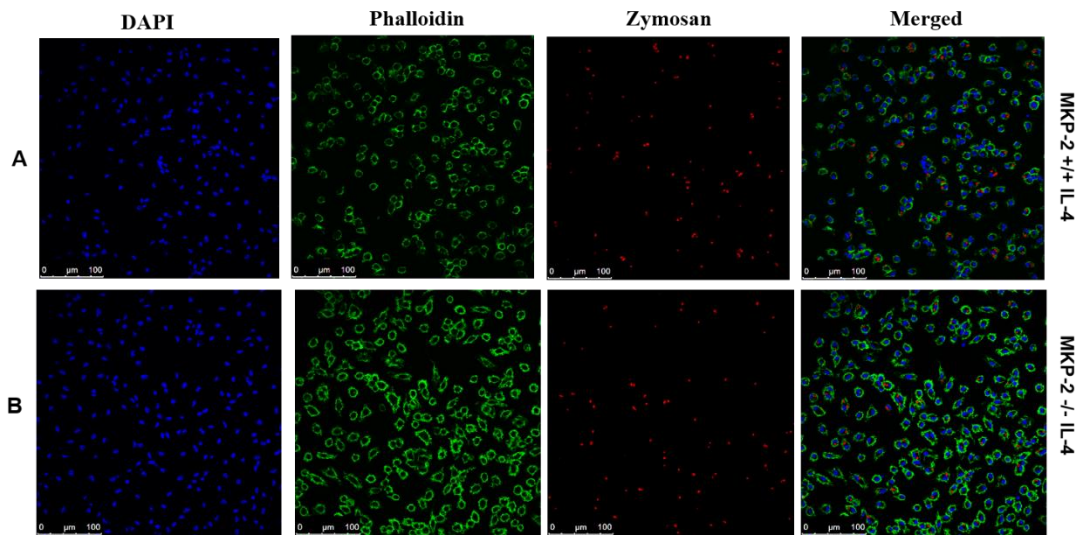
Figure 4. 6 The effect of MKP-2 deletion on IL-4 induced macrophage phagocytosis

Macrophages were harvested on day 7 of culture and 0.5 x10^6 cells seeded on coverslips in 12-well plates and left to attach overnight. Next day cells were stimulated with 100ng/ml IL-4 or left untreated as controls one hour before adding opsonized zymosan particles for further one hour and phagocytosis assayed as outlined in section 2.5. Panel (A) represents MKP-2 $^{+/+}$ and panel (B) represents MKP-2 $^{-/-}$. Each condition was performed in triplicate and 5 fields assessed for each coverslip (3-5 coverslips per each conditions). Scale bars are 100µm. n=3. Each figure is representative of at least 3 experiments and represented as bar chart in Figure 4.7.

As shown in Figure 4.7, it was found that the phagocytic index (cells that engulfed zymosan/total cells x100) in the MKP-2$^{+/+}$ increased by approximately 2 fold to 33.68% ±1.420 when cells were stimulated by LPS compared to the control values of 16.13% ±1.070. In MKP-2$^{-/-}$ macrophages, LPS stimulation increased phagocytosis by approximately 1.5 fold to 40.3% ± 6.30 comparing to the control values of 26 % ± 9.0. This results suggests that MKP-2 deficiency can affect both basal and M1 stimulated phagocytosis, however, due to the experimental variation this difference was not statistically significant.

Stimulation of cells with IL-4 to induce an M2 phenotype in MKP-2$^{+/+}$ macrophages resulted in a significant 3-4 fold increase in phagocytosis reaching 51.64% ± 5.14 compared to the controls 16.13 % ±1.07. On the other hand, stimulation of MKP-2$^{-/-}$ macrophages with IL-4 only increased phagocytosis to 35.42% ± 1.28 when compared to the control values of 26 % ± 9, this was less than their WT counterparts. This suggests that the M2 phenotype has more phagocytic activity than the M1 phenotype in WT but not KO MKP-2 macrophages. Thus deletion of MKP-2 leads to an increase in the phagocytic function of M1 macrophage phenotype whilst reducing this activity in the M2 phenotype figure 4.7.
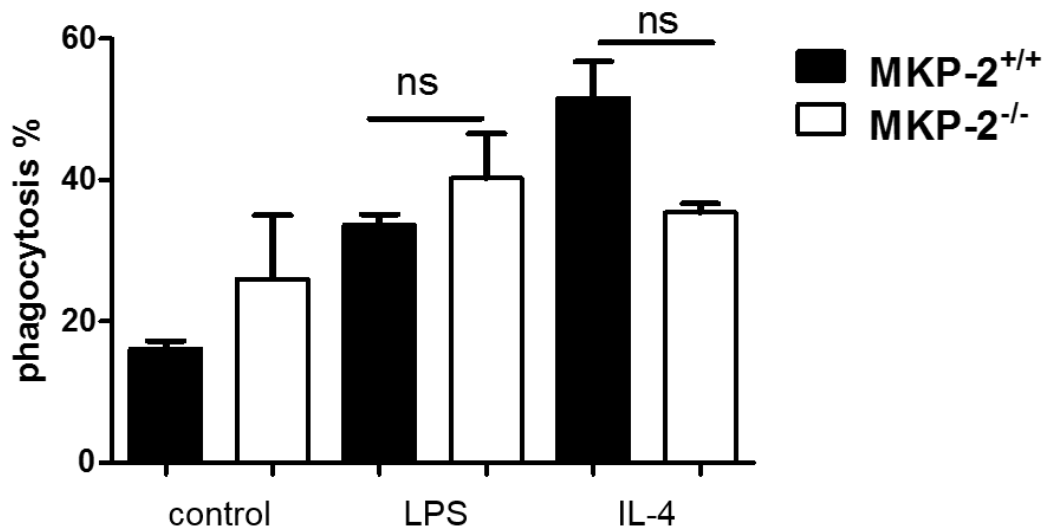
Figure 4. 7 MKP-2 deletion does not affect macrophage phenotype function of phagocytosis

Macrophages were harvested on day 7 of culture and 0.5 x10^{6} cells seeded on coverslips in 12-well plates and left to attach overnight. Next day cells were stimulated with either 100ng/ml LPS or 100ng/ml IL-4 or left untreated (control) for 60 minutes before adding opsonized zymosan particles for a further 60 min and phagocytosis assayed as in section 2.5. Each condition was performed in triplicate and 5 fields was taken for each coverslip (3-5 coverslips per each conditions) and cells internalizing zymosan were counted manually up to 1000 cells/coverslip. Error bars represents mean ± SEM, n=3 for MKP-2^{+/+} versus MKP-2^{-/-} .

In order to further confirm the role of MKP-2 deletion on macrophage phagocytic activity, a cytoselect 96-well phagocytosis assay kit (detailed in methods section 2.5.1) was used. Results (Figure 4.8) showed no differences in the phagocytosis between the conditions and indicated that the assay did not work well possibly because of the high density of cells which was chosen according to the manufacturer's instructions in the first place. However, one experiment was carried out using wild type MKP-2 macrophages to assess phagocytosis. For this, macrophages were seeded at increasing cell densities (from 1×10^4 and up to 2×10^5) (Figure 4.9). Results showed increased phagocytosis of zymosan at the lowest cell density which was 1×10^4 cells/well and this increase followed to peak at 2×10^5 which was used previously. (Figure 4.9). Due to the time limitation these experiments were not continued.

Further confocal imaging analysis indicated a number of other differences between wild type and knockout macrophages. For example, there where clear differences in the phagocytic capacity (the ability to engulf more than one particle of zymosan) observed during the determination of the phagocytic index. Therein, control MKP-2$^{-/-}$ macrophages seemed to engulf (1-2 particles) about 10% more than wild type macrophages (37.22% ± 1.25 and 27.64% ± 0.78). For the different activators, there did not seem to be any difference in this parameter in wild type macrophages versus knockout.

For 3-4 particles the situation was far more marked, unstimulated MKP-2$^{-/-}$ macrophages showed higher uptake compared to their wild type controls (176% ± 3.18 versus 60% ± 2.43). MKP-2$^{+/+}$ macrophages seemed to be more active in engulfing 3-4 particles, more than MKP-2 deleted phagocyte but only in response to IL-4 (WT= 470% ± 5.48, KO= 9.2% ± 0.05). LPS treated phagocytes showed slight differences in the number of particles that were engulfed (Figure 4.10). This result demonstrates MKP-2 to have an effect on the phagocytic capacity of alternatively activated macrophages. Thus, deleting this gene reduced the number of internalised zymosan particles upon IL-4 stimulation.

Macrophage uptake of more than 4 particles is shown in the third panel of figure 4.10. There was higher uptake of the particles in the control group and the LPS treated MKP-2$^{-/-}$, 111% and 135% respectively, compared to their wild type counterparts. Interestingly, again IL-4 pre-treatment reduced the uptake in MKP-2$^{-/-}$ macrophages relative to MKP-2$^{+/+}$ counterparts (WT = 118% ± 4.37, KO= 0.8% ±0.06. In all cells

during uptake of more than 4 particles, condensed cytoplasm was observed near the nucleus and was granulated (Third line in Fig.4.10).

To conclude, IL-4 pre-treatment reduced the capacity of zymosan uptake in MKP-2 deleted macrophage but that was reversed upon LPS pre-treatment suggesting possible mechanistic differences in the MAP kinase signalling pathway that is mediating macrophage phagocytosis of zymosan.
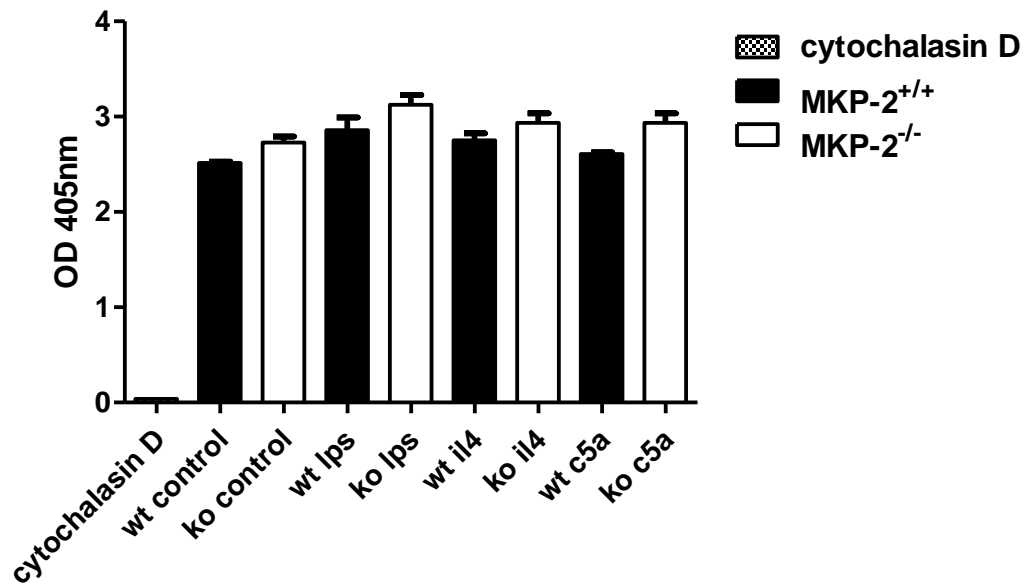
Figure 4. 8 Phagocytosis uptake using Cytoselect 96-well assay

Macrophages were harvested on day 7 of culture, seeded into 96-well plates (2x105 cells/well), left to attach overnight, then pre-treated with 100ng/ml LPS or 100ng/ml IL-4 or 20nM c5a or 2µM of Cytochalasin D (as appositive control to inhibit phagocytosis) for 4 hours prior to addition of zymosan particles as described in section 2.5.1. Absorbance measurements were performed on the microplate reader with a 405 filter n=2.
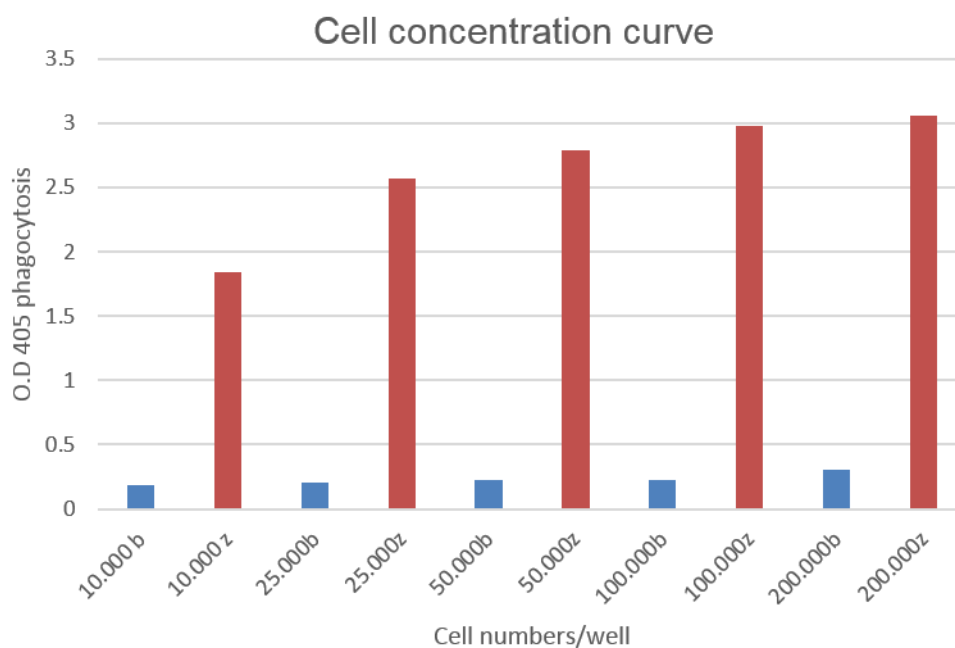
Figure 4. 9 The effect of cell density on the phagocytosis assay

Macrophages from MKP-2$^{+/+}$ were used to optimize the phagocytosis assay kit. Cells were grown for 7 days and harvested and re seeded in each well of a 96-well plate in different concentrations with a triplicate wells for each concentration. Cells were incubated with zymosan particles (MOI of 10) for one hour and assessed for phagocytosis as described in section 2.5.1. For each concentration, blank cells (b) were included alongside samples with zymosan (z). Phagocytosis was measured using a plate reader (POLAR star Omega –BMG). The absorbance was read using 405nm. Data represents a single experiment.
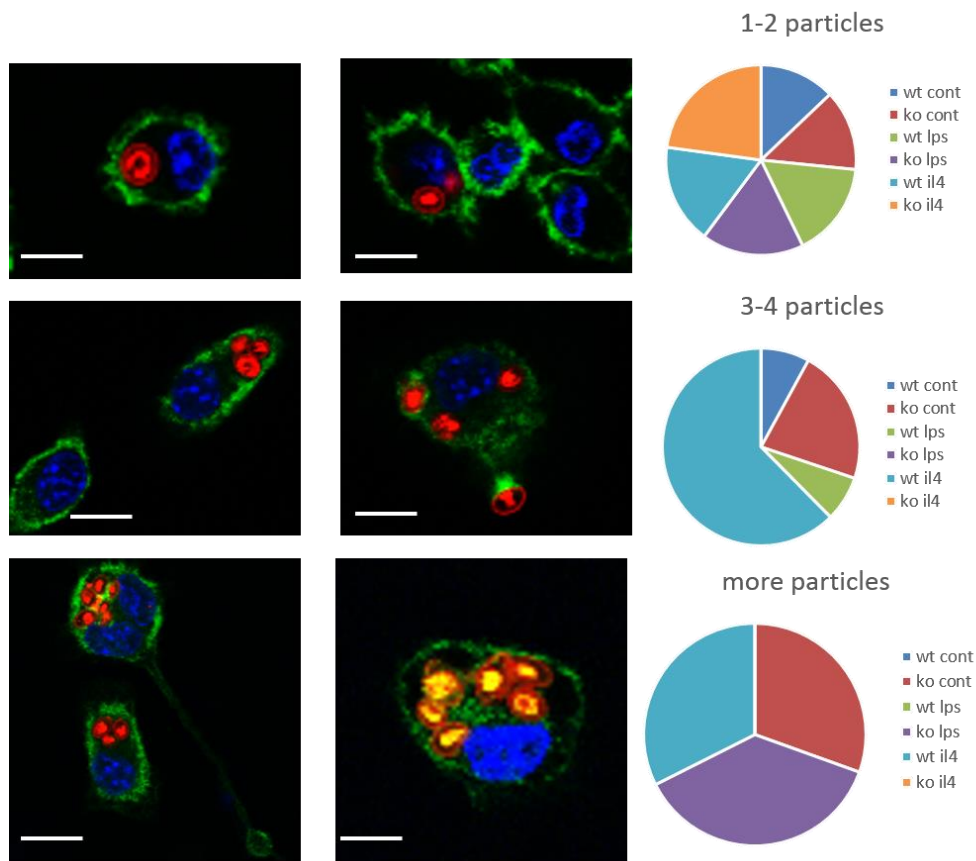
Figure 4. 10 Phagocytic capacity is altered in MKP-2 deleted BMDMs

Macrophages were harvested on day 7 of culture and 0.5 x10^6 cells seeded on coverslips in 12-well plates and left to attach overnight. Next day cells were stimulated with 100ng/ml LPS, IL-4 or left untreated as controls one hour before addition of opsonized zymosan particles for further one hour and phagocytosis assayed as indicated in section 2.5. Each condition was performed in triplicate and 5 fields were taken from each coverslip and cells internalizing zymosan particles categorized and was counted manually up to 1000 cells/coverslip. Data is representative of 3 more other independent experiments. Scale bars are 10µm.

4.2.2 MKP-2 deletion alters macrophage migration

Having established the potential for MKP-2 to play a role in the regulation of macrophage phagocytosis, in the next part of the study the effect of MKP-2 deletion on macrophage migration was investigated. BMDMs from both WT and MKP-2 KO mice were tested for their migratory activity towards different chemotactic factors. Firstly, the migratory activity towards a C5a gradient was tested and the results shown in Figure 4.11. Addition of C5a to the bottom chamber caused a significant increase in the migration of WT macrophages compared to untreated cells, giving an approximate 4 fold increase (RFU/100; stim vs cont. 168.45 ± 5.52, 46.93 ± 2.53). In contrast, whilst control MKP-2$^{-/-}$ macrophages showed a similar level of migration to their wild type counterparts, there was less than a 2 fold increase in migration towards C5a compared to control (RFU/100 stim vs control; 77.52 ± 1.26, 42.99 ± 2.54). Thus, deletion of MKP-2 reduced macrophage motility by approximately 50%. This indicates that deletion of the MKP-2 gene significantly reduced the migratory function of macrophages towards C5a compared to their wild type counterparts.

Next, macrophage migration towards different agents such as LPS, IL-4 and zymosan particles was examined in order to find out the pathway that drives this migration in both MKP-2$^{+/+}$ and MKP-2$^{-/-}$ macrophages. Figure 4.12 shows that in contrast to previous experiments deletion of MKP-2 significantly increased control migration from 42.99 ± 7.38 to 73.71 ± 2.33. Following addition of LPS, migration increased in MKP-2 wild type macrophages by approximately 3 fold (118.98 ± 0.74, versus 30.92 ± 0.48). However in MKP-2$^{-/-}$ macrophages that increase was virtually abolished relative to the counterpart controls (LPS stim = 83.85 ± 0.57, control = 73.71 ± 2.33).

In response to IL-4 the pattern was considerably different. In WT macrophages the response to IL-4 was smaller than that observed for LPS giving a 2 fold increase in migration (61.05 ± 0.38). However in MKP-2$^{-/-}$ macrophages stimulated by IL-4, migration was markedly reduced to 28.87 ± 0.22 RFU respectively and was virtually no different to WT controls. For zymogen particles again the pattern was unique. In WT macrophages zymogen particles caused a small 1.6 fold increase in migration relative to controls (52.44 ± 2.06). Interestingly, in MKP-2 deleted macrophages the migratory response to zymosan particles was exacerbated considerably increasing to (165.78 ± 3.86, RFU). Taking into account the increase in basal migration in MKP-2$^{-/-}$ macrophages this represents an overall increase in response relative to either LPS

or IL-4. Taken together MKP-2 deletion abrogates migration activated by M1 and M2 ligands.

Overall, for both macrophage functions of phagocytosis and migration it seems that WT MKP-2 has a more migratory effect towards LPS than KO MKP-2 macrophages while this effect was reversed in phagocytosis where MKP-2 deficient macrophages show more phagocytic activity than their wild type counterparts when pre-treated with LPS. Meanwhile, MKP-2 deleted macrophages that are activated alternatively, showed less phagocytic activity and less migration than MKP-2 wild type macrophages

One possible reason for these differences may involve possible differences in actin polymerization kinetics. Both migration and phagocytosis involve actin polymerization which is regulated mainly by the MAPK pathway (Rougerie *et al.*, 2013). Examination by confocal imaging supported the idea of actin polymerization and changes in the cell morphology between both groups. Figure 4.13 shows a representative image of MKP-2$^{+/+}$ macrophages and the characteristics. Many zymosan particles were observed on the surface of the phagocytic cup in which the distal margin remained open. Two membrane protrusions were seen, first, a broad sheet- like which is called lamellipodium and second a spike-like protrusion called filopodia. Both protrusions are indicative of macrophage migration to phagocytize zymosan. Also stress fibres were observed within the retracting actin filament tail confirming cell motility towards yeast particles (Fig.4.13). It was therefore, decided to track these morphological features in MKP-2 deleted macrophages to investigate any differences compared to the wild type.
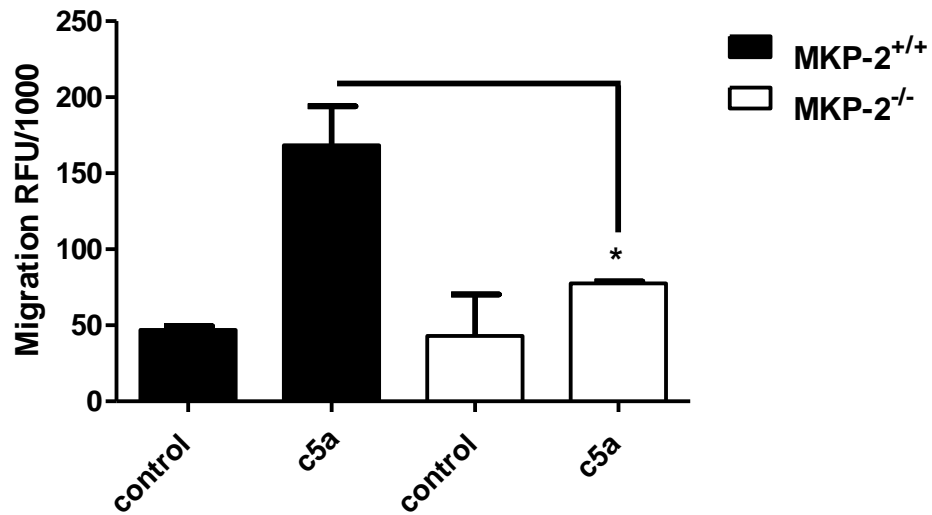
Figure 4. 11 MKP-2 deletion reduces macrophage migration towards C5a

Macrophages were cultured for seven days and harvested. Cells were then seeded in the upper chamber of a 24-well Boyden plate at a density of 2×10^5 cells and 20 nM of C5a added to the lower chamber and migration assayed over 24 hours as outlined in section 2.6. Relative Fluorescent units (RFU) was measured using an Omega Polar Star plate reader excitation 485 nm, emission 520 nm. Error bars represents Mean ±SEM, n=3, *P<0.05 MKP-2$^{+/+}$ versus MKP-2$^{-/-}$.
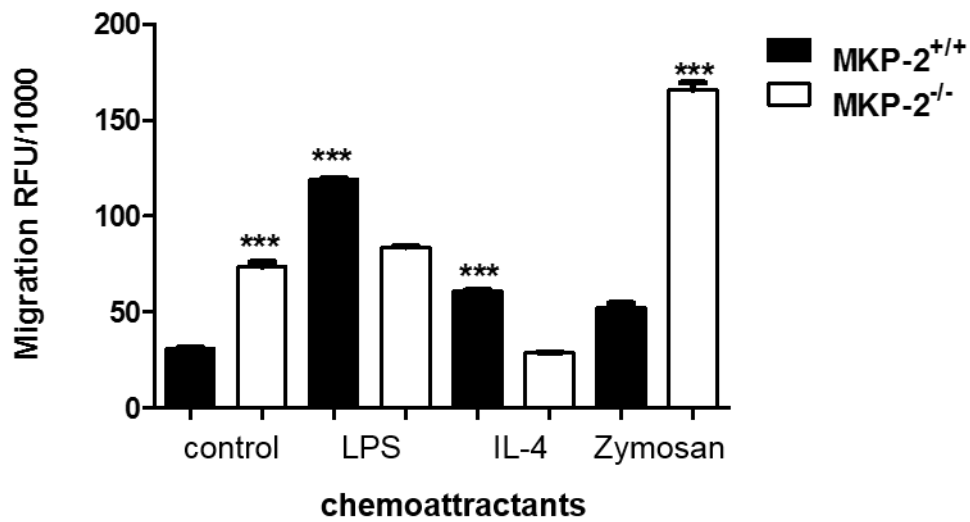
Figure 4. 12 MKP-2 deletion alters macrophage migration towards LPS, zymosan and IL-4

Macrophages from both groups were cultured for seven days and harvested. Cells were then seeded in upper chamber of a 24-well Boyden plate at a density of $2x10^5$ cells and 100ng/ml of LPS or IL-4 or zymosan (MOI of 10) was added to the lower chamber and migration assayed after 24 hours as outlined in section 2.6. The 0.8µm pore size insert was used. Relative Fluorescent Units (RFU) was measured using an Omega Polar Star plate reader excitation 485 nm, emission 520 nm. Error bars represents Mean ±SEM, n=3, ***P<0.001 MKP-2$^{+/+}$ versus MKP-2$^{-/-}$.
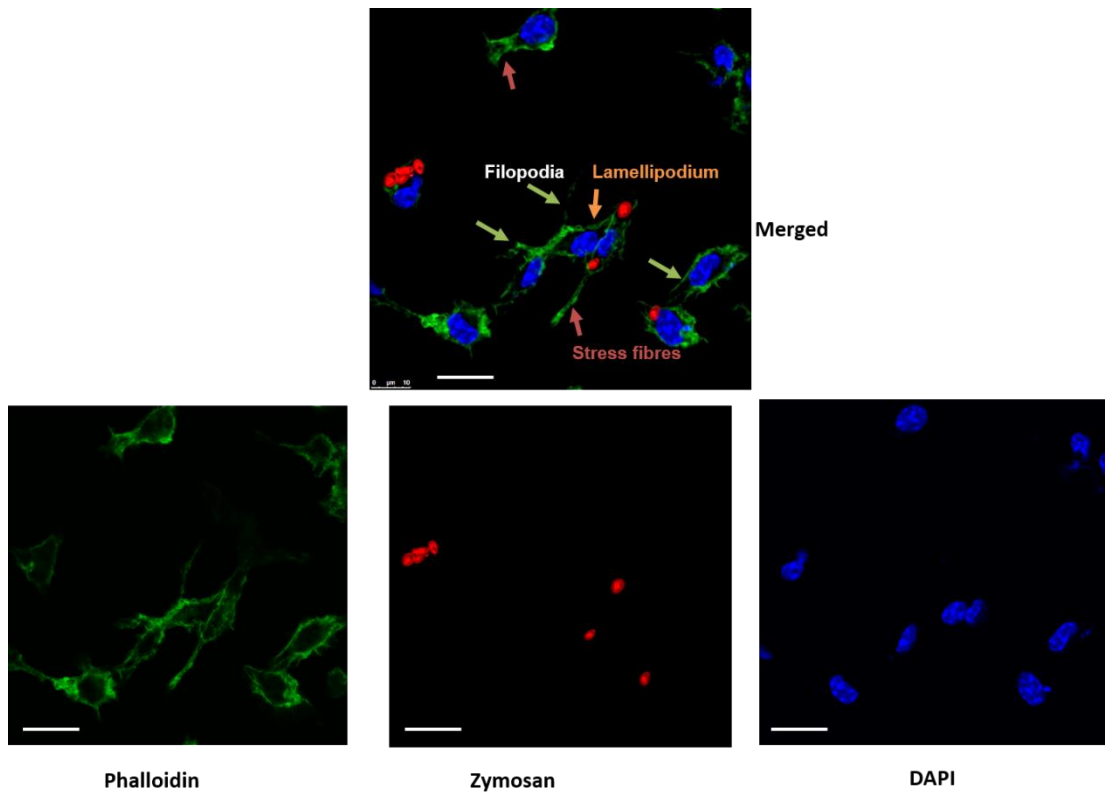
Figure 4. 13 Actin polymerization during phagocytosis

Macrophages from MKP-2$^{+/+}$ were assessed for phagocytosis assay using zymosan bio-particles (red), phalloidin (green) for the actin cytoskeleton, and DAPI (blue) for the nucleus. Green arrows are filopodia, orange arrow is lamellipodium and the red arrow is stress fibres. Data is representative of three other experiments. Scale bar is 10 μm.

Closer analysis using confocal microscopy showed that macrophages deficient in MKP-2 differed from their wild type in their morphology. Spike-like filopodia were observed in unstimulated MKP-2$^{-/-}$ macrophages and showed more phagocytic cup closure than wild type counterparts (Fig.4.14 first panel). LPS treated MKP-2$^{+/+}$ macrophages showed dense thick and long pseudopods and three or more short cytoplasmic lamellipodial extensions terminating in spiky filopods and giving a bushy appearance to cells. In contrast, LPS treated MKP-2$^{-/-}$ macrophages had more filopods than their controls and had thinner pseudopods and less spikes (filopods) than their wild type macrophages (Fig4.14, second panel).

IL-4 treated MKP-2$^{+/+}$ macrophages showed similar morphology to their controls, where the phagocytic cups were mostly opened. But MKP-2$^{-/-}$ macrophages showed extensive branches of thin filaments (filopods) and pseudopods with the cell body more oval and elongated than their wild types and with more pseudopods (Fig.4.14, third panel). The latter finding is indicative of more phagocytosis whilst more spikes are indicative of more migration. These results indicate some differences in the direction and the morphology of actin filaments.

In summary, the morphological study of phagocytosis and migration, shows that MKP-2 deleted macrophages had more phagocytic activity when treated with LPS (M1 like) but where less motile compared to MKP-2 wild type under same conditions. In contrast, MKP-2 deleted macrophages showed less phagocytosis and less motility when alternatively activated with IL-4.
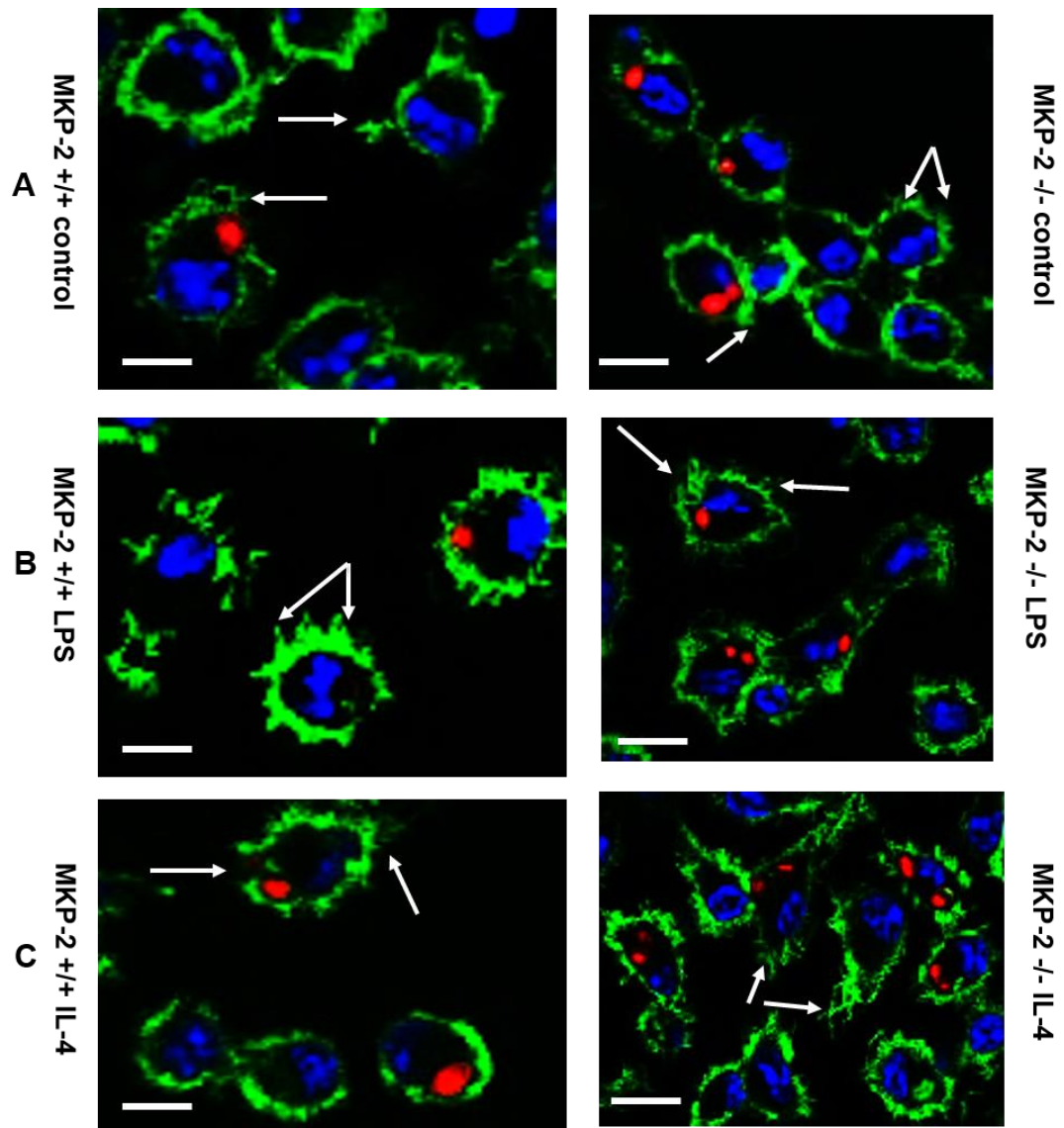
Figure 4. 14 Increased actin polymerization in MKP-2 deleted macrophages

Macrophages were harvested on day 7 of the culture and 0.5 x10^6 cells seeded on coverslips in 12-well plates and left to attach overnight. Next day cells were stimulated with 100ng/ml IL-4, LPS or left untreated as controls one hour before addition of opsonized zymosan particles for further one hour and phagocytosis assayed as outlined in section in 2.5. Each condition was performed in triplicate and with confocal microscopy 5 fields were taken from each coverslip (3-5 coverslips per each conditions) and cells internalizing zymosan was counted manually up to 1000 cells/coverslip. Panel A&B arrow shows filopodia, panel C shows pseudopodia. Scale bars are 10µm. n=3.

4.2.3 The role of MKP-2 deletion in macrophage differentiation and proliferation

During macrophage culture, there was a consistent observation that MKP-2$^{-/-}$ bone marrow progenitors gave rise to fewer macrophages than MKP-2$^{+/+}$. Equal numbers of bone marrow cells suspension containing monocyte/macrophage progenitors were isolated and cultured for seven days however, the MKP-2$^{+/+}$ preparation produced higher numbers of cells than MKP-2$^{-/-}$. Based on these observations and also previous findings from the Plevin laboratory that MKP-2 deletion altered cell cycle progression and proliferation in MEFs (Lawan *et al.*, 2012) it was hypothesised that a similar effect of MKP-2 deletion on macrophage proliferation would be observed.

As outlined in the methods chapter (2.2.3) L929 conditional medium was used as a source of M-CSF which is required for macrophage development and differentiation. For the proliferation assay, macrophages from both MKP-2$^{+/+}$ and MKP-2$^{-/-}$ mice were cultured for three days in the growth media containing M-CSF (L-929 source) and harvested on day three to track the proliferative rate of these cells for up to 72 hours which would then be day seven when the macrophages are fully differentiated.

Results outlined in Figure 4.15 shows the effect of MKP-2 deletion on macrophage proliferation under different conditions. The results indicate a significant increase in macrophage proliferation rate in both MKP-2$^{+/+}$ and MKP-2$^{-/-}$ after 24 hr, M-CSF stimulation was approximately 3-4 fold in both populations with a slight increase in the wild type MKP-2 population over MKP-2 deleted macrophages. After 48 hr (panel B) proliferation increased further in the WT MKP-2 macrophages, however in MKP-2 KO macrophages cell growth lagged significantly. By 72 hr proliferation rates for both cultures had fallen and were similar (panel C).

Furthermore, pre-addition of LPS had marked effects on M-CSF mediated-macrophage proliferation in both groups. At 24 hours LPS significantly reduced stimulation in both WT and KO cultures reducing levels back towards basal values (WT stim = 0.83 ± 0.19 (absorbance), LPS= 0.15 ± 0.01; KO stim = 0.74 ± 0.006, LPS= 0.16 ± 0.02). This pattern of inhibition continued at both 48 and 72 hours although the relative inhibition at 72 hours was reduced due to the much reduced stimulation by M-CSF and generally lower levels of stimulation.

In contrast IL-4 pre-treatment seemed to enhance M-CSF induced proliferation in MKP-2$^{+/+}$ compared to MKP-2$^{-/-}$ macrophages over the time course examined. For example at 24 hours, IL-4 increased M-CSF stimulation from 0.73 ± 0.19 to 1.5 ± 0.26

with a smaller effect on KO macrophages. At 48 hours when M-CSF increased proliferation further the effect of IL-4 was relatively smaller but retained the enhancing effect on the MKP-2$^{-/-}$ cultures relatively better than for MKP-2 WT counterparts. At 72 hours the effect was still apparent but due to the low levels of incorporation at this time point there were no significant differences relative to other conditions.

These results confirms that deletion of the MKP-2 gene results in a decrease in macrophage proliferation rates and that the M2 phenotype cells are more proliferative than M1 like macrophages. Results show that in response to M-CSF there were clear differences between MKP-2$^{+/+}$ and MKP-2$^{-/-}$ proliferative activity.
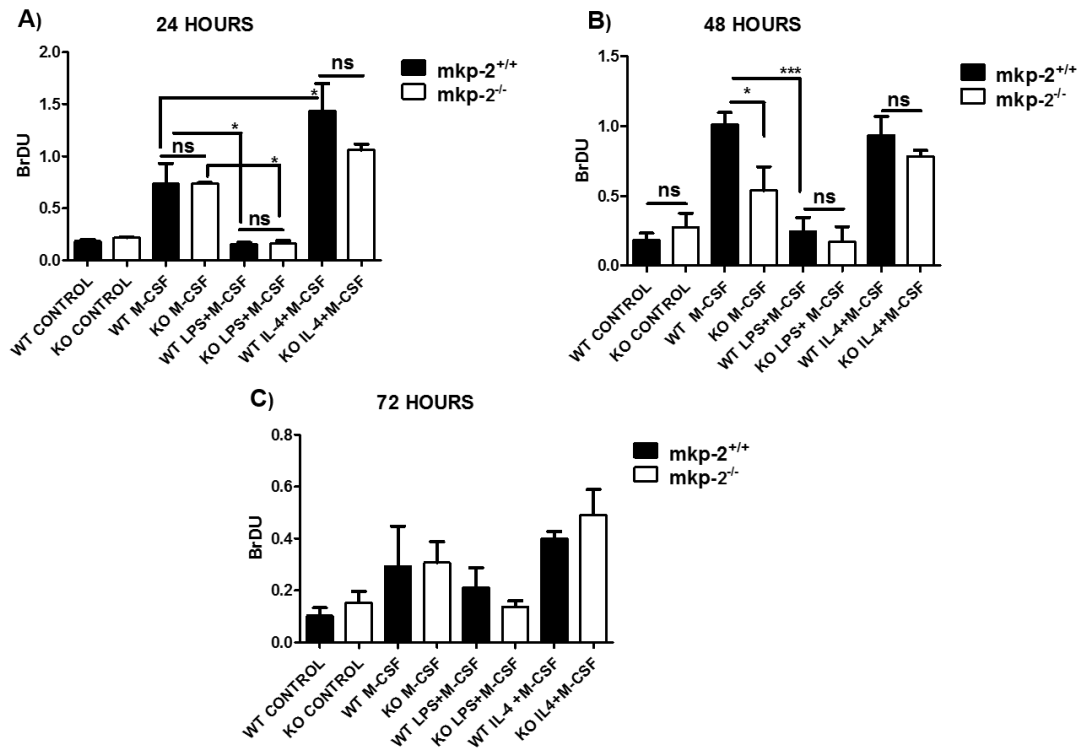
Figure 4. 15 The effect of MKP-2 deletion on BMDM proliferation in response to different agents

Macrophages from both MKP-2$^{+/+}$ and MKP-2$^{-/-}$ were harvested on day 3 of culture, seeded at 4x10^4 cells/well in a 96-well plate and incubated overnight. Cells were then pre-treated with 100ng/ml of LPS, 100ng/ml of IL-4 for 1 hour or left untreated as controls. Cells were stimulated with 10ng/ml M-CSF for A) 24h, B) 48 and C) 72 hours. Finally, 10μM BrDU was added each well and cells were incubated for 6 hours. Incorporated BrDU was measured using Polar Star Omega plate reader at absorbance of 450nM. Data represents mean ± SEM of three independent experiments, *P<0.05 MKP-2$^{+/+}$ versus MKP-2$^{-/-}$ in 48 h but *P<0.05 at 24h represents stim vs M-CSF and also ***P<0.05 at 48h.

4.2.4 The role of MKP-2 in the metabolomics profile underling macrophage functions

A number of recent studies have revealed the role that metabolites play in shaping macrophage activation and function. Such metabolic approaches have demonstrated that macrophages can readily re-programme their metabolic phenotype in order to support general cellular activities linked to survival, growth and proliferation or to carry out specific effector functions such as migration, phagocytosis and cytokine production (Geeraerts *et al.*, 2017). It has been shown that amongst the MAPKs, ERK signalling is the main pathway involved in the central metabolism which leads to the activation of oxidative and nitrosative bursts and proinflammatory macrophage polarization (Traves *et al.*, 2012). Inhibition of MEK/ERK signalling interferes with the central metabolism in the normal state and also in response to LPS or other external stimuli (Wang *et al.*, 2018, Marchetti *et al.*, 2018).

From results in this chapter and from previous results showing that MKP-2 can influence macrophage phagocytosis, migration and proliferation, it was decided to examine the metabolic profiles under different conditions in both WT and KO macrophages. This would allow a mapping of metabolic pathways which may support these functional outcomes. An experimental design was set as described in methods section 2.11 for an untargeted metabolomics profile. Samples were run on LC-MS to determine changes in the metabolite concentration in MKP-2$^{+/+}$ and MKP-2$^{-/-}$ macrophages as described in section 2.11.

4.2.4.1 Metabolic changes underlying zymosan uptake

Initially metabolic profiles in MKP-2$^{+/+}$ and MKP-2$^{-/-}$ were compared in macrophages stimulated in response to zymosan, the agent used previously to promote phagocytosis. Results in table 4.1 show upregulated metabolites of the glycolysis pathway (D-glucose 6-phosphate,D- fructose 1, 6-biphosphate, DL-Glyceraldehyde 3-phosphate, ATP and NADP+) in MKP-2$^{-/-}$ macrophages which was detected as early as 5 minutes stimulation with opsonized zymosan when compared to their levels in counterpart MKP-2$^{+/+}$macrophages. The glutathione metabolic pathway (L-Glutamate, NADP+, and Glutathione disulphate) was upregulated in MKP-2 deleted macrophages after 5 minutes stimulation of zymosan. At the same time the pentose phosphate pathway was elevated in MKP-2 deleted macrophages (D-Ribose 5-phosphate and NADP+) which links this pathway to glycolysis (illustrated in Figure 4.16). Also a slight increase was observed in taurine and hypo-taurine metabolism,

ascorbate and alderate metabolism, purine and pyrimidine metabolism (UDP-glucose, UDP, GMP and UTP) in MKP-2$^{-/-}$ macrophages when compared to their wild type controls. Some of the amino acids such as leucine and alanine were upregulated in MKP-2 deficient phagocytes.

By contrast, there were some metabolites downregulated in the MKP-2$^{-/-}$ macrophages after 5 minutes incubation with zymosan particles. A combination of amino acids including Leu-Thr-pro (commonly named as ornithokinin) was significantly reduced in MKP-2 deleted macrophages by about 13 fold compared to the wild type (* P< 0.01). Downregulation of the glutathione intermediate S-allyl cysteine was shown to be decreased about 2 fold in MKP-2 deleted macrophages but this was not statistically significant.

Table 4. 1 The list of top 20 detected metabolites that were upregulated in MKP-2$^{-/-}$ in 5 minutes zymosan stimulation

NO.	DM	m/z	RT	Name	5WZ F WT	5KZ F KO	P
1	P	148.06	11.57	L-Glutamate	3.22	8.45	0.003
2	P	261.04	16.37	D-Glucose 6-phosphate	4.44	6.47	0.07
3	P	156.08	15.96	L-Histidine	0.07	6.07	0.02
4	N	742.07	17.02	NADP+	0.71	3.81	0.01
5	P	744.08	17.02	NADP+	1.35	3.69	0.01
6	p	203.14	5.03	Leu-Ala	2.46	3.75	0.002
7	P	405.01	16.57	UDP	1.15	3.52	0.05
8	N	229.01	16.07	D-Ribose 5-phosphate	0.21	3.40	0.24
9	P	221.09	4.49	5-Hydroxy-L-tryptophan	1.36	3.40	0.02
10	N	338.99	18.39	D-Fructose 1,6-bisphosphate	0.57	2.80	0.04
11	N	168.99	16.32	DL-Glyceraldehyde 3-phosphate	0.57	2.53	0.12
12	P	364.06	16.96	GMP	1.01	2.53	0.11
13	N	482.96	18.28	UTP	0.77	2.46	0.05
14	P	508.00	17.00	ATP	0.90	2.37	0.07
15	N	259.02	16.45	D-Glucose 6-phosphate	0.61	2.28	0.01
16	P	244.11	7.57	Biotin amide	0.70	2.12	0.05
17	N	565.05	16.55	UDP-glucose	0.62	2.00	0.03
18	N	611.15	17.66	Glutathione disulfide	0.37	1.88	0.03
19	P	613.16	17.67	Glutathione disulfide	0.31	1.85	0.02
20	P	126.02	15.19	Taurine	0.87	1.76	0.01
21	N	267.07	11.22	2(alpha-D-Mannosyl)-D-glycerate	0.09	1.60	0.03

Macrophages were treated as outlined in section 2.11.1 and analysed in section 2.11.3. DM refers to detection zone, M/Z to mass ratio, RT to raw retention time, WZF and KZF to fold changes in wild type and knockout MKP-2 compared to their controls and according to their P values n=3.
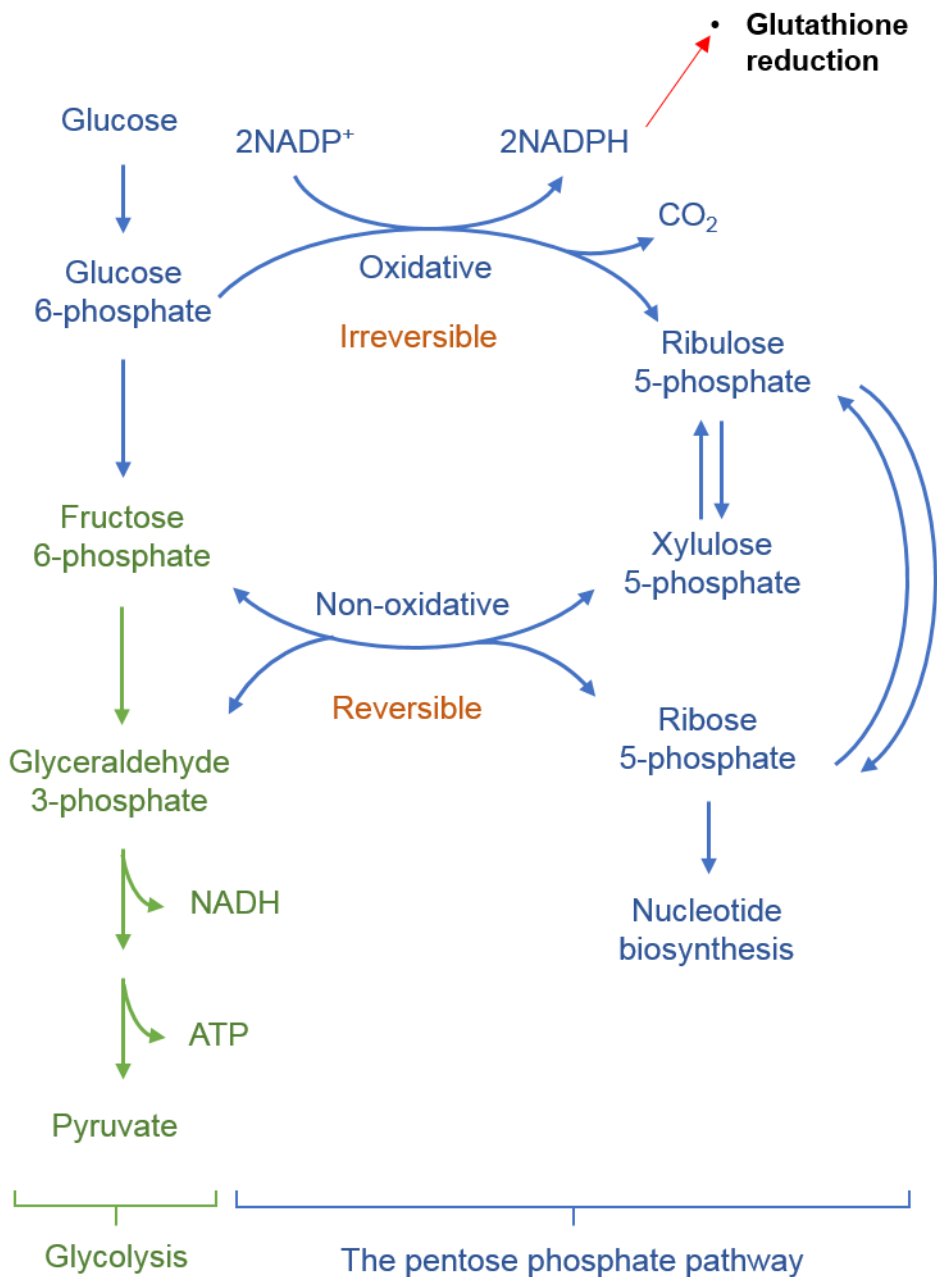
Figure 4. 16 Illustration of the link between the Glycolysis pathway and the pentose phosphate pathway

Glucose is metabolised to G-6-P which either oxidized to Ribulose 5-posphate activating the Pentose phosphate pathway (PPP), two NADP+ will convert to two NADPH or G-6-P initiate the glycolysis pathway and gives F-6-p. The latter provides the PPP pathway into R-5-p or continues the glycolysis pathway to form Pyruvate. R 5-P will further contribute in Nucleotide biosynthesis. Adapted from (Xu *et al.*, 2015).

Table 4. 2 The list of detected metabolites that were downregulated in MKP-2$^{-/-}$ macrophages following 5 minute zymosan stimulation

No	DM	M/Z	RT	Name	5WZ F* WT	5KZ F* KO	**P
1	P	330.25	3.93	4-Methyl-4-aza-5-pregnene-3,20-dione	31.83	7.44	0.001
2	P	330.20	4.47	Leu-Thr-Pro	20.69	6.75	0.01
3	P	162.06	5.07	Allyl cysteine	6.80	3.55	0.01
4	P	346.20	4.41	Leu-Val-Asp	5.23	4.86	0.01
5	P	188.10	14.30	5-guanidino-3-methyl-2-oxo-pentanoate	5.12	2.86	0.05

Macrophages were treated as outlined in section 2.11.1 and analysed in section 2.11.3. DM refers to detection zone, M/Z to mass ratio, RT to raw retention time, WZF and KZF to fold changes in wild type and knockout MKP-2 compared to their controls and according to their P values, n=3.

After 15 minutes incubation with zymosan particles, the time at which ERK and JNK phosphorylation was maximal and also the time of phagosome formation, MKP-2 deleted macrophages showed upregulation of multiple metabolites when compared to the MKP-2$^{+/+}$ macrophages (Table 4.3). Purine catabolism amino acids (Asp-Trp-Asp-Cys) were increased significantly and by about 37 fold in MKP-2$^{-/-}$ macrophages compared to only 0.48 in MKP-2$^{+/+}$ macrophages. Key components of the cell lipid bilayer ([FA amino (9:0)] 9-amino-nonanoic acid and PE (18:0/22:4(7Z, 10Z, 13Z, 16Z) were upregulated in MKP-2 deficient macrophages (**P<0.001, 23 and 2 folds) respectively. An intermediate in starch and sucrose metabolism (1-4-beta-D-Glucan) was significantly elevated (**P<0.002) by about 12 fold in MKP-2 deleted macrophages after 15 minutes of zymosan stimulation (Table 4.3).

More down regulated metabolites were found in MKP-2$^{-/-}$ macrophages after 15 minutes stimulation with zymosan particles. Of those metabolites, benzamide significantly declined in MKP-2 deleted macrophages by about 155 fold compared to wild type macrophage (**P<0.003). Glycolysis pathway metabolites and TCA cycle intermediates (D-Glucose 6-phosphate, 2(alpha-D-Mannosyl)-D-glycerate, D-Fructose 1, 6-bisphosphate, DL-Glyceraldehyde 3-phosphate, S-Malate and Phenyl pyruvate) were down regulated (Table 4.4). PS (14:0/16:0), which is a phosphatidyl serine, was also reduced in MKP-2 deleted macrophages after 15 minutes by greater than 90% compared to the wild type counterparts. The purine pathway metabolite (Guanosine) was decreased by about 2 fold in MKP-2$^{-/-}$ macrophages. Non-enoyl-carnitine, which is derived from methionine metabolism was also down regulated when the MKP-2 gene was deleted in macrophages (Table 4.4).

Table 4. 3 The list of top 20 detected metabolites that were upregulated in MKP-2$^{-/-}$ Macrophages after 15 minutes zymosan stimulation

No	DM	M/Z	RT	Name	15WZ F WT	15KZ F KO	P value
1	P	538.16	3.997	Asp-Trp-Asp-Cys	0.48	37.32	0.0001
2	P	174.15	8.192	[FA amino(9:0)] 9-amino-nonanoic acid	3.88	26.23	0.05
3	P	537.17	4.009	1-4-beta-D-Glucan	0.65	12.89	0.002
4	P	330.20	4.470	Leu-Thr-Pro	1.53	10.50	0.001
5	P	288.29	4.785	[SP (17:0)] heptadecasphinganine	0.82	5.66	0.002
6	P	785.65	7.465	3-demethylubiquinol-9	0.93	4.30	0.04
7	P	445.12	4.018	Cys-Cys-Gly-Tyr	0.39	3.57	0.03
8	P	731.60	7.495	Ubiquinol	0.76	3.08	0.05
9	N	616.47	7.232	[SP (16:0)] N-(hexadecanoyl)-sphing-4-enine-1-phosphate	1.39	3.06	0.01
10	P	788.61	4.183	[PC (18:0/18:1)] 1-octadecanoyl-2-(9Z-octadecenoyl)-sn-glycero-3-phosphocholine	0.95	2.99	0.05
11	P	796.59	4.171	PE(18:0/22:4(7Z,10Z,13Z,16Z))	0.86	2.91	0.005
12	N	701.56	7.521	[SP (16:0)] N-(hexadecanoyl)-sphing-4-enine-1-phosphocholine	0.82	2.89	0.02
13	N	763.56	7.283	[PR] Loroxanthin ester/ Loroxanthin dodecenoate	1.20	2.57	0.03
14	P	538.52	4.057	[SP (16:0)] N-(hexadecanoyl)-sphing-4-enine	0.94	2.55	0.05
15	P	223.06	4.107	2-(3'-methylthio)propylmalate	0.56	2.35	0.01
16	P	703.57	7.430	[SP (16:0)] N-(hexadecanoyl)-sphing-4-enine-1-phosphocholine	0.81	2.27	0.01
17	P	703.57	7.501	[SP (16:0)] N-(hexadecanoyl)-sphing-4-enine-1-phosphocholine	0.80	2.24	0.01
18	P	371.32	4.809	2-monooleoylglycerol	1.95	2.15	0.007
19	P	689.56	7.537	[SP (18:0/14:0)] N-(octadecanoyl)-tetradecasphing-4-enine-1-phosphoethanolamine	0.80	1.99	0.01
20	P	223.00	14.340	2,4-substituted-furan	1.35	1.88	0.0004

Macrophages were treated as outlined in section 2.11.1 and analysed in section 2.11.3. DM refers to detection zone, M/Z to mass ratio, RT to raw retention time, WZF and KZF to fold changes in wild type and knockout MKP-2 compared to their controls and according to their P values, n=3.

Table 4. 4 The list of top 20 detected metabolite that were downregulated in MKP-2$^{-/-}$ macrophages following 15 minutes zymosan stimulation

No.	Polarity	m/z	RT	Name	15WZ F WT	15KZ F KO	P value
1	N	120.04	7.367	Benzamide	156.58	0.96	0.03
2	P	193.12	13.791	[FA (12:4)] 2E,4E,8Z,10E-dodecatetraenoic acid	30.51	0.90	0.001
3	P	261.04	16.372	D-Glucose 6-phosphate	22.49	0.33	0.002
4	P	302.21	4.670	Leu-Leu-Gly	20.91	5.66	0.05
5	P	303.24	7.703	nonenoylcarnitine	16.77	0.64	0.04
6	P	708.49	4.188	PS(14:0/16:0)	14.39	1.35	0.0007
7	P	320.18	4.773	Leu-Thr-Ser	9.18	1.44	0.03
8	P	269.09	11.235	2(alpha-D-Mannosyl)-D-glycerate	4.95	2.67	0.0002
9	N	338.99	18.389	D-Fructose 1,6-bisphosphate	2.37	0.28	0.02
10	N	282.08	12.972	Guanosine	2.11	0.53	0.02
11	P	746.10	17.238	NADPH	1.89	1.58	0.002
12	N	168.99	16.322	DL-Glyceraldehyde 3-phosphate	1.83	0.34	0.03
13	N	620.02	17.014	ADP ribose 1",2"-phosphate	1.81	0.42	0.04
14	P	148.06	11.565	L-Glutamate	1.61	0.25	0.05
15	P	613.16	17.666	Glutathione disulfide	1.59	0.28	0.04
16	P	212.04	15.454	Phosphocreatine	1.54	0.47	0.001
17	P	608.09	15.347	UDP-N-acetyl-D-glucosamine	1.46	0.60	0.004
18	N	742.07	17.018	NADP+	1.37	0.42	0.04
19	N	133.01	16.235	(S)-Malate	1.35	0.68	0.01
20	N	163.04	13.409	Phenyl pyruvate	1.35	0.88	0.05

Macrophages were treated as outlined in section 2.11.1 and analysed in section 2.11.3. DM refers to detection zone, M/Z to mass ratio, RT to raw retention time, WZF and KZF to fold changes in wild type and knockout MKP-2 compared to their controls and according to their P values, n=3.

Results in Table 4.5 for 2 hr stimulation with zymosan, during which time phagocytosis was largely complete, showed no upregulation at any metabolites. Instead many metabolites were downregulated in MKP-2 deleted macrophages. Some of these were similar to 15 minutes such as amino acid profiles but largely the metabolites were different. An ascorbate and alderate pathway metabolite (trihydroxy-butanoic acid), known as Threonic acid, was down regulated in MKP-2$^{-/-}$ macrophages by approximately 20-37 fold compared to wild type. A mannocyl- glyceride degradation intermediate (2-O-(6-phospho-α-mannosyl)-D-glycerate) was significantly decreased by over 90% in MKP-2 deleted macrophages compared to wild type.

Interestingly, glycolysis pathway metabolites (D-Glucose 6-phosphate, D-Fructose 1, 6-bisphosphate, DL-Glyceraldehyde 3-phosphate and UDP-glucose (a mannose receptor agonist) were all down regulated in MKP-2$^{-/-}$ macrophages (Table 4.5). TCA cycle metabolites (L-Glutamate, GMP, and S- Malate) were downregulated in MKP-2 deleted macrophages compared to their wild type counterparts (Table 4.5), indicative of a different metabolic signature between 5 minutes and 2 hours. Metabolites of the purine metabolism pathway (Guanosine, Guanine, GMP, ADP and GDP) and pyrimidine metabolism (UMP, UDP and UDP-glucose) were all decreased in MKP-2$^{-/-}$ macrophages compared to MKP-2$^{+/+}$ macrophages treated with zymosan particles for two hours.

Table 4. 5 Down regulated metabolites after 2 hours zymosan stimulation in MKP-2$^{-/-}$ macrophages

No	DM	m/z	RT	Name	2WZ F WT	2KZ F KO	P value
1	P	137.05	15.71	[FA trihydroxy(4:0)] 2,3,4-trihydroxy-butanoic acid	50.39	31.13	0.001
2	N	135.03	11.34	[FA trihydroxy(4:0)] 2,3,4-trihydroxy-butanoic acid/ Threonic acid	48.80	11.85	0.003
3	N	267.07	11.22	2(alpha-D-Mannosyl)-D-glycerate	44.15	14.99	0.0006
4	N	347.04	15.71	2-O-(6-phospho-α-mannosyl)-D-glycerate	39.38	7.31	0.002
5	P	538.16	4.00	Asp-Trp-Asp-Cys	13.68	1.89	0.02
6	P	261.04	16.37	D-Glucose 6-phosphate	10.36	1.52	0.72895
7	N	338.99	18.39	D-Fructose 1,6-bisphosphate	9.64	3.35	0.003
8	N	211.00	15.58	P-DPD	9.15	2.04	0.03
9	N	282.08	12.97	Guanosine	8.29	0.21	0.0005
10	P	148.06	11.57	L-Glutamate	6.94	3.51	0.008
11	N	362.05	16.96	GMP	4.02	0.75	0.002
12	N	323.03	15.54	UMP	3.94	0.76	0.05
13	P	152.06	12.76	Guanine	3.71	0.42	0.01
14	N	442.02	18.30	GDP	2.88	0.70	0.04
15	N	346.06	14.07	AMP	2.56	0.78	0.03
16	N	403.00	16.87	UDP	2.38	0.80	0.004
17	N	168.99	16.32	DL-Glyceraldehyde 3-phosphate	2.37	0.41	0.001
18	P	444.03	18.30	GDP	2.20	0.63	0.05
19	N	565.05	16.55	UDP-glucose	2.19	0.52	0.002
20	N	426.02	15.63	ADP	1.79	0.48	0.001
21	N	133.01	16.23	(S)-Malate	1.67	0.72	0.02
22	N	540.05	14.54	Cyclic ADP-ribose	1.34	0.52	0.00

Macrophages were treated as outlined in section 2.11 and analysed in section 2.11.3. DM refers to detection zone, M/Z to mass ratio, RT to raw retention time, WZF and KZF to fold changes in wild type and knockout MKP-2 compared to their controls and according to their P values, n=3.

One of the mechanisms that macrophages use to kill pathogens that are phagocytosed is through releasing toxic substances such as ROS (Aderem and Underhill, 1999). Thus, it was expected to see changes in the metabolic pathway that generate these substances. Not-surprisingly, results show that after 24 hours incubation with zymosan particles, there was a significant (**$P<0.01$) upregulation in components of the arginine and proline metabolism pathway (L-Ornithine, Creatine, and L-Citrulline) in MKP-2$^{-/-}$ macrophages compared to MKP-2$^{+/+}$ macrophages (Table 4.6). The Acyl CoA intermediate suberic acid was elevated by approximately 29 fold in MKP-2 deleted macrophages after 24 hours. Purine metabolism pathway intermediates (Hypoxanthine and Adenine Mono Phosphate, AMP) were upregulated in MKP-2$^{-/-}$ macrophages by 12 and 3 fold respectively. UDP-glucose, which is a key intermediate in the carbohydrate metabolism, was upregulated 11 fold in MKP-2 deleted macrophages following 24 hour zymosan stimulation. Pyrimidine metabolism (5, 6-Dihydrouracil and UMP) was also found to be elevated (Table 4.6).

After 24 hours of zymosan stimulation, down regulation of the glutathione pathway was indicated in MKP-2$^{-/-}$ macrophages with a high production of metabolites such as S-allyl cysteine and prenyl-L-cysteine compared to their levels in MKP-2$^{+/+}$ macrophages (Table 4.7). This pattern returned to that observed for 5 minutes stimulation (Table 4.2).

In conclusion, the glycolysis pathway seemed to be mostly regulated when phagocytizing zymosan in both MKP-2$^{+/+}$and MKP-2$^{-/-}$ macrophages. A summary of the glycolytic metabolite uptake profile during phagocytosis of zymosan is shown in figure 4.17. MKP-2 deleted macrophages showed a different pattern in glycolysis during phagocytosis from MKP-2 wild type macrophages. For example, at an early time point, 5 minutes, glycolysis metabolites were upregulated in MKP-2 deleted macrophages (shown as purple in Fig.4.17), decreased towards 15 minutes of zymosan incubation and then downregulated after 2 hours. This pattern was reversed in MKP-2$^{+/+}$ phagocytes (shown as green in Fig.4.18) when glycolysis metabolites started at low levels at 5 minutes and increased towards 15 minutes and then reached a maximum at 2 hours. By 24 hours, glycolysis metabolites were not changed in either group. These results demonstrate an important role for MKP-2 in controlling glycolysis and phagocytosis function.

Table 4. 6 List of metabolites upregulated in MKP-2$^{-/-}$ macrophages after 24 hours zymosan

No.	DM	m/z	RT	Name	ZW F WT	ZK F KO	ZK P
1	N	132.09	16.53	L-Ornithine	12.32	1050.29	0.05
2	N	131.07	15.30	Creatine	44.84	223.11	0.05
3	N	800.56	3.74	PG(18:0/20:3(5Z,8Z,11Z)	1.28	31.86	0.04
4	P	317.29	4.75	[SP hydrox] 4-hydroxysphinganine	0.42	30.41	0.04
5	N	174.09	3.95	Suberic acid	0.01	29.19	0.01
6	N	446.06	17.01	CDP-ethanolamine	0.03	12.18	0.04
7	P	136.04	16.07	Hypoxanthine	0.29	12.06	0.04
8	N	566.06	16.91	UDP-glucose	0.01	11.77	0.05
9	P	165.06	13.60	3-Methylguanine	0.56	6.32	0.01
10	P	612.15	17.90	Glutathione disulfide	1.84	5.28	0.002
11	N	307.08	17.89	Glutathione	1.89	4.55	0.002
12	P	177.06	10.75	4-Hydroxy-4-methylglutamate	0.36	4.50	0.002
13	P	114.04	15.86	5,6-Dihydrouracil	0.76	3.80	0.004
14	P	347.06	14.61	AMP	1.22	3.77	0.005
15	N	324.04	16.92	UMP	0.09	3.74	0.01
16	N	507.33	4.77	[PC (17:0)] 1-(10Z-heptadecenoyl)-sn-glycero-3-phosphocholine	1.65	3.14	0.002
17	N	501.28	4.06	[PE (20:4)] 1-(5Z,8Z,11Z,14Z-eicosatetraenoyl)-sn-glycero-3-phosphoethanolamine	2.61	3.02	0.003
18	P	175.10	16.17	L-Citrulline	0.32	2.39	0.02
19	N	347.06	14.70	AMP	0.51	2.34	0.03
20	P	183.07	15.25	Choline phosphate	0.58	1.50	0.05

Macrophages were treated as outlined in section 2.11.1 and analysed in section 2.11.3. DM refers to detection zone, M/Z to mass ratio, RT to raw retention time, WZF and KZF to fold changes in wild type and knockout MKP-2 compared to their controls and according to their P values, n=3.

Table 4. 7 Down regulated metabolites in MKP-2$^{-/-}$ macrophages after 24 hours incubation with zymosan

No	DM	M/Z	RT	Name	ZW FC WT	ZKO FC KO	P value
1	P	161.05	7.651	Allyl cysteine	115.02	1.63	0.03
2	P	189.08	4.823	Prenyl-L-cysteine	57.62	1.20	0.03
3	P	189.08	7.408	Prenyl-L-cysteine	38.88	1.34	0.03

Macrophages were treated as outlined in section 2.11.1 and analysed in section 2.11.3. DM refers to detection zone, M/Z to mass ratio, RT to raw retention time, WZF and KZF to fold changes in wild type and knockout MKP-2 compared to their controls and according to their P values, n=3.
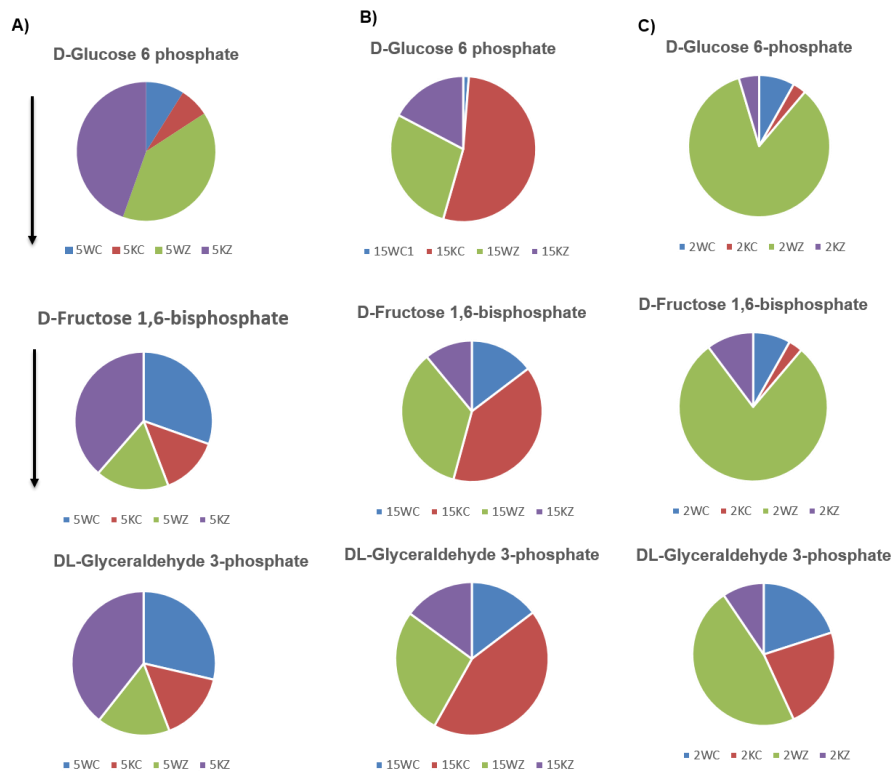
Figure 4. 17 Changes in Glycolysis pathway metabolites following Zymosan phagocytosis

MKP-2$^{+/+}$ and MKP-2$^{-/-}$ macrophages were incubated with opsonized zymosan particles for 5, 15 or 120 minutes or left untreated. Cell extracts were prepared for untargeted metabolomics as described in section 2.11. Results show A) upregulated metabolites of glycolysis pathway in MKP-2 deleted macrophages (purple) after 5 minutes phagocytosis of zymosan). B), and C) shows down regulated glycolysis metabolites after 15 minutes and 2 hours. Results represents 3 independent experiments. Fold changes and p values are presented in tables 4.1, 4.4, 4.6.

4.2.4.2 Metabolic changes underlying LPS stimulation in BMDMs in MKP-2$^{-/-}$ macrophages

Having established changes in macrophage metabolomics during phagocytosis, the effect of LPS was investigated in order to further understand metabolic changes that accompany LPS-mediated macrophage phagocytosis, migration and proliferation. Unsurprisingly, some of the changes were different. Increases in glycolysis pathway metabolites (D-Glucose 6 phosphate, Glycerol 3-phosphate) are observed in both MKP-2$^{+/+}$ and MKP-2$^{-/-}$ macrophages following LPS stimulation for 5 minutes to 11.71 and 14.61 folds respectively (see Table 4.8). Upregulation of the pentose phosphate pathway and purine metabolism was shown in MKP-2 deleted macrophages via the uptake of metabolites (D-Ribose 5-phosphate, Guanosine monophosphate, GMP, Guanine, Guanosine diphosphate, GDP and Guanosine triphosphate). The TCA cycle intermediate ((2S)-2-Isopropylmalate) was increased in both MKP-2$^{+/+}$ and MKP-2$^{-/-}$ macrophages (Table 4.8).

Following LPS stimulation, some groups of metabolites were downregulated following MKP-2 gene deletion. For example, results show decreased metabolites that are involved in ascorbate and alderate metabolism pathway via a threonic acid intermediate ([FA trihydroxy (4:0)] 2, 3, 4-trihydroxy-butanoic acid) which approximately decreased 10 fold relative to their wild type MKP-2 counterparts (*** $P<0.001$). Glutathione, histidine and citrate cycle (TCA cycle) metabolites were decreased in MKP-2$^{-/-}$ macrophages compared to MKP-2$^{+/+}$ macrophages (Table 4.9).

Table 4. 8 Upregulated metabolites in MKP-2^{-/-} macrophages after 5 minutes LPS stimulation

DM	m/z	RT	Name	5WL F WT	5KL F KO	P
P	261.036	16.4	D-Glucose 6-phosphate	11.71	14.61	0.03
N	229.012	16.1	D-Ribose 5-phosphate	0.32	10.32	0.03
N	528.310	7.6	LysoPE(0:0/22:4(7Z,10Z,13Z,16Z)) lysophospholipid	0.72	5.74	0.05
P	148.060	11.6	L-Glutamate	2.75	5.40	0.03
N	362.051	17.0	GMP	1.05	5.15	0.05
P	364.064	17.0	GMP	1.76	5.04	0.05
P	502.302	4.7	Arg-Leu-Val-Asp	1.92	4.11	0.05
N	211.001	13.9	P-DPD	0.60	4.02	0.03
P	405.008	16.6	UDP	1.81	3.89	0.05
P	161.092	7.6	D-Alanyl-D-alanine	1.93	3.85	0.008
P	152.056	12.8	Guanine	2.15	3.81	0.03
P	444.030	18.3	GDP	2.24	3.59	0.006
P	156.076	16.0	L-Histidine	0.08	3.54	0.001
P	523.997	19.7	GTP	1.61	3.24	0.03
P	744.081	17.0	NADP+	2.39	2.95	0.009
N	613.139	17.7	CMP-N-acetylneuraminate	0.48	2.87	0.02
N	175.060	10.2	(2S)-2-Isopropylmalate	1.57	2.80	0.02
P	428.036	15.6	ADP	1.68	2.64	0.01
P	336.086	14.9	S-Formylglutathione	1.66	2.63	0.004
N	306.077	14.7	Glutathione	1.57	2.43	0.04
N	171.006	14.9	sn-Glycerol 3-phosphate	1.34	2.36	0.03
N	346.056	17.0	AMP	1.39	2.34	0.04
P	447.066	16.6	CDP-ethanolamine	1.52	2.29	0.02
P	720.017	13.2	Phosphoribosyl-ATP	1.76	2.25	0.005
P	508.002	17.0	ATP	1.42	2.16	0.04
N	606.075	15.3	UDP-N-acetyl-D-glucosamine	1.32	2.12	0.01
P	248.149	11.8	Hydroxybutyrylcarnitine	1.50	2.08	0.01
P	110.027	15.4	Hypotaurine	1.37	2.08	0.04
P	212.042	15.5	Phosphocreatine	1.38	2.03	0.01
P	126.022	15.2	Taurine	1.43	1.91	0.003

Macrophages were treated as outlined in section 2.11.1 and analysed in section 2.11.3. DM refers to detection zone, M/Z to mass ratio, RT to raw retention time, WZF and KZF to fold changes in wild type and knockout MKP-2 compared to their controls and according to their P values, n=3.

Table 4. 9 Downregulated metabolites in MKP-2^{-/-} macrophages after 5 minutes LPS stimulation

DM	m/z	RT	Name	5WL F WT	5KL F KO	P
P	137.045	15.7	[FA trihydroxy(4:0)] 2,3,4-trihydroxy-butanoic acid	12.55	1.83	0.001
P	159.076	16.3	4-Methylene-L-glutamine	6.50	1.60	0.001
P	198.087	7.0	N-Acetyl-L-histidine	6.25	3.44	0.01
P	162.058	5.1	Allyl cysteine	5.15	1.94	0.005
P	148.060	10.6	L-Glutamate	3.08	2.09	0.004
P	269.087	11.2	2(alpha-D-Mannosyl)-D-glycerate	2.84	1.99	0.004
P	249.106	10.0	Glu-Thr	2.52	1.03	0.008
P	349.053	15.7	2-O-(6-phospho-α-mannosyl)-D-glycerate	2.50	1.68	0.007
P	427.094	17.3	S-glutathionyl-L-cysteine	2.47	1.35	0.001
N	151.983	16.6	Thiocysteine	1.89	0.97	0.009
P	170.092	13.3	N(pi)-Methyl-L-histidine	1.64	1.53	0.007
P	221.018	14.9	4,4'-dithiodipyridine	1.63	2.45	0.0009
N	239.016	16.6	L-Cystine	1.62	1.16	0.007
P	203.150	22.0	NG,NG-Dimethyl-L-arginine	1.47	1.20	0.002
N	191.019	18.4	Citrate	1.35	0.82	0.05

Macrophages were treated as outlined in section 2.11.1 and analysed in section 2.11.3. DM refers to detection zone, M/Z to mass ratio, RT to raw retention time, WZF and KZF to fold changes in wild type and knockout MKP-2 compared to their controls and according to their P values, n=3.

After 15 minutes of LPS treatment a new pattern emerged, upregulation of pentose phosphate pathway metabolites (D-Ribose 5- phosphate) was detected which feeds the formation of more D-Fructose 1, 6-bisphosphate within glycolysis (Figure 4.18). Both metabolites were significantly upregulated in MKP-2$^{-/-}$ macrophages compared to MKP-2$^{+/+}$ macrophages; 35,438 ± 6,869 vs 6,128 ± 994, for D-Ribose 5- phosphate and 851.36 ± 100 vs 304.89 ± 16.79 for D-Fructose 1, 6-bisphosphate respectively. Metabolites of purine metabolism (AMP, GMP and GDP) were elevated in MKP-2$^{-/-}$ macrophages however, this was not significant compared to MKP-2$^{+/+}$ macrophages (Table 4.10).

Furthermore, the purine metabolism intermediate guanosine, was reduced by approximately 3 fold in MKP-2 deleted macrophages after 15 minutes of LPS stimulation (Table 4.11). This is a different pattern from that observed after 5 minutes when it was upregulated. The arginine and proline pathway metabolites (L-Glutamate, Ornithine and N-Acetyl ornithine) started to decline as early as 15 minutes post LPS treatment.
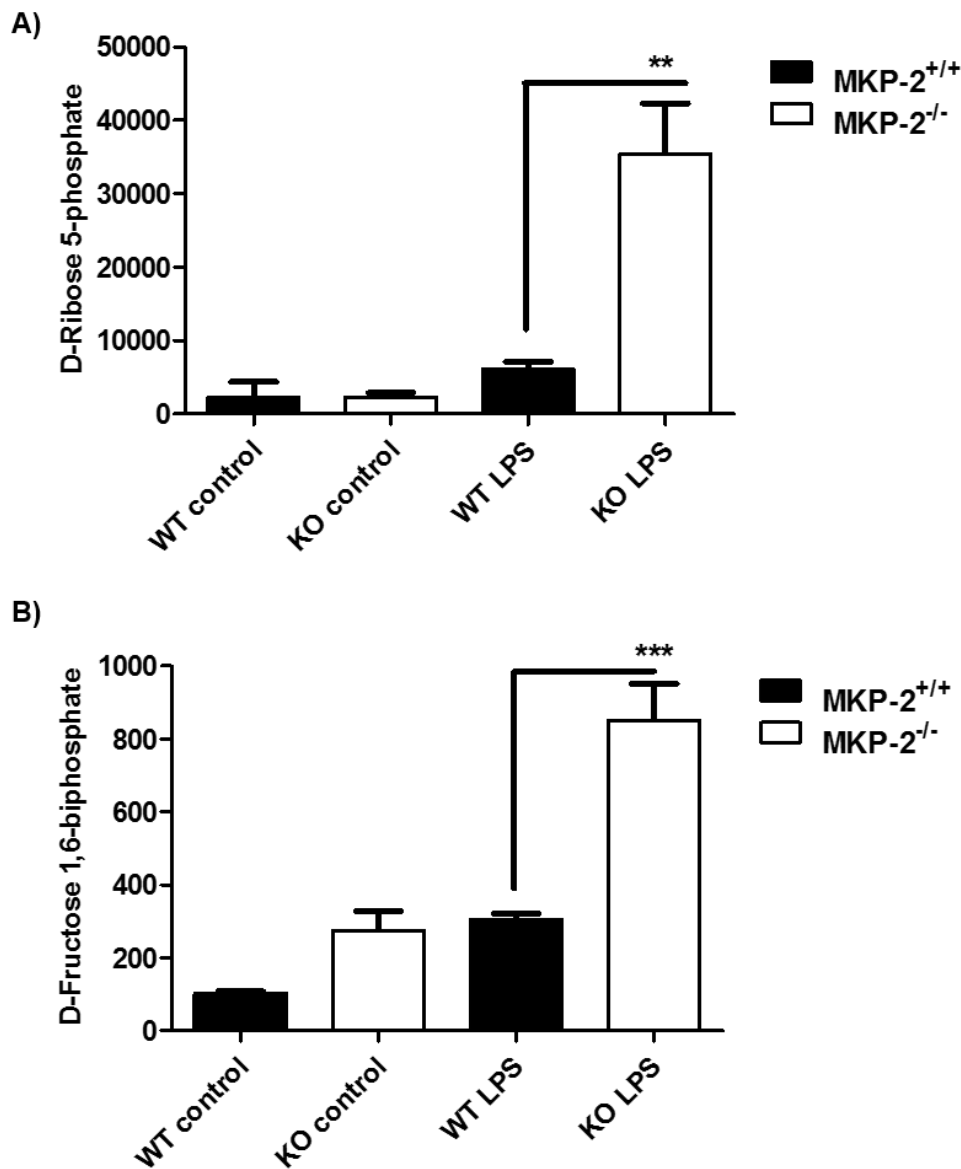
Figure 4. 18 Upregulation of pentose phosphate pathway and glycolysis in MKP-2 deleted BMDMs stimulated with LPS

MKP-2^{+/+} and MKP-2^{-/-} macrophages were seeded in 6-well plates at a density of 2×10^6 cells /well and stimulated with 100ng/ml of LPS for 15 minutes or left untreated as controls. Cell extracts were prepared for untargeted metabolomics as described in section 2.2.10. Results show A) Upregulated metabolites of the pentose phosphate pathway in MKP-2 deleted macrophages. B) Upregulated metabolites of the glycolysis pathway. Data represents mean ± SEM of n=3 (5 mice were used from each group in each experiment), Bonferroni's multiple comparison test were ** $P<0.01$, *** $P<0.001$ for MKP-2^{+/+} versus MKP-2^{-/-}.

Table 4. 10 Upregulated metabolites in MKP-2$^{-/-}$ after 15 minutes LPS stimulation

DM	m/z	RT	Name	15WL F WT	15KL F KO	15KL P
N	229.01	16.066	D-Ribose 5-phosphate	0.83	15.45	0.008
N	135.03	11.337	[FA trihydroxy(4:0)] 2,3,4-trihydroxy-butanoic acid	6.77	7.84	0.02
N	346.06	14.066	AMP	1.51	3.45	0.04
N	338.99	18.389	D-Fructose 1,6-bisphosphate	2.98	3.09	0.007
P	364.06	16.957	GMP	1.59	3.06	0.009
N	362.05	16.961	GMP	1.71	2.96	0.01
P	165.06	13.460	dimethylsulfonio-2-hydroxybutyrate	1.53	2.13	0.00004
N	442.02	18.302	GDP	1.54	1.64	0.05

Macrophages were treated as outlined in section 2.11.1 and analysed in section 2.11.3. DM refers to detection zone, M/Z to mass ratio, RT to raw retention time, WZF and KZF to fold changes in wild type and knockout MKP-2 compared to their controls and according to their P values, n=3.

Table 4. 11 Downregulated metabolites in MKP-2$^{-/-}$ after 15 minutes LPS stimulation

DM	m/z	RT	Name	15WL F WT	15KL F KO	P
P	284.10	12.962	Guanosine	4.27	1.62	0.05
P	148.06	11.565	L-Glutamate	4.00	1.15	0.01
P	180.09	15.425	D-Glucosamine	3.56	0.92	0.03
N	620.02	17.014	ADP ribose 1'',2''-phosphate	2.94	1.78	0.008
P	190.09	4.814	Prenyl-L-cysteine	2.82	1.12	0.002
P	162.06	5.070	allylcysteine	2.76	1.20	0.004
N	742.07	17.018	NADP+	2.68	1.84	0.04
P	744.08	17.017	NADP+	2.45	1.87	0.03
P	156.08	15.963	L-Histidine	2.42	0.98	0.05
P	198.09	6.954	N-Acetyl-L-histidine	2.29	1.43	0.04
N	151.03	11.576	Xanthine	1.92	1.40	0.001
N	425.08	17.260	S-glutathionyl-L-cysteine	1.82	0.94	0.02
P	198.09	8.930	N-Acetyl-L-histidine	1.71	0.94	0.02
N	191.02	18.353	Citrate	1.70	0.96	0.02
P	444.03	18.305	GDP	1.69	1.62	0.008
P	746.10	17.238	NADPH	1.62	0.22	0.0002
N	154.06	16.484	L-Histidine	1.60	1.06	0.01
P	175.11	13.917	N-Acetylornithine	1.56	0.90	0.02
N	167.02	12.799	Urate	1.56	1.34	0.02
N	306.08	17.277	Glutathione	1.54	1.07	0.02
N	131.08	26.600	L-Ornithine	1.53	0.91	0.02
P	114.07	10.068	Creatinine	1.52	0.93	0.01
N	239.02	16.580	L-Cystine	1.52	1.16	0.03
P	120.07	14.875	L-Threonine	1.51	1.02	0.01
P	150.06	11.929	L-Methionine	1.51	0.96	0.02
P	204.13	12.490	Lys-Gly	1.51	0.90	0.02
N	180.07	13.463	L-Tyrosine	1.49	0.89	0.05
P	106.05	16.145	L-Serine	1.48	0.96	0.03
P	133.10	23.579	L-Ornithine	1.47	0.89	0.04
P	166.09	10.618	L-Phenylalanine	1.47	0.96	0.02

Macrophages were treated as outlined in section 2.11.1 and analysed in section 2.11.3. DM refers to detection zone, M/Z to mass ratio, RT to raw retention time, WZF and KZF to fold changes in wild type and knockout MKP-2 compared to their controls and according to their P values, n=3.

After two hours stimulation by LPS, the metabolic profiling showed an increased uptake of Threonic acid in both MKP-2$^{+/+}$ and MKP-2$^{-/-}$ macrophages compared to their controls (61.53 and 52.53 fold) respectively (Table 4.12). Threonic acid is a glycated protein and a substrate of L-threonate 3-dehydrogenase in the ascorbate and alderate metabolism pathway.

D-Fructose 1, 6-bisphosphate is one of the metabolites that involved in both glycolytic and pentose phosphate pathways and shown earlier to be upregulated earlier after 15 min LPS stimulation. Overall results show significant upregulation of D-Fructose 1, 6-bisphosphate starting from 5 minutes and peaking at 15 minutes in MKP-2$^{-/-}$ macrophages compared to MKP-2$^{+/+}$ macrophages (851.36 ± 100.02 versus 304.89 ± 16.79) and remaining upregulated for up to two hours (Figure 4.19, A,B and C). After 24 hours these metabolites were not different from basal values recorded at the start of the experiment. To conclude, results demonstrate a significant upregulation in glycolysis and the pentose phosphate pathway in MKP-2 deleted macrophages following LPS stimulation.

Table 4. 12 Upregulated metabolites in MKP-2$^{-/-}$ after 2 hours LPS stimulation

DM	m/z	RT	Name	2WL F WT	2KL F KO	P
P	137.05	11.197	[FA trihydroxy(4:0)] 2,3,4-trihydroxy-butanoic acid/ Thrionic acid	52.35	61.53	0.00002
N	267.07	11.218	2(alpha-D-Mannosyl)-D-glycerate	27.95	51.65	0.00002
P	261.04	16.372	D-Glucose 6-phosphate/ glycolysis	9.79	15.78	0.002
N	338.99	18.389	D-Fructose 1,6-bisphosphate/ glycolysis	5.40	9.89	0.0002
P	203.14	5.034	Leu-Ala	2.15	3.76	0.0003
N	168.99	16.322	DL-Glyceraldehyde 3-phosphate	0.99	1.76	0.0001
P	502.30	4.673	Arg-Leu-Val-Asp	1.55	1.71	0.001
N	323.03	16.538	UMP / Pyrimidine metabolism	1.17	1.65	0.00004
N	482.96	18.285	UTP/ Pyrimidine metabolism	0.75	1.37	0.0006
N	742.07	17.018	NADP+/ pentose phosphate pathway	0.67	1.29	0.07
N	306.08	14.668	Glutathione	0.62	1.19	0.01
N	131.08	26.600	L-Ornithine	0.64	0.70	0.01
N	505.99	17.005	ATP / Purine metabolism	0.31	0.65	0.0002
N	426.02	17.005	ADP/ Purine metabolism	0.30	0.65	0.0001
P	508.00	17.000	ATP/ Purine metabolism	0.58	0.64	0.00007
N	133.01	16.235	(S)-Malate/ TCA- cycle	1.05	1.44	0.0006

Macrophages were treated as outlined in section 2.11.1 and analysed in section 2.11.3. DM refers to detection zone, M/Z to mass ratio, RT to raw retention time, WZF and KZF to fold changes in wild type and knockout MKP-2 compared to their controls and according to their P values, n=3.
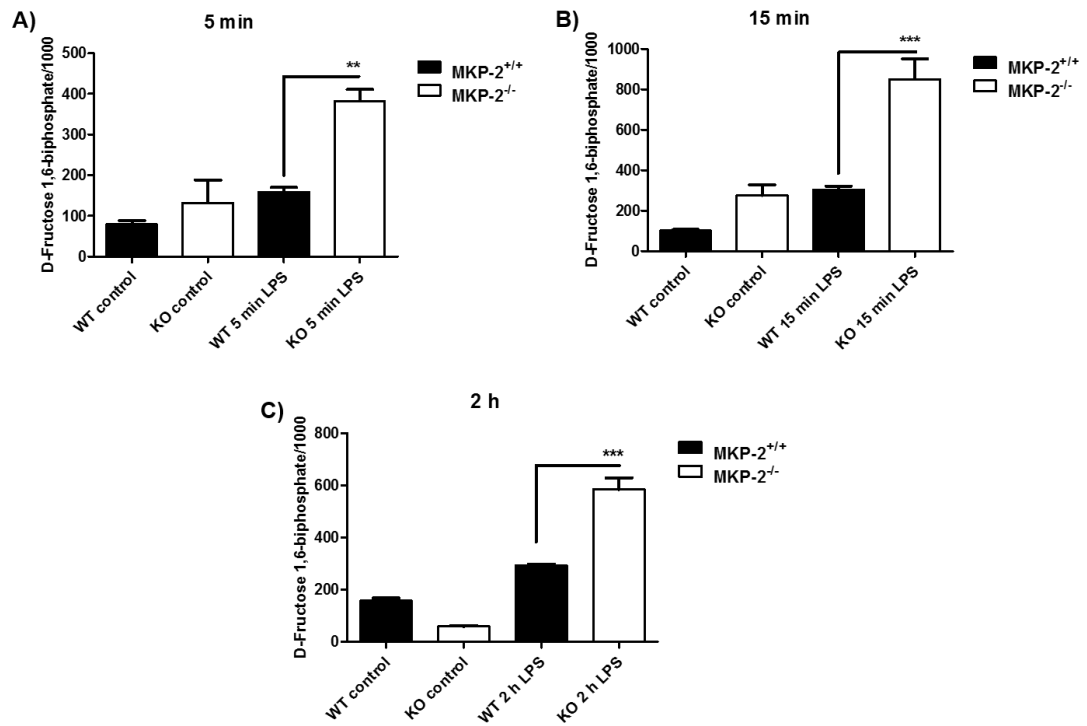
Figure 4. 19 Upregulation of Glycolysis pathway metabolites in MKP-2^{-/-} BMDMs stimulated with LPS

MKP-2 [+/+] and MKP-2 [-/-] macrophages were seeded in 6-well plates at a density of $2x10^6$ cells /well and stimulated with 100ng/ml of LPS for 5,15 or 120 minutes or left untreated as controls. Cell extracts were prepared for untargeted metabolomics as described in section 2.11. Results show A) Upregulated D-Fructose 1, 6-bisphosphate after 5 minutes of LPS in MKP-2 deleted macrophages. B) 15 minutes. C) 120 minutes. Data represents mean ± SEM of n=3 (5 mice were used from each group in each experiment), Bonferroni's multiple comparison test, ** P<0.01, *** P<0.001 in MKP-2^{+/+} versus MKP-2^{-/-}.

Metabolic changes were observed at early time points following LPS stimulation that differed when the MKP-2 gene was deleted. However, LPS is well recognised to have long term cellular actions linked to inflammation for example, enhanced cytokine release. Also well recognised are changes in the arginine and proline pathway products such as nitric oxide that was previously shown to be affected by MKP-2 deletion in parasite infected macrophages through effects upon iNOS expression (Al-Mutairi *et al.*, 2010). Therefore, investigating the metabolic changes in this context would clarify the exact mechanism and pathways involved in these changes.

The metabolites produced after 24 hours of LPS stimulation showed increased levels of phosphoglycerate and glycerophosphoglycerol, these metabolites were upregulated in MKP-2$^{-/-}$ macrophages compared to their controls (555 and 188 folds respectively). Enhanced amino sugar and nucleotide sugar metabolism was indicated by increased UDP-glucose concentration in MKP-2 deleted macrophages which increased by 28 fold compared to only 2.79 folds in the WT (Table 4.13). An accumulation of L-Citrulline was observed to be higher in MKP-2 deleted macrophages compared to wild types by about 8 fold. This metabolite belongs to the Arginine and Proline metabolic pathway. In contrast however, other metabolites of this pathway such as Creatine, L-Ornithine, L-Arginine and L-Proline were shown to be down regulated in MKP-2$^{-/-}$ macrophages compared to their levels in MKP-2$^{+/+}$ macrophages (Table 4.14). Also, the TCA-cycle metabolite (citrate) was reduced by about 4 fold in MKP-2 deleted macrophages.

Table 4. 13 Upregulated metabolites in MKP-2⁻ᐟ⁻ macrophages after 24 hours LPS stimulation

DM	m/z	RT	Name	LW F WT	LW P	LK F KO	LK P
N	800.56	3.744	PG(18:0/20:3(5Z,8Z,11Z)	2.19	0.00185	557.04	0.1
N	246.05	13.567	Glycerophosphoglycerol	2.97	0.78448	188.22	0.2
P	159.13	7.579	DL-2-Aminooctanoicacid	11.85	0.39030	86.84	0.2
N	566.06	16.910	UDP-glucose	1.77	0.05857	28.80	0.4
P	358.16	4.165	Cilastatin	0.38	0.00891	23.17	0.5
P	175.10	16.174	L-Citrulline	10.18	0.00608	18.94	0.00003
P	136.04	11.545	[FA trihydroxy(4:0)] 2,3,4-trihydroxy-butanoic acid	1.47	0.19529	12.99	0.001
P	165.06	13.603	3-Methylguanine	1.34	0.53315	9.86	0.01
P	177.06	10.753	4-Hydroxy-4-methylglutamate	1.29	0.58564	7.09	0.006
P	612.15	17.900	Glutathione disulfide	4.97	0.00300	7.01	0.003
P	136.04	16.070	Hypoxanthine	0.46	0.04294	6.88	0.1
P	769.56	4.226	PC(15:0/20:3(5Z,8Z,11Z))	3.10	0.01610	5.86	0.3
P	177.06	10.948	4-Hydroxy-4-methylglutamate	1.54	0.40802	5.73	0.02
N	612.15	17.907	Glutathione disulfide	4.13	0.00876	5.71	0.01
N	307.08	17.890	Glutathione	3.38	0.00340	3.92	0.008
P	109.02	15.632	Hypotaurine	3.34	0.00022	3.65	0.002
P	114.04	15.863	5,6-Dihydrouracil	1.98	0.12553	3.63	0.02
P	459.26	4.262	Trp-Val-Arg	0.59	0.03126	3.58	0.2
N	347.06	14.698	AMP	1.80	0.05343	3.21	0.01
N	307.08	5.023	Glutathione	1.16	0.56421	3.03	0.02

Macrophages were treated as outlined in section 2.11.1 and analysed in section 2.11.3. DM refers to detection zone, M/Z to mass ratio, RT to raw retention time, WZF and KZF to fold changes in wild type and knockout MKP-2 compared to their controls and according to their P values n=3.

Table 4. 14 Down regulated metabolites in MKP-2$^{-/-}$ macrophages after 24 hours LPS stimulation

DM	m/z	RT	Name	LW F WT	LW P	LK F KO	LK P
P	99.01	8.323	Allylisothiocyanate	4926.78	0.05150	2.31	0.10692
N	131.07	15.297	Creatine / Arginine and proline metabolism	2143.97	0.04656	167.25	0.21263
P	189.08	4.823	Prenyl-L-cysteine	285.49	0.22669	2.00	0.07850
P	238.07	4.554	Xanthopterin-B2	278.11	0.12089	0.33	0.13550
P	188.08	11.572	N-Acetylglutamine	256.36	0.10387	1.04	0.93065
N	446.06	17.010	CDP-ethanolamine/ Glycerophospholipid metabolism	170.54	0.16932	54.94	0.40635
P	189.08	7.408	Prenyl-L-cysteine	167.89	0.16628	1.89	0.03062
N	785.60	4.181	[PC (18:1/18:1)] 1-(9Z-octadecenoyl)-2-(9Z-octadecenoyl)-sn-glycero-3-phosphocholine	23.03	0.00256	7.73	0.05763
N	299.01	15.292	2-Methyl-4-amino-5-hydroxymethylpyrimidine diphosphate	9.33	0.00976	5.50	0.01391
P	145.16	15.339	Spermidine / Arginine and proline metabolism	8.85	0.00001	0.62	0.34098
N	663.11	14.986	NAD+	7.67	0.61837	5.25	0.74381
P	703.51	4.22	[PC (14:0/16:1)] 1-tetradecanoyl-2-(9Z-hexadecenoyl)-sn-glycero-3-phosphocholine /Glycerophospholipid metabolism	7.15	0.00003	5.13	0.00201
P	677.50	4.260	[PC (14:0/14:0)] 1,2-ditetradecanoyl-sn-glycero-3-phosphocholine	6.78	0.00001	4.38	0.00053
P	161.05	5.142	Allyl cysteine	5.45	0.00777	1.77	0.00164
N	192.03	18.581	Citrate / TCA- cycle	4.19	0.01806	0.27	0.06315
P	441.34	7.686	3-Hydroxy-11Z-octadecenoylcarnitine	4.15	0.00692	2.29	0.00024
P	195.08	10.345	2-Amino-2-deoxy-D-gluconate	4.04	0.00219	2.92	0.08566
P	114.04	15.324	5,6-Dihydrouracil / Pyrimidine metabolism	3.94	0.00338	3.17	0.00055
P	479.30	4.753	[PE (18:0)] 1-(9Z-octadecenoyl)-sn-glycero-3-phosphoethanolamine	3.90	0.00173	3.62	0.05237
N	324.04	16.917	UMP / Pyrimidine metabolism	3.89	0.02834	1.37	0.41226
N	494.20	4.847	Asp-Phe-Val-Asp	3.82	0.02991	0.34	0.16393

DM	M/Z	RT		WZF		KZF	
P	343.27	5.010	1,2-dioctanoyl-1-amino-2,3-propanediol	3.55	0.00011	1.65	0.02264
P	424.04	15.744	Thiamin diphosphate	3.54	0.00868	2.73	0.00281
P	131.09	11.173	L-Leucine / Aminoacyl-tRNA biosynthesis	3.09	0.11536	0.94	0.91151
P	211.04	15.884	Phosphocreatine/ Arginine and proline metabolism	2.84	0.00004	2.32	0.00177
P	759.61	14.034	PE (20:0/dm18:0)	2.17	0.00126	0.72	0.44875
N	458.24	4.282	[GP (20:4)] 1-(5Z,8Z,11Z,14Z-eicosatetraenoyl)-sn-glycero-3-phosphate	2.17	0.00270	1.83	0.16509
P	369.29	4.933	cis-5-Tetradecenoylcarnitine	2.17	0.00105	1.75	0.00259
N	427.03	16.989	ADP	1.91	0.02066	0.87	0.50257
N	175.06	4.572	Indole-3-acetate	1.36	0.04357	0.44	0.03481
P	197.08	9.681	N-Acetyl-L-histidine	1.30	0.04172	0.57	0.00978
P	244.14	13.419	N-hexenoylglutamine	1.27	0.04792	0.93	0.28792
P	663.11	15.010	NAD+	1.25	0.01927	0.92	0.52615
P	147.05	15.474	L-Glutamate /Arginine and proline metabolism	1.25	0.05875	0.98	0.80042
P	131.06	15.123	L-Glutamate 5-semialdehyde/ Arginine and proline metabolism	1.21	0.12307	0.61	0.06221
P	113.06	10.354	Creatinine	1.16	0.18465	0.67	0.01902
N	180.06	14.659	D-Glucose	1.16	0.12796	0.52	0.04140
N	132.09	25.614	L-Ornithine / Arginine and proline metabolism	1.12	0.33853	0.47	0.00267
N	174.11	25.611	L-Arginine / Arginine and proline metabolism	1.07	0.62844	0.46	0.00387
P	115.06	13.535	L-Proline/ Arginine and proline metabolism	1.05	0.75394	0.66	0.00202

Macrophages were treated as outlined in section 2.11.1 and analysed in section 2.11.3. DM refers to detection zone, M/Z to mass ratio, RT to raw retention time, WZF and KZF to fold changes in wild type and knockout MKP-2 compared to their controls and according to their P values, n=3.

4.2.4.3 Metabolic changes underlying C5a stimulation

Finally, the metabolic changes underlying macrophage migration towards C5a stimulation was investigated in this section. This was significantly altered in MKP-2$^{-/-}$ macrophages. Results showed a rapid increase in the glycolysis intermediate, Glucose-6-phosphate, following 5 minutes stimulation with C5a in MKP-2$^{-/-}$ macrophages compared to MKP-2$^{+/+}$ macrophages (MKP-2$^{-/-}$ = 7330.15 ± 993.5, MKP-2$^{+/+}$ = 369.32 ± 993.53) (Figure 4.20 panel A). D-Fructose 1,6-bisphosphate uptake was also upregulated significantly in MKP-2$^{-/-}$ macrophages compared to MKP-2$^{+/+}$ counterparts (731.74 ± 41.60 vs 230.28 ± 29.20) (Figure 4.20 panel B). In addition, the pentose phosphate pathway metabolite, D-Ribose 5-phosphate which links with to the glycolysis pathway was increased by over 3 fold (17.93 ± 2.51 vs 5.45 ± 1.23) (Figure 4.21). Sphingolipid linked metabolites were also upregulated in MKP-2 deleted macrophages after 5 minutes of C5a stimulation. Those metabolites were SP [(16:0)]N-(hexadecanoyl)-sphing-4-enine-1-phosphocholine and SM (d18:1/24:1(15Z)). Prostaglandin A$_2$, an intermediate of the cyclooxygenase pathway was increased by about 2 fold in MKP-2 deleted macrophages compared to its levels in their wild type counterparts (Table 4.15). Interestingly, results showed no downregulated metabolites in MKP-2$^{-/-}$ macrophages compared to MKP-2$^{+/+}$ macrophages after 5 minutes of C5a stimulation.

After 15 minutes C5a stimulation there were additional significant changes in the metabolite profiles and contrasts between MKP-2$^{-/-}$ and MKP-2$^{+/+}$ macrophages. Phosphatidylserine is an acidic (anionic) phospholipid in glycerophospholipid metabolism and was found to be upregulated by about 9 fold in MKP-2$^{-/-}$ compared with MKP-2$^{+/+}$macrophages (936.26 ± 34.32 versus 104.14 ± 17.14) (Figure 4.22). The sphingolipid metabolism pathway metabolite, sphingomyelin was also upregulated about 3 fold in MKP-2$^{-/-}$ macrophages to 3081.36 ± 635.57 compared to 990.65 ± 77.28 in MKP-2$^{+/+}$ (Figure 4.23). Components of the purine and pyrimidine metabolism pathway were down regulated in MKP-2 deleted macrophages as shown in Table 4.16. Creatinine is one of the metabolites that facilitates cell migration via ATP exchange and hydrolysis (Kuiper *et al.*, 2009). Both creatinine and ATP were decreased in MKP-2$^{-/-}$ macrophages compared to their wild type counterparts which may be the reason why more MKP-2$^{+/+}$ macrophages migrate towards C5a than in MKP-2$^{-/-}$ counterparts (Table 4.16).
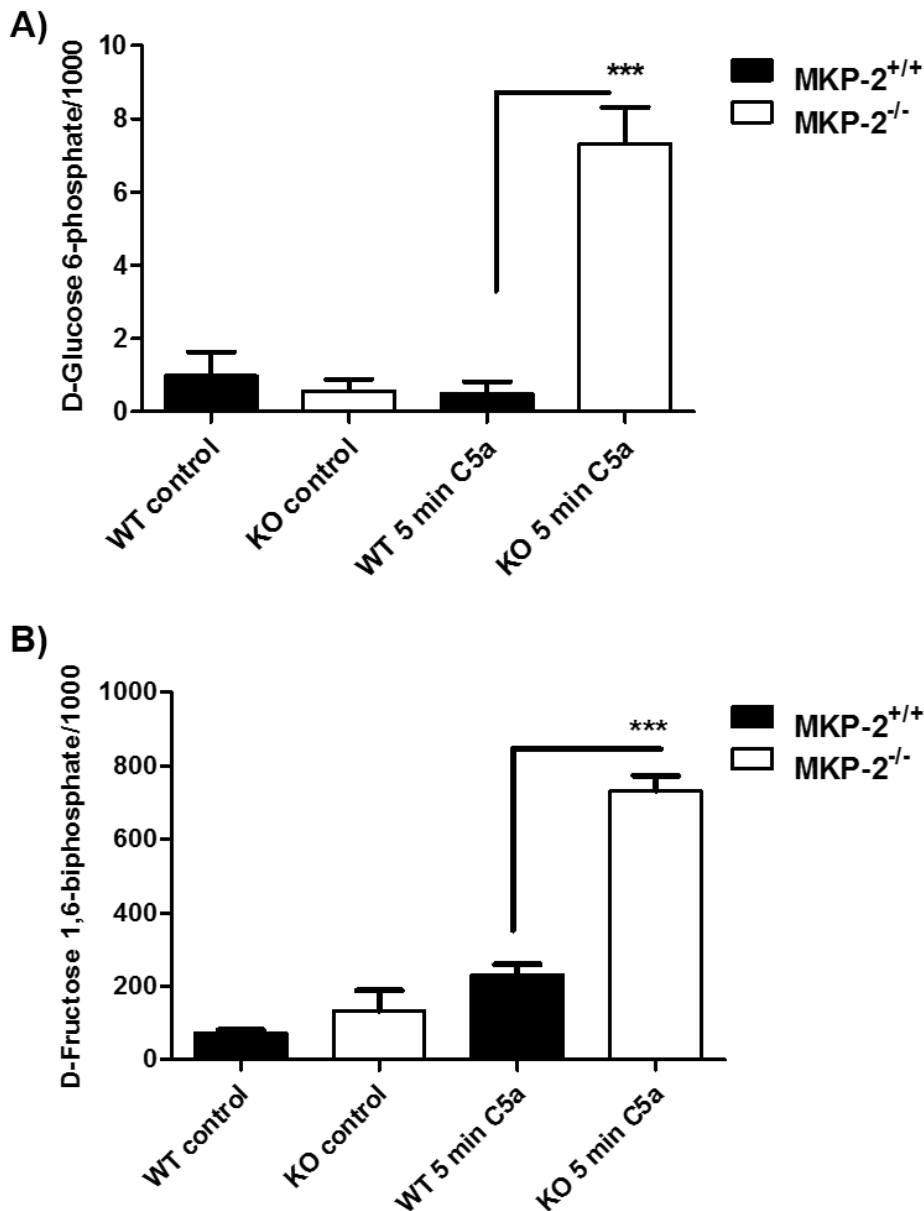
Figure 4. 20 Upregulated glycolysis pathway metabolites in MKP-2^{-/-} BMDMs stimulated with C5a

MKP-2 [+/+] and MKP-2 [-/-] macrophages were seeded in 6-well plates at a density of 2×10^6 cells/well and stimulated with 20nM C5a for 5 minutes or left untreated as controls. Cell extracts were prepared for untargeted metabolomics as described in section 2.11. Results show A) Upregulated D-Glucose 6-phosphate after 5 minutes of C5a in MKP-2 deleted macrophages. B) Upregulated D-Fructose 1, 6-bisphosphate. Data represents mean ± SEM of n=3 (5 mice were used from each group in each experiment), Bonferroni's multiple comparison test, *** $P<0.001$ for MKP-2^{+/+} versus MKP-2^{-/-}.
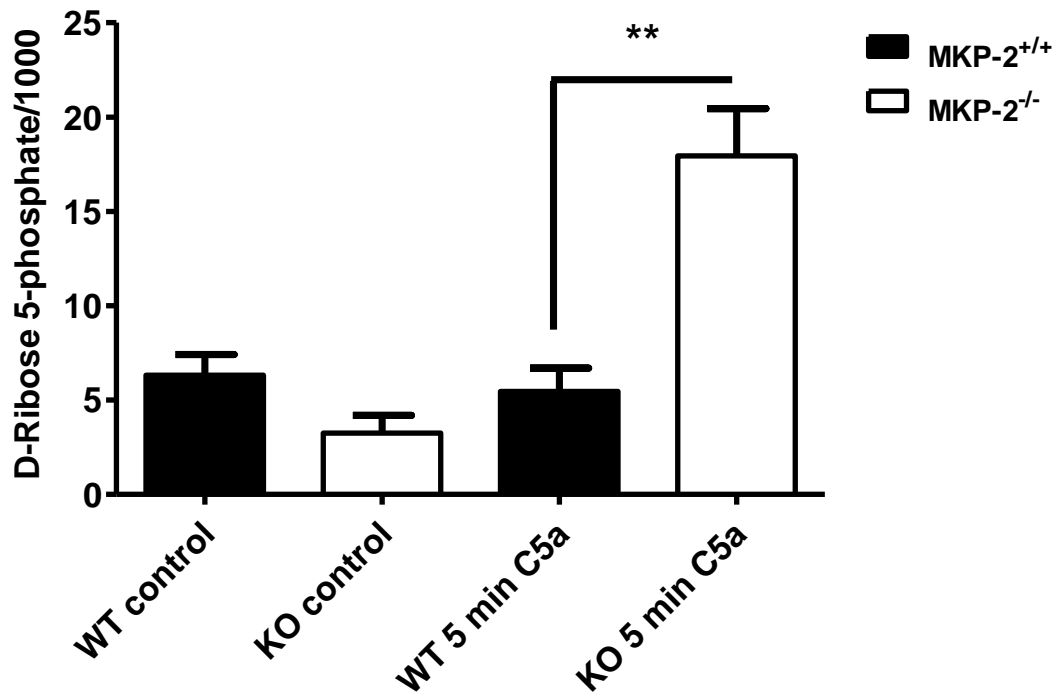
Figure 4. 21 Upregulated pentose phosphate pathway metabolites in MKP-2^{-/-} BMDMs stimulated with C5a

MKP-2 [+/+] and MKP-2 [-/-] macrophages were seeded in 6-well plates at a density of 2×10^6 cells/well and stimulated with 20nM C5a for 5 minutes or left untreated as controls. Cell extract were prepared for untargeted metabolomics as described in section 2.11. Results show upregulated D-Ribose 5-phosphate after 5 minutes of C5a in MKP-2 deleted macrophages. Data represents mean ± SEM of n=3 (5 mice were used from each group in each experiment), Bonferroni's multiple comparison test, ** $P<0.01$ in MKP-2^{+/+} versus MKP-2^{-/-}.

Table 4. 15 Upregulated metabolites in MKP-2^{-/-} following 5 minutes C5a stimulation

DM	m/z	RT	Name	5WCA F WT	5WCA P	5KCA F KO	5KCA P
P	261.04	16.372	D-Glucose 6-phosphate	0.50	0.67679	12.81	0.01539
N	229.01	16.066	D-Ribose 5-phosphate	0.43	0.61042	11.12	0.01813
P	349.05	15.709	2-O-(6-phospho-α-mannosyl)-D-glycerate	4.09	0.20875	8.90	0.00144
N	135.03	11.337	[FA trihydroxy(4:0)] 2,3,4-trihydroxy-butanoic acid	0.21	0.45159	7.55	0.00289
P	346.20	4.410	Leu-Val-Asp	2.33	0.33052	6.92	0.14824
N	267.07	11.218	2(alpha-D-Mannosyl)-D-glycerate	0.26	0.47947	6.71	0.00161
P	703.57	7.430	[SP (16:0)] N-(hexadecanoyl)-sphing-4-enine-1-phosphocholine	0.94	0.91266	5.66	0.04251
N	338.99	18.389	D-Fructose 1,6-bisphosphate	0.59	0.63978	5.52	0.00680
P	813.68	7.390	SM(d18:1/24:1(15Z))	1.07	0.90743	5.07	0.11836
P	790.56	6.583	PS(18:0/18:1(9Z))	1.02	0.96787	4.95	0.05472
N	616.47	7.442	[SP (16:0)] N-(hexadecanoyl)-sphing-4-enine-1-phosphate	0.97	0.95221	4.87	0.03825
P	689.56	7.537	[SP (18:0/14:0)] N-(octadecanoyl)-tetradecasphing-4-enine-1-phosphoethanolamine	0.87	0.80239	4.83	0.04429
P	388.30	4.936	2-Hydroxymyristoylcarnitine	1.59	0.57300	3.44	0.00088
P	405.01	16.568	UDP	0.99	0.99058	3.43	0.03701
N	613.14	17.666	CMP-N-acetylneuraminate	0.35	0.03278	2.72	0.21457
P	734.57	4.226	[PC (16:0/16:0)] 1-hexadecanoyl-2-hexadecanoyl-sn-glycero-3-phosphocholine	0.90	0.83150	2.71	0.05980
P	746.60	4.206	PC (16:0/P-18:0)	0.77	0.61586	2.55	0.05918
N	442.02	18.302	GDP	0.67	0.45199	2.53	0.03046
P	746.10	17.238	NADPH	1.11	0.85252	2.47	0.06535
P	868.61	3.721	1-24:1-2-18:3-phosphatidylserine	0.83	0.70763	2.29	0.05100
N	171.01	14.894	sn-Glycerol 3-phosphate	0.88	0.79553	2.27	0.06437
P	110.03	15.361	Hypotaurine	0.84	0.73002	2.03	0.08749
P	666.13	13.658	NADH	0.84	0.73112	2.00	0.13756
P	212.04	15.454	Phosphocreatine	1.04	0.94167	2.00	0.10756
N	214.05	16.033	sn-glycero-3-Phosphoethanolamine	0.86	0.76399	2.00	0.10729
N	133.01	16.235	(S)-Malate	0.86	0.74827	1.95	0.07828
P	208.10	4.937	N-Acetyl-L-phenylalanine	0.77	0.52522	1.84	0.05365
N	147.03	15.054	(R)-2-Hydroxyglutarate	0.97	0.93083	1.84	0.03942
P	335.22	4.197	Prostaglandin A2	0.80	0.60712	1.75	0.05809
P	133.10	13.159	L-Ornithine	0.96	0.92591	1.66	0.34558
P	234.13	7.638	Hydroxypropionylcarnitine	0.83	0.62442	1.59	0.00982
N	611.15	17.662	Glutathione disulfide	0.32	0.01811	1.48	0.40770

P	187.11	12.102	Ala-Pro	0.63	0.01617	1.19	0.28632
P	189.12	15.450	Glycyl-leucine	0.72	0.04048	1.12	0.48309
P	156.08	15.963	L-Histidine	0.07	0.00006	0.22	0.16844

Macrophages were treated as outlined in section 2.11.1 and analysed in section 2.11.3. DM refers to detection zone, M/Z to mass ratio, RT to raw retention time, WZF and KZF to fold changes in wild type and knockout MKP-2 compared to their controls and according to their P values, n=3.

Figure 4. 22 Upregulated Glycerophospholipid metabolism in MKP-2 deleted BMDMs stimulated by C5a

MKP-2^{+/+} and MKP-2^{-/-} macrophages were seeded in 6-well plates at a density of 2×10^6 cells /well and stimulated with 20nM of C5a for 15 minutes or left untreated as controls. Cell extracts were prepared for untargeted metabolomics as described in section 2.11. Results show upregulated phosphatidylserine in MKP-2 deleted macrophages. Data represents mean ± SEM of n=3 (5 mice were used from each group in each experiment), Bonferroni's multiple comparison test, *** $P<0.001$ in MKP-2^{+/+} versus MKP-2^{-/-}.
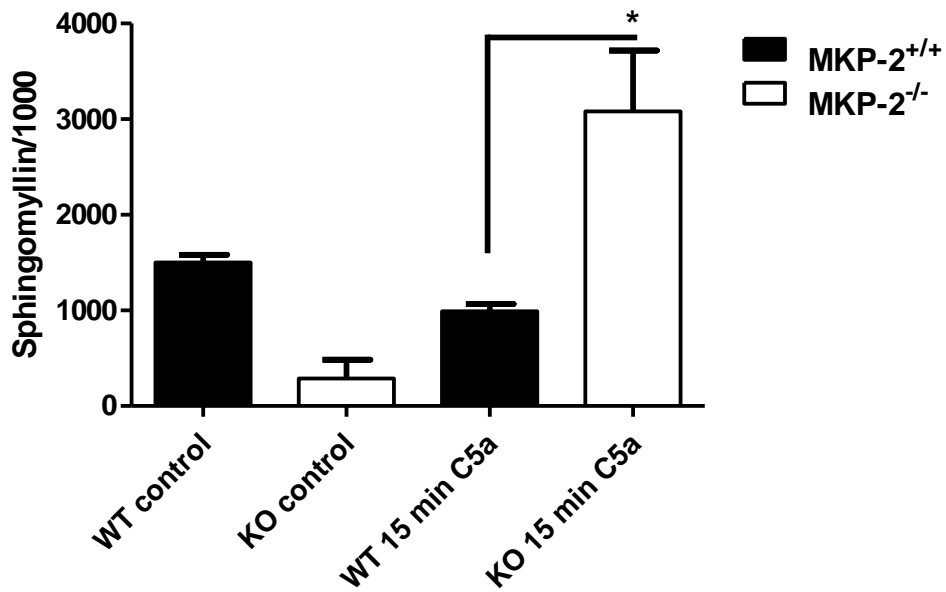
Figure 4. 23 Sphingolipid metabolism pathway is altered by MKP-2 deletion in macrophages stimulated by C5a

MKP-2^{+/+} and MKP-2^{-/-} macrophages were seeded in 6-well plates at a density of 2×10^6 cells /well and stimulated with 20nM of C5a for 15 minutes or left untreated as controls. Cell extracts were prepared for untargeted metabolomics as described in section 2.11. Data represents mean ± SEM of n=3 (5 mice were used from each group in each experiment), Bonferroni's multiple comparison test, * P<0.05 in MKP-2^{+/+} versus MKP-2^{-/-}.

Table 4. 16 Downregulated metabolites after 15 min C5a stimulation in MKP-2$^{-/-}$ BMDMs

DM	m/z	RT	Name	15WCA F WT	P	15KCA F KO	P
P	284.09	12.96	Guanosine/ Purine Metabolism	4.52	0.03	0.66	0.18
P	148.06	11.57	L-Glutamate	3.63	0.00002	0.07	0.02
P	203.13	5.03	Leu-Ala//Ile-Ala	3.15	0.00002	0.22	0.03
P	130.05	5.25	L-1-Pyrroline-3-hydroxy-5-carboxylate	2.91	0.03	1.39	0.79
N	620.02	17.01	ADP ribose 1'',2''-phosphate	2.71	0.00000	0.37	0.09
P	444.03	18.30	GDP / Purine Metabolism	2.28	0.005	0.29	0.01
N	742.06	17.02	NADP+	1.97	0.004	0.34	0.06
N	442.01	18.30	GDP	1.88	0.004	0.43	0.01
P	198.08	6.95	N-Acetyl-L-histidine	1.87	0.03	0.55	0.23
P	744.08	17.02	NADP+	1.81	0.0001	0.37	0.06
N	362.05	16.96	GMP / Purine Metabolism	1.69	0.009	0.29	0.01
N	402.99	16.87	UDP	1.68	0.02	0.46	0.06
P	428.03	15.62	ADP / Purine Metabolism	1.64	0.005	0.38	0.003
N	323.02	15.54	UMP/ Pyrimidine Metabolism	1.58	0.02	0.38	0.01
P	364.0	16.96	GMP/ Purine Metabolism	1.52	0.05	0.28	0.01
P	523.99	19.73	GTP/ Purine Metabolism	1.37	0.01	0.36	0.03
N	346.05	17.00	AMP/ Purine Metabolism	1.27	0.04	0.37	0.02
P	132.07	15.04	Creatine	1.26	0.01	0.42	0.01
P	114.06	14.96	Creatinine	1.25	0.007	0.71	0.04
N	540.05	14.54	Cyclic ADP-ribose	1.25	0.04	0.56	0.005
P	508.002	17.00	ATP	1.21	0.03368	0.45	0.02

Macrophages were treated as outlined in section 2.11.1 and analysed in section 2.11.3. DM refers to detection zone, M/Z to mass ratio, RT to raw retention time, WZF and KZF to fold changes in wild type and knockout MKP-2 compared to their controls and according to their P values, n=3.

The metabolic profile after 2 hours of C5a stimulation differed from the other time points. Here the metabolites of the purine metabolism pathway (guanosine diphosphate; GDP, adenine monophosphate; AMP, guanosine monophosphate; GMP and Guanosine) were upregulated in MKP-2$^{-/-}$ macrophages compared to their wild type counterpart (Table 4.17). Metabolites were increased in the pyrimidine metabolism pathway, tryptophan, and glycine, serine and threonine metabolism (Table 4.17). Results shows no downregulated metabolites in MKP-2$^{-/-}$ macrophages at this point. One of the purine metabolism pathway metabolites, GMP, was assessed over the whole time period after C5a stimulation. Results in figure 4.24 shows increased levels of GMP from 5 minutes in MKP-2$^{-/-}$ macrophages, about 2 fold greater than MKP-2$^{+/+}$ counterparts (MKP-2 $^{+/+}$ = 26.36 ± 3.81, MKP-2 $^{-/-}$ =47.33 ± 2.6). The converse occurred after 15 minutes when the GMP levels were reduced to 14.47 ± 1.03 in MKP-2$^{-/-}$ macrophages compared to MKP-2$^{+/+}$ cells which actually increased to 42.36 ± 4.81. At 2 hours levels recovered with no significant difference between wild type and knockout (Figure 4.24).

Finally, 24 hours stimulation with C5a showed upregulation in arginine and proline metabolism, glutathione metabolism and pyrimidine metabolism (Table 4.18). One of the metabolites that was highly upregulated in the arginine and proline metabolism pathway was L-citrulline in MKP-2$^{-/-}$ macrophages compared to WT. However, another metabolite from the same pathway, creatine, was down regulated in MKP-2 deleted macrophages at the same time point making it unclear if there was a consistent effect on this pathway (Table 4.19).

Table 4. 17 Upregulated metabolites after 2 hours C5a stimulation in MKP-2$^{-/-}$ BMDMs

DM	m/z	RT	Name	2WCA F WT	2WCA P	2KCA F KO	2KCA P
P	137.05	15.7	[FA trihydroxy(4:0)] 2,3,4-trihydroxy-butanoic acid	83.71	0.001	338.35	0.002
P	269.09	11.23	2(alpha-D-Mannosyl)-D-glycerate	48.13	0.003	272.49	0.001
P	137.05	11.19	[FA trihydroxy(4:0)] 2,3,4-trihydroxy-butanoic acid	55.68	0.005	137.40	0.0005
P	349.05	15.70	2-O-(6-phospho-α-mannosyl)-D-glycerate	40.06	0.0006	108.07	0.003
N	267.07	11.21	2(alpha-D-Mannosyl)-D-glycerate	25.68	0.14	105.81	0.0006
N	135.03	11.33	[FA trihydroxy(4:0)] 2,3,4-trihydroxy-butanoic acid	27.52	0.14	87.45	0.001
N	347.04	15.71	2-O-(6-phospho-α-mannosyl)-D-glycerate	20.65	0.12	66.68	0.002
P	284.10	12.96	Guanosine	9.72	0.001	21.88	0.06
N	338.99	18.38	D-Fructose 1,6-bisphosphate	5.29	0.16	13.84	0.0005
N	211.00	15.58	P-DPD	5.56	0.14	12.89	0.006
P	340.32	7.80	9-Hexadecenoylcholine	1.86	0.01	7.78	0.03
N	282.08	12.97	Guanosine	4.98	0.09	5.54	0.001
N	207.08	11.28	L-Kynurenine	3.40	0.3	4.94	0.04
P	364.06	16.95	GMP	4.22	0.001	4.57	0.01
N	362.05	16.96	GMP	2.87	0.1	4.05	0.003
P	130.05	5.24	L-1-Pyrroline-3-hydroxy-5-carboxylate	1.58	0.04	3.37	0.1
P	181.07	7.40	D-Glucose	1.39	0.73	3.31	0.13
N	403.00	16.86	UDP	1.59	0.32	2.24	0.004
N	442.02	18.30	GDP	1.90	0.15	2.17	0.004
P	348.07	14.06	AMP	2.11	0.02	1.95	0.04
P	132.08	15.03	Creatine	1.79	0.003	1.79	0.03
P	303.24	7.70	nonenoylcarnitine	0.28	0.04	1.58	0.6

Macrophages were treated as outlined in section 2.11.1 and analysed in section 2.11.3. DM refers to detection zone, M/Z to mass ratio, RT to raw retention time, WZF and KZF to fold changes in wild type and knockout MKP-2 compared to their controls and according to their P values, n=3.
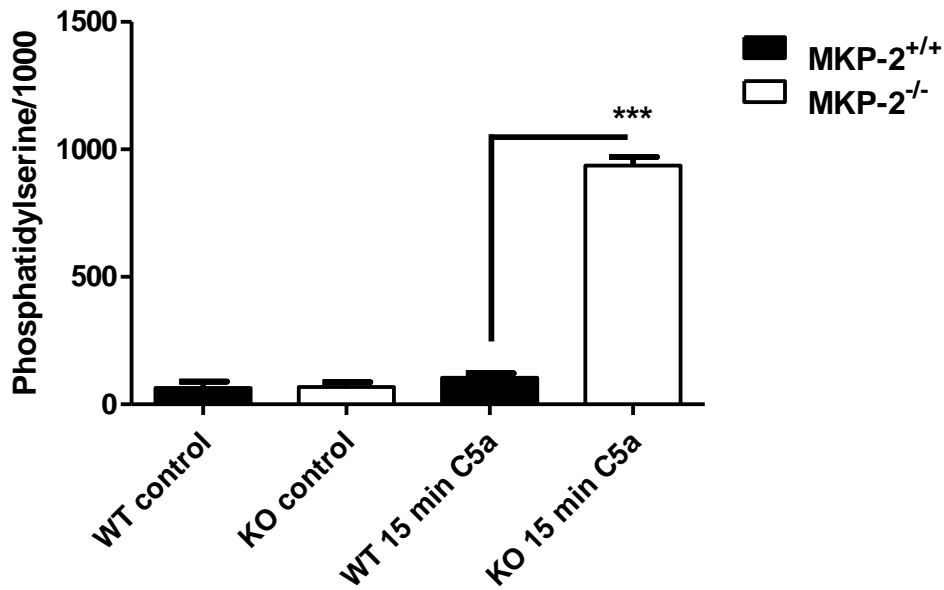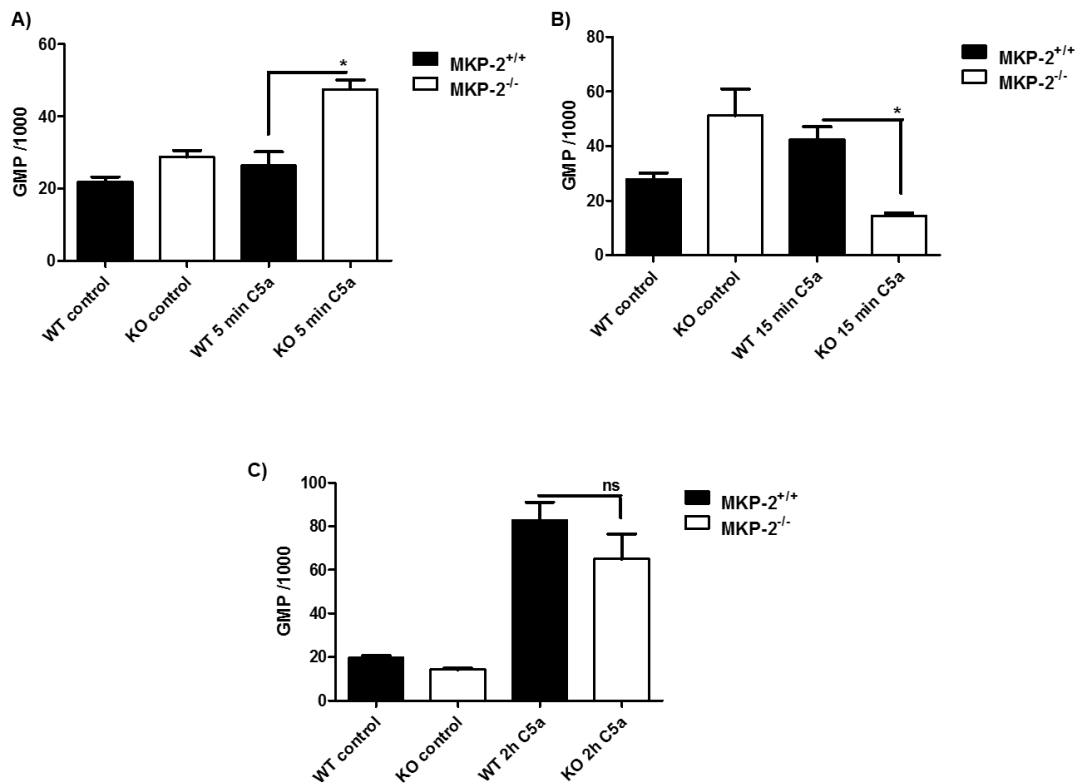
Figure 4. 24 Purine metabolism pathway is altered in MKP-2 deleted BMDMs stimulated with C5a

MKP-2^{+/+} and MKP-2^{-/-} macrophages were seeded in 6-well plates at a density of 2×10^6 cells/well and stimulated with 20nM of C5a for 5,15 and 120 minutes or left untreated as controls. Cell extracts were prepared for untargeted metabolomics as described in section 2.11. Results show A) upregulated Guanosine mono phosphate after 5 minutes of C5a in MKP-2 deleted macrophages. B), and C) Down regulated GMP in MKP-2^{-/-} macrophages. Data represents mean ± SEM of n=3 (5 mice were used from each group in each experiment), Bonferroni's multiple comparison test, * P<0.05 in MKP-2^{+/+} versus MKP-2^{-/-}.

Table 4. 18 Upregulated metabolites in 24h stimulation with C5a

DM	m/z	RT	Name	C5AW F WT	C5AW P	C5AK F KO	C5AK P
N	132.09	16.53	L-Ornithine / Glutathione metabolism, Arginine and proline metabolism	4972.35	0.05	13766.41	0.02
N	566.06	16.91	UDP-glucose	0.45	0.01	24.06	0.4
P	175.10	16.53	L-Citrulline	9.34	0.002	15.51	0.0006
P	158.07	16.42	4-Methylene-L-glutamine	8.36	0.002	15.02	0.0005
P	715.51	4.21	[PE (16:0/18:2)] 1-hexadecanoyl-2-(9Z,12Z-octadecadienoyl)-sn-glycero-3-phosphoethanolamine	12.93	0.004	14.20	0.003
N	174.09	3.95	Suberic acid	0.26	0.1	12.27	0.4
P	151.06	8.36	(Z)-4-Hydroxyphenylacetaldehyde-oxime	0.11	0.09	9.28	0.08
P	177.06	10.95	4-Hydroxy-4-methylglutamate	4.06	0.03	8.44	0.001
P	165.06	13.60	3-Methylguanine	1.03	0.9	7.42	0.009
P	177.06	10.75	4-Hydroxy-4-methylglutamate	2.63	0.08	7.12	0.001
P	136.04	10.30	[FA trihydroxy(4:0)] 2,3,4-trihydroxy-butanoic acid	2.20	0.1	5.85	0.001
P	703.51	4.22	[PC (14:0/16:1)] 1-tetradecanoyl-2-(9Z-hexadecenoyl)-sn-glycero-3-phosphocholine	4.17	0.004	5.78	0.0001
P	612.15	17.90	Glutathione disulfide	4.41	0.004	5.69	0.0035
N	294.26	3.76	[FA methyl(18:0)] 9,10-methylene-9-octadecenoic acid	0.92	0.8	5.41	0.003
N	694.46	4.21	1-18:2-2-18:3-phosphatidate	3.46	0.0001	5.39	0.0002
P	677.50	4.26	[PC (14:0/14:0)] 1,2-ditetradecanoyl-sn-glycero-3-phosphocholine	4.82	0.001	5.22	0.0001
P	821.59	4.15	PE(18:4(6Z,9Z,12Z,15Z)/24:1(15Z)	1.89	0.01	4.57	0.005
N	307.08	17.89	Glutathione	3.11	0.007	4.20	0.002
P	799.61	4.16	[PE (20:0/20:2)] 1-eicosanoyl-2-(11Z,14Z-eicosadienoyl)-sn-glycero-3-phosphoethanolamine	2.40	0.05	4.01	0.02
P	154.09	15.48	creatinine acetonitrile adduct	3.94	0.003	3.99	0.01
N	418.25	4.05	CPA(18:1(11Z)/0:0)	1.88	0.02	3.94	0.007
N	612.15	17.91	Glutathione disulfide	3.38	0.007	3.79	0.04
N	757.56	4.19	[PC (16:0/18:2)] 1-hexadecanoyl-2-(9Z,12Z-octadecadienoyl)-sn-glycero-3-phosphocholine	2.69	0.01	3.79	0.004
N	347.06	14.70	AMP	2.63	0.003	3.66	0.01
N	479.30	4.71	[PE (18:0)] 1-(9Z-octadecenoyl)-sn-glycero-3-phosphoethanolamine	2.22	0.02	3.55	0.003

DM	M/Z	RT	Metabolite	WZF		KZF	
P	771.58	4.18	[PE (18:0/20:2)] 1-octadecanoyl-2-(11Z,14Z-eicosadienoyl)-sn-glycero-3-phosphoethanolamine	2.60	0.01	3.53	0.0006
N	324.04	16.92	UMP	1.60	0.3	3.02	0.006

Macrophages were treated as outlined in section 2.11.1 and analysed in section 2.11.3. DM refers to detection zone, M/Z to mass ratio, RT to raw retention time, WZF and KZF to fold changes in wild type and knockout MKP-2 compared to their controls and according to their P values, n=3.

Table 4. 19 Down regulated metabolites in MKP-2 deleted mice after 24h stimulation with C5a

DM	m/z	RT	Name	C5AW F WT	C5AW P	C5AK F KO	C5AK P
N	131.07	15.30	Creatine/ Arginine and proline metabolism, Glycine, serine and threonine metabolism	3014.63	0.04	302.04	0.08
P	145.02	8.41	3,4-Dehydrothiomorpholine-3-carboxylate	463.29	0.1	4.26	0.01
P	133.02	9.18	L-thiazolidine-4-carboxylate	442.88	0.09	3.23	0.01
P	161.05	7.65	Allyl cysteine	358.43	0.1	2.85	0.02
P	189.08	7.41	Prenyl-L-cysteine	215.88	0.1	2.42	0.1
N	456.23	4.26	Vindoline	163.86	0.1	14.92	0.009
N	580.30	3.91	Lys-Phe-Thr-Trp	93.62	0.2	3.57	0.02
N	785.60	4.18	[PC (18:1/18:1)] 1-(9Z-octadecenoyl)-2-(9Z-octadecenoyl)-sn-glycero-3-phosphocholine	18.15	0.003	13.25	0.01
N	299.01	15.29	2-Methyl-4-amino-5-hydroxymethylpyrimidine diphosphate	12.40	0.006	9.64	0.0009
P	175.10	16.17	L-Citrulline/ Arginine and proline metabolism	10.82	0.008	8.25	0.004
P	769.56	4.23	PC(15:0/20:3(5Z,8Z,11Z))hexadecanoyl-2-(9Z,12Z,15Z-nonadecatrienoyl)-sn-glycero-3-phosphocholine	5.65	0.004	3.68	0.3
P	114.04	15.32	5,6-Dihydrouracil/ pantothenate and CoA biosynthesis,beta-Alanine metabolism,Pyrimidine metabolism	5.30	0.001	4.41	0.0002
P	797.59	4.18	PE(18:1(11Z)/22:2(13Z,16Z))	4.86	0.03	3.60	0.005
P	347.06	14.61	AMP / Purine metabolism	4.77	0.001	4.28	0.01
P	459.26	4.26	Trp-Val-Arg	4.37	0.03	0.73	0.5
P	280.13	4.30	Phaseic acid	4.11	0.05	0.80	0.7
P	811.61	4.21	PC(16:1(9Z)/22:2(13Z,16Z))/1-hexadecanoyl-2-(13Z,16Z,19Z-docosatrienoyl)-sn-glycero-3-phosphocholine	4.01	0.01	2.15	0.3
N	674.54	4.45	SM(d18:1/14:0)	3.11	0.0006	2.09	0.01
P	413.31	7.68	3-Hydroxy-9-hexadecenoylcarnitine	2.33	0.01	1.82	0.01
N	172.01	15.16	sn-Glycerol 3-phosphate / Glycerophospholipid metabolism,Glycerolipid metabolism	0.59	0.0003	0.83	0.5

Macrophages were treated as outlined in section 2.11.1 and analysed in section 2.11.3. DM refers to detection zone, M/Z to mass ratio, RT to raw retention time, WZF and KZF to fold changes in wild type and knockout MKP-2 compared to their controls and according to their P values, n=3.

4.2.4.4 Metabolic changes linked to NO and cytokine profiles in MKP-2 deleted macrophages

The metabolomics studies showed a strong upregulation of L-citrulline in LPS stimulated MKP-2$^{-/-}$ macrophages relative to wild type controls. Since citrulline is linked to nitric oxide synthesis it was decided to measure NO in macrophages comparing WT and KO mice. In addition, NO has been found to activate focal adhesion kinase (FAK) signalling which is important in both phagocytosis and migration linking this metabolite to these parameters (Martin-Lorenzo *et al.*, 2015, Rhoads, 2004). It has also been shown that changes in the glycolytic pathway can influence the production of cytokines such as IL-6 and IL-10 (Chiba *et al.*, 2017). Therefore it was decided to measure nitric oxide as nitrite/nitrate via the Greiss assay and IL1β and IL-10 by ELISA.

Figure 4.25 shows the effect of LPS on cellular nitrite levels over a time course up to 48 hours in both WT and knockout macrophages. Nitrite levels started to increase after 12 hours in both groups to the same level. After 24 hours, MKP-2$^{+/+}$ macrophages showed higher levels of nitrite than MKP-2$^{-/-}$ macrophages. This difference became significant after 48 hours stimulation with LPS when nitrite production was 64.60 μM ± 10.42 in MKP-2$^{+/+}$ macrophages and 44.29 μM ± 0.44 in MKP-2$^{-/-}$ (Figure 4.25).

Supernatants from the same wells that were used for the metabolomics experiment was also used to measure cytokines. First, IL-1β was measured as a pro-inflammatory cytokine. Results in Figure 4.26 panel A, show increased levels of IL-1β in MKP-2$^{-/-}$ after 24 hours treatment with either LPS, C5a or zymosan compared to their levels in MKP-2$^{+/+}$ macrophages. However, this increase was not significant for either LPS or C5a treatment groups. Zymosan treated MKP-2$^{-/-}$ macrophages, showed a significant increase of 122.15 ± 13.96 pg/ml in IL-1β levels, compared to MKP-2$^{+/+}$ macrophages which was 81.41 ± 9.73 pg/ml (Figure 4.26). The production of IL-10 which is an anti-inflammatory cytokine was not altered and almost identical between MKP-2$^{+/+}$ and MKP-2$^{-/-}$ macrophages (Figure 4.26, panel B). Both groups showed increased levels of IL-10 production when treated with LPS and C5a but not for zymosan treatment which was reduced in both groups.
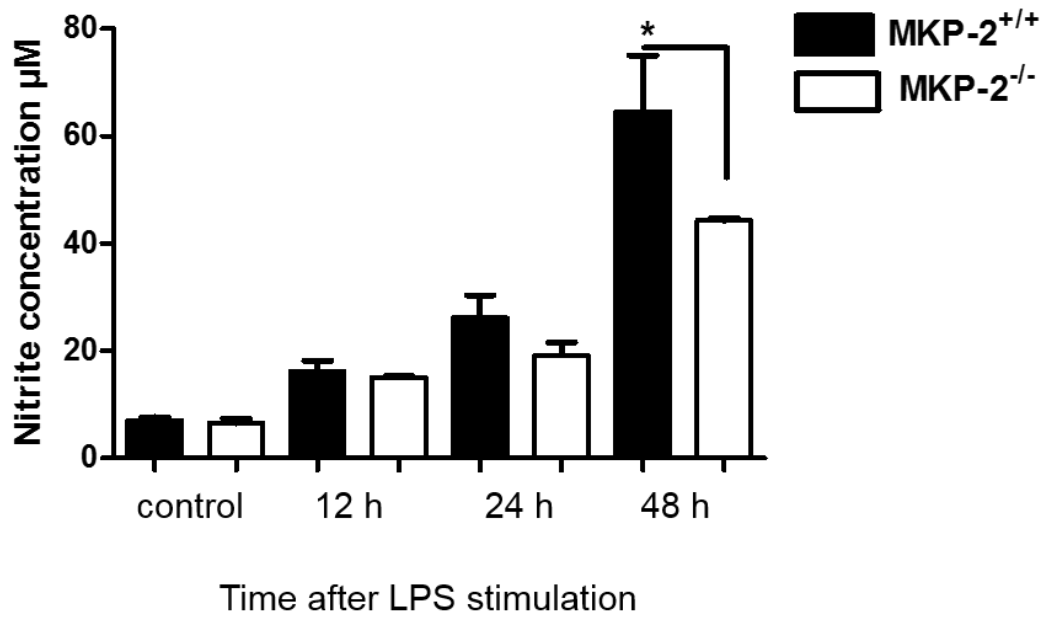
Figure 4. 25 MKP-2 deletion reduces LPS mediated nitric oxide production from macrophages

BMDMs were generated from MKP-2^{+/+} and MKP-2^{-/-} mice and stimulated with LPS (100 ng/ml) for 12, 24 or 48 hours, or left untreated as controls. Cell culture supernatant was collected at each time point and nitrite concentrations determined by Griess Assay as described in section 2.10. Data represent mean ± SEM of three independent experiments (n=3), * $P<0.05$ in MKP-2^{+/+} versus MKP-2^{-/-}.
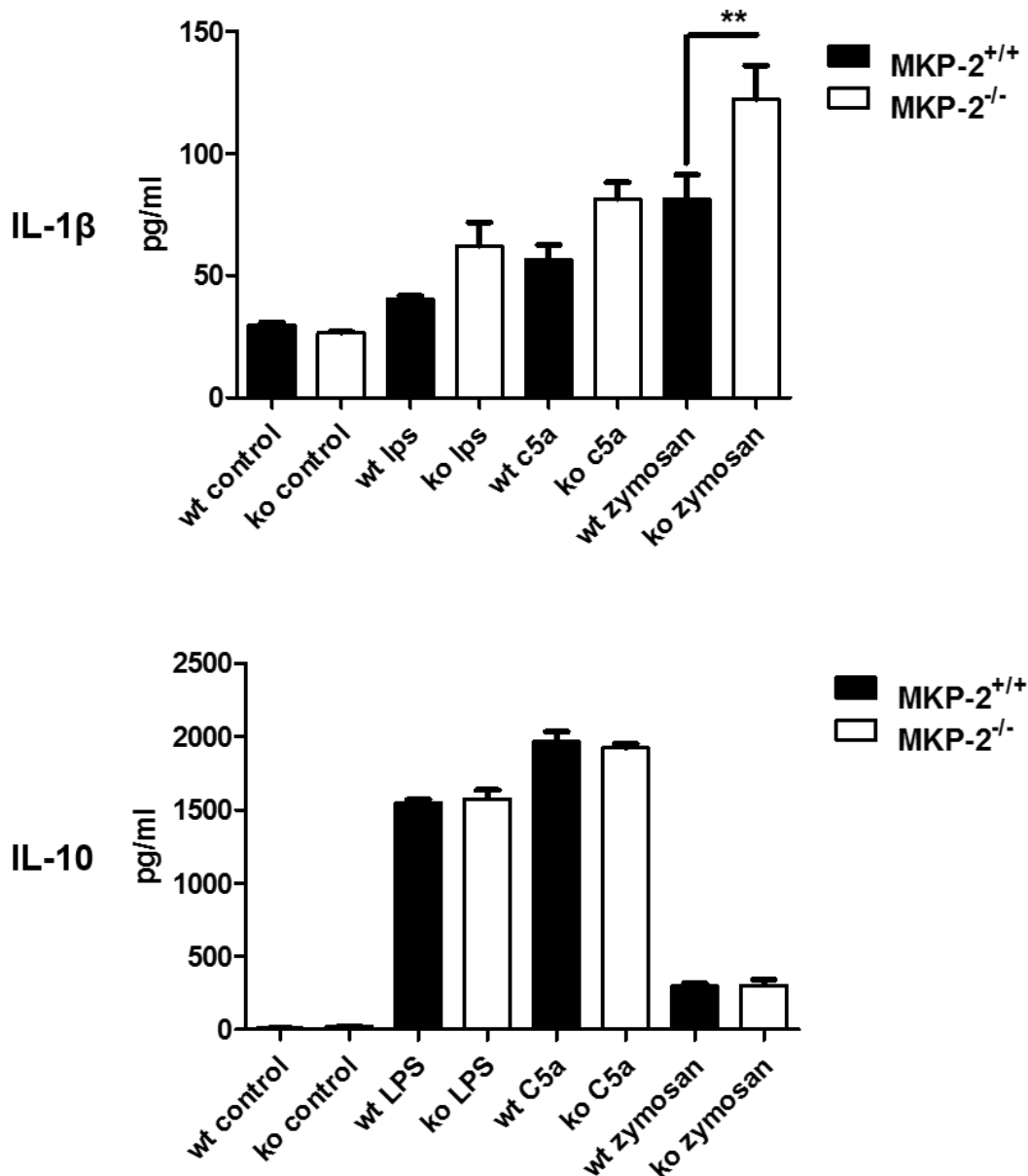
Figure 4. 26 Effect of MKP-2 deletion on the cytokine profile that accompanied the metabolic changes in stimulated macrophages

Macrophages from both MKP-2$^{+/+}$ and MKP-2$^{-/-}$ were seeded in 6-well plates at a density of 2x10^6 cells/ml and stimulated with 100ng/ml LPS, 20 nM C5a, 10 MOI zymosan or left untreated as controls for 24 hours. Supernatants were collected and cytokine expression analysed by ELISA. Graphs shows A) levels of IL-1β and B) shows IL-10 expression. Data is representative of two other experiments (n=5 mice pooled per group). Bonferroni's multiple comparison test, ** P<0.01 for MKP-2$^{+/+}$ versus MKP-2$^{-/-}$.

4.3 Discussion

The current chapter aimed to investigate the effect of MKP-2 deletion on a number of macrophage functions including phagocytosis, migration and proliferation in response to a diverse array of signals. These outcomes were then linked to metabolic profiles to determine if any differences in these cascades could be linked to differences in function. This was the first time these elements had been studied in relation to MKP-2 using the DUSP-4 knockout model developed in the Plevin laboratory.

The first group of experiments in this chapter demonstrated that MKP-2 deletion resulted in enhanced phagocytic activity and zymosan uptake in both basal conditions. The zymosan bio-particles used in the present study were opsonised with IgG before incubation with macrophages in order to lessen the number of receptors involved in zymosan phagocytosis with a key role for FcγR in recognition (Rougerie *et al.*, 2013). This is important as a study showed that stimulation by LPS reduced or increased phagocytic activity depending on the receptors available (Wonderling *et al.*, 1996). Another group (Feng *et al.*, 2011) also showed that LPS is unable to change macrophage uptake in response to activated yeast which is not opsonized.

In this study treatment with LPS enhanced zymosan uptake in MKP-2$^{-/-}$ macrophages although the increase was not statistically significant possibly due to lack of n-numbers. Morphological examination confirmed these differences between the macrophage populations; longer pseudopods and thinner filaments were observed in MKP-2 deleted phagocytes. The effect of MKP-2 deletion may be linked to observed differences in MAP kinase signalling. LPS mediated TLR4 activation is known to increase JNK1/2 and ERK1/2 phosphorylation in turn leading to enhanced actin polymerization and thus phagocytosis. Both ERK and JNK have been shown to be increased upon LPS stimulation (as confirmed in chapter 3) and both have been reported to be involved in cell membrane protrusion (Mendoza *et al.*, 2015) and transformation of G-actin into F-actin which is required for lamellipodium formation and the phagocytic cup (Tanimura *et al.*, 2016, Mengistu *et al.*, 2011).

Therefore the small one fold enhancement in LPS mediated phagocytosis that was observed in MKP-2$^{-/-}$ macrophages may be due to increased JNK signalling in chapter 3. A study in support of this possibility showed JNK co-localisation with F-actin and stress fibres consistent with a role for this MAPK in actin cytoskeleton re-arrangement (Mengistu *et al.*, 2011). JNK was also found to control TLR2 mediated phagocytosis of Staphylococcus aureus by RAW 264.7 macrophages (Fang *et al.*, 2014), whilst

another group linked zymosan phagocytosis with increased ERK activation at 30 minutes (Farnebo *et al.*, 2015). These findings are also consistent with another report that showed Syk promoted phagocytosis of *Francisella tularensis* through the activation of ERK (Parsa *et al.*, 2008). Furthermore another group found ERK to be required for FcgR mediated phagocytosis of opsonized particles (Ninkovic, 2011). However, MKP-2 deletion did not significantly alter ERK activation over this time span (see chapter 3 and (Al-Mutairi *et al.*, 2010)) therefore the effects of MKP-2 deletion is not significant in this context.

Another finding is that IL-4 induced phagocytosis in both MKP-2$^{+/+}$ and MKP-2$^{-/-}$ macrophages but was higher in the latter indicative of an M2 like macrophage phenotype inducing more phagocytic activity than the M1 like phenotype. This idea is consistent with previous studies in our laboratory which indicate a more pronounced M2 phenotype for MKP-2$^{-/-}$ macrophages (Woods *et al.*, 2013). A study by (Rubio *et al.*, 2015) demonstrated increased phagocytosis of zymosan particles in IL-4 treated human macrophages. The known phagocytic receptors enhanced by IL-4 are MRC-1 and dectin-1 alone or with TLR2 both of which involved in zymosan uptake by macrophages (Gordon and Martinez, 2010). A future study may involve a direct comparison of these receptors in both WT and MKP-2 knockout macrophages.

The balance of the M1 and M2 phenotypes may be relevant in differences in the cell capacity of internalised zymosan numbers. The uptake of 3-4 or more particles clearly showed higher percentages of internalised zymosan in MKP-2$^{-/-}$ macrophages but was reversed and reduced significantly when pre-treated with IL-4. Therefore, perhaps MKP-2 plays a role in the phagocytic capacity of alternatively activated macrophages. This may be significant at the morphological level, another group has shown an inhibitory role for IL-4 on phagocytic cup closure, many zymosan particles were observed on the cell surface instead of inside the phagocytic cup (Varin *et al.*, 2010). The MKP-2 gene may therefore have a role in the cross talk between PI3K, ERK and STAT6 as all three are known to be involved in IL-4 signalling (Mccormick and Heller, 2015). Examination of these parameters would add a better insight in the role of the MKP-2 gene in macrophage phagocytosis and is recommended for future work.

The second macrophage function that was investigated in this chapter was migration. The chemoattractant used was C5a which has been reported for its chemotactic effect in immune cells such as monocytes, macrophages and neutrophils and has been

identified in proinflammatory cytokines in the synovial fluid in cases of rheumatoid arthritis (Grant *et al.*, 2002).

The current study is the first to examine migratory function in relation to DUSP-4 deletion. A transwell migration assay revealed a significant reduction in macrophage migration towards a C5a gradient in in MKP-2 deleted macrophages compared to their wild type counterparts (Fig.4.11). Studies have previously shown C5a stimulation of ERK which is in turn linked to chemotaxis (Liu *et al.*, 2012, Hsu *et al.*, 2014). In chapter 3 it was demonstrated that in neutrophils from MKP-2 KO mice, ERK activation by C5a is almost abolished. Also in macrophage precursors ERK activation via stimulation with CSF is also markedly reduced (Neamatallah, 2014). Other studies have surprisingly linked C5a with TLR4 when assessing cell chemotaxis and migration (Liu *et al.*, 2010, Kurihara *et al.*, 2010) or via another GPCR called C5L2 which facilitates C5aR internalization in an ERK dependent pathway (Hsu *et al.*, 2014). It is unclear if any of these intermediates including the C5a receptor are compromised in MKP-2 deletion macrophages.

None of the above studies mention a role of the JNK activation. A study by (Chiou *et al.*, 2004) revealed that JNK was not essential for C5a induced cell migration, while they confirmed the role of ERK and p38. Our study demonstrated that in MKP-2$^{-/-}$ macrophages motility towards IL-4 was markedly reduced compared to wild type counterparts. This finding may again link to the idea that macrophages lacking MKP-2 already have an M2 phenotype and this is what contributes to the basal activation and the range of responses. IL-4 is known to increase macrophage motility even more so than LPS (Vereyken *et al.*, 2011) but regulates motility by different signalling mechanisms. So once again, whilst MKP-2 deletion has a significant effect on macrophage motility in response to different agents ascribing the effect to changes in MAP kinase signalling is difficult.

One of the additional confounding issues, but also significant, which emerged during these sets of experiments was the high rates of migration in resting MKP-2$^{-/-}$ macrophages and this obscured the levels of stimulation with each agent. One aspect emerging from migration biology is the potential of specific water channels called aquaporin (AQPs) (Hara-Chikuma and Verkman, 2006, Tyteca *et al.*, 2015, Zhu *et al.*, 2011). It has been shown that AQP1 supresses migration in resting macrophages (Tyteca *et al.*, 2015). Also potentially involved is GRK2 which can inhibit neutrophil migration through effects mediated by ERK itself (Liu *et al.*, 2012). Thus MKP-2

deletion could enhance resting ERK thus increasing GRK2 function and therefore migration.

The morphological studies again showed fundamental changes in cellular actin following deletion MKP-2. Resting MKP-2$^{-/-}$ macrophages showed more phagocytic cup closure than their wild type counterparts (Fig.4.14 first line). LPS treated MKP-2$^{+/+}$ showed dense thick and long pseudopods and had more lamellipods terminated in spiky filopods, whilst, MKP-2 deleted macrophages had thinner pseudopods and less spikes (filopods) than their wild type. It is well established that JNK is involved in the control of the actin polymerization and is required for the formation of filopodia and lamillipodia in the dorsal and thorax closure of *Drosophila* (Homsy *et al.*, 2006, Martin-Blanco *et al.,* 2000). JNK signalling is also reported to contribute to the migration via its effect on the formation of stress fibres which was found to be increased upon JNK inhibition (Rennefahrt *et al.*, 2002). Thus, in the presence of the MKP-2 gene when JNK is down regulated, there would be an accumulation of stress fibres and the data shown in Fig.4.13 confirmed enhanced levels of stress fibre in MKP-2$^{+/+}$ relative to MKP-2$^{-/-}$ macrophages. This might explain the increase in the motility of MKP-2 deleted macrophages towards zymosan particles which was also significant.   A study by Huang and co-workers revealed that one of the actin proteins called paxillin, which is a focal adhesion adapter, is activated downstream of both JNK and ERK and regulates adhesion dynamic and thus in cell migration (Huang *et al.*, 2004). Future studies could examine this particular axis relative to MKP-2 deletion.

This chapter also investigated the regulation of M-CSF induced proliferation. There was a significant difference which was marked after 48 h stimulation; MKP-2 deleted macrophages showed reduced proliferation and entry into S-phase compared to their wild type controls. M-CSF or CSF-1 are known regulators of macrophage differentiation and proliferation via Src/PI3K, Akt, MAPK or STAT pathways (Huynh *et al.*, 2012, Cypher *et al.*, 2016). The proliferative deficit may be linked to the inability of GPCR linked receptors to activate ERK signalling in MKP-2$^{-/-}$ mice, ERK activation is essential for G1 progression into S-phase which was measured via the assay. Other studies have shown that MKP-2 deficiency causes block in G$_2$/M phase which is correlated with cyclin B accumulation and elevated cdc2 phosphorylation (Lawan *et al.*, 2011). Another study demonstrated that overexpression of the MKP-2 gene increased proliferation of colorectal cancer cell line, suggesting that MKP-2 acts to increase cell growth rather than inhibit it (Groschl *et al.*, 2013).

It is noted that LPS and IL-4 had additional regulatory effects. In particular IL-4 is of interest as this agent enhanced proliferation in response to M-CSF in both WT and MKP-2$^{-/-}$ cells but less so for the KO group. This may link to the previous finding with respect to motility and again raises the question regarding the M2 phenotype in macrophages deficient in MKP-2 and their responsiveness to IL-4. This might imply a dysregulation of the IL-4 receptor or signalling events further downstream.

The second part of the study linked the effects of these functions on metabolic changes. Early time points were chosen to determine which metabolites might accompany the phagocytic process at the times when MAPKs were phosphorylated (5 and 15 minutes) and at 2 hours when the process of phagocytosis is almost finished but when MKP-2 in WT macrophages is highly expressed. A longer time point of 24 hours was included to determine if metabolic changes are linked to post-translational activity (which may involve cytokine production). The role of DUSPs in regulation of metabolism in general has only recently been examined; MKP-1 was revealed as an important sensor of metabolic stress where it is inactivated and degraded due to s-glutathionylation (Kim *et al.*, 2016). The loss of MKP-1 in monocytes and macrophages has been reported very recently in the context of a metabolomics profile and is linked to dysregulation of monocyte adhesion and migration (Kim and Asmis, 2017). In contrast, no study has attempted to examine the effect of MKP-2 deletion in metabolic reprogramming in macrophages and the current work is the first to the author's knowledge.

The first notable pathway that seemed to be affected by MKP-2 deletion was glycolysis. The pathway was upregulated as early as 5 minutes in MKP-2$^{-/-}$ compared to their wild type counterparts. A possible explanation could be that MAPKs such as JNK may contribute. In this regards a study by (Deng *et al.*, 2008) supports the link between JNK and glycolysis, they found that JNK1 activation promotes glycolysis in MEF cells via activation of phosphofructokinase -1 (PFK-1). A recent study has demonstrated a strong bond between glycolysis and phagocytosis, thus inhibiting glycolysis by 2-deoxy-D-glucose reduced phagocytosis of peritoneal macrophages (Pavlou *et al.*, 2017). Therefore, MKP-2 through the regulation of JNK may have a role. These results contrast with MKP-1 which favours the ERK pathway but still this DUSP contributes to the glycolytic flux albeit via a different mechanism (Kim and Asmis, 2017).

One of the oxidative stress markers, nicotinamide adenine dinucleotide phosphate; oxidised form (NADP+), was also upregulated. As shown in the schematic in Fig.4.17, during glycolysis and pentose phosphate pathway two molecules of NADP+ are reduced to NADPH. The latter is required for NADPH oxidase, expressed in the cell wall of professional phagocytes, to transfer electrons into the cytoplasm of cells (Cross and Segal, 2004, Quinn *et al.*, 2006) and mediate phagocytic closure. This facilitates the uptake of opsonized zymosan particles by macrophages. This result might explain the higher uptake that was observed in MKP-2 deleted resting macrophages. The pentose phosphate pathway was also elevated through D- Ribose 5- phosphate which links this pathway to glycolysis as shown in Fig.4.17. This pathway is recently used to identify the biological functions of the yeast *Saccharomyces cerevisiae* and to develop a strain that is clinically attractive (Kim *et al.*, 2015). The fact that zymosan is derived from *S. cerevisiae*, again indicates a role for the MKP-2/DUSP4 gene in early phagocytosis.

Interestingly, in MKP-2 deleted macrophages one of the downregulated metabolites was ornithokinin, which is one of the oligopeptides located within the cytoplasm and found to increase nitric oxide production (Guabiraba *et al.*, 2017). Also the glutathione intermediate S-allyl cysteine was also found to decrease. These metabolites are moderately acidic which may be of significant in the acidic environment of the phagosome and could explain the increase in the phagocytic capacity of 3-4 particles following MKP-2 deletion. Acidification linked to phagocytosis was reported to be via Myd-D88 dependent pathway (Ip *et al.*, 2010). Taken together, these findings suggest emerging patterns in metabolite production which fits in with possible effects on functional outcomes.

Findings from 15 minutes of zymosan stimulation showed upregulation of purine catabolism amino acids and cell lipid bilayer components in MKP-2 deleted macrophages, whilst, Glycolysis pathway and TCA cycle metabolites were down regulated compared to their levels in wild type. Interestingly, one of the metabolites that was downregulated in MKP-2 deleted phagocytes is phosphatidylserine which is an acidic phospholipid in the macrophage membrane confirming the differences in the phagocytic capacity between both groups. This finding is in agreement with another study examining macrophage membrane fatty acids components and their contribution in particle uptake (Schumann, 2016).

Unsurprisingly, the pattern for the 2 hours stimulation changed from those at other time points. Glycolysis, the TCA cycle and Purine and Pyrimidine pathways were all downregulated at this time point in MKP-2 deficient macrophages. One possible reason might be that alongside the immediate phagocytosis process, many metabolic changes occur to provide relevant metabolites and energy requirements to fulfil other cellular needs including the regulation of signalling functions. In support to this idea, a recent study found that inhibition of glycolysis downregulated ERK phosphorylation (Chiba *et al.*, 2017). Another early study also revealed that phagocytosis of opsonized zymosan is glycolysis dependent and essential for active actin cytoskeleton remodelling (Venter *et al.*, 2014). This indicates a reciprocal influence of signalling on cellular metabolism and vice versa.

It was also found that deletion of MKP-2 had considerable effects when cells were stimulated with LPS which, as outlined previously, is a key driver of macrophage function. Interestingly, it was found that that MKP-2 deleted macrophages showed upregulated pentose phosphate pathway (PPP) metabolite, D- ribose 5- phosphate. This metabolite is the last step in the oxidative reaction within the PPP which generates fructose 6-phosphate and glyceraldehyde 3-phosphate, both are also intermediates in glycolysis. Ribose 5- phosphate is also a precursor for nucleotides (Boer and Sperling, 1995). Both pathways continued to be enhanced in MKP-2$^{-/-}$ macrophages relative to WT controls. Thus both PPP and glycolysis may be influenced by enhanced JNK activity within this early time frame. Indeed, a previous report has demonstrated JNK1 as a controller of glycolytic activity via phosphofructokinase-1 (Deng *et al.*, 2008). This metabolite was found later to be reduced after ERK and JNK inhibition (Traves *et al.,* 2012). Consistent with the zymosan metabolic profile, LPS treatment confirmed the link between PPP and glycolysis and upregulation following MKP-2 deletion. This explanation is in agreement with another finding where the selective ERK inhibitor PD325901 decreased glucose consumption and lactate production in different types of macrophages (Traves *et al.*, 2012). Thus, MAPKs and in particular for this study JNK, can be correlated with the upregulation of glycolysis although it remains unclear if changes in JNK can explain all the effects of DUSP4 deletion.

Another key finding in the study of LPS metabolomics was enhanced accumulation of L-citrulline in MKP-2$^{-/-}$ macrophages after 24 hours stimulation while other metabolites of the Arginine and proline pathway were down regulated. One study revealed that L-

citrulline recycling does not play a major role in the cell under basal conditions in airways (Sopi *et al.*, 2012), the same group however also showed that L-citrulline accumulation blocks L-Arginine generation of L-Ornithine and urea metabolites known to be important in cellular proliferation. These findings might be relevant to the current study in that enhanced L-Citrulline accumulation in MKP-2 deleted macrophages may block the formation of L-ornithine/urea/polyamine and perhaps is the reason why LPS reduced the proliferation rate detailed in Fig.4.15. MKP-2 deleted macrophage may have reduced polyamine formation and a targeted metabolomics of this metabolite may help to understand the proliferative changes resulting from MKP-2 deletion.

Metabolic profiles that accompanied macrophage migration towards C5a was investigated in the final part of this chapter. As expected, early upregulation of glycolysis metabolites was observed as early as 5 minutes C5a stimulation in MKP-2$^{-/-}$ macrophages (Fig.4.21). The PPP was also upregulated confirming that both pathways are changed in a parallel direction. These findings demonstrate an important role for metabolic changes in motility and indeed it has been found that glycolysis regulates dendritic cell morphology and motility (Guak *et al.*, 2018). This finding is consistent with the effects observed in MKP-2$^{-/-}$ macrophages.

A host of other metabolites were also upregulated and two are briefly discussed here. Sphingolipids pathway metabolites were also found to be upregulated in MKP-2 deleted macrophage. These are a family of proteins (Gault *et al.*, 2010) within the cell membrane and also known for their role in signalling. However sphingolipids are also a part of lipid raft formation, a function important in actin polymerisation. Creatine is a metabolite that is also involved in cell migration via ATP exchange hydrolysis (Kuiper *et al.*, 2009). Both creatine and ATP are decreased in MKP-2 deleted macrophages after 15 minutes of C5a stimulation (Table 4.16) and this may explain the reduction in MKP-2$^{-/-}$ migration towards C5a. One of the metabolites that was significantly upregulated in MKP-2$^{-/-}$ was phosphatidylserine (PS). PS is located in the inner part of the cell membrane but translocate to the outer site of the membrane during apoptosis and provide a signal to the phagocytic cells (an eat me signal) (Dill *et al.*, 2015). This indicates that MKP-2 deleted macrophages are more prone towards apoptosis than MKP-2$^{+/+}$which would be another area of interest to study.

 Overall, the upregulation of host of metabolic intermediates correlate well with enhanced migration following MKP-2 deletion.

A key and surprising element in the study of metabolomics is that a number of intermediates can have strong regulatory effects on the inflammatory response of macrophages including not only NO release but the production of cytokines (Rattigan *et al.*, 2018, Kelly and O'neill, 2015). Interestingly, zymosan treatment showed a significant increase in the concentration of IL-1β in MKP-2 deleted macrophages. IL-1β is found to be a pro-inflammatory cytokine (Lu *et al.*, 2018). On the other hand, IL-10 production seemed to be unaffected or decreased to the basal levels in zymosan treated macrophages in both groups. This may indicate that zymosan drives MKP-2 deleted microphages towards a pro-inflammatory phenotype. IL-1β and IL-10 has shown to be involved in arginine metabolism (Rodriguez *et al.*, 2017), thus the pro-inflammatory signal generated by IL-1β correlates with citrulline accumulation and decreased NO which was shown to be down regulated in MKP-2 deleted macrophages (Fig.4.26). This confirms previous findings in our laboratory regarding NO production (Al-Mutairi *et al.*, 2010) and might be JNK regulated. The reduction in the NO could be due to uncoupled iNOS where it produce superoxide anion O_2^- instead of NO (Fig.4.25).

Chapter Five

General Discussion

5. General discussion

The role of MKPs in regulating MAPKs has been studied to some extent but relative to the MAP kinases, major deficits in our understanding remain. From the literature the focus has been mostly on MKP-1 which revealed the answers to many questions surrounding MAPKs and their function. However, many other questions are still unanswered, a growing body including previous and recent work in our laboratory and also other groups have demonstrated important roles for MKP-2 in inflammation, parasite infection, the cardiovascular system and multiple sclerosis (Cornell *et al.*, 2010, Al-Mutairi *et al.*, 2010, Lawan *et al.*, 2011, Barbour *et al.*, 2016). Macrophages are one of the innate immune cell types known to be required for the immune response in the above conditions/diseases. However, the molecular mechanisms that drive macrophages function is still poorly studied.

This thesis is the first body of work to demonstrate the role of MKP-2 (DUSP4) in a number of key macrophage functions using a novel MKP-2 deleted mouse model. Findings in chapter 3 demonstrated that in a M1 "like" phenotype, JNK signalling was significantly elevated in MKP-2 deleted macrophage following LPS challenge. This indicates that MKP-2 mainly dephosphorylates JNK over ERK and p38 in this system. Thus, deleting this gene leads to JNK upregulation consistent with a similar results obtained previously from our laboratory (Al-Mutairi *et al.*, 2010) where JNK and p38 MAPK was significantly increased in MKP-2 deleted macrophages with no effect on ERK. This is not consistent with other studies in which considerable changes in MAP kinase signalling are observed due to the differences in the methods that was used to produce MKP-2 KO cells. For example, our laboratory has developed MKP-2 deleted mice using targeted homologous recombination method (Al-Mutairi *et al.*, 2010). Whilst, others developed tissue specific MKP-2 knockdown (Cornell *et al.*, 2012).

LPS also enhanced MKP-2 expression in a time dependent manner where the maximal expression was 2 hours which is well beyond the time at which ERK, JNK and p38 phosphorylation returned to basal values. This might suggest that MKP-2 does not play a role in regulating MAP kinase activity, however given that MKP-2 is a nuclear phosphatase, assessing the activity status of JNK and ERK in the nucleus would be essential to determine if this was the case. A new finding here was that MKP-2 expression was decreased upon ERK inhibition and to a lesser extent by JNK but not p38 MAPK suggesting the potential of cross talk between ERK and JNK but via the induction of MKP-2. With regards to ERK signalling which was not significantly

altered in MKP-2 deletion macrophages, there might be redundancy between the MKPs such that MKP-1, MKP-3, MKP-X and MKP-4 are able to dephosphorylate ERK in the absence of MKP-2 (Kidger and Keyse, 2016). Thus, the exact effect on ERK might not be due to one DUSP activity and needs more investigation using approaches to delete a number or all nuclear phosphatases together in one study to exactly identify their respective roles.

Having established MAPK signalling in macrophages relative to MKP-2 gene deletion, the next task was to investigate this signalling in another immune cell type for comparison. Neutrophils were chosen due to their interaction with macrophages at the sight of injury or inflammation resolution and also in tumour environment (Galdiero *et al.*, 2013). Investigating the role of MKP-2 in neutrophil MAPK signalling was completely new and this study is first to investigate MAPK signalling towards different agents that contributes in neutrophil functions using MKP-2 deleted neutrophil for a comparison. From those agents, C5a and LTB4 induced ERK activation was significantly reduced in MKP-2$^{-/-}$ neutrophils. This effect was unexpected the assumption was ERK activity would be enhanced. However preliminary results in our laboratory suggested a similar phenomenon in macrophage precursors (Neamatallah personal communication). This suggests a dysfunction within MAP kinase cascade but only with respect to GPCRs. This would imply a deficit in G-protein function, activation of PKCs or perhaps β-arrestins, all elements implicated in the coupling of GPCRs to ERK signalling. In any event this effect might regulate neutrophil function with respect to migration towards the inflammation site and indeed studies in the laboratory are currently examining this concept.

Next it was decided next to investigate one of the genes that is correlated with JNK signalling. Endolthelin-1 was the gene that chosen having previously been shown to be regulated by JNK signalling (Gadea *et al.*, 2008). Also a previous gene array study had shown the upregulation of EDN1 in response to LPS thus it was of important to determine if this was a real effect. An interesting observation was that when the MKP-2 gene was deleted, levels of endothelin-1 gene expression and peptide release were significantly increased. To the author's knowledge, this thesis is the first study to investigate the role of MKP-2 in the regulation of the EDN1 gene. Endothelin-1 is a vasoconstrictor agent that found to contribute in many cardiac dysfunctions via its effect on smooth muscle cell contraction and proliferation (Elisa *et al.*, 2015). Studies have indicated that EDN1 release works in opposition to NO, a well-known vasodilator

molecule (Labonte *et al.*, 2008, Mckenna *et al.*, 2015). This suggests that MKP-2 deletion may result in hypertension under inflammatory conditions and could easily be tested. However, given that MKP-2 is expressed in most cells, a tissue specific KO mouse would have to be developed to delete macrophage MKP-2 but retain MKP-2 expression intact in other cell types.

However, there were clear caveats with these results, there was a dissociation between JNK signalling and the expression of MKP-2, and inhibitor studies did not suggest that altering JNK activity would have any effect on END1 expression. This was even more clearly marked for END1 protein release, the inhibitors were ineffective, suggesting that MAPK does not play a role to any extent at this level. Whilst this seems unlikely, and more optimisation of the ELISA might be required to show the same outcome as for the mRNA, it is apparent that the effect of MKP-2 deletion on END1 expression is not easily explained by changes in MAP kinase activity that are minimal.

Nevertheless in preliminary studies an attempt was made to link MKP-2 deletion and enhanced END1 expression and release to a physiological function. The author was able to carry out one experiment which was to co-culture BMDMs from both MKP-2$^{+/+}$ and MKP-2$^{-/-}$ mice with rat pulmonary vascular smooth muscle cells (PVSMs) gifted from Dr. Paul Coats group (SIPBS). Interestingly MKP-2$^{-/-}$ macrophages, but not WT, stimulated with LPS were able to increase smooth muscle proliferation in the lower chamber (results not shown). Clearly, properly controlled experiments should be conducted including the use of specific EDN1 receptor a (ETa) inhibitors, but it does give rise to the possibility that MKP-2 deletion at the level of the macrophage could affect smooth muscle cell function *in vivo* via enhanced END1 gene expression.

Contained with this thesis is also the first study to uncover the effect MKP-2 gene plays in regulating macrophage functions. Results from chapter 4 demonstrated a novel role for the MKP-2 gene in regulating macrophage phagocytosis and migration via regulation of actin rearrangement and other morphological differences that was observed in the absence of the MKP-2 gene. An interesting finding was that the MKP-2 gene regulates macrophage phagocytosis and migration in a different context depending to the activation mode. MKP-2 deleted macrophages had higher phagocytic activity and were less motile than MKP-2$^{+/+}$ macrophages. This effect is reversed in IL-4 activated macrophages which also had lowered uptake of zymosan particles in MKP-2 deleted cells which was completely novel finding for the MKP-2

gene and has been not recorded for any other DUSPs family. Using a phagocytosis inhibitor such as Cytochalasin -D would be a possible way to further investigate the role of MKP-2 in this function. Such idea could be confirmed by measuring MKP-2 protein expression by Western blotting to check whether phagocytosis inhibition would affect MKP-2 expression or not. Also using MAPK inhibitors in LPS or IL-4 induced phagocytosis and migration would be also another possible suggestion to further understanding influence of MKP-2 on stress fibre formation and morphological features of both phagocytosis and migration.

A third aspect that was investigated in this thesis was proliferation. An interesting finding in this section was that the MKP-2 gene regulates M-CSF induced macrophage proliferation and MKP-2 deleted macrophages showed reduced proliferation compared to the wild type counterpart. This result is confirmed the role of MKP-2 in cell proliferation observed previously in our lab in MEF cells (Lawan *et al.*, 2011) although in the previous study an effect in G2/M-phase was identified rather than a deficient in S-phase progression. A possible explanation for that is that macrophage progenitor themselves could be dysfunctional in some way. Less progenitor cells means less proliferation and less differentiated macrophages. Such a hypothesis could be further confirmed by isolating bone marrow monocytes using specific magnetic beads in which equal numbers of isolated monocytes could be then cultured and monitored for proliferation and differentiation markers.

This thesis also presents for the first time the metabolic changes underlying MKP-2 regulation of macrophage function. Using an untargeted metabolomics profile revealed thousands of metabolites in response to each stimulus used. This metabolic approach is now used very recently to study cells such as macrophage reprogramming which widened the understanding of innate immune response better than studying the functions alone (Kelly and O'neill, 2015). In this context, the LPS stimulated metabolic profile has been investigated by different groups to identify macrophages and DCs functions in more details (Galvan-Pena and O'neill, 2014). They demonstrated that cellular metabolism is controlled by many signalling pathways including MAPK pathway, thus they correlated these functions to MKP-1, and this is the only phosphatase that has been studied very recently for its regulatory effect on macrophages during atherosclerosis (Kim *et al.*, 2016). The main pathway that was found to be regulated by MKP-1 is linked to metabolic stress which affects macrophage polarization towards the M1/M2 activation phenotype. The role of

MAPKs in macrophage metabolism was studied previously and it was found that the MEK/ERK cascade is important in regulating central metabolism in response to LPS stimulation via glycolytic flux (Traves *et al.*, 2012).

This thesis attempted to assess metabolic changes in MKP-2 deleted macrophages that underpin effects upon macrophage phagocytosis, migration and proliferation. Novel findings were found for a number of metabolic changes linked to zymosan phagocytosis. Glycolysis and the pentose phosphate pathway were main metabolic pathways upregulated in MKP-2 deleted macrophages. Their intermediate metabolites are key factors for providing the energy required for phagocytosis thus indicating a regulatory effect for MKP-2 in controlling macrophage phagocytosis albeit indirectly. The pattern of glycolysis and pentose phosphate pathway paralleled MAPK phosphorylation suggesting that MAPK was driving metabolic activity however, studies to assess the effect of inhibiting MAP kinase signalling in either WT or MKP-2 deletion macrophages could not be completed in the time available. It is interesting that upregulation of glycolysis and fatty acid β-oxidation can be recorded in the plasma samples following zymosan induced peritonitis (Fujieda *et al.*, 2013, Venter *et al.*, 2014), therefore one future study might be to conduct some equivalent studies in MKP-2 KO mice *in vivo*.

LPS induced phagocytosis and migration also showed similar pattern which confirms strong correlation in metabolic changes and macrophage functions. Results from LPS metabolic profiling conducted in this thesis suggests an important role of MKP-2 in the arginine and proline pathway. MKP-2 deleted macrophages showed enhanced accumulated citrulline which is one of the metabolites that is derived from nitric oxide synthase (NOS) activity. Citrulline accumulation blocks L-arginine to generate L-Ornithine and urea thus prevents the formation of polyamines which is required for cell proliferation. This might be the reason behind reduced proliferation in MKP-2 deleted macrophages and also may explain reduced NO production in this cell type. In order to confirm these effects, it would be good to employ inhibitors of the relevant pathways to mimic the effects of MKP-2 deletion on proliferation.

In addition novel metabolic changes have been demonstrated following C5a stimulation with again an upregulation of glycolysis and the PPP in MKP-2$^{-/-}$ macrophages. These results further confirmed that MKP-2 has a key regulatory role in macrophage motility and chemotaxis. Further investigation of MAPK signalling in response to C5a is an essential next step to clarify further these metabolic changes

with respect to macrophage cell function given, that as described in chapter 3 neutrophil, ERK signalling is significantly compromised in response to C5a.

In conclusion, novel findings from this thesis highlight the significant role of MKP-2 in the immune response via regulating macrophage functions and adds new findings which help in understanding the role of MKP-2 in immune biology.

Chapter six

Appendices

1- OPLSDA
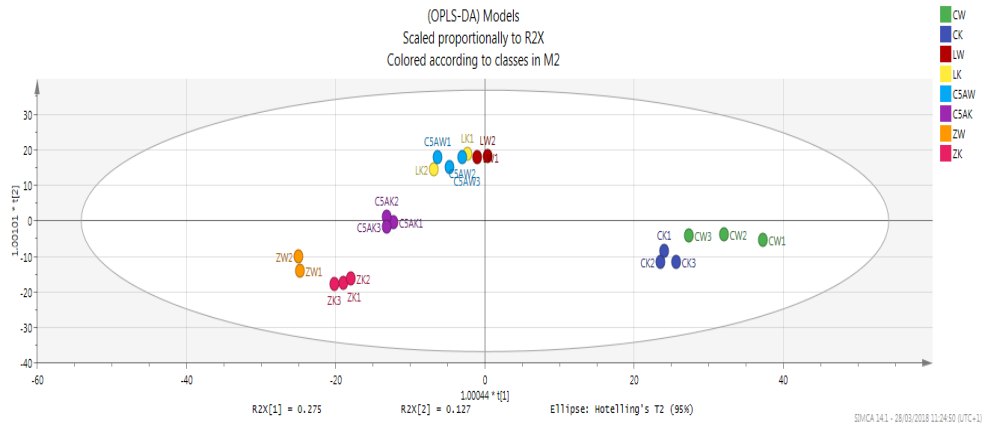
2- PCA

3- Permutations

203
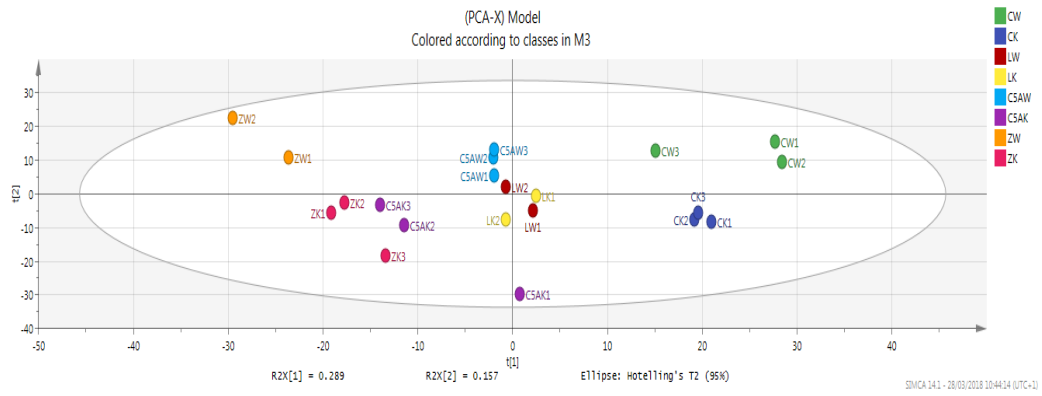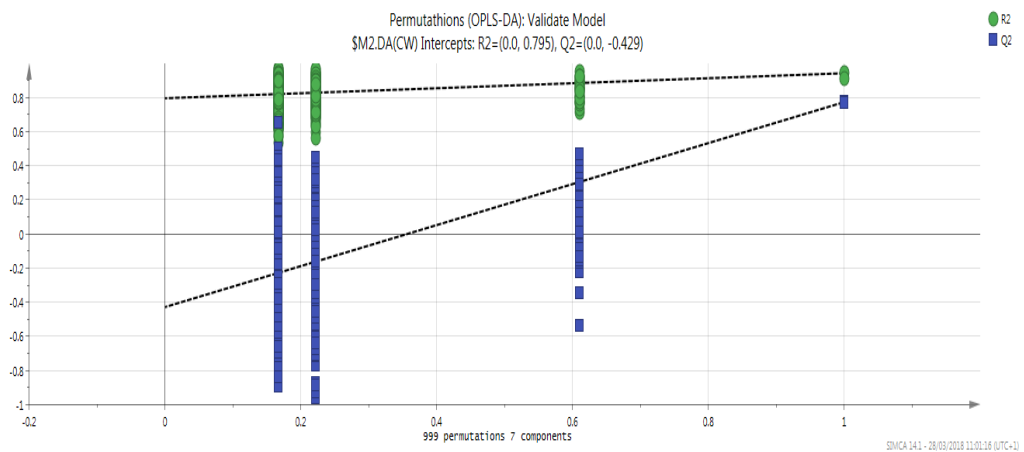
4- Outliers
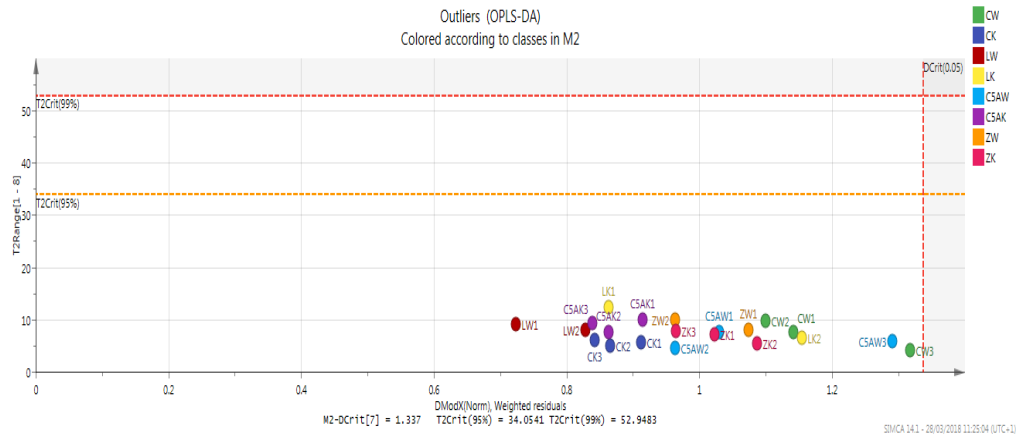
5-ROC
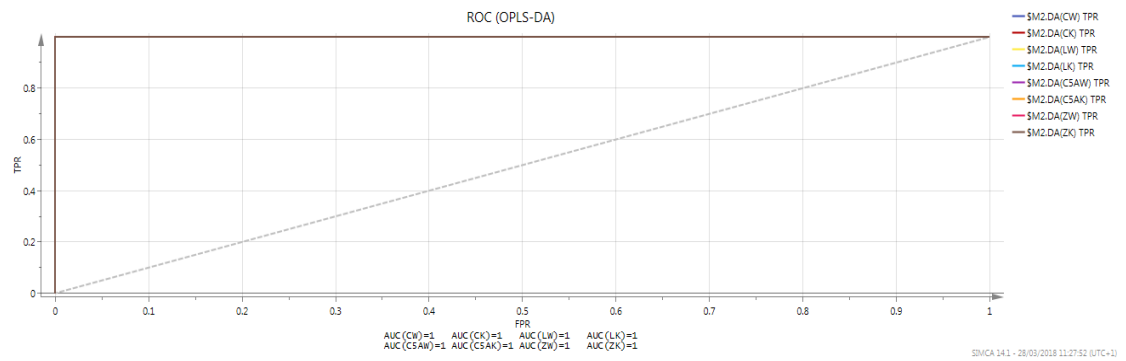
6-Model Anova

OPLS-DA	SS	DF	MS	F	p	SD
Total corr.	140	140	1			1
Regression	74.66	84	0.888809	0.761759	0.872043	0.942767
Residual	65.34	56	1.16679			1.08018

7- HCA

HCA (PCA-X)
Hierarchical Clustering
t[1 2 3 4]

Calculated with ward and sorted by size.

SIMCA 14.1 - 28/03/2018 11:31:42 (UTC+1)
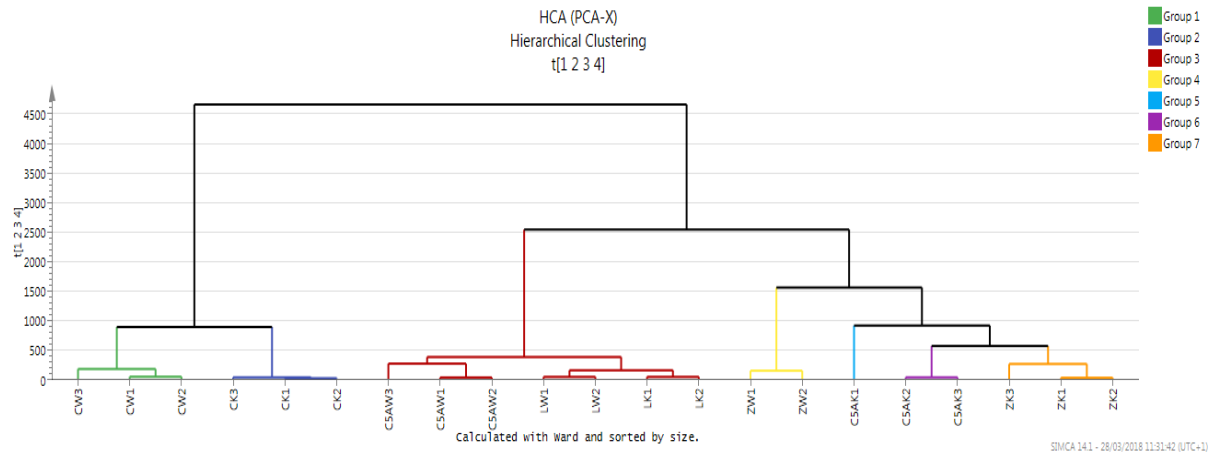
8- Misclassification table

	Members	Correct	CW	CK	LW	LK	C5AW	C5AK	ZW	ZK	No class (YPred <= 0)
CW	3	100%	3	0	0	0	0	0	0	0	0
CK	3	100%	0	3	0	0	0	0	0	0	0
LW	2	100%	0	0	2	0	0	0	0	0	0
LK	2	100%	0	0	0	2	0	0	0	0	0
C5AW	3	100%	0	0	0	0	3	0	0	0	0
C5AK	3	100%	0	0	0	0	0	3	0	0	0
ZW	2	100%	0	0	0	0	0	0	2	0	0
ZK	3	100%	0	0	0	0	0	0	0	3	0
Total	21	100%	3	3	2	2	3	3	2	3	0

9- Distance to model is a summary of the deviations of an observation. The larger the deviation, the further away from the model is the observation. Observations well above the red line are significantly dissimilar from the others.

Macrophages W vs K - 24 h.M2 (OPLS-DA)
Colored according to marked groups

1 - R2X(cum)[7] = 0.2568 M2-DCrit[7] = 1.337

SIMCA 14.1 - 28/03/2018 11:39:33 (UTC+1)
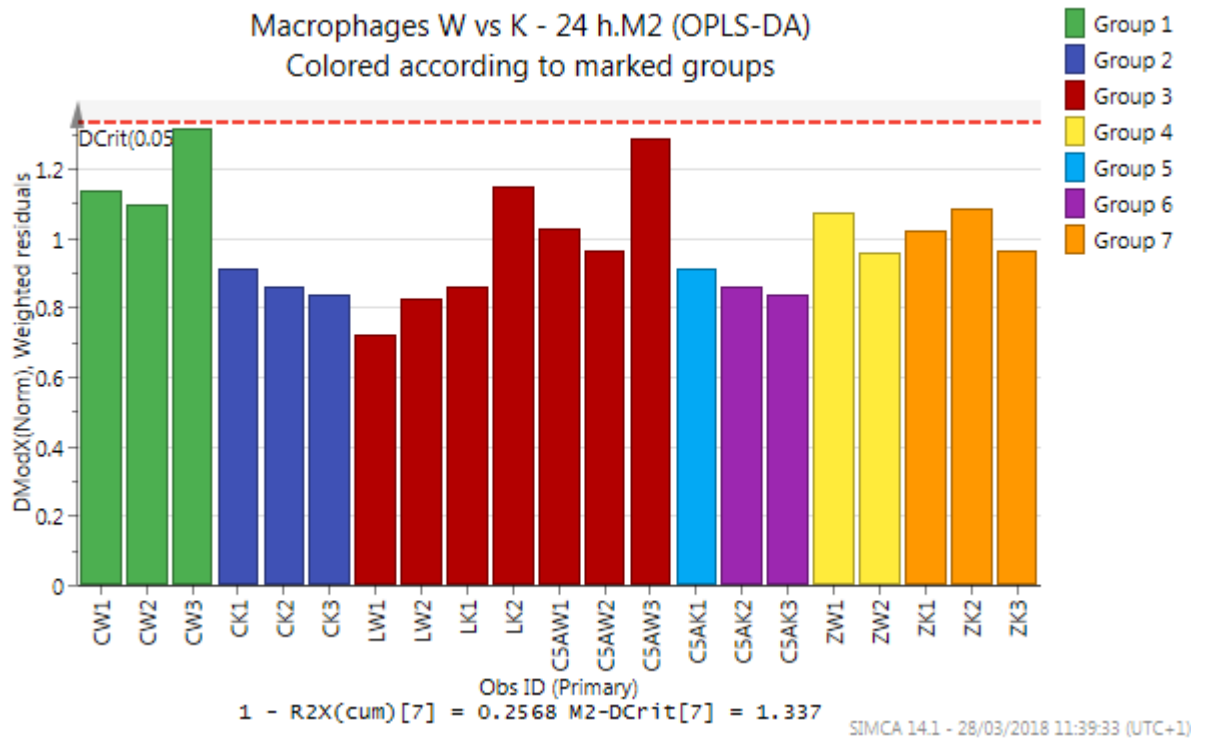
Chapter Seven

References

Abraham, S. M., Lawrence, T., Kleiman, A., Warden, P., Medghalchi, M., Tuckermann, J., Saklatvala, J. & Clark, A. R. 2006. Antiinflammatory effects of dexamethasone are partly dependent on induction of dual specificity phosphatase 1. *J Exp Med,* 203**,** 1883-9.

Aderem, A. & Underhill, D. M. 1999. Mechanisms of phagocytosis in macrophages. *Annu Rev Immunol,* 17**,** 593-623.

Adhikari, A., Xu, M. & Chen, Z. J. 2007. Ubiquitin-mediated activation of TAK1 and IKK. *Oncogene,* 26**,** 3214-26.

Akashi, K., Traver, D., Miyamoto, T. & Weissman, I. L. 2000. A clonogenic common myeloid progenitor that gives rise to all myeloid lineages. *Nature,* 404**,** 193-7.

Akira, S. & Takeda, K. 2004. Toll-like receptor signalling. *Nat Rev Immunol,* 4**,** 499-511.

Al-Mutairi, M. S., Cadalbert, L. C., Mcgachy, H. A., Shweash, M., Schroeder, J., Kurnik, M., Sloss, C. M., Bryant, C. E., Alexander, J. & Plevin, R. 2010. MAP kinase phosphatase-2 plays a critical role in response to infection by Leishmania mexicana. *PLoS Pathog,* 6**,** e1001192.

Amano, S. U., Cohen, J. L., Vangala, P., Tencerova, M., Nicoloro, S. M., Yawe, J. C., Shen, Y., Czech, M. P. & Aouadi, M. 2014. Local proliferation of macrophages contributes to obesity-associated adipose tissue inflammation. *Cell Metab,* 19**,** 162-171.

Aouadi, M., Binetruy, B., Caron, L., Le Marchand-Brustel, Y. & Bost, F. 2006. Role of MAPKs in development and differentiation: lessons from knockout mice. *Biochimie,* 88**,** 1091-8.

Arancibia, S. A., Beltran, C. J., Aguirre, I. M., Silva, P., Peralta, A. L., Malinarich, F. & Hermoso, M. A. 2007. Toll-like receptors are key participants in innate immune responses. *Biol Res,* 40**,** 97-112.

Arbour, N., Naniche, D., Homann, D., Davis, R. J., Flavell, R. A. & Oldstone, M. B. 2002. c-Jun NH(2)-terminal kinase (JNK)1 and JNK2 signaling pathways have divergent roles in CD8(+) T cell-mediated antiviral immunity. *J Exp Med,* 195**,** 801-10.

Arce, I., Martinez-Munoz, L., Roda-Navarro, P. & Fernandez-Ruiz, E. 2004. The human C-type lectin CLECSF8 is a novel monocyte/macrophage endocytic receptor. *Eur J Immunol,* 34**,** 210-20.

Arthur, J. S. & Ley, S. C. 2013. Mitogen-activated protein kinases in innate immunity. *Nat Rev Immunol,* 13**,** 679-92.

Auffray, C., Sieweke, M. H. & Geissmann, F. 2009. Blood monocytes: development, heterogeneity, and relationship with dendritic cells. *Annu Rev Immunol,* 27**,** 669-92.

Avruch, J. 2007. MAP kinase pathways: the first twenty years. *Biochim Biophys Acta,* 1773**,** 1150-60.

Balko, J. M., Schwarz, L. J., Bhola, N. E., Kurupi, R., Owens, P., Miller, T. W., Gomez, H., Cook, R. S. & Arteaga, C. L. 2013. Activation of MAPK pathways due to DUSP4 loss promotes cancer stem cell-like phenotypes in basal-like breast cancer. *Cancer Res,* 73**,** 6346-58.

Barbosa, C. M., Leon, C. M., Nogueira-Pedro, A., Wasinsk, F., Araujo, R. C., Miranda, A., Ferreira, A. T. & Paredes-Gamero, E. J. 2011. Differentiation of hematopoietic stem cell and myeloid populations by ATP is modulated by cytokines. *Cell Death Dis,* 2**,** e165.

Barbour, M., Plevin, R. & Jiang, H. R. 2016. MAP kinase phosphatase 2 deficient mice develop attenuated experimental autoimmune encephalomyelitis through regulating dendritic cells and T cells. *Sci Rep,* 6**,** 38999.

Bezbradica, J. S., Rosenstein, R. K., Demarco, R. A., Brodsky, I. & Medzhitov, R. 2014. A role for the ITAM signaling module in specifying cytokine-receptor functions. *Nat Immunol,* 15**,** 333-42.

Biteau, B., Hochmuth, C. E. & Jasper, H. 2008. JNK activity in somatic stem cells causes loss of tissue homeostasis in the aging Drosophila gut. *Cell Stem Cell,* 3**,** 442-55.

Bobryshev, Y. V., Ivanova, E. A., Chistiakov, D. A., Nikiforov, N. G. & Orekhov, A. N. 2016. Macrophages and Their Role in Atherosclerosis: Pathophysiology and Transcriptome Analysis. *Biomed Res Int,* 2016**,** 9582430.

Bode, J. G., Ehlting, C. & Haussinger, D. 2012. The macrophage response towards LPS and its control through the p38(MAPK)-STAT3 axis. *Cell Signal,* 24**,** 1185-94.

Boer, P. & Sperling, O. 1995. Role of cellular ribose-5-phosphate content in the regulation of 5-phosphoribosyl-1-pyrophosphate and de novo purine synthesis in a human hepatoma cell line. *Metabolism,* 44**,** 1469-74.

Boggiatto, P. M., Jie, F., Ghosh, M., Gibson-Corley, K. N., Ramer-Tait, A. E., Jones, D. E. & Petersen, C. A. 2009. Altered dendritic cell phenotype in response to Leishmania amazonensis amastigote infection is mediated by MAP kinase, ERK. *Am J Pathol,* 174**,** 1818-26.

Borregaard, N. & Herlin, T. 1982. Energy metabolism of human neutrophils during phagocytosis. *J Clin Invest,* 70**,** 550-7.

Bourque, S. L., Davidge, S. T. & Adams, M. A. 2011. The interaction between endothelin-1 and nitric oxide in the vasculature: new perspectives. *Am J Physiol Regul Integr Comp Physiol,* 300**,** R1288-95.

Bozza, M., Satoskar, A. R., Lin, G., Lu, B., Humbles, A. A., Gerard, C. & David, J. R. 1999. Targeted disruption of migration inhibitory factor gene reveals its critical role in sepsis. *J Exp Med,* 189**,** 341-6.

Burdon, P. C., Martin, C. & Rankin, S. M. 2008. Migration across the sinusoidal endothelium regulates neutrophil mobilization in response to ELR + CXC chemokines. *Br J Haematol,* 142**,** 100-8.

Bylesjo, M., Sjodin, A., Eriksson, D., Antti, H., Moritz, T., Jansson, S. & Trygg, J. 2006. MASQOT-GUI: spot quality assessment for the two-channel microarray platform. *Bioinformatics,* 22**,** 2554-5.

Canagarajah, B. J., Khokhlatchev, A., Cobb, M. H. & Goldsmith, E. J. 1997. Activation mechanism of the MAP kinase ERK2 by dual phosphorylation. *Cell,* 90**,** 859-69.

Carr, E. L., Kelman, A., Wu, G. S., Gopaul, R., Senkevitch, E., Aghvanyan, A., Turay, A. M. & Frauwirth, K. A. 2010. Glutamine uptake and metabolism are coordinately regulated by ERK/MAPK during T lymphocyte activation. *J Immunol,* 185**,** 1037-44.

Caunt, C. J. & Keyse, S. M. 2013. Dual-specificity MAP kinase phosphatases (MKPs): shaping the outcome of MAP kinase signalling. *Febs j,* 280**,** 489-504.

Chambard, J. C., Lefloch, R., Pouyssegur, J. & Lenormand, P. 2007. ERK implication in cell cycle regulation. *Biochim Biophys Acta,* 1773**,** 1299-310.

Chang, L. & Karin, M. 2001. Mammalian MAP kinase signalling cascades. *Nature,* 410**,** 37-40.

Chaplin, D. D. 2010. Overview of the immune response. *J Allergy Clin Immunol,* 125**,** S3-23.

Charles, C. H., Sun, H., Lau, L. F. & Tonks, N. K. 1993. The growth factor-inducible immediate-early gene 3CH134 encodes a protein-tyrosine-phosphatase. *Proc Natl Acad Sci U S A,* 90**,** 5292-6.

Chen, P. 2002. Restraint of proinflammatory cytokine biosynthesis by mitogen-activated protein kinase phosphatase-1 in lipopolysaccharide-stimulated macrophages. *J. Immunol.,* 169**,** 6408-6416.

Chi, H. 2006. Dynamic regulation of pro- and anti-inflammatory cytokines by MAPK phosphatase 1 (MKP-1) in innate immune responses. *Proc. Natl Acad. Sci. USA,* 103**,** 2274.

Chi, H. & Flavell, R. A. 2008. Acetylation of MKP-1 and the control of inflammation. *Sci Signal,* 1**,** pe44.

Chiba, S., Hisamatsu, T., Suzuki, H., Mori, K., Kitazume, M. T., Shimamura, K., Mizuno, S., Nakamoto, N., Matsuoka, K., Naganuma, M. & Kanai, T. 2017. Glycolysis regulates LPS-induced cytokine production in M2 polarized human macrophages. *Immunol Lett,* 183**,** 17-23.

Chiou, W. F., Tsai, H. R., Yang, L. M. & Tsai, W. J. 2004. C5a differentially stimulates the ERK1/2 and p38 MAPK phosphorylation through independent signaling pathways to induced chemotactic migration in RAW264.7 macrophages. *Int Immunopharmacol,* 4**,** 1329-41.

Chu, Y., Solski, P. A., Khosravi-Far, R., Der, C. J. & Kelly, K. 1996. The mitogen-activated protein kinase phosphatases PAC1, MKP-1, and MKP-2 have unique substrate specificities and reduced activity in vivo toward the ERK2 sevenmaker mutation. *J. Biol. Chem.,* 271**,** 6497-6501.

Clynes, R., Maizes, J. S., Guinamard, R., Ono, M., Takai, T. & Ravetch, J. V. 1999. Modulation of immune complex-induced inflammation in vivo by the coordinate expression of activation and inhibitory Fc receptors. *J Exp Med,* 189**,** 179-85.

Comalada, M., Lloberas, J. & Celada, A. 2012. MKP-1: a critical phosphatase in the biology of macrophages controlling the switch between proliferation and activation. *Eur J Immunol,* 42**,** 1938-48.

Cornell, T. T., Fleszar, A., Mchugh, W., Blatt, N. B., Le Vine, A. M. & Shanley, T. P. 2012. Mitogen-activated protein kinase phosphatase 2, MKP-2, regulates early inflammation in acute lung injury. *Am J Physiol Lung Cell Mol Physiol,* 303**,** L251-8.

Cornell, T. T., Rodenhouse, P., Cai, Q., Sun, L. & Shanley, T. P. 2010. Mitogen-activated protein kinase phosphatase 2 regulates the inflammatory response in sepsis. *Infect Immun,* 78**,** 2868-76.

Cross, A. R. & Segal, A. W. 2004. The NADPH oxidase of professional phagocytes--prototype of the NOX electron transport chain systems. *Biochim Biophys Acta,* 1657**,** 1-22.

Crowell, S., Wancket, L. M., Shakibi, Y., Xu, P., Xue, J., Samavati, L., Nelin, L. D. & Liu, Y. 2014. Post-translational regulation of mitogen-activated protein kinase phosphatase (MKP)-1 and MKP-2 in macrophages following lipopolysaccharide stimulation: the role of the C termini of the phosphatases in determining their stability. *J Biol Chem,* 289**,** 28753-64.

Crowley, M. T., Costello, P. S., Fitzer-Attas, C. J., Turner, M., Meng, F., Lowell, C., Tybulewicz, V. L. J. & Defranco, A. L. 1997. A Critical Role for Syk in Signal Transduction and Phagocytosis Mediated by Fcγ Receptors on Macrophages. *The Journal of Experimental Medicine,* 186**,** 1027-1039.

Cypher, L. R., Bielecki, T. A., Adepegba, O., Huang, L., An, W., Iseka, F., Luan, H., Tom, E., Storck, M. D., Hoppe, A. D., Band, V. & Band, H. 2016. CSF-1 receptor signalling is governed by pre-requisite EHD1 mediated receptor display on the macrophage cell surface. *Cell Signal,* 28**,** 1325-35.

Dangaj, D., Abbott, K. L., Mookerjee, A., Zhao, A., Kirby, P. S., Sandaltzopoulos, R., Powell, D. J., Jr., Lamaziere, A., Siegel, D. L., Wolf, C. & Scholler, N. 2011. Mannose receptor (MR) engagement by mesothelin GPI anchor polarizes

tumor-associated macrophages and is blocked by anti-MR human recombinant antibody. *PLoS One,* 6**,** e28386.

Deguine, J. & Barton, G. M. 2014. MyD88: a central player in innate immune signaling. *F1000Prime Rep,* 6**,** 97.

Deng, H., Yu, F., Chen, J., Zhao, Y., Xiang, J. & Lin, A. 2008. Phosphorylation of Bad at Thr-201 by JNK1 promotes glycolysis through activation of phosphofructokinase-1. *J Biol Chem,* 283**,** 20754-60.

Dickinson, R. J. 2002. Characterization of a murine gene encoding a developmentally regulated cytoplasmic dual-specificity mitogen-activated protein kinase phosphatase. *Biochem. J.,* 364**,** 145-155.

Dill, B. D., Gierlinski, M., Hartlova, A., Arandilla, A. G., Guo, M., Clarke, R. G. & Trost, M. 2015. Quantitative proteome analysis of temporally resolved phagosomes following uptake via key phagocytic receptors. *Mol Cell Proteomics,* 14**,** 1334-49.

Dong, C., Davis, R. J. & Flavell, R. A. 2001. Signaling by the JNK group of MAP kinases. c-jun N-terminal Kinase. *J Clin Immunol,* 21**,** 253-7.

Doyle, S. L. & O'neill, L. A. 2006. Toll-like receptors: from the discovery of NFkappaB to new insights into transcriptional regulations in innate immunity. *Biochem Pharmacol,* 72**,** 1102-13.

Dudley, D. T., Pang, L., Decker, S. J., Bridges, A. J. & Saltiel, A. R. 1995. A synthetic inhibitor of the mitogen-activated protein kinase cascade. *Proc Natl Acad Sci U S A,* 92**,** 7686-9.

Dzopalic, T., Rajkovic, I., Dragicevic, A. & Colic, M. 2012. The response of human dendritic cells to co-ligation of pattern-recognition receptors. *Immunol Res,* 52**,** 20-33.

Edwards, J. P., Zhang, X., Frauwirth, K. A. & Mosser, D. M. 2006. Biochemical and functional characterization of three activated macrophage populations. *J Leukoc Biol,* 80**,** 1298-307.

Elisa, T., Antonio, P., Giuseppe, P., Alessandro, B., Giuseppe, A., Federico, C., Marzia, D., Ruggero, B., Giacomo, M., Andrea, O., Daniela, R., Mariaelisa, R. & Claudio, L. 2015. Endothelin Receptors Expressed by Immune Cells Are Involved in Modulation of Inflammation and in Fibrosis: Relevance to the Pathogenesis of Systemic Sclerosis. *J Immunol Res,* 2015**,** 147616.

Enslen, H., Brancho, D. M. & Davis, R. J. 2000. Molecular determinants that mediate selective activation of p38 MAP kinase isoforms. *Embo j,* 19**,** 1301-11.

Epelman, S., Lavine, K. J. & Randolph, G. J. 2014. Origin and functions of tissue macrophages. *Immunity,* 41**,** 21-35.

Fang, L., Wu, H. M., Ding, P. S. & Liu, R. Y. 2014. TLR2 mediates phagocytosis and autophagy through JNK signaling pathway in Staphylococcus aureus-stimulated RAW264.7 cells. *Cell Signal,* 26**,** 806-14.

Fanger, N. A., Wardwell, K., Shen, L., Tedder, T. F. & Guyre, P. M. 1996. Type I (CD64) and type II (CD32) Fc gamma receptor-mediated phagocytosis by human blood dendritic cells. *J Immunol,* 157**,** 541-8.

Farnebo, L., Shahangian, A., Lee, Y., Shin, J. H., Scheeren, F. A. & Sunwoo, J. B. 2015. Targeting Toll-like receptor 2 inhibits growth of head and neck squamous cell carcinoma. *Oncotarget,* 6**,** 9897-907.

Farooq, A. & Zhou, M. M. 2004. Structure and regulation of MAPK phosphatases. *Cell Signal,* 16**,** 769-79.

Favata, M. F., Horiuchi, K. Y., Manos, E. J., Daulerio, A. J., Stradley, D. A., Feeser, W. S., Van Dyk, D. E., Pitts, W. J., Earl, R. A., Hobbs, F., Copeland, R. A., Magolda, R. L., Scherle, P. A. & Trzaskos, J. M. 1998. Identification of a novel inhibitor of mitogen-activated protein kinase kinase. *J Biol Chem,* 273**,** 18623-32.

Feng, X., Deng, T., Zhang, Y., Su, S., Wei, C. & Han, D. 2011. Lipopolysaccharide inhibits macrophage phagocytosis of apoptotic neutrophils by regulating the production of tumour necrosis factor alpha and growth arrest-specific gene 6. *Immunology,* 132**,** 287-95.

Fielding, C. A., Mcloughlin, R. M., Mcleod, L., Colmont, C. S., Najdovska, M., Grail, D., Ernst, M., Jones, S. A., Topley, N. & Jenkins, B. J. 2008. IL-6 regulates neutrophil trafficking during acute inflammation via STAT3. *J Immunol,* 181**,** 2189-95.

Fleming, B. D. & Mosser, D. M. 2011. Regulatory macrophages: setting the threshold for therapy. *Eur J Immunol,* 41**,** 2498-502.

Fogg, D. K., Sibon, C., Miled, C., Jung, S., Aucouturier, P., Littman, D. R., Cumano, A. & Geissmann, F. 2006. A clonogenic bone marrow progenitor specific for macrophages and dendritic cells. *Science,* 311**,** 83-7.

Freeman, B. D., Machado, F. S., Tanowitz, H. B. & Desruisseaux, M. S. 2014. Endothelin-1 and its role in the pathogenesis of infectious diseases. *Life Sci,* 118**,** 110-9.

Friedl, P. & Weigelin, B. 2008. Interstitial leukocyte migration and immune function. *Nat Immunol,* 9**,** 960-9.

Fujieda, Y., Manno, A., Hayashi, Y., Rhodes, N., Guo, L., Arita, M., Bamba, T. & Fukusaki, E. 2013. Inflammation and resolution are associated with upregulation of fatty acid beta-oxidation in Zymosan-induced peritonitis. *PLoS One,* 8**,** e66270.

Fukuyama, K., Yoshida, M., Yamashita, A., Deyama, T., Baba, M., Suzuki, A., Mohri, H., Ikezawa, Z., Nakajima, H., Hirai, S. & Ohno, S. 2000. MAPK upstream kinase (MUK)-binding inhibitory protein, a negative regulator of MUK/dual leucine zipper-bearing kinase/leucine zipper protein kinase. *J Biol Chem,* 275**,** 21247-54.

Gadea, A., Schinelli, S. & Gallo, V. 2008. Endothelin-1 Regulates Astrocyte Proliferation and Reactive Gliosis via a JNK/c-Jun Signaling Pathway. *Journal of Neuroscience,* 28**,** 2394-2408.

Galdiero, M. R., Bonavita, E., Barajon, I., Garlanda, C., Mantovani, A. & Jaillon, S. 2013. Tumor associated macrophages and neutrophils in cancer. *Immunobiology,* 218**,** 1402-10.

Galvan-Pena, S. & O'neill, L. A. 2014. Metabolic reprograming in macrophage polarization. *Front Immunol,* 5**,** 420.

Garrington, T. P. & Johnson, G. L. 1999. Organization and regulation of mitogen-activated protein kinase signaling pathways. *Curr Opin Cell Biol,* 11**,** 211-8.

Gault, C. R., Obeid, L. M. & Hannun, Y. A. 2010. An overview of sphingolipid metabolism: from synthesis to breakdown. *Adv Exp Med Biol,* 688**,** 1-23.

Gautier, E. L., Jakubzick, C. & Randolph, G. J. 2009. Regulation of the migration and survival of monocyte subsets by chemokine receptors and its relevance to atherosclerosis. *Arterioscler Thromb Vasc Biol,* 29**,** 1412-8.

Geeraerts, X., Bolli, E., Fendt, S. M. & Van Ginderachter, J. A. 2017. Macrophage Metabolism As Therapeutic Target for Cancer, Atherosclerosis, and Obesity. *Front Immunol,* 8**,** 289.

Geissmann, F., Manz, M. G., Jung, S., Sieweke, M. H., Merad, M. & Ley, K. 2010. Development of monocytes, macrophages, and dendritic cells. *Science,* 327**,** 656-61.

Gentek, R., Molawi, K. & Sieweke, M. H. 2014. Tissue macrophage identity and self-renewal. *Immunol Rev,* 262**,** 56-73.

Goerdt, S. & Orfanos, C. E. 1999. Other functions, other genes: alternative activation of antigen-presenting cells. *Immunity,* 10**,** 137-42.

Gomes, N. E., Brunialti, M. K. C., Mendes, M. E., Freudenberg, M., Galanos, C. & Salomão, R. 2010. Lipopolysaccharide-induced expression of cell surface receptors and cell activation of neutrophils and monocytes in whole human blood. *Brazilian Journal of Medical and Biological Research,* 43**,** 853-858.

Gonzalez, S., Gonzalez-Rodriguez, A. P., Suarez-Alvarez, B., Lopez-Soto, A., Huergo-Zapico, L. & Lopez-Larrea, C. 2011. Conceptual aspects of self and nonself discrimination. *Self Nonself,* 2**,** 19-25.

Gordon, S. & Martinez, F. O. 2010. Alternative activation of macrophages: mechanism and functions. *Immunity,* 32**,** 593-604.

Gordon, S. & Taylor, P. R. 2005. Monocyte and macrophage heterogeneity. *Nat Rev Immunol,* 5**,** 953-64.

Goyal, S., Castrillon-Betancur, J. C., Klaile, E. & Slevogt, H. 2018. The Interaction of Human Pathogenic Fungi With C-Type Lectin Receptors. *Front Immunol,* 9**,** 1261.

Grant, E. P., Picarella, D., Burwell, T., Delaney, T., Croci, A., Avitahl, N., Humbles, A. A., Gutierrez-Ramos, J. C., Briskin, M., Gerard, C. & Coyle, A. J. 2002. Essential role for the C5a receptor in regulating the effector phase of synovial infiltration and joint destruction in experimental arthritis. *J Exp Med,* 196**,** 1461-71.

Gratchev, A., Kzhyshkowska, J., Kannookadan, S., Ochsenreiter, M., Popova, A., Yu, X., Mamidi, S., Stonehouse-Usselmann, E., Muller-Molinet, I., Gooi, L. & Goerdt, S. 2008. Activation of a TGF-beta-specific multistep gene expression program in mature macrophages requires glucocorticoid-mediated surface expression of TGF-beta receptor II. *J Immunol,* 180**,** 6553-65.

Grimsey, N. J., Aguilar, B., Smith, T. H., Le, P., Soohoo, A. L., Puthenveedu, M. A., Nizet, V. & Trejo, J. 2015. Ubiquitin plays an atypical role in GPCR-induced p38 MAP kinase activation on endosomes. *J Cell Biol,* 210**,** 1117-31.

Grisham, M. B., Johnson, G. G. & Lancaster, J. R., Jr. 1996. Quantitation of nitrate and nitrite in extracellular fluids. *Methods Enzymol,* 268**,** 237-46.

Groschl, B., Bettstetter, M., Giedl, C., Woenckhaus, M., Edmonston, T., Hofstadter, F. & Dietmaier, W. 2013. Expression of the MAP kinase phosphatase DUSP4 is associated with microsatellite instability in colorectal cancer (CRC) and causes increased cell proliferation. *Int J Cancer,* 132**,** 1537-46.

Guabiraba, R., Garrido, D., Bailleul, G., Trotereau, A., Pinaud, M., Lalmanach, A. C., Chanteloup, N. K. & Schouler, C. 2017. Unveiling the participation of avian kinin ornithokinin and its receptors in the chicken inflammatory response. *Vet Immunol Immunopathol,* 188**,** 34-47.

Guak, H., Al Habyan, S., Ma, E. H., Aldossary, H., Al-Masri, M., Won, S. Y., Ying, T., Fixman, E. D., Jones, R. G., Mccaffrey, L. M. & Krawczyk, C. M. 2018. Glycolytic metabolism is essential for CCR7 oligomerization and dendritic cell migration. *Nat Commun,* 9**,** 2463.

Guan, K. L. & Butch, E. 1995. Isolation and characterization of a novel dual specific phosphatase, HVH2, which selectively dephosphorylates the mitogen-activated protein kinase. *J. Biol. Chem.,* 270**,** 7197-7203.

Guilliams, M., Ginhoux, F., Jakubzick, C., Naik, S. H., Onai, N., Schraml, B. U., Segura, E., Tussiwand, R. & Yona, S. 2014. Dendritic cells, monocytes and macrophages: a unified nomenclature based on ontogeny. *Nat Rev Immunol,* 14**,** 571-8.

Guo, F., He, H., Fu, Z. C., Huang, S., Chen, T., Papasian, C. J., Morse, L. R., Xu, Y., Battaglino, R. A., Yang, X. F., Jiang, Z., Xin, H. B. & Fu, M. 2015. Adipocyte-derived PAMM suppresses macrophage inflammation by inhibiting MAPK signalling. *Biochem J,* 472**,** 309-18.

Guo, J., Qiu, X., Zhang, L. & Wei, R. 2018. Smurf1 regulates macrophage proliferation, apoptosis and migration via JNK and p38 MAPK signaling pathways. *Mol Immunol,* 97**,** 20-26.

Gupta, S., Barrett, T., Whitmarsh, A. J., Cavanagh, J., Sluss, H. K., Derijard, B. & Davis, R. J. 1996. Selective interaction of JNK protein kinase isoforms with transcription factors. *Embo j,* 15**,** 2760-70.

Guzman-Beltran, S., Perez-Torres, A., Coronel-Cruz, C. & Torres-Guerrero, H. 2012. Phagocytic receptors on macrophages distinguish between different Sporothrix schenckii morphotypes. *Microbes Infect,* 14**,** 1093-101.

Hall, A. 1998. Rho GTPases and the actin cytoskeleton. *Science,* 279**,** 509-14.

Hallgren, J. & Gurish, M. F. 2011. Mast cell progenitor trafficking and maturation. *Adv Exp Med Biol,* 716**,** 14-28.

Hara-Chikuma, M. & Verkman, A. S. 2006. Aquaporin-1 facilitates epithelial cell migration in kidney proximal tubule. *J Am Soc Nephrol,* 17**,** 39-45.

Hardison, S. E. & Brown, G. D. 2012. C-type lectin receptors orchestrate antifungal immunity. *Nat Immunol,* 13**,** 817-22.

Hart, S. P., Alexander, K. M. & Dransfield, I. 2004. Immune Complexes Bind Preferentially to Fc RIIA (CD32) on Apoptotic Neutrophils, Leading to Augmented Phagocytosis by Macrophages and Release of Proinflammatory Cytokines. *The Journal of Immunology,* 172**,** 1882-1887.

Hashimoto, R., Kakigi, R., Nakamura, K., Itoh, S., Daida, H., Okada, T. & Katoh, Y. 2017. LPS enhances expression of CD204 through the MAPK/ERK pathway in murine bone marrow macrophages. *Atherosclerosis,* 266**,** 167-175.

Hirosumi, J. 2002. A central role for JNK in obesity and insulin resistance. *Nature,* 420**,** 333-336.

Homsy, J. G., Jasper, H., Peralta, X. G., Wu, H., Kiehart, D. P. & Bohmann, D. 2006. JNK signaling coordinates integrin and actin functions during Drosophila embryogenesis. *Dev Dyn,* 235**,** 427-34.

Horinouchi, T., Terada, K., Higashi, T. & Miwa, S. 2013. Endothelin receptor signaling: new insight into its regulatory mechanisms. *J Pharmacol Sci,* 123**,** 85-101.

Howard, C. J., Charleston, B., Stephens, S. A., Sopp, P. & Hope, J. C. 2004. The role of dendritic cells in shaping the immune response. *Anim Health Res Rev,* 5**,** 191-5.

Hsiao, W. Y., Lin, Y. C., Liao, F. H., Chan, Y. C. & Huang, C. Y. 2015. Dual-Specificity Phosphatase 4 Regulates STAT5 Protein Stability and Helper T Cell Polarization. *PLoS One,* 10**,** e0145880.

Hsu, W. C., Yang, F. C., Lin, C. H., Hsieh, S. L. & Chen, N. J. 2014. C5L2 is required for C5a-triggered receptor internalization and ERK signaling. *Cell Signal,* 26**,** 1409-19.

Hu, J. H., Chen, T., Zhuang, Z. H., Kong, L., Yu, M. C., Liu, Y., Zang, J. W. & Ge, B. X. 2007. Feedback control of MKP-1 expression by p38. *Cell Signal,* 19**,** 393-400.

Huang, C., Jacobson, K. & Schaller, M. D. 2004. MAP kinases and cell migration. *J Cell Sci,* 117**,** 4619-28.

Huang, C. Y. & Tan, T. H. 2012. DUSPs, to MAP kinases and beyond. *Cell Biosci,* 2**,** 24.

Huang, S. C., Everts, B., Ivanova, Y., O'sullivan, D., Nascimento, M., Smith, A. M., Beatty, W., Love-Gregory, L., Lam, W. Y., O'neill, C. M., Yan, C., Du, H., Abumrad, N. A., Urban, J. F., Jr., Artyomov, M. N., Pearce, E. L. & Pearce, E. J. 2014. Cell-intrinsic lysosomal lipolysis is essential for alternative activation of macrophages. *Nat Immunol,* 15**,** 846-55.

Huynh, J., Kwa, M. Q., Cook, A. D., Hamilton, J. A. & Scholz, G. M. 2012. CSF-1 receptor signalling from endosomes mediates the sustained activation of Erk1/2 and Akt in macrophages. *Cell Signal,* 24**,** 1753-61.

Ingersoll, M. A., Platt, A. M., Potteaux, S. & Randolph, G. J. 2011. Monocyte trafficking in acute and chronic inflammation. *Trends Immunol,* 32**,** 470-7.

Ip, W. K., Sokolovska, A., Charriere, G. M., Boyer, L., Dejardin, S., Cappillino, M. P., Yantosca, L. M., Takahashi, K., Moore, K. J., Lacy-Hulbert, A. & Stuart, L. M. 2010. Phagocytosis and phagosome acidification are required for pathogen processing and MyD88-dependent responses to Staphylococcus aureus. *J Immunol,* 184**,** 7071-81.

Italiani, P. a. B., Diana 2017. Development and functional differentiation of tissue - resident versus monocyte - derived macrophages in inflammatory reaction. *In:* KLOC, M. (ed.) *Macrophages: Origin, Functions and Biointervention*

Springer International Publishing.

Ivashkiv, L. B. 2011. Inflammatory signaling in macrophages: transitions from acute to tolerant and alternative activation states. *Eur J Immunol,* 41**,** 2477-81.

Jamur, M. C. & Oliver, C. 2011. Origin, maturation and recruitment of mast cell precursors. *Front Biosci (Schol Ed),* 3**,** 1390-406.

Janeway, C. A., Jr. 2001. How the immune system works to protect the host from infection: a personal view. *Proc Natl Acad Sci U S A,* 98**,** 7461-8.

Jeffrey, K. L. 2006. Positive regulation of immune cell function and inflammatory responses by phosphatase PAC-1. *Nature Immunol.,* 7**,** 274-283.

Jenkins, S. J., Ruckerl, D., Cook, P. C., Jones, L. H., Finkelman, F. D., Van Rooijen, N., Macdonald, A. S. & Allen, J. E. 2011. Local macrophage proliferation, rather than recruitment from the blood, is a signature of TH2 inflammation. *Science,* 332**,** 1284-8.

Jiang, J. X., Zhang, S. J., Xiong, Y. K., Jia, Y. L., Sun, Y. H., Lin, X. X., Shen, H. J., Xie, Q. M. & Yan, X. F. 2015. EETs Attenuate Ox-LDL-Induced LTB4 Production and Activity by Inhibiting p38 MAPK Phosphorylation and 5-LO/BLT1 Receptor Expression in Rat Pulmonary Arterial Endothelial Cells. *PLoS One,* 10**,** e0128278.

Jiang, K., Zhong, B., Gilvary, D. L., Corliss, B. C., Vivier, E., Hong-Geller, E., Wei, S. & Djeu, J. Y. 2002. Syk regulation of phosphoinositide 3-kinase-dependent NK cell function. *J Immunol,* 168**,** 3155-64.

Jiao, H., Tang, P. & Zhang, Y. 2015. MAP kinase phosphatase 2 regulates macrophage-adipocyte interaction. *PLoS One,* 10**,** e0120755.

Jiao, H. & Zhang, Y. 2014. MAP kinase phosphatase 2 (MKP-2) regulates the innate immune response to influenza infection (INM8P.436). *The Journal of Immunology,* 192**,** 124.2.

Jin, X., Liu, L., Zhang, Y., Xiang, Y., Yin, G., Lu, Y., Shi, L., Dong, J. & Shen, C. 2018. Advanced Glycation End Products Enhance Murine Monocyte Proliferation in Bone Marrow and Prime Them into an Inflammatory Phenotype through MAPK Signaling. *J Diabetes Res,* 2018**,** 2527406.

Johnson, G. L. & Lapadat, R. 2002. Mitogen-activated protein kinase pathways mediated by ERK, JNK, and p38 protein kinases. *Science,* 298**,** 1911-2.

Johnson, G. L. & Nakamura, K. 2007. The c-jun kinase/stress-activated pathway: regulation, function and role in human disease. *Biochim Biophys Acta,* 1773**,** 1341-8.

Jones, G. E. 2000. Cellular signaling in macrophage migration and chemotaxis. *J Leukoc Biol,* 68**,** 593-602.

Jonsson, A. H. & Yokoyama, W. M. 2009. Natural killer cell tolerance licensing and other mechanisms. *Adv Immunol,* 101**,** 27-79.

Jutras, I. & Desjardins, M. 2005. Phagocytosis: at the crossroads of innate and adaptive immunity. *Annu Rev Cell Dev Biol,* 21**,** 511-27.

Karp, G. 2013. *Cell and Molecular Biology Concepts and Experiments* United States of America, John Wiley and Sons.

Katz, M., Amit, I. & Yarden, Y. 2007. Regulation of MAPKs by growth factors and receptor tyrosine kinases. *Biochim Biophys Acta,* 1773**,** 1161-76.

Keesler, G. A., Bray, J., Hunt, J., Johnson, D. A., Gleason, T., Yao, Z., Wang, S. W., Parker, C., Yamane, H., Cole, C. & Lichenstein, H. S. 1998. Purification and activation of recombinant p38 isoforms alpha, beta, gamma, and delta. *Protein Expr Purif,* 14**,** 221-8.

Kelly, B. & O'neill, L. A. 2015. Metabolic reprogramming in macrophages and dendritic cells in innate immunity. *Cell Res,* 25**,** 771-84.

Keyse, S. M. 2000. Protein phosphatases and the regulation of mitogen-activated protein kinase signalling. *Curr. Opin. Cell Biol.,* 12**,** 186-192.

Kidger, A. M. & Keyse, S. M. 2016. The regulation of oncogenic Ras/ERK signalling by dual-specificity mitogen activated protein kinase phosphatases (MKPs). *Semin Cell Dev Biol,* 50**,** 125-32.

Kim, D. & Haynes, C. L. 2013. The role of p38 MAPK in neutrophil functions: single cell chemotaxis and surface marker expression. *Analyst,* 138**,** 6826-33.

Kim, E. K. & Choi, E. J. 2015. Compromised MAPK signaling in human diseases: an update. *Arch Toxicol,* 89**,** 867-82.

Kim, H. S. & Asmis, R. 2017. Mitogen-activated protein kinase phosphatase 1 (MKP-1) in macrophage biology and cardiovascular disease. A redox-regulated master controller of monocyte function and macrophage phenotype. *Free Radic Biol Med,* 109**,** 75-83.

Kim, H. S., Tavakoli, S., Piefer, L. A., Nguyen, H. N. & Asmis, R. 2016. Monocytic MKP-1 is a Sensor of the Metabolic Environment and Regulates Function and Phenotypic Fate of Monocyte-Derived Macrophages in Atherosclerosis. *Sci Rep,* 6**,** 34223.

Kim, K. H., An, D. R., Song, J., Yoon, J. Y., Kim, H. S., Yoon, H. J., Im, H. N., Kim, J., Kim, D. J., Lee, S. J., Kim, K. H., Lee, H. M., Kim, H. J., Jo, E. K., Lee, J. Y. & Suh, S. W. 2012. Mycobacterium tuberculosis Eis protein initiates suppression of host immune responses by acetylation of DUSP16/MKP-7. *Proc Natl Acad Sci U S A,* 109**,** 7729-34.

Kim, S. R., Xu, H., Lesmana, A., Kuzmanovic, U., Au, M., Florencia, C., Oh, E. J., Zhang, G., Kim, K. H. & Jin, Y. S. 2015. Deletion of PHO13, encoding haloacid dehalogenase type IIA phosphatase, results in upregulation of the pentose phosphate pathway in Saccharomyces cerevisiae. *Appl Environ Microbiol,* 81**,** 1601-9.

Kinne, R. W., Brauer, R., Stuhlmuller, B., Palombo-Kinne, E. & Burmester, G. R. 2000. Macrophages in rheumatoid arthritis. *Arthritis Res,* 2**,** 189-202.

Kitanaka, T., Nakano, R., Kitanaka, N., Kimura, T., Okabayashi, K., Narita, T. & Sugiya, H. 2017. JNK activation is essential for activation of MEK/ERK signaling in IL-1beta-induced COX-2 expression in synovial fibroblasts. *Sci Rep,* 7**,** 39914.

Koh, T. J. & Dipietro, L. A. 2011. Inflammation and wound healing: the role of the macrophage. *Expert Rev Mol Med,* 13**,** e23.

Kondo, M. 2010. Lymphoid and myeloid lineage commitment in multipotent hematopoietic progenitors. *Immunol Rev,* 238**,** 37-46.

Kondoh, K. & Nishida, E. 2007. Regulation of MAP kinases by MAP kinase phosphatases. *Biochim Biophys Acta,* 1773**,** 1227-37.

Kruger, P., Saffarzadeh, M., Weber, A. N., Rieber, N., Radsak, M., Von Bernuth, H., Benarafa, C., Roos, D., Skokowa, J. & Hartl, D. 2015. Neutrophils: Between

host defence, immune modulation, and tissue injury. *PLoS Pathog,* 11**,** e1004651.

Kuiper, J. W., Van Horssen, R., Oerlemans, F., Peters, W., Van Dommelen, M. M., Te Lindert, M. M., Ten Hagen, T. L., Janssen, E., Fransen, J. A. & Wieringa, B. 2009. Local ATP generation by brain-type creatine kinase (CK-B) facilitates cell motility. *PLoS One,* 4**,** e5030.

Kumar, S. & Jack, R. 2006. Origin of monocytes and their differentiation to macrophages and dendritic cells. *J Endotoxin Res,* 12**,** 278-84.

Kurihara, R., Yamaoka, K., Sawamukai, N., Shimajiri, S., Oshita, K., Yukawa, S., Tokunaga, M., Iwata, S., Saito, K., Chiba, K. & Tanaka, Y. 2010. C5a promotes migration, proliferation, and vessel formation in endothelial cells. *Inflamm Res,* 59**,** 659-66.

Kurokawa, K., Itoh, R. E., Yoshizaki, H., Nakamura, Y. O. & Matsuda, M. 2004. Coactivation of Rac1 and Cdc42 at lamellipodia and membrane ruffles induced by epidermal growth factor. *Mol Biol Cell,* 15**,** 1003-10.

Kurosaki, T. 2010. B-lymphocyte biology. *Immunol Rev,* 237**,** 5-9.

Labonte, J., Brochu, I., Simard, E. & D'orleans-Juste, P. 2008. Distinct modulation of the endothelin-1 pathway in iNOS-/- and eNOS-/- mice. *Can J Physiol Pharmacol,* 86**,** 516-25.

Lamprou, I., Mamali, I., Dallas, K., Fertakis, V., Lampropoulou, M. & Marmaras, V. J. 2007. Distinct signalling pathways promote phagocytosis of bacteria, latex beads and lipopolysaccharide in medfly haemocytes. *Immunology,* 121**,** 314-27.

Lancaster, G. I., Kraakman, M. J., Kammoun, H. L., Langley, K. G., Estevez, E., Banerjee, A., Grumont, R. J., Febbraio, M. A. & Gerondakis, S. 2014. The dual-specificity phosphatase 2 (DUSP2) does not regulate obesity-associated inflammation or insulin resistance in mice. *PLoS One,* 9**,** e111524.

Lawan, A., Al-Harthi, S., Cadalbert, L., Mccluskey, A. G., Shweash, M., Grassia, G., Grant, A., Boyd, M., Currie, S. & Plevin, R. 2011. Deletion of the dual specific phosphatase-4 (DUSP-4) gene reveals an essential non-redundant role for MAP kinase phosphatase-2 (MKP-2) in proliferation and cell survival. *J Biol Chem,* 286**,** 12933-43.

Lawan, A., Torrance, E., Al-Harthi, S., Shweash, M., Alnasser, S., Neamatallah, T., Schroeder, J. & Plevin, R. 2012. MKP-2: out of the DUSP-bin and back into the limelight. *Biochem Soc Trans,* 40**,** 235-9.

Lawrence, T. & Natoli, G. 2011. Transcriptional regulation of macrophage polarization: enabling diversity with identity. *Nat Rev Immunol,* 11**,** 750-61.

Le Page, C., Genin, P., Baines, M. G. & Hiscott, J. 2000. Interferon activation and innate immunity. *Rev Immunogenet,* 2**,** 374-86.

Lee, J., Hun Yun, J., Lee, J., Choi, C. & Hoon Kim, J. 2015. Blockade of dual-specificity phosphatase 28 decreases chemo-resistance and migration in human pancreatic cancer cells. *Sci Rep,* 5**,** 12296.

Lee, J., Tam, H., Adler, L., Ilstad-Minnihan, A., Macaubas, C. & Mellins, E. D. 2017. The MHC class II antigen presentation pathway in human monocytes differs by subset and is regulated by cytokines. *PLoS One,* 12**,** e0183594.

Letourneux, C., Rocher, G. & Porteu, F. 2006. B56-containing PP2A dephosphorylate ERK and their activity is controlled by the early gene IEX-1 and ERK. *Embo j,* 25**,** 727-38.

Littlewood-Evans, A., Sarret, S., Apfel, V., Loesle, P., Dawson, J., Zhang, J., Muller, A., Tigani, B., Kneuer, R., Patel, S., Valeaux, S., Gommermann, N., Rubic-Schneider, T., Junt, T. & Carballido, J. M. 2016. GPR91 senses extracellular succinate released from inflammatory macrophages and exacerbates rheumatoid arthritis. *J Exp Med,* 213**,** 1655-62.

Liu, X., Ma, B., Malik, A. B., Tang, H., Yang, T., Sun, B., Wang, G., Minshall, R. D., Li, Y., Zhao, Y., Ye, R. D. & Xu, J. 2012. Bidirectional regulation of neutrophil migration by mitogen-activated protein kinases. *Nat Immunol,* 13**,** 457-64.

Liu, Y., Shepherd, E. G. & Nelin, L. D. 2007. MAPK phosphatases [mdash] regulating the immune response. *Nat Rev Immunol,* 7**,** 202-212.

Liu, Z. M., Zhu, S. M., Qin, X. J., Cheng, Z. D., Liu, M. Y., Zhang, H. M. & Liu, D. X. 2010. Silencing of C5a receptor gene with siRNA for protection from Gram-negative bacterial lipopolysaccharide-induced vascular permeability. *Mol Immunol,* 47**,** 1325-33.

Livak, K. J. & Schmittgen, T. D. 2001. Analysis of relative gene expression data using real-time quantitative PCR and the 2(-Delta Delta C(T)) Method. *Methods,* 25**,** 402-8.

Lloberas, J., Valverde-Estrella, L., Tur, J., Vico, T. & Celada, A. 2016. Mitogen-Activated Protein Kinases and Mitogen Kinase Phosphatase 1: A Critical Interplay in Macrophage Biology. *Front Mol Biosci,* 3**,** 28.

Lu, W., Wang, L., Yao, J., Wang, W. & Chen, Y. 2018. Inhibition of C5a prevents IL-1beta-induced alternations in rat synoviocytes in vitro. *Mol Cell Probes.*

Lue, H., Kapurniotu, A., Fingerle-Rowson, G., Roger, T., Leng, L., Thiele, M., Calandra, T., Bucala, R. & Bernhagen, J. 2006. Rapid and transient activation of the ERK MAPK signalling pathway by macrophage migration inhibitory factor (MIF) and dependence on JAB1/CSN5 and Src kinase activity. *Cell Signal,* 18**,** 688-703.

Lulai, E. C., Neubauer, J. D., Olson, L. L. & Suttle, J. C. 2015. Wounding induces changes in tuber polyamine content, polyamine metabolic gene expression, and enzyme activity during closing layer formation and initiation of wound periderm formation. *J Plant Physiol,* 176**,** 89-95.

Ma, Y. & Pope, R. M. 2005. The role of macrophages in rheumatoid arthritis. *Curr Pharm Des,* 11**,** 569-80.

Mao, Y. & Finnemann, S. C. 2015. Regulation of phagocytosis by Rho GTPases. *Small GTPases,* 6**,** 89-99.

Marchetti, P., Trinh, A., Khamari, R. & Kluza, J. 2018. Melanoma metabolism contributes to the cellular responses to MAPK/ERK pathway inhibitors. *Biochim Biophys Acta,* 1862**,** 999-1005.

Marshall, C. J. 1994. MAP kinase kinase kinase, MAP kinase kinase and MAP kinase. *Curr Opin Genet Dev,* 4**,** 82-9.

Martin-Blanco, E., Pastor-Pareja, J. C. & Garcia-Bellido, A. 2000. JNK and decapentaplegic signaling control adhesiveness and cytoskeleton dynamics during thorax closure in Drosophila. *Proc Natl Acad Sci U S A,* 97**,** 7888-93.

Martin-Lorenzo, M., Zubiri, I., Maroto, A. S., Gonzalez-Calero, L., Posada-Ayala, M., De La Cuesta, F., Mourino-Alvarez, L., Lopez-Almodovar, L. F., Calvo-Bonacho, E., Ruilope, L. M., Padial, L. R., Barderas, M. G., Vivanco, F. & Alvarez-Llamas, G. 2015. KLK1 and ZG16B proteins and arginine-proline metabolism identified as novel targets to monitor atherosclerosis, acute coronary syndrome and recovery. *Metabolomics,* 11**,** 1056-1067.

Martinez, F. O. & Gordon, S. 2014. The M1 and M2 paradigm of macrophage activation: time for reassessment. *F1000Prime Rep,* 6**,** 13.

Masuda, K., Shima, H., Watanabe, M. & Kikuchi, K. 2001. MKP-7, a novel mitogen-activated protein kinase phosphatase, functions as a shuttle protein. *J Biol Chem,* 276**,** 39002-11.

Matsuno, R., Aramaki, Y., Arima, H., Adachi, Y., Ohno, N., Yadomae, T. & Tsuchiya, S. 1998. Contribution of CR3 to nitric oxide production from macrophages stimulated with high-dose of LPS. *Biochem Biophys Res Commun,* 244**,** 115-9.

Mccormick, S. M. & Heller, N. M. 2015. Commentary: IL-4 and IL-13 receptors and signaling. *Cytokine,* 75**,** 38-50.

Mckenna, S., Gossling, M., Bugarini, A., Hill, E., Anderson, A. L., Rancourt, R. C., Balasubramaniyan, N., El Kasmi, K. C. & Wright, C. J. 2015. Endotoxemia Induces IkappaBbeta/NF-kappaB-Dependent Endothelin-1 Expression in Hepatic Macrophages. *J Immunol,* 195**,** 3866-79.

Medzhitov, R., Preston-Hurlburt, P. & Janeway, C. A., Jr. 1997. A human homologue of the Drosophila Toll protein signals activation of adaptive immunity. *Nature,* 388**,** 394-7.

Mellman, I. & Steinman, R. M. 2001. Dendritic cells: specialized and regulated antigen processing machines. *Cell,* 106**,** 255-8.

Mendoza, M. C., Vilela, M., Juarez, J. E., Blenis, J. & Danuser, G. 2015. ERK reinforces actin polymerization to power persistent edge protrusion during motility. *Sci Signal,* 8**,** ra47.

Meng, A., Zhang, X. & Shi, Y. 2014. Role of p38 MAPK and STAT3 in lipopolysaccharide-stimulated mouse alveolar macrophages. *Exp Ther Med,* 8**,** 1772-1776.

Meng, F. & Lowell, C. A. 1997. Lipopolysaccharide (LPS)-induced macrophage activation and signal transduction in the absence of Src-family kinases Hck, Fgr, and Lyn. *J Exp Med,* 185**,** 1661-70.

Mengistu, M., Brotzman, H., Ghadiali, S. & Lowe-Krentz, L. 2011. Fluid shear stress-induced JNK activity leads to actin remodeling for cell alignment. *J Cell Physiol,* 226**,** 110-21.

Michelucci, A., Cordes, T., Ghelfi, J., Pailot, A., Reiling, N., Goldmann, O., Binz, T., Wegner, A., Tallam, A., Rausell, A., Buttini, M., Linster, C. L., Medina, E., Balling, R. & Hiller, K. 2013. Immune-responsive gene 1 protein links metabolism to immunity by catalyzing itaconic acid production. *Proc Natl Acad Sci U S A,* 110**,** 7820-5.

Mills, J. C., Lee, V. M. & Pittman, R. N. 1998. Activation of a PP2A-like phosphatase and dephosphorylation of tau protein characterize onset of the execution phase of apoptosis. *J Cell Sci,* 111 (Pt 5)**,** 625-36.

Misra-Press, A., Rim, C. S., Yao, H., Roberson, M. S. & Stork, P. J. 1995. A novel mitogen-activated protein kinase phosphatase. Structure, expression, and regulation. *J Biol Chem,* 270**,** 14587-96.

Moriwaki, K. & Asahi, M. 2017. Augmented TME O-GlcNAcylation Promotes Tumor Proliferation through the Inhibition of p38 MAPK. *Mol Cancer Res,* 15**,** 1287-1298.

Morrison, D. K. 2012. MAP kinase pathways. *Cold Spring Harb Perspect Biol,* 4.

Mosser, D. M. & Edwards, J. P. 2008. Exploring the full spectrum of macrophage activation. *Nat Rev Immunol,* 8**,** 958-69.

Mosser, D. M. & Zhang, X. 2011. Measuring opsonic phagocytosis via Fcgamma receptors and complement receptors on macrophages. *Curr Protoc Immunol,* Chapter 14**,** Unit 14 27.

Muller, W. A. 2001. New mechanisms and pathways for monocyte recruitment. *J Exp Med,* 194**,** F47-51.

Murray, P. J. & Wynn, T. A. 2011. Protective and pathogenic functions of macrophage subsets. *Nat Rev Immunol,* 11**,** 723-37.

Na, Y. R., Je, S. & Seok, S. H. 2018. Metabolic features of macrophages in inflammatory diseases and cancer. *Cancer Lett,* 413**,** 46-58.

Naor, Z., Benard, O. & Seger, R. 2000. Activation of MAPK cascades by G-protein-coupled receptors: the case of gonadotropin-releasing hormone receptor. *Trends Endocrinol Metab,* 11**,** 91-9.

Nathan, C. 2002. Points of control in inflammation. *Nature,* 420**,** 846-52.

Nawaz, A., Aminuddin, A., Kado, T., Takikawa, A., Yamamoto, S., Tsuneyama, K., Igarashi, Y., Ikutani, M., Nishida, Y., Nagai, Y., Takatsu, K., Imura, J., Sasahara, M., Okazaki, Y., Ueki, K., Okamura, T., Tokuyama, K., Ando, A., Matsumoto, M., Mori, H., Nakagawa, T., Kobayashi, N., Saeki, K., Usui, I., Fujisaka, S. & Tobe, K. 2017. CD206(+) M2-like macrophages regulate systemic glucose metabolism by inhibiting proliferation of adipocyte progenitors. *Nat Commun,* 8**,** 286.

Neamatallah, T. A. 2014. *The role of mitogen-activated protein kinase phosphatase - 2 (MKP-2) in macrophage development and gene expression.* Doctor of philosophy, University of Strathclyde.

Newling, M., Hoepel, W., Vogelpoel, L. T. C., Heineke, M. H., Van Burgsteden, J. A., Taanman-Kueter, E. W. M., Eggink, D., Kuijpers, T. W., Beaumont, T., Van Egmond, M., Kapsenberg, M. L., Baeten, D. L. P., Den Dunnen, J. & De Jong, E. C. 2018. Fc gamma receptor IIa suppresses type I and III interferon production by human myeloid immune cells. *Eur J Immunol.*

Nick, J. A., Avdi, N. J., Young, S. K., Lehman, L. A., Mcdonald, P. P., Frasch, S. C., Billstrom, M. A., Henson, P. M., Johnson, G. L. & Worthen, G. S. 1999. Selective activation and functional significance of p38alpha mitogen-activated protein kinase in lipopolysaccharide-stimulated neutrophils. *J Clin Invest,* 103**,** 851-8.

Niedergang, F. & Chavrier, P. 2005. Regulation of phagocytosis by Rho GTPases. *Curr Top Microbiol Immunol,* 291**,** 43-60.

Niedzielska, M., Bodendorfer, B., Munch, S., Eichner, A., Derigs, M., Da Costa, O., Schweizer, A., Neff, F., Nitschke, L., Sparwasser, T., Keyse, S. M. & Lang, R. 2014. Gene trap mice reveal an essential function of dual specificity phosphatase Dusp16/MKP-7 in perinatal survival and regulation of Toll-like receptor (TLR)-induced cytokine production. *J Biol Chem,* 289**,** 2112-26.

Nieminen, R., Lahti, A., Jalonen, U., Kankaanranta, H. & Moilanen, E. 2006. JNK inhibitor SP600125 reduces COX-2 expression by attenuating mRNA in activated murine J774 macrophages. *Int Immunopharmacol,* 6**,** 987-96.

Ninkovic, J. 2011. *Morphin Inhibition of macrophage phagocytosis and bactericidal functions.* Doctor of Philosophy PhD, University of Minnesota.

Ogata, S., Kubota, Y., Yamashiro, T., Takeuchi, H., Ninomiya, T., Suyama, Y. & Shirasuna, K. 2007. Signaling pathways regulating IL-1alpha-induced COX-2 expression. *J Dent Res,* 86**,** 186-91.

Okazawa, H. & Estus, S. 2002. The JNK/c-Jun cascade and Alzheimer's disease. *Am J Alzheimers Dis Other Demen,* 17**,** 79-88.

Orr, M. T. & Lanier, L. L. 2010. Natural Killer Cell Education and Tolerance. *Cell,* 142**,** 847-856.

Ozinsky, A., Smith, K. D., Hume, D. & Underhill, D. M. 2000. Co-operative induction of pro-inflammatory signaling by Toll-like receptors. *J Endotoxin Res,* 6**,** 393-6.

Pages, G., Guerin, S., Grall, D., Bonino, F., Smith, A., Anjuere, F., Auberger, P. & Pouyssegur, J. 1999. Defective thymocyte maturation in p44 MAP kinase (Erk 1) knockout mice. *Science,* 286**,** 1374-7.

Palsson-Mcdermott, E. M. & O'neill, L. A. 2004. Signal transduction by the lipopolysaccharide receptor, Toll-like receptor-4. *Immunology,* 113**,** 153-62.

Park, S. A., Kim, E. H., Na, H. K. & Surh, Y. J. 2007. KG-135 inhibits COX-2 expression by blocking the activation of JNK and AP-1 in phorbol ester-stimulated human breast epithelial cells. *Ann N Y Acad Sci,* 1095**,** 545-53.

Parri, M. & Chiarugi, P. 2010. Rac and Rho GTPases in cancer cell motility control. *Cell Commun Signal,* 8**,** 23.

Parsa, K. V., Butchar, J. P., Rajaram, M. V., Cremer, T. J. & Tridandapani, S. 2008. The tyrosine kinase Syk promotes phagocytosis of Francisella through the activation of Erk. *Mol Immunol,* 45**,** 3012-21.

Parveen, S., Chowdhury, A. R., Jawed, J. J., Majumdar, S. B., Saha, B. & Majumdar, S. 2018. Immunomodulation of dual specificity phosphatase 4 during visceral leishmaniasis. *Microbes Infect,* 20**,** 111-121.

Passlick, B., Flieger, D. & Ziegler-Heitbrock, H. W. 1989. Identification and characterization of a novel monocyte subpopulation in human peripheral blood. *Blood,* 74**,** 2527-34.

Patterson, K. I., Brummer, T., O'brien, P. M. & Daly, R. J. 2009. Dual-specificity phosphatases: critical regulators with diverse cellular targets. *Biochem J,* 418**,** 475-89.

Pavlou, S., Wang, L., Xu, H. & Chen, M. 2017. Higher phagocytic activity of thioglycollate-elicited peritoneal macrophages is related to metabolic status of the cells. *J Inflamm (Lond),* 14**,** 4.

Peters-Golden, M. 2009. Putting on the brakes: cyclic AMP as a multipronged controller of macrophage function. *Sci Signal,* 2**,** pe37.

Petit, I., Jin, D. & Rafii, S. 2007. The SDF-1-CXCR4 signaling pathway: a molecular hub modulating neo-angiogenesis. *Trends Immunol,* 28**,** 299-307.

Pimienta, G. & Pascual, J. 2007. Canonical and alternative MAPK signaling. *Cell Cycle,* 6**,** 2628-32.

Pixley, F. J. 2012. Macrophage Migration and Its Regulation by CSF-1. *Int J Cell Biol,* 2012**,** 501962.

Platko, K., Lebeau, P. & Austin, R. C. 2018. MAPping the kinase landscape of macrophage activation. *J Biol Chem,* 293**,** 9910-9911.

Pluskal, T., Castillo, S., Villar-Briones, A. & Oresic, M. 2010. MZmine 2: modular framework for processing, visualizing, and analyzing mass spectrometry-based molecular profile data. *BMC Bioinformatics,* 11**,** 395.

Qian, B. Z. & Pollard, J. W. 2010. Macrophage diversity enhances tumor progression and metastasis. *Cell,* 141**,** 39-51.

Quehenberger, P., Bierhaus, A., Fasching, P., Muellner, C., Klevesath, M., Hong, M., Stier, G., Sattler, M., Schleicher, E., Speiser, W. & Nawroth, P. P. 2000. Endothelin 1 transcription is controlled by nuclear factor-kappaB in AGE-stimulated cultured endothelial cells. *Diabetes,* 49**,** 1561-70.

Quinn, M. T., Ammons, M. C. & Deleo, F. R. 2006. The expanding role of NADPH oxidases in health and disease: no longer just agents of death and destruction. *Clin Sci (Lond),* 111**,** 1-20.

Rao, K. M., Meighan, T. & Bowman, L. 2002. Role of mitogen-activated protein kinase activation in the production of inflammatory mediators: differences between primary rat alveolar macrophages and macrophage cell lines. *J Toxicol Environ Health A,* 65**,** 757-68.

Rapoport, R. M. 2014. Acute nitric oxide synthase inhibition and endothelin-1-dependent arterial pressure elevation. *Front Pharmacol,* 5**,** 57.

Rattigan, K. M., Pountain, A. W., Regnault, C., Achcar, F., Vincent, I. M., Goodyear, C. S. & Barrett, M. P. 2018. Metabolomic profiling of macrophages determines the discrete metabolomic signature and metabolomic interactome triggered by polarising immune stimuli. *PLoS One,* 13**,** e0194126.

Ravetch, J. V. 1997. Fc receptors. *Curr Opin Immunol,* 9**,** 121-5.

Rennefahrt, U. E., Illert, B., Kerkhoff, E., Troppmair, J. & Rapp, U. R. 2002. Constitutive JNK activation in NIH 3T3 fibroblasts induces a partially transformed phenotype. *J Biol Chem,* 277**,** 29510-8.

Rhoads, J. M. 2004. Arginine stimulates intestinal cell migration through a focal adhesion kinase dependent mechanism. *Gut,* 53**,** 514-522.

Riedemann, N. C., Guo, R. F., Hollmann, T. J., Gao, H., Neff, T. A., Reuben, J. S., Speyer, C. L., Sarma, J. V., Wetsel, R. A., Zetoune, F. S. & Ward, P. A. 2004. Regulatory role of C5a in LPS-induced IL-6 production by neutrophils during sepsis. *FASEB J,* 18**,** 370-2.

Rizzetto, L., De Filippo, C., Rivero, D., Riccadonna, S., Beltrame, L. & Cavalieri, D. 2013. Systems biology of host-mycobiota interactions: dissecting Dectin-1 and Dectin-2 signalling in immune cells with DC-ATLAS. *Immunobiology,* 218**,** 1428-37.

Rodriguez-Prados, J. C., Traves, P. G., Cuenca, J., Rico, D., Aragones, J., Martin-Sanz, P., Cascante, M. & Bosca, L. 2010. Substrate fate in activated macrophages: a comparison between innate, classic, and alternative activation. *J Immunol,* 185**,** 605-14.

Rodriguez, P. C., Ochoa, A. C. & Al-Khami, A. A. 2017. Arginine Metabolism in Myeloid Cells Shapes Innate and Adaptive Immunity. *Front Immunol,* 8**,** 93.

Roger, T., David, J., Glauser, M. P. & Calandra, T. 2001. MIF regulates innate immune responses through modulation of Toll-like receptor 4. *Nature,* 414**,** 920-4.

Rohan, P. J., Davis, P., Moskaluk, C. A., Kearns, M., Krutzsch, H., Siebenlist, U. & Kelly, K. 1993. PAC-1: a mitogen-induced nuclear protein tyrosine phosphatase. *Science,* 259**,** 1763-6.

Romano, A., Carneiro, M. B. H., Doria, N. A., Roma, E. H., Ribeiro-Gomes, F. L., Inbar, E., Lee, S. H., Mendez, J., Paun, A., Sacks, D. L. & Peters, N. C. 2017. Divergent roles for Ly6C+CCR2+CX3CR1+ inflammatory monocytes during primary or secondary infection of the skin with the intra-phagosomal pathogen Leishmania major. *PLoS Pathog,* 13**,** e1006479.

Rosa, S. I., Rios-Santos, F., Balogun, S. O. & Martins, D. T. 2016. Vitexin reduces neutrophil migration to inflammatory focus by down-regulating pro-inflammatory mediators via inhibition of p38, ERK1/2 and JNK pathway. *Phytomedicine,* 23**,** 9-17.

Rougerie, P., Miskolci, V. & Cox, D. 2013. Generation of membrane structures during phagocytosis and chemotaxis of macrophages: role and regulation of the actin cytoskeleton. *Immunol Rev,* 256**,** 222-39.

Roux, P. P. & Blenis, J. 2004. ERK and p38 MAPK-activated protein kinases: a family of protein kinases with diverse biological functions. *Microbiol Mol Biol Rev,* 68**,** 320-44.

Rubio, J. M., Rodriguez, J. P., Gil-De-Gomez, L., Guijas, C., Balboa, M. A. & Balsinde, J. 2015. Group V secreted phospholipase A2 is upregulated by IL-4 in human macrophages and mediates phagocytosis via hydrolysis of ethanolamine phospholipids. *J Immunol,* 194**,** 3327-39.

Sahara, N., Murayama, M., Lee, B., Park, J. M., Lagalwar, S., Binder, L. I. & Takashima, A. 2008. Active c-jun N-terminal kinase induces caspase cleavage of tau and additional phosphorylation by GSK-3beta is required for tau aggregation. *Eur J Neurosci,* 27**,** 2897-906.

Salojin, K. V. 2006. Essential role of MAPK phosphatase-1 in the negative control of innate immune responses. *J. Immunol.,* 176**,** 1899.

Sato, K., Yang, X. L., Yudate, T., Chung, J. S., Wu, J., Luby-Phelps, K., Kimberly, R. P., Underhill, D., Cruz, P. D., Jr. & Ariizumi, K. 2006. Dectin-2 is a pattern recognition receptor for fungi that couples with the Fc receptor gamma chain to induce innate immune responses. *J Biol Chem,* 281**,** 38854-66.

Schroeder, J., Mcgachy, H. A., Woods, S., Plevin, R. & Alexander, J. 2013. T cell hypo-responsiveness against Leishmania major in MAP kinase phosphatase (MKP) 2 deficient C57BL/6 mice does not alter the healer disease phenotype. *PLoS Negl Trop Dis,* 7**,** e2064.

Schumann, J. 2016. It is all about fluidity: Fatty acids and macrophage phagocytosis. *Eur J Pharmacol,* 785**,** 18-23.

Sen, R. & Smale, S. T. 2010. Selectivity of the NF-{kappa}B response. *Cold Spring Harb Perspect Biol,* 2**,** a000257.

Seow, V., Lim, J., Iyer, A., Suen, J. Y., Ariffin, J. K., Hohenhaus, D. M., Sweet, M. J. & Fairlie, D. P. 2013. Inflammatory responses induced by lipopolysaccharide are amplified in primary human monocytes but suppressed in macrophages by complement protein C5a. *J Immunol,* 191**,** 4308-16.

Serbina, N. V., Jia, T., Hohl, T. M. & Pamer, E. G. 2008. Monocyte-mediated defense against microbial pathogens. *Annu Rev Immunol,* 26**,** 421-52.

Shearer, J. D., Richards, J. R., Mills, C. D. & Caldwell, M. D. 1997. Differential regulation of macrophage arginine metabolism: a proposed role in wound healing. *Am J Physiol,* 272**,** E181-90.

Shweash, M. 2010. *The Pathological Effects of Leishmania mexicana Infection on Macrophage Cell Signalling and Immune Responses.* Doctor of Philosophy PhD, University of Strathclyde.

Shweash, M., Adrienne Mcgachy, H., Schroeder, J., Neamatallah, T., Bryant, C. E., Millington, O., Mottram, J. C., Alexander, J. & Plevin, R. 2011. Leishmania mexicana promastigotes inhibit macrophage IL-12 production via TLR-4 dependent COX-2, iNOS and arginase-1 expression. *Mol Immunol,* 48**,** 1800-8.

Sikkeland, L. I., Dahl, C. P., Ueland, T., Andreassen, A. K., Gude, E., Edvardsen, T., Holm, T., Yndestad, A., Gullestad, L., Kongerud, J., Aukrust, P. & Oie, E. 2012. Increased levels of inflammatory cytokines and endothelin-1 in alveolar macrophages from patients with chronic heart failure. *PLoS One,* 7**,** e36815.

Simard, F. A., Cloutier, A., Ear, T., Vardhan, H. & Mcdonald, P. P. 2015. MEK-independent ERK activation in human neutrophils and its impact on functional responses. *J Leukoc Biol,* 98**,** 565-73.

Simo-Cheyou, E. R., Vardatsikos, G. & Srivastava, A. K. 2016. Src tyrosine kinase mediates endothelin-1-induced early growth response protein-1 expression via MAP kinase-dependent pathways in vascular smooth muscle cells. *Int J Mol Med,* 38**,** 1879-1886.

Sloss, C. M., Cadalbert, L., Finn, S. G., Fuller, S. J. & Plevin, R. 2005. Disruption of two putative nuclear localization sequences is required for cytosolic localization of mitogen-activated protein kinase phosphatase-2. *Cell Signal,* 17**,** 709-16.

Small, J. V., Stradal, T., Vignal, E. & Rottner, K. 2002. The lamellipodium: where motility begins. *Trends Cell Biol,* 12**,** 112-20.

Sopi, R. B., Zaidi, S. I., Mladenov, M., Sahiti, H., Istrefi, Z., Gjorgoski, I., Lajci, A. & Jakupaj, M. 2012. L-citrulline supplementation reverses the impaired airway relaxation in neonatal rats exposed to hyperoxia. *Respir Res,* 13**,** 68.

Stanciu, M. & Defranco, D. B. 2002. Prolonged nuclear retention of activated extracellular signal-regulated protein kinase promotes cell death generated by oxidative toxicity or proteasome inhibition in a neuronal cell line. *J Biol Chem,* 277**,** 4010-7.

Stein, M., Keshav, S., Harris, N. & Gordon, S. 1992. Interleukin 4 potently enhances murine macrophage mannose receptor activity: a marker of alternative immunologic macrophage activation. *J Exp Med,* 176**,** 287-92.

Steinman, R. M. & Cohn, Z. A. 1973. Identification of a novel cell type in peripheral lymphoid organs of mice. I. Morphology, quantitation, tissue distribution. *J Exp Med,* 137**,** 1142-62.

Stokoe, D., Campbell, D. G., Nakielny, S., Hidaka, H., Leevers, S. J., Marshall, C. & Cohen, P. 1992. MAPKAP kinase-2; a novel protein kinase activated by mitogen-activated protein kinase. *Embo j,* 11**,** 3985-94.

Sturgill, T. W. & Ray, L. B. 1986. Muscle proteins related to microtubule associated protein-2 are substrates for an insulin-stimulatable kinase. *Biochem Biophys Res Commun,* 134**,** 565-71.

Sugiyama, T. & Nagasawa, T. 2015. Myeloid Cells Stimulate Their Progenitors in an Emergency. *Immunity,* 42**,** 13-14.

Sutterwala, F. S., Noel, G. J., Salgame, P. & Mosser, D. M. 1998. Reversal of proinflammatory responses by ligating the macrophage Fcgamma receptor type I. *J Exp Med,* 188**,** 217-22.

Swanson, J. A. & Hoppe, A. D. 2004. The coordination of signaling during Fc receptor-mediated phagocytosis. *J Leukoc Biol,* 76**,** 1093-103.

Swirski, F. K., Hilgendorf, I. & Robbins, C. S. 2014. From proliferation to proliferation: monocyte lineage comes full circle. *Semin Immunopathol,* 36**,** 137-48.

Szent-Gyorgyi, A. G. 2004. The early history of the biochemistry of muscle contraction. *J Gen Physiol,* 123**,** 631-41.

Tabas, I. & Bornfeldt, K. E. 2016. Macrophage Phenotype and Function in Different Stages of Atherosclerosis. *Circ Res,* 118**,** 653-67.

Takeda, K. & Akira, S. 2004. TLR signaling pathways. *Semin Immunol,* 16**,** 3-9.

Takeuchi, O. & Akira, S. 2010. Pattern recognition receptors and inflammation. *Cell,* 140**,** 805-20.

Tanimura, S., Hashizume, J., Arichika, N., Watanabe, K., Ohyama, K., Takeda, K. & Kohno, M. 2016. ERK signaling promotes cell motility by inducing the localization of myosin 1E to lamellipodial tips. *J Cell Biol,* 214**,** 475-89.

Tannahill, G. M., Curtis, A. M., Adamik, J., Palsson-Mcdermott, E. M., Mcgettrick, A. F., Goel, G., Frezza, C., Bernard, N. J., Kelly, B., Foley, N. H., Zheng, L., Gardet, A., Tong, Z., Jany, S. S., Corr, S. C., Haneklaus, M., Caffrey, B. E., Pierce, K., Walmsley, S., Beasley, F. C., Cummins, E., Nizet, V., Whyte, M., Taylor, C. T., Lin, H., Masters, S. L., Gottlieb, E., Kelly, V. P., Clish, C., Auron, P. E., Xavier, R. J. & O'neill, L. A. 2013. Succinate is an inflammatory signal that induces IL-1beta through HIF-1alpha. *Nature,* 496**,** 238-42.

Taylor, P. R., Martinez-Pomares, L., Stacey, M., Lin, H. H., Brown, G. D. & Gordon, S. 2005. Macrophage receptors and immune recognition. *Annu Rev Immunol,* 23**,** 901-44.

Theodosiou, A., Smith, A., Gillieron, C., Arkinstall, S. & Ashworth, A. 1999. MKP5, a new member of the MAP kinase phosphatase family, which selectively dephosphorylates stress-activated kinases. *Oncogene,* 18**,** 6981-8.

Thompson, M. R., Kaminski, J. J., Kurt-Jones, E. A. & Fitzgerald, K. A. 2011. Pattern recognition receptors and the innate immune response to viral infection. *Viruses,* 3**,** 920-40.

Tohyama, Y. & Yamamura, H. 2009. Protein tyrosine kinase, syk: a key player in phagocytic cells. *J Biochem,* 145**,** 267-73.

Towbin, H., Staehelin, T. & Gordon, J. 1979. Electrophoretic transfer of proteins from polyacrylamide gels to nitrocellulose sheets: procedure and some applications. *Proc Natl Acad Sci U S A,* 76**,** 4350-4.

Traves, P. G., De Atauri, P., Marin, S., Pimentel-Santillana, M., Rodriguez-Prados, J. C., Marin De Mas, I., Selivanov, V. A., Martin-Sanz, P., Bosca, L. & Cascante, M. 2012. Relevance of the MEK/ERK signaling pathway in the metabolism of activated macrophages: a metabolomic approach. *J Immunol,* 188**,** 1402-10.

Treanor, B. 2012. B-cell receptor: from resting state to activate. *Immunology,* 136**,** 21-7.

Trygg, J., Holmes, E. & Lundstedt, T. 2007. Chemometrics in metabonomics. *J Proteome Res,* 6**,** 469-79.

Turjanski, A. G., Vaque, J. P. & Gutkind, J. S. 2007. MAP kinases and the control of nuclear events. *Oncogene,* 26**,** 3240-53.

Tyteca, D., Nishino, T., Debaix, H., Van Der Smissen, P., N'kuli, F., Hoffmann, D., Cnops, Y., Rabolli, V., Van Loo, G., Beyaert, R., Huaux, F., Devuyst, O. & Courtoy, P. J. 2015. Regulation of macrophage motility by the water channel aquaporin-1: crucial role of M0/M2 phenotype switch. *PLoS One,* 10**,** e0117398.

Tzouvelekis, A., Xylourgidis, N., Kisuk, M., Yu, G., Herazo-Maya, J., Aurelien, N., Adams, T., Woolard, T., Ibarra, G., Deiuliis, G., Binzenhöfer, L., Bennett, A. & Kaminski, N. 2016. P056 Loss of MAP Kinase Phosphatase 5 (MKP5) attenuates fibrotic responses in-vitro and in-vivo. *QJM: An International Journal of Medicine,* 109**,** S40-S40.

Underhill, D. M. & Goodridge, H. S. 2012. Information processing during phagocytosis. *Nat Rev Immunol,* 12**,** 492-502.

Van Furth, R., Cohn, Z. A., Hirsch, J. G., Humphrey, J. H., Spector, W. G. & Langevoort, H. L. 1972. The mononuclear phagocyte system: a new classification of macrophages, monocytes, and their precursor cells. *Bull World Health Organ,* 46**,** 845-52.

Varin, A. & Gordon, S. 2009. Alternative activation of macrophages: immune function and cellular biology. *Immunobiology,* 214**,** 630-41.

Varin, A., Mukhopadhyay, S., Herbein, G. & Gordon, S. 2010. Alternative activation of macrophages by IL-4 impairs phagocytosis of pathogens but potentiates microbial-induced signalling and cytokine secretion. *Blood,* 115**,** 353-62.

Varol, C., Landsman, L., Fogg, D. K., Greenshtein, L., Gildor, B., Margalit, R., Kalchenko, V., Geissmann, F. & Jung, S. 2007. Monocytes give rise to mucosal, but not splenic, conventional dendritic cells. *J Exp Med,* 204**,** 171-80.

Venter, G., Oerlemans, F. T., Wijers, M., Willemse, M., Fransen, J. A. & Wieringa, B. 2014. Glucose controls morphodynamics of LPS-stimulated macrophages. *PLoS One,* 9**,** e96786.

Vereyken, E. J., Heijnen, P. D., Baron, W., De Vries, E. H., Dijkstra, C. D. & Teunissen, C. E. 2011. Classically and alternatively activated bone marrow derived macrophages differ in cytoskeletal functions and migration towards specific CNS cell types. *J Neuroinflammation,* 8**,** 58.

Wahl, J. R., Goetsch, N. J., Young, H. J., Van Maanen, R. J., Johnson, J. D., Pea, A. S. & Brittingham, A. 2005. Murine macrophages produce endothelin-1 after microbial stimulation. *Exp Biol Med (Maywood),* 230**,** 652-8.

Wakeman, D., Schneider, J. E., Liu, J., Wandu, W. S., Erwin, C. R., Guo, J., Stappenbeck, T. S. & Warner, B. W. 2012. Deletion of p38-alpha mitogen-activated protein kinase within the intestinal epithelium promotes colon tumorigenesis. *Surgery,* 152**,** 286-93.

Wang, G., Li, Y., Yang, Z., Xu, W., Yang, Y. & Tan, X. 2018. ROS mediated EGFR/MEK/ERK/HIF-1alpha Loop Regulates Glucose metabolism in pancreatic cancer. *Biochem Biophys Res Commun,* 500**,** 873-878.

Wang, J. 2018. Neutrophils in tissue injury and repair. *Cell Tissue Res,* 371**,** 531-539.

Warburg, O., Wind, F. & Negelein, E. 1927. THE METABOLISM OF TUMORS IN THE BODY. *J Gen Physiol,* 8**,** 519-30.

Weischenfeldt, J. & Porse, B. 2008. Bone Marrow-Derived Macrophages (BMM): Isolation and Applications. *CSH Protoc,* 2008**,** pdb prot5080.

Witte, M. B. & Barbul, A. 2003. Arginine physiology and its implication for wound healing. *Wound Repair Regen,* 11**,** 419-23.

Wonderling, R. S., Ghaffar, A. & Mayer, E. P. 1996. Lipopolysaccharide-induced suppression of phagocytosis: effects on the phagocytic machinery. *Immunopharmacol Immunotoxicol,* 18**,** 267-89.

Woods, S., Schroeder, J., Mcgachy, H. A., Plevin, R., Roberts, C. W. & Alexander, J. 2013. MAP kinase phosphatase-2 plays a key role in the control of infection with Toxoplasma gondii by modulating iNOS and arginase-1 activities in mice. *PLoS Pathog,* 9**,** e1003535.

Wu, J. J., Roth, R. J., Anderson, E. J., Hong, E. G., Lee, M. K., Choi, C. S., Neufer, P. D., Shulman, G. I., Kim, J. K. & Bennett, A. M. 2006. Mice lacking MAP kinase phosphatase-1 have enhanced MAP kinase activity and resistance to diet-induced obesity. *Cell Metab,* 4**,** 61-73.

Xu, X. D., Shao, S. X., Jiang, H. P., Cao, Y. W., Wang, Y. H., Yang, X. C., Wang, Y. L., Wang, X. S. & Niu, H. T. 2015. Warburg effect or reverse Warburg effect? A review of cancer metabolism. *Oncol Res Treat,* 38**,** 117-22.

Yamamoto, M., Sato, S., Hemmi, H., Hoshino, K., Kaisho, T., Sanjo, H., Takeuchi, O., Sugiyama, M., Okabe, M., Takeda, K. & Akira, S. 2003. Role of adaptor TRIF in the MyD88-independent toll-like receptor signaling pathway. *Science,* 301**,** 640-3.

Yamauchi, J., Nagao, M., Kaziro, Y. & Itoh, H. 1997. Activation of p38 mitogen-activated protein kinase by signaling through G protein-coupled receptors. Involvement of Gbetagamma and Galphaq/11 subunits. *J Biol Chem,* 272**,** 27771-7.

Yan, Z. Q. & Hansson, G. K. 2007. Innate immunity, macrophage activation, and atherosclerosis. *Immunol Rev,* 219**,** 187-203.

Yanagisawa, M., Kurihara, H., Kimura, S., Tomobe, Y., Kobayashi, M., Mitsui, Y., Yazaki, Y., Goto, K. & Masaki, T. 1988. A novel potent vasoconstrictor peptide produced by vascular endothelial cells. *Nature,* 332**,** 411-5.

Yang, D. D., Kuan, C. Y., Whitmarsh, A. J., Rincon, M., Zheng, T. S., Davis, R. J., Rakic, P. & Flavell, R. A. 1997. Absence of excitotoxicity-induced apoptosis in the hippocampus of mice lacking the Jnk3 gene. *Nature,* 389**,** 865-70.

Yang, Q., Jeremiah Bell, J. & Bhandoola, A. 2010. T-cell lineage determination. *Immunol Rev,* 238**,** 12-22.

Yang, S. H., Whitmarsh, A. J., Davis, R. J. & Sharrocks, A. D. 1998. Differential targeting of MAP kinases to the ETS-domain transcription factor Elk-1. *Embo j,* 17**,** 1740-9.

Yang, Y., Kim, S. C., Yu, T., Yi, Y. S., Rhee, M. H., Sung, G. H., Yoo, B. C. & Cho, J. Y. 2014. Functional roles of p38 mitogen-activated protein kinase in macrophage-mediated inflammatory responses. *Mediators Inflamm,* 2014**,** 352371.

Zarubin, T. & Han, J. 2005. Activation and signaling of the p38 MAP kinase pathway. *Cell Res,* 15**,** 11-8.

Zhang, H., Chi, Y., Gao, K., Zhang, X. & Yao, J. 2015. p53 protein-mediated up-regulation of MAP kinase phosphatase 3 (MKP-3) contributes to the establishment of the cellular senescent phenotype through dephosphorylation of extracellular signal-regulated kinase 1/2 (ERK1/2). *J Biol Chem,* 290**,** 1129-40.

Zhang, T., Choy, M., Jo, M. & Roberson, M. S. 2001. Structural organization of the rat mitogen-activated protein kinase phosphatase 2 gene. *Gene,* 273**,** 71-9.

Zhang, X., Kimura, Y., Fang, C., Zhou, L., Sfyroera, G., Lambris, J. D., Wetsel, R. A., Miwa, T. & Song, W. C. 2007. Regulation of Toll-like receptor-mediated inflammatory response by complement in vivo. *Blood,* 110**,** 228-36.

Zhang, Y., Blattman, J. N., Kennedy, N. J., Duong, J., Nguyen, T., Wang, Y., Davis, R. J., Greenberg, P. D., Flavell, R. A. & Dong, C. 2004. Regulation of innate

and adaptive immune responses by MAP kinase phosphatase 5. *Nature,* 430**,** 793-7.

Zhang, Y., Hoppe, A. D. & Swanson, J. A. 2010. Coordination of Fc receptor signaling regulates cellular commitment to phagocytosis. *Proc Natl Acad Sci U S A,* 107**,** 19332-7.

Zhao, Q. 2005. The role of mitogen-activated protein kinase phosphatase-1 in the response of alveolar macrophages to lipopolysaccharide: attenuation of proinflammatory cytokine biosynthesis via feedback control of p38. *J. Biol. Chem.,* 280**,** 8101-8108.

Zhou, B. & Zhang, Z. Y. 2002. The activity of the extracellular signal-regulated kinase 2 is regulated by differential phosphorylation in the activation loop. *J Biol Chem,* 277**,** 13889-99.

Zhou, D., Huang, C., Lin, Z., Zhan, S., Kong, L., Fang, C. & Li, J. 2014. Macrophage polarization and function with emphasis on the evolving roles of coordinated regulation of cellular signaling pathways. *Cell Signal,* 26**,** 192-7.

Zhu, N., Feng, X., He, C., Gao, H., Yang, L., Ma, Q., Guo, L., Qiao, Y., Yang, H. & Ma, T. 2011. Defective macrophage function in aquaporin-3 deficiency. *Faseb j,* 25**,** 4233-9.

Zhu, X., Castellani, R. J., Takeda, A., Nunomura, A., Atwood, C. S., Perry, G. & Smith, M. A. 2001. Differential activation of neuronal ERK, JNK/SAPK and p38 in Alzheimer disease: the 'two hit' hypothesis. *Mech Ageing Dev,* 123**,** 39-46.

Ziegler-Heitbrock, L. 2015. Blood Monocytes and Their Subsets: Established Features and Open Questions. *Front Immunol,* 6**,** 423.